



VNiVERSiDAD D SALAMANCA

Gravitational Shock Waves and Holography

Álvaro Dueñas Vidal

UNIVERSIDAD DE SALAMANCA
Departamento de Física Fundamental



Gravitational Shock Waves and Holography

TESIS PRESENTADA POR **D. ÁLVARO DUEÑAS VIDAL**
PARA OPTAR AL TÍTULO DE DOCTOR EN FÍSICA

Tesis dirigida por el profesor **Dr. D. Miguel Ángel Vázquez Mozo.**

Salamanca, Mayo 2015.

D. MIGUEL ÁNGEL VÁZQUEZ MOZO, Profesor Titular de Universidad del Departamento de Física Fundamental de la Universidad de Salamanca

Autoriza la presentación de la memoria de tesis titulada “Gravitational Shock Waves and Holography”, realizada bajo su dirección, por D. ÁLVARO DUEÑAS VIDAL.

Salamanca, a 15 de Mayo de 2015

Fdo.: Miguel Ángel Vázquez Mozo

*All knowledge, the totality of all questions
and all answers, is contained in the dog.*

– Franz Kafka's holographic principle

Agradecimientos

- A mis compañeros de doctorado y amigos, que han combatido en el mismo barro: Edu, Alberto Soria, Alberto “Séneca”, Cris y, como no, Cuchi. Teresa no es alumna de doctorado, pero sin duda merece estar también presente. Vuestros ánimos, consejos y largas horas aguntando mis pensamientos en voz alta han sido de gran ayuda para mí. Han sido grandes momentos, sin duda, los que hemos pasado juntos.
- A mi familia, que siempre ha sido un apoyo incondicional, y a los que nunca he visto flaquear. En especial mis padres, incansables día tras día, con una confianza ciega sobre mí.
- A Fátima, cuya sonrisa cada mañana me ha permitido volar más allá de mis propios sueños. No es aire, si no aliento de vida lo que con cada uno de los momentos que he pasado a su lado ha conseguido insuflar en mí. Lo cierto es que para ella no tengo palabras suficientes (ni rosas).
- Por último, mi mayor agradecimiento es para mi director de tesis, Miguel Ángel. Con su guía a lo largo de estos años ha sabido llevar este trabajo hacia buen puerto y, por el camino, haciendo gala de una paciencia infinita, me ha enseñado mucho. Este trabajo nunca habría sido posible sin él.

A todos vosotros, gracias.

Esta tesis fue realizada con el apoyo económico de la Consejería de Educación de la Junta de Castilla y León a través del programa de becas de Formación de Personal Investigador.

Salamanca, Idus Maius MMXV.

Contents

1	Introduction	1
1.1	The Quark-Gluon Plasma	2
1.2	The holographic tool	6
1.3	Gravitational duals for sQGP production	10
1.4	Gauge symmetries in noncommutative spaces	16
1.5	A note about conventions	19
2	Gravitational waves	21
2.1	Weak gravitational waves	22
2.2	Exact gravitational waves in flat background	24
2.2.1	Flat pp-waves	24
2.2.2	Shock waves in flat background	27
2.3	Aichelburg-Sexl boost	29
2.4	Exact gravitational waves in the AdS space	33
2.4.1	Basics on coordinates in the AdS space	34
2.4.2	Conformal pp-waves	36
2.4.3	AdS gravitational shock waves	37
2.5	Colliding gravitational shock waves in AdS background	39
2.5.1	Setup	40
2.5.2	Regions I, II and III	40
2.5.3	Region IV	42
2.5.4	Penrose trapped surface	45
3	Reissner-Nordström and Fat shock waves in AdS_D	51
3.1	AdS-RN shock waves	52
3.1.1	Shock wave metric computation	52
3.1.2	Electromagnetic field and energy-momentum tensor	57
3.1.3	Some remarks	62
3.2	Fat gravitational shock waves	65
3.3	Holography for AdS-RN and fat gravitational shock waves	70
3.3.1	Holographic stress tensor	70

3.3.2	Holographic dual for colliding shock waves	74
3.3.3	Comparison with boosted Woods-Saxon potential	78
4	Critical phenomena in collisions of AdS gravitational shock waves	83
4.1	AdS-Sch shock wave collision	84
4.1.1	head-on collision	85
4.1.2	Off-center collision	88
4.1.3	Holographic interpretation	96
4.2	Gravitational dual of nonequal sized energy lumps	98
4.3	Improving the model: Colliding AdS-RN shock waves	104
5	Gauge symmetries in noncommutative geometry	109
5.1	Basics on noncommutative field theory	110
5.1.1	Noncommutative geometry and noncommutative flat space	110
5.1.2	Weyl correspondence and Moyal product	111
5.1.3	Non-commutative functional actions	114
5.1.4	Non-commutative Yang-Mills theories	117
5.2	Star-gauge invariance	121
5.3	Twist-gauge invariance	123
5.4	Star- and twist-gauge invariances as true symmetries	127
5.5	Star-twisted gauge invariances	131
6	Conclusions and outlook	137
6.1	Collisions of gravitational shock waves and plasma thermalization	137
6.2	Gauge invariances in noncommutative Yang-Mills theories	141
A	Anti-de Sitter space	143
B	Anti-de Sitter Reissner-Nordström solution	151
B.1	Line element, equations of motion and action	151
B.2	Horizons	153
B.3	Mass and charge	154
C	Mathematical supplement	159
C.1	A useful lemma	159
C.2	Computation of some improper integrals	160

Chapter 1

Introduction

One of the most exciting discoveries in the high energy physics of the new century is the existence of (at least one) deconfined phase of Quantum Chromodynamics (QCD) [1, 2]. Roughly speaking, under suitable temperature and baryon density conditions, quarks and gluons can be extracted from hadrons to form a new matter state called the Quark-Gluon Plasma (QGP), where quarks and gluons are the effective degrees of freedom rather than baryons and mesons [3]. A theoretical description of how quarks and gluons deconfine and the properties of the QGP would be a very desirable result to go into a deep understanding of the fundamentals of QCD.

Experimentally, the QGP is produced colliding heavy ion in modern accelerators at high energy. Measures performed after the QGP is formed in the collisions show that the transition from confinement to the QGP phase happens in a region where QCD is still strongly coupled [4]. Thus usual techniques based in perturbative approaches to QCD are not useful to understand the physics involved in. As a consequence, nowadays the deconfinement phenomenon as well as the nature of the QGP are poorly understood.

The crash of the perturbative techniques to analyze the QGP physics has highlighted the necessity to develop new models constructed in non-perturbative frameworks to go towards a definitive understanding of the deconfinement phenomenon. In this PhD Thesis, taking advantage of the gauge/gravity connection provided by string theory [5, 6, 7], gravitational duals are used to develop models for the QGP production in high energy collisions. In particular, the critical formation of the QGP in high energy collisions is discussed from gravitational duals consisting in colliding gravitational shock waves obtained boosting black hole solutions in an AdS background .

Not directly related to the strongly coupled QCD world and the deconfinement of quarks and gluons, in this PhD Thesis the formulation of gauge theories in noncommutative geometries is also studied. In general terms, a

noncommutative space consists in some kind of space where the coordinates do not commute among themselves [8]. Usually in scientific literature, a field theory living in a noncommutative space is referred as a Non-Commutative Field Theory or NCFT. Because of the noncommutativity of the coordinates causes a lack of locality in NCFTs, the construction of gauge symmetries in noncommutative geometries must be revised [9, 10, 11, 12, 13, 14]. Here we discuss in detail the different ways in which this can be done, introducing an infinite family of realizations interpolating between the two usual constructions of gauge invariance in NCFTs: star-gauge and twist-gauge symmetries.

The goal of this chapter is to put into context the work contained in this Thesis and give a briefly description of the results obtained. Neither too many equations nor exhaustive technicalities will be used along it in order to gain clarity and concision. At the end of the chapter there is a brief section dedicated to some convections and terminology which will be used in the next chapters.

1.1 The Quark-Gluon Plasma

As has already been mentioned, the physical interest in the results presented in the first part of this Thesis rests over the phenomenon called the Quark-Gluon Plasma. Therefore, a good way to begin the introduction chapter is giving a brief picture of what the QGP is and how it can be produced.

As a physics phenomenon, the quark-gluon plasma fits in the framework of Quantum Chromodynamics. Mathematically, QCD is a gauge theory with gauge group $SU(3)$ [15], constructed for modeling the strong interaction between hadrons and, in the last microscopic frontier, between quarks and gluons. Together with the electroweak interaction theory (Yang-Mills theory with $SU(2) \times U(1)$ gauge group) and the spontaneous symmetry breaking, it composes the most accurate fundamental particle theory written up to date: the standard model.

Unlike Quantum Electrodynamics (QED), QCD is a nonabelian gauge theory. Physically that means the gluons couple among themselves, having vertices of three and four gluons. As a consequence, two relevant phenomena that do not appear in QED do in QCD: asymptotic freedom and confinement [16].

- **Asymptotic freedom.** At low energies, QCD is nonperturbative. That is, the bare gauge coupling constant is large. On the other hand, the color charge of the gluons leads to an anti-screening of the quarks. This phenomenon, after renormalization, results in a negative beta

function, and therefore the coupling constant of the renormalized theory decreases when the energy scale increases. Thus, although QCD is strongly coupled at low energy, it becomes weakly coupled for enough high energy, being tractable through perturbative expansions in Feynman diagrams. In fact, at very high energies the theory approaches asymptotically a free regime. This behavior of the theory is called asymptotic freedom.

- **Confinement.** At low energy it is observed that quarks and gluons associate forming color singlets (hadrons), in such a way that color charge is always confined. In other words, at low temperature, free color does not exist. This is called color confinement. Note that it happens at strong coupling, and thus perturbative tools are useless to study it: up to date there is not any full analytical proof for color confinement¹. In four dimensions² it is believed to be a consequence of the color charge of gluons rather than a nonperturbative phenomenon [16] (note that QED does not exhibit confinement even at strong coupling).

In short, asymptotic freedom and color confinement are two rival phenomena which happen at opposite energy scales. The first one means “free quarks”, whereas the second one means “confined quarks”. Thus it is not crazy to hope that at some middle point in the energy scale a confined-deconfined phase transition (or crossover) could exist, such that, in the deconfined phase, quarks and gluons would interact without forming color singlets. This new phase is what is called the Quark-Gluon Plasma.

Following an heuristic reasoning, the deconfinement of quarks and gluons from hadrons must consists in a kind of process where the energy scale involved is large enough to make hadrons overlap with each other. Experimentally, this can be achieved following two different strategies [3]: heating up the QCD vacuum or increasing the baryonic density.

- **Heating the vacuum.** Suppose we heat up the QCD vacuum in some bounded region. At low temperature colorless particles, i.e. hadrons, will be excited from the vacuum. However, if we increase enough the temperature, hadrons will start to overlap at a certain critical temperature T_c . Above such critical temperature, the mixing process continues, breaking completely the structure of hadrons. Then hadrons dissolve into some kind of quarks and gluons foam, the QGP.

¹A mechanism for total confinement of quarks was defined by Wilson in [17] using a discrete lattice in flat space.

²It has been observed that compact abelian gauge theories also can exhibit confinement in two dimensions [18].

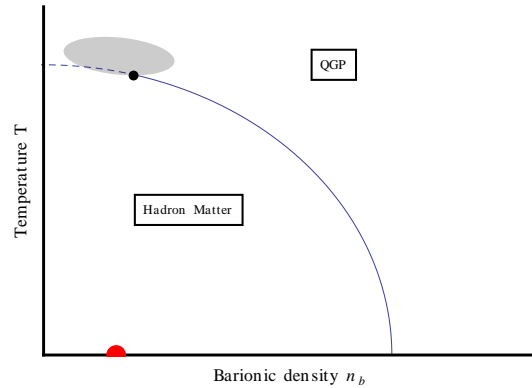


Figure 1.1: Phase diagram for QCD. The blue curve marks the confined-deconfined phase transition discussed in the text. The black and red points in the graph corresponds to the critical point for the phase transition and nuclear matter respectively. The dashed curve beyond the critical point represents that a crossover happens in this region between confined and deconfined phase. Finally, gray region shows where the sQGP created at RHIC and LHC is.

- **Increasing the baryonic density n_b .** In a similar way to the first point, for large enough baryonic density, hadrons overlap and mix. Then quarks and gluons begin to interact without being associated in hadrons, forming the QGP.

These two strategies are not exclusive, and both can be combined to achieve a thermalized QGP from the hadronic phase. Therefore, in a phase diagram with thermodynamical variables n_b and T , the confined-deconfined phase transition must corresponds to some curve $T_c = T_c(n_b)$ dividing the phase space into two regions. In fig. 1.1 it is showed a sketch of how could be such QCD phase diagram. Note that the curve $T_c = T_c(n_b)$ starts at some critical point. It is expected that this critical point exits, such that for temperatures and densities beyond it a sudden change between the hadron phase and the QGP does not happen, but a crossover [19].

Until date nobody has been successful in giving any analytical proof for the existence of the QGP beyond the heuristic explanation previously exposed based on a cross over between asymptotic freedom and confinement at some energy scale. Only lattice computations have had some success showing (numerically) the existence of the phase transition [20]. Surprisingly, simulations in the lattice has shown that deconfinement could happen in a region where QCD is still strongly coupled ($T \sim 150 - 200$ Mev for low baryonic densities). In other words, lattice simulations signal that the phase transition between ordinary baryonic matter and QGP could be nonperturbative. This would explain the fact that perturbative QCD has not had success in find

an analytical description of the confined-deconfined QCD phase transition nowadays.

Of course, theoretical lucubrations and equations in a paper are a beautiful way to understand nature, but physics sinks its roots in experimental facts. It is necessary to produce the QGP in the laboratory to “play” with it and measure its properties, beyond the theoretical predictions given by lattice formulations or other models. From an empirical point of view, the range of temperatures to produce the QGP predicted by lattice calculations are almost prohibitive. Note that $T \sim 200$ MeV corresponds to $10^{12}K$, being $1.5 \cdot 10^7K$ the temperature at the core of the Sun. The only known way to obtain such so elevate temperatures in the Earth is through heavy ion collisions at high energy inside modern accelerators: just after collision, a hot region called “fireball” is created for a very sort time, being the temperature large enough to deconfine quarks and gluons form hadrons. Then the fireball expands and cools down, resulting finally in jets of relativistic particles running away from the collision region (hadronization) [3].

The first efforts in creating a QGP from high energy collisions were done at the Super Proton Synchrotron (SPS) in the 1980s and 1990s. The results led CERN to announce indirect evidence of some kind of quark matter, but without neither details of its production nor data [1]. It was necessary to wait until 2010 to have a complete evidence for QGP creation in high energy collisions: experiments colliding heavy ions at the Relativistic Heavy Ion Collider (RHIC) produced a large elliptic flow and quenching parameter, which indicate the creation of a plasma fireball after collision by a very short time [21, 22, 23, 24]. Nowadays, apart from the RHIC experiments, current experiments at the Large Hadron Collider (LHC) with colliding heavy ions are also been done for advancing in the understanding of the QGP production and its nature [25, 26, 27].

Experimental measures at RHIC and LHC are in accordance with the previous lattice predictions. In particular, measures show the created plasma is still strongly coupled in spite of being a deconfined phase [4]. This support the hypothesis that the phase transition could be a nonperturbative phenomenon, such that the created QGP in RHIC and LHC would be near the phase transition. Usually scientific literature refers to this kind of plasma as strongly QGP (sQGP). In fig. 1.1 it is shown the zone of the phase diagram for QCD where the sQGP from RHIC and LHC experiments is being created. It is believed, from lattice simulations, that experiments are near to the critical point. However, the critical point has not been observed yet. In fact, the exact phase transition curve and the location of the critical point are currently being actively studied.

Unraveling the QCD phase structure is an important goal in present and

future theoretical and experimental physics. Understanding the physics behind the QGP nature and the conditions for its creation may be important for the study of neutron stars and the early Universe. In the first case, it is supposed that pressure in the core of neutron stars could increase the baryon density enough to deconfine quarks and gluons from hadrons, even at low temperatures. On the other hand, temperature and pressure about 10^{-5} s after the Big Bang could be adequate to form and thermalize a QGP at low baryon density. Also knowing the details of the phase transition could give us fundamental information about the confinement mechanism of color and, in general, of the nonperturbative aspects of QCD.

1.2 The holographic tool

Since the confined-deconfined phase transition happens in a region where the field theory is still strongly coupled, the phenomenon of deconfinement cannot be addressed in perturbative QCD. As a consequence, nonperturbative tools, as lattice QCD (e.g. see [28]) and the gauge/gravity correspondence, must be used to get some insight inside the phenomenon of sQGP. In this section we provide a brief review of the holographic principle as well as the AdS/CFT correspondence, being the latest the framework we shall use in next chapter to develop model for the sQGP production in high energy collisions. The reader interested in a detailed study of string theory and the Maldacena conjecture can satisfy its curiosity in, for example, [6, 7, 29, 30, 31, 32].

The holographic principle was first proposed by Gerard 't Hooft in 1993, and latter by Leonard Susskind in 1995, from the original idea of Bekenstein [33] for the maximum entropy of a region of space. Proposing the Planck scale as a natural cut-off for any quantum field theory³, Bekenstein proposed that the maximum entropy of a region of space does not grow with the volume of the region, but with the area of the boundary surrounding it. Later 't Hooft and Susskind proposed a more radical interpretation of Bekenstein's idea [34, 35]: given that the entropy measures the number of degrees of freedom of a configuration, it was proposed that the dynamics of any quantum theory of gravitation in a bounded region of spacetime must be encoded in some field theory living at the boundary of the region, with “one bit” of information per Planck area. In other words, gravity emerges from a lower dimensional field theory in what could be called a holographic way.

The holographic principle proposes a bridge connecting (quantum) grav-

³Beyond Planck scale the energy density is high enough in order to a micro black hole forms at each point of space. Then entropy is given by the Bekenstein-Hawking formula for the black hole entropy at Planck scale.

ity with a field theory in a lower dimension. This enables the possibility to handle quantum gravity phenomena from their images in the lower dimensional theory (and vice versa). However the holographic principle only establishes the existence of such connection but it does not explicitly formulate it. In other words, the principle by itself has not any associated mathematical construction that let us to compute anything. Searching for an explicit realization of the holographic principle, Susskind highlighted in 1995 that perhaps it could be done inside the framework of string theory since it is a theory containing quantum gravity [35]. Finally, Maldacena ended the search in 1998 formulating an explicit realization of the principle which is called nowadays as the Maldacena conjecture [5].

Maldacena conjecture establishes the existence of a one-to-one map between Yang Mills field theory with gauge group $SU(N)$ and four supersymmetries ($\mathcal{N} = 4$ SYM) in flat 4-dimensional space and IIB string theory in⁴ $AdS_5 \times S^5$, such that

$$g_s = g_{YM}^2, \quad L^2 = \alpha' \sqrt{4\pi g_s N}, \quad \int_{S^5} F^5 = N, \quad (1.1)$$

where g_s and g_{YM} are the string and gauge coupling constants respectively, L the scale of AdS_5 and radius of S^5 , α' the Regge slope parameter and F^5 the 5-form field strength of the self-dual 4-form of the IIB supergravity. In addition, given that the conformal boundary of AdS_5 is 4-dimensional Minkowski spacetime, usually the Maldacena conjecture is formulated defining the $\mathcal{N} = 4$ SYM over the AdS_5 boundary.

The connection between the string and gauge worlds proposed by Maldacena arises from a detailed study of the $D3$ -brane solution in type IIB string theory. From the stringy point of view, Dp -branes are the locus where open strings end, such that the world-volume low energy dynamics (that is $\alpha' \rightarrow 0$) is given by some gauge theory with $g_{YM}^2 = g_s$. In particular, for a stack of N $D3$ -branes, it is $\mathcal{N} = 4$ SYM field theory with gauge group $SU(N)$. In addition, the bulk dynamics approaches free SUGRA for low energies, and the interacting term between bulk and world-volume dynamics vanishes. Thus, from this point of view, the effective action at low energy for a stack of N $D3$ -branes is

$$S = \underbrace{S_{\mathcal{N}=4}^{\text{SYM}}}_{\text{World-Volume}} + \underbrace{S_{\text{SUGRA}}^{\text{FREE}}}_{\text{Bulk}}. \quad (1.2)$$

On the other hand, from the "brany" point of view, a Dp -brane (with p odd) in the low energy regime is a solution of supergravity (SUGRA) IIB equations. Taking certain low energy limit in which the bulk dynamics decouples from

⁴ AdS_D stands for D -dimensional Anti de Sitter space.

that of the brane (near horizon limit), closed strings inside the "throat" of the brane solution decouple from the closed strings living far away of the brane, in flat space. In addition, the near-horizon geometry becomes $\text{AdS}_5 \times S^5$ with $L^2 = \alpha' \sqrt{4\pi g_s N}$ and $\int_{S^5} F^5 = N$. Thus, from this point of view, the dynamics at low energy is given by the action,

$$S = \underbrace{S_{\text{AdS}_5 \times S^5}^{\text{IIB}}}_{\text{Throat}} + \underbrace{S_{\text{Flat space}}^{\text{FREE SUGRA}}}_{\text{Flat space}}. \quad (1.3)$$

Then a direct identification between (1.2) and (1.3) gives the Maldacena conjecture,

$$S_{\text{SYM}}^{N=4} + \cancel{S_{\text{SUGRA}}^{\text{FREE}}} \iff S_{\text{AdS}_5 \times S^5}^{\text{IIB}} + \cancel{S_{\text{SUGRA}}^{\text{FREE}}} \quad (1.4)$$

Note that this is just a heuristic reasoning to sketch out the mechanism under which the conjecture works. An identification between (1.2) and (1.3) is not rigorous. The main reason for it is that quantized strings are well understood in flat space time, but are not in curved spaces, like $\text{AdS}_5 \times S^5$. In fact, nowadays no analytic proof exist for the Maldacena conjecture.

The main advantage of the Maldacena conjecture is that it relates a theory containing quantum gravity with a quantum field theory *without gravity* at lower dimension. That is one step beyond the original idea of 't Hooft and Susskind. However, because it is not known how to formulate string theory in $\text{AdS}_5 \times S^5$, the Maldacena conjecture in its strongest form (1.4) cannot be fully exploited. Fortunately, there are various highly non trivial limits of the correspondence that can be useful. In particular, consider the large N -limit fixing the 't Hooft coupling constant of the gauge theory, $\lambda = Ng_{YM}^2$. Given that $g_s = g_{YM}^2$, at fixed 't Hooft coupling, the string coupling scales as $1/N$, so the large N -limit at fixed 't Hooft coupling in the SYM side corresponds to take the tree level in the string side. In this way, the conjecture simplifies, but the string side is still highly nontrivial to be useful since it remains necessary to quantize noninteracting strings in $\text{AdS}_5 \times S^5$. The solution comes taking also the strong 't Hooft coupling limit ($\lambda \gg 1$) after the large N -limit. In the string side of the conjecture it corresponds to take the low-energy limit, since $L^2/\alpha' \sim \sqrt{\lambda}$. Thus, in the $N \gg 1, \lambda \gg 1$ regime, the conjecture identify large N and strongly coupled SYM field theory with IIB SUGRA in $\text{AdS}_5 \times S^5$:

$$\begin{array}{ccc} N \gg 1, & \lambda \gg 1 & \\ & \Downarrow & \\ \text{Large N} & & \text{IIB SUGRA} \\ \text{Strongly coupled} & \iff & \text{AdS}_5 \times S^5 \\ \mathcal{N} = 4 \text{ SYM} & & \end{array} \quad (1.5)$$

Now this connection can be fully exploited: the two theories related in (1.5) are known and perfectly defined.

The correspondence (1.5) relates a strongly coupled quantum Yang-Mills theory in four dimensions with a classical theory of gravitation in $\text{AdS}_5 \times S^5$, where “classical” means “nonquantum”. A relevant characteristic that can be used to roughly justify the connection established in (1.5) is the fact that the symmetry groups of the two theory involved coincide: on one hand, $\mathcal{N} = 4$ SYM is a Conformal Field Theory (CFT), being $\text{SO}(2,4)$ the group of the conformal symmetry in four dimensions, and on the other hand, $\text{SO}(2,4)$ is also the isometry group in AdS_5 . In addition, the R-symmetry group for four supersymmetries in four dimensions is $\text{SO}(5)$, which also coincides with the isometry group of S^5 .

Note that (1.4) establishes a full equivalence between two theories, something that can not be proved or tested in any way and, in addition, is not useful, since IIB strings in AdS_5 is an unknown theory. In some sense (1.4) is oversized for current physics: for all practical purposes it is enough to conjecture that the equivalence happens in certain limit, being exact just at the level of (1.5), where the conjecture can be tested and is useful. Relation (1.4) is referred as the Maldacena conjecture in its strongest form, while (1.5) is called the weak formulation of the Maldacena conjecture or, according to the connection previously discussed between the symmetry groups of the two theories, the AdS/CFT correspondence. In this PhD Thesis, the weak version of the conjecture will even be relaxed following the spirit of the holographic principle for including arbitrary dimensions and products of the AdS space with arbitrary compact manifolds. Enunciated in a rigorous way, this extended AdS/CFT correspondence conjectures that there exists a bijective map between classical gravity in AdS_D and observables of some strongly coupled conformal field theory at the boundary of AdS_D .

The explicit form of the AdS/CFT map (or Maldacena dictionary) follows from (1.5) equaling the partition functions⁵ of the two theories: given any supergravity field ϕ inside AdS space which takes the value ϕ_0 over the conformal boundary, there is an operator \mathcal{O} in the boundary field theory which couples to ϕ_0 according to

$$\left\langle e^{-\int \mathcal{O}(x)\Phi_0(x)} \right\rangle_{\text{CFT}} = e^{-S_{\text{IIB}}(\phi_0)}, \quad (1.6)$$

⁵A Wick rotation to Euclidean time has been done such that the generation functional of a theory for some field Φ is given by $Z[J] = \int \mathcal{D}\Phi \text{Exp} [-S_E(\Phi) - \int d^d x \Phi(x)J(x)]$, where S_E stands for the Euclidean functional action. In addition, in the semiclassical limit the functional integral can be evaluated in the saddle point approximation with the result $\text{Exp} [-S_E(\Phi_{cl}) - \int d^d x \Phi_{cl}(x)J(x)]$, where $\Phi_{cl}(x)$ is a solution to the classical field equations of the theory.

being S_{IIB} the classical (super)gravity action. An example of such connection (which will be useful in subsequent chapters) is that the graviton in AdS space couples to the energy-momentum tensor operator in the gauge theory defined in the conformal boundary of AdS.

By connecting strongly coupled gauge theories to classical (super)gravity, the AdS/CFT correspondence becomes a powerful tool to perform nonperturbative computations in the gauge side of the correspondence from gravitational duals inside the AdS space. In particular, it can be used to study nonperturbative phenomena in strongly coupled QCD. Of course, QCD is far away from $\mathcal{N} = 4$ SYM theory: the former is neither supersymmetric nor conformal. Also, the gauge group of QCD is $SU(3)$. This corresponds to $N = 3$ in (1.5), which is not an excessively large number as required. However, it is expected that, in spirit of the holographic principle, the gravitational dynamics in AdS_D captures enough physics of QCD in $D - 1$ flat dimensions, such that the gravitational duals could be useful to describe at least qualitatively nonperturbative QCD phenomena.

1.3 Gravitational duals for sQGP production

In the previous section it has been introduced the concept of the gauge/gravity duality and it has been pointed out that it can be used as a powerful tool to analyze nonperturbative phenomena in strongly coupled QCD. As an important application, it can be used to study the properties of the sQGP. In particular, in this PhD Thesis the AdS/CFT correspondence is used to study the production of the sQGP in high energy collisions. This section tries to fix what are the gravitational duals for the sQGP production in high energy collision and discuss briefly what are the results obtained from them, which will be exposed in detail in subsequent chapters.

The first question to answer is what is the (super)gravitational dual for a thermalized plasma. Note that, in gravitational physics, black holes are thermal objects that obey the laws of thermodynamics: given any event horizon, it has associated a Hawking temperature [36]. Then, following the spirit of the holographic principle, it is tempting to believe that an event horizon is described holographically by a thermal quantum field theory living in some hypersurface surrounding the event horizon. This seems to indicate that AdS black holes are the gravitational duals for thermal field theories. In fact, the AdS/CFT correspondence shows that a nonextremal D3-brane solution of supergravity is the gravitational dual of $\mathcal{N} = 4$ SYM at finite temperature [6], such that the Hawking temperature of the brane coincides with the temperature of the supersymmetric plasma. This connection between event horizons

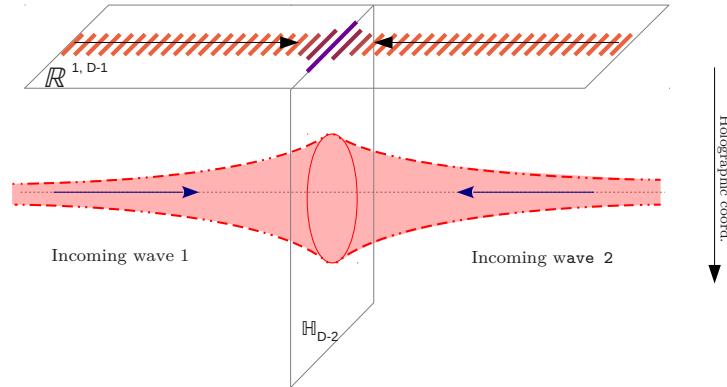


Figure 1.2: Schematic picture for the gravitational dual proposed in the text. The AdS boundary corresponds to the horizontal plane, and the AdS space spreads from top to down. The arrows signal the colliding gravitational shock waves inside the AdS space. The dashed “trumpet” around the colliding shock waves represents the Penrose trapped surface, which forms before the collision happens.

and finite temperature field theory has been used successfully to study the hydrodynamics of strongly coupled Yang-Mills plasmas [37, 38, 39, 40, 41].

From the connection between black holes and thermalized plasmas, it follows that the gravitational dual for plasma thermalization after a high energy collision must be some dynamical process inside the AdS space which yields to the creation of an event horizon. Inspired from the generation of horizons after the collision of gravitational waves in flat spacetime, it has been proposed in [42, 43] that the gravitational dual for colliding relativistic energy lumps in the boundary of AdS space must be colliding gravitational shock waves inside AdS space, such that the appearance of an event horizon after the collision is signaling the thermalization of a plasma in the boundary theory (see fig. 1.2). In this way, it is possible to study the production of thermalized strongly coupled Yang-Mills plasma after high energy collisions from solving colliding gravitational shock waves, a problem that, although is not trivial, is much more feasible than the original, where perturbative tools cannot be used.

The concepts and details in gravitational waves and shock waves will be given in Chaps. 2 and 3. From the time being, it will be enough to have an intuitive picture of the issue. Roughly speaking, a gravitational wave is any geometrical ripple which propagates at the speed of light in some stationary background. Usually gravitational waves are referred to perturbative

solutions in the weak field approximation over a stationary vacuum solution. Gravitational shock waves are a special case in this sense since they are not approximate solutions to Einstein equations, but exact. In addition, gravitational shock waves are “finite”; they begin and end at some point, such that before and after the wave passes the spacetime recovers the background geometry. As an example, the gravitational field of a relativistic particle is infinitely Lorentz-contracted in the direction of motion until it is confined in the transverse plane to the particle propagation, traveling with the particle and forming a gravitational shock wave.

As we have explained, the production of a thermalized plasma in the boundary theory is given by the creation of a event horizon in the future light cone of the collision of two gravitational waves inside AdS space. However, to solve the causal structure of the spacetime after a gravitational wave collision is a complicated task since, unlike electromagnetic waves, gravitational waves cannot generally be superposed linearly⁶. In general terms, at the instant of collision the two waves pass through one another, and nonlinearly interact by shearing and focusing. The analytical solution after such highly nonlinear process is only known in a few cases with high degree of symmetry and in flat spacetime [44]. In fact, for colliding gravitational shock waves no analytical solution for the metric in the future light cone of the collision is known until date, even in flat background (see [45] for some important progress in AdS space), which results in an impossibility to use the holographic approach to study the production of thermalized plasma in the boundary field theory. A possibility to circumvent this inconvenient is to search for the so called Penrose trapped surface, a marginally outer trapped surface defined over the past light cone of the collision [46], and to take the appearance of this trapped surface as signaling an eventual horizon formation in the future light cone of the collision⁷ [47, 48, 49, 50]. In this way, the appearance of such trapped surface in the collision of two gravitational shock waves is taken as the gravitational dual for plasma thermalization in the boundary theory [51].

The holographic model explained above for studying the sQGP production in high energy collisions has been tested with relative success. It was first time used in [51, 52, 53], taking the gravitational shock waves produced by ultrarelativistic particles in AdS₅ as the gravitational dual for modeling

⁶Except in the weak field limit, or outside the future light cone of the collision of two shock waves

⁷Note that it has been not proved in general terms the existence of a marginally outer trapped surface in a spacetime implies the eventual evolution of the geometry to a event horizon. Only in highly controlled environments (asymptotically flat and static spacetimes in 4 dimensions) it has been proved. However, it seems a reasonable conjecture to assume the generalization to any globally hyperbolic spacetime from a physical point of view.

two colliding energy lumps in the boundary theory. These shock waves are achieved by performing an infinite boost over the AdS-Schwarzschild black hole with a suitable scaling of the mass, following a procedure first time fixed by Aichelburg and Sexl in flat spacetime [54]. With this type of shock waves, [51] analyzed the central collision, whereas in [53] the collision with small impact parameter parallel to the boundary was studied (in the boundary theory, this corresponds to a collision with the a small impact parameter between the two energy lumps). In both cases, it was found that a Penrose trapped surface appears in the collision, which can be interpreted as signaling an eventual thermalization after collision in the boundary theory.

From a physical point of view, it is intuitive to believe that for off-center collisions, two colliding energy lumps in a gauge theory must no longer result in a thermalized plasma once a critical value of the impact parameter is reached. In addition, this maximum impact parameter for plasma thermalization must depend on the energy collision. For the gravitational dual, this phenomenon must translate in an absence of a Penrose trapped surface⁸ in the shock wave collision beyond the maximum impact parameter. This critical behavior of the impact parameter in AdS₅ was found in [52] using a numerical spectral method to compute the Penrose trapped surface in the collision of two shock waves obtained from the AdS-Schwarzschild black hole following the procedure previously described⁹.

Following with the gravitational dual developed in [51, 52, 53], in Chapter 4 it is presented a detailed study of the dependence of the critical impact parameter with the dimension of the AdS space and the energy of the collision [55]. Using a numerical method based on finite differences [56], the gravitational shock wave collision with a non zero impact parameter parallel to the boundary is numerically solved for dimensions 4, 5, 6, 7 and 8 for several values of the impact parameter and energy collision. The obtained results yields a simple scaling relating the critical impact parameter b_c and the energy of the collision μ :

$$\frac{b_c}{L} \sim \left(\frac{G_D \mu}{L^{D-3}} \right)^{\frac{1}{D-2}}. \quad (1.7)$$

⁸Note that, as it has been already explained, the absence of the Penrose trapped surface does not guarantee the eventual evolution of an event horizon after the collision. It is a good conjecture to suppose it happens in this way while there are not a better model. But, however, it is possible that, although the Penrose trapped surface does not appear in a collision, other trapped surface does it in the future light cone of the collision, which may yields to an eventual event horizon.

⁹In [53] the authors did not find any critical behaviour with the impact parameter because of the collision was solved perturbatively in the impact parameter. The results of [53] and [52] coincide at low impact parameters.

As we have pointed out in the previous section, the isometry group of AdS space and the group of conformal symmetry of the boundary theory is identified via the AdS/CFT correspondence. Following this connection, a suitable rotation of the collision scenario with non zero impact parameter inside the AdS space leads to a central collision in the boundary theory between two energy lumps of different size. As we will show in Chapter 4, the criticality in the impact parameter is then transported to a critical relation between the size of two colliding energy lumps to produce a thermalized plasma [55]: when the difference of size is large enough, the energy lumps pass through one another without interaction, since the smallest energy lump does not see enough degrees of freedom in the biggest one to thermalize. Intuitively this is an expected result which, together with the existence of a critical impact parameter, helps to legitimize the use of colliding gravitational shock waves as gravitational duals for modeling the strongly coupled plasma production in high energy collisions.

According to the Bekenstein-Hawking formula relating the black hole entropy to the event horizon area and the holographic principle, in [51, 52] the area of the Penrose trapped surface has been used to compute the entropy production in the collision between energy lumps in the boundary theory, giving an estimate to the entropy production in heavy ion collisions at high energy when a sQGP is produced. From central collisions, it is obtained a scaling of the entropy S of the collision with the energy μ given by

$$S \sim \mu^{2/3}. \quad (1.8)$$

However the behavior observed in heavy ion collisions at RHIC gives a scaling $S \sim \mu^{1/2}$. There are several factors for the discordance between (1.8) and the experimental results. The first one is that the AdS-Schwarzschild solution, from which the model is constructed, is dual to thermal $\mathcal{N} = 4$ SYM, far away from real QCD. Mainly, $\mathcal{N} = 4$ SYM has a conformal symmetry and thus it cannot exhibit confinement. It is expected that confinement in real QCD decreases the production of entropy in sQGP creation, since, until deconfinement happens in the early stages of the collision, the number of degrees of freedom are negligible compared to the number of degrees of freedom of the sQGP, a fact that is not taken into account by the gravitational dual. In [53] it is proposed to introduce an infrared cut-off in the model to take into account confinement in QCD and improved the entropy prediction, together with a ultraviolet cut-off to avoid the asymptotic freedom of QCD. According with the connection between energy scale in the boundary theory and deep inside the AdS space, these cut-offs correspond to eliminate the internal and external shells of the AdS space or computing the area of the Penrose surface. By this method, it is achieved an scaling $S \sim \mu^{1/3}$ for large

μ , a better prediction than the previous one, but still far away from real QCD.

Other reason for the excessive entropy production predicted by the model so far discussed is that point-sourced gravitational shock waves are not very suitable to describe heavy-ions. In fact, the energy-momentum tensor for the boundary theory (or holographic stress tensor) extracted from the gravitational shock waves used to get (1.8) results in a Lorentzian potential, very different from the expected Woods-Saxon potential. Also there are large freedom in choosing the source for the gravitational shock waves. In general, any source invariant under rotations around the collision axis gives the same energy-momentum tensor in the boundary gauge theory. Taking advantage of this fact, in [57] it is proposed to spread the sources of the gravitational shock waves in the transverse space to the collision, substituting point-like sources by transverse energy densities. Introducing such “fat waves” it is possible to increase the energy without changing the entropy production if the energy is sufficiently diffused [51]. However, following this strategy one runs the risk of generating a shock wave which is a solution of Einstein equations but not a supergravity solution, as required by the AdS/CFT correspondence. In fact, in [57] it is analyzed the central collision of fat shock waves and it is found that there is a critical dependence in the size of the sources: for enough diffused fat waves, the Penrose trapped surface does not form in the collision. However, since the holographic energy-momentum tensor is the same for all the sources invariant under rotations around the collision axis, it is not found any reason for this critical behavior in the thermalization of the plasma in the boundary theory. Together with the fact that conserved currents are not the same in the bulk and the boundary, it seems to indicate that fat waves are not in general a supergravity solutions by themselves such that we need to consider additional supergravity fields which would couple to global background charges in the boundary [58].

As an additional effort to improve the gravitational dual model so far discussed, it is possible to consider the collision between gravitational shock waves constructed from other AdS black hole solutions different from the AdS-Schwarzschild black hole, following the mechanism developed by Aichelburg and Sexl in [54]. In particular, the Reissner-Nordström solution has the advantage that it can be extended to a supergravity solution, and perhaps the novel features in the shock wave metric introduced by the presence of charge can improved the model. Intuitively, the presence of charge could reduce the Penrose trapped surface [59], decreasing the expected entropy production in the collision. However, this effect is excessively strong, and in Chapter 4 it is shown how the presence of charge fully prevents the formation of the Penrose trapped surface, even for small charge [60]. Naively we would

expect that searching for topologies with non zero genus solves the problem, since a “hole” in the Penrose surface around the collision could isolate the influence of the charge. However, even taking into account this possibility it is not possible to find a Penrose surface. This same situation is found in flat spacetime. At this point, it is important to remember that the absence of Penrose trapped surface does not exclude the possibility of an eventual horizon formation after the collision happens. Indeed, in [61] a trapped surface is found, similar to the Penrose one, over the future light cone of the collision for the head-on collisions of gravitational shock waves constructed from the Reissner-Nordström solution in flat spacetime.

1.4 Gauge symmetries in noncommutative spaces

The second part of this Thesis will deal with the physics of noncommutative spacetimes. Although this is an issue not directly related to holography or its applications to the study of the sQGP, field theories in noncommutative spaces incorporate nonlocality to interactions, which eventually could be useful to describe gravity at some level between string theory and general relativity. Nevertheless, in the second part of this Thesis, we will focus on the construction of gauge invariance in this kind of spaces and not over the importance of noncommutative field theories as a rude approach to quantum gravity.

In general terms, a noncommutative space is a topological space where the ordinary coordinates have been substituted by operators satisfying some noncommutative algebra. Here, “coordinates” means the generators of the (noncommutative) algebra of continuous complex functions¹⁰ over the noncommutative space that we are considering. Note that this notion of coordinates as the generators of the algebra of functions over the space is not so different from the one we have in ordinary spaces. For example, in \mathbb{R}^n the coordinates $\{x^1, \dots, x^n\}$ are the generators for the (commutative) algebra of continuous complex functions over \mathbb{R}^n vanishing at infinity.

At the end, the change from ordinary spaces to noncommutative ones reduces to considering noncommutative algebras of functions instead of commutative ones. For practical purposes, this translates in substituting the ordinary commutative product by a noncommutative one. Of course, the explicit way in which the noncommutative product is implemented depends on the noncommutative space that we are considering. In Chapter 5 we

¹⁰If the space is locally compact but no compact, the algebra generated by the coordinates is the one of continuous complex functions vanishing at infinity.

work over the most direct generalization of the commutative space \mathbb{R}^d : the noncommutative space \mathbb{R}_θ^d , defined as the noncommutative space where the coordinate operators satisfy the algebra

$$[\hat{x}^\mu, \hat{x}^\nu] = i\theta^{\mu\nu}, \quad (1.9)$$

$\theta^{\mu\nu}$ being some $d \times d$ real antisymmetric matrix. The noncommutative product which follows from this algebra is the so called Moyal product or star product.

Surprisingly, once a noncommutative geometry has been established, the original construction of field theory can be followed with few changes. In \mathbb{R}_θ^d , the ordinary commutative product is substituted by the Moyal one in the Lagrangian formalism, and the (noncommutative) quantum field theory is constructed from it in the usual way [62, 63, 64]. Basically, the novel features of the NCFTs constructed in this way are nonlocality, because of the existence of Heisenberg inequalities between coordinates, and the breaking of Lorentz invariance, since only the subgroup of the Lorentz group keeping invariant the noncommutative algebra of coordinates is allowed. In addition, the lack of locality leads to a mixing of scales (IR/UV mixing) in the quantum theory [65].

Because of the breakdown of Lorentz invariance, NCFT has been relegated to a second place in the theoretical physics of the last century¹¹. However, the formal development of noncommutative geometry by Alain Connes [67] together with the renewed interest in NCFT as a particular low-energy limit of open-string theory [9] around the end of 20th century revived the interest in noncommutative theories. From a physical point of view, NCFT may be useful to formulate effective theories of gravitation at Planck scale halfway between string theory and classical Einstein gravitation.

Either looking NCFT as an alternative framework to develop effective theories of quantum gravity or as a pure mathematical deformation of the ordinary field theory, it is obvious that introducing gauge symmetries in noncommutative geometries is an interesting task. On the one hand, gauge symmetries are intrinsically local in ordinary field theory and it is not clear the way in which local transformations can be constructed in noncommutative geometries where locality is lost. On the other, gauge symmetries are the cornerstone of the standard model, and thus they must be kept in mind in any effort to go beyond the standard model.

Basically there are two ways in which gauge transformations can be defined in field theories over \mathbb{R}_θ^d : star-gauge transformations [10, 11, 12] or

¹¹As early as 1947, Snyder considered the possibility to construct field theories in spaces where the coordinates do not commute [66].

twist-gauge [13, 14, 68] transformations. The first one solves the implementation of gauge invariance by introducing the star product in the local action of the gauge group over the field algebra. The second one keeps the ordinary product for the action of the gauge group over the fields, but modifies the Leibniz rule to be compatible with the noncommutative structure of the field algebra. At this level, the two ways to build gauge transformations in \mathbb{R}_θ^d are equivalent.

Despite of star- and twist-gauge transformations are conceptually different, both are symmetries of the noncommutative Yang-Mills action¹², and necessarily they coexist [69]. Thus both invariances compete to be the physical symmetry (the one with real physical meaning) of the noncommutative gauge theories. The problem is to decide what of them is the true symmetry, or if the two may have real physical relevance.

Basically there are two reason to think that star-gauge invariance is the only one with relevant physical meaning in noncommutative Yang-Mills theories. First, it has been argued in [70] that Noether currents do not follow from the twist-gauge invariance by means of the standard procedure, but from the star-gauge one. Second, the star-gauge symmetry appears in the low energy Seiberg-Witten limit of string theory [71]. Thus, it seems that the star-gauge symmetry is the true physical symmetry of noncommutative Yang Mills theories, whereas the twist-gauge invariance plays an accidental role, watched over by the star-gauge one.

In Chapter 5 we show it can be constructed an infinite family of twisted invariances interpolating continuously between twist- and star-gauge symmetries [72]. All of these invariances are conceptually equivalent to the original twist-gauge invariance (in the sense that the Leibniz rule is modified in all of them), and all are watched over by the star-gauge symmetry. From this point of view, the twist-gauge invariance is a particular case of an infinite family of accidental symmetries and thus there is no reason to consider it as a real symmetry with physical meaning, reinforcing the idea of the star-gauge symmetry as the true physical symmetry supervising all the twisted invariances. Also, as a particular case of the family of twisted symmetries, it appears a spurious symmetry for the ordinary Yang-Mills theory.

¹²The noncommutative Yang-Mills action functional is constructed from the commutative one by substituting the commutative product by the Moyal one in the ordinary Yang-Mills Lagrangian.

1.5 A note about conventions

In the next three chapters (as well as the related appendices) we shall work with different coordinate systems in several spaces. Thus it is convenient to fix *a priori* some generalities about the index notation that we will use in Chapters 2, 3 and 4. Coordinates in the D -dimensional AdS space will be indexed by lowercase Latin letters $a, b, c \dots$, while coordinates in the conformal boundary of it will be denoted by Greek indices μ, ν, σ, \dots . Moreover, the D -dimensional AdS spacetime (which we will denote as AdS_D) can be viewed as a D -dimensional hyperboloid embedded in a flat background with $D + 1$ dimensions. In general it will be used capital letters $A, B, C \dots$ to refer to the coordinates in this flat space. Respect to the collision scheme, lowercase Latin letters $i, j, k \dots$ will refer to the transverse space to the shock wave propagation without including the Poincaré coordinate z . Summarizing:

$$\begin{aligned}
 A, B, C \dots &\in \{0, 1 \dots D\}, \\
 a, b, c \dots &\in \{0, 1 \dots D - 1\}, \\
 \mu, \nu, \sigma \dots &\in \{0, 1 \dots D - 2\}, \\
 i, j, k \dots &\in \{1, 2 \dots D - 3\}.
 \end{aligned}
 \tag{1.10}$$

Also we will use Greek indices in the general discussions of the Chapter 2 to describe gravitational waves in arbitrary spacetimes as well as in flat spacetime, and in Chapter 5 to construct gauge symmetries in \mathbb{R}_g^d .

To avoid an excessively cumbersome jargon, we shall resort to abbreviations commonly used in scientific literature, as GR for General Relativity or AdS for Anti-de Sitter, as well as “AdS-Sch shock waves” and “AdS-RN shock waves” to refer to the gravitational shock waves obtained boosting the AdS-Schwarzschild and AdS-Reissner-Nordström solutions respectively.

At the end of the text there are included several mathematical appendices in order to complement the physical discussions of the main text. Those readers not familiar with AdS coordinate systems are advised to read Appendices A and B before proceeding to Chapters 2, 3 and 4. Likewise, in Appendix C there are the demonstration of some equations that are widely used along the text.

Finally, all the equations are written in unities where $\hbar = c = 1$, being G_D the Newton constant in D dimensions, and we take the Minkowski metric with signature $\eta_{\mu\nu} = (-, +, +, \dots, +)$.

Chapter 2

Gravitational waves

Gravitational waves are a central topic in General Relativity. Usually the concept refers to solutions to linearized gravity representing a weak gravitational disturbance propagating in some spacetime, i.e. gravitational radiation. Sources of gravitational radiation are supposed to be physical systems where the geometric configuration changes in time as in binary stars or supernovae events¹. In any case, gravitational radiation is an approximate solution to Einstein equations where the amplitude of the gravitational waves are treated as a weak perturbation over a stationary background configuration. For this reason, we shall refer to gravitational radiation as weak gravitational waves.

Together with the weak gravitational waves previously mentioned, there are also exact solutions to Einstein equations which are nonstationary and represent geometric ripples propagating in some background. We shall call exact gravitational waves to these solutions. A particular example of this kind of gravitational waves are shock waves. In contrast to weak gravitational waves, exact gravitational waves describe, for example, the gravitational field associated to a particle or an electromagnetic pulse traveling through the spacetime.

The aim of this Chapter is to introduce the general concept of gravitational waves, paying special attention to gravitational shock waves. In Section 2.1 we briefly discuss the issue of gravitational radiation in general backgrounds, showed here for completeness and as a counterpoint to exact gravitational waves. The Section 2.2 are entirely dedicated to define exact

¹To date no direct measure of gravitational radiation has been yet achieved. The observation of the orbital decay of some binary pulsars is the only evidence of gravitational radiation as predicted by Einstein field equations up to date [73, 74]. On the other hand, recent claims of primordial gravitational wave detection through their imprints on the CMB have turned out to be premature [75, 76].

gravitational waves and gravitational shock waves in flat background. In Section 2.3 it is discussed how this type of waves can be constructed from black hole solutions by means of a suitable ultrarelativistic limit first time introduced by Aichelburg and Sexl [54]. The generalization of exact gravitational waves and, in particular, gravitational shock waves to the AdS space is studied in Section 2.4. Finally, in Section 2.5 the collision of two gravitational shock waves in AdS background is set out.

2.1 Weak gravitational waves

As we have already mentioned, gravitational radiation is the propagation of a weak gravitational disturbance over some stationary solution to the Einstein equations. Here we are interested in obtaining the equation which governs such evolution through spacetime. Classically it has been obtained from a perturbative treatment designed for linearizing the Einstein field equations. Usually this weak gravitational waves are presented on a flat background, but here we will follow a general derivation on some arbitrary stationary background. A more exhaustive study of weak gravitational waves can be found in classical texts such as [77, 78, 79, 80].

Let $g_{\mu,\nu}^{(0)}$ be the metric of some stationary solution to D -dimensional Einstein equations, with a possible nonvanishing cosmological constant Λ and energy-momentum tensor $T_{\mu\nu}^{(0)}$,

$$R_{\mu\nu}^{(0)} - \frac{1}{2}g_{\mu\nu}^{(0)} (R^{(0)} - 2\Lambda) = 8\pi G_D T_{\mu\nu}^{(0)}. \quad (2.1)$$

where the (0) superindex refers to the metric $g^{(0)}$ and G_D is the Newton constant in D dimensions. Now, consider a weak disturbance over $g_{\mu\nu}^{(0)}$ such that the disturbed metric is

$$g_{\mu\nu} = g_{\mu\nu}^{(0)} + h_{\mu\nu}, \quad (2.2)$$

where $h_{\mu\nu}$ is a symmetric 2-covariant tensor such that there exists a coordinate system where $|h_{\mu\nu}| \ll 1$. This condition ensures it is possible to approximate the geometry to first order in $h_{\mu\nu}$. In this way, the contravariant metric $g^{\mu\nu}$ will be given by

$$g^{\mu\nu} = g^{(0)\mu\nu} - h^{\mu\nu} + O(h^2). \quad (2.3)$$

The indices of $h_{\mu\nu}$ are lowered and raised with $g_{\mu\nu}^{(0)}$ to first order in h . Also, it is possible to perform a series expansion of the Ricci curvature to first order in h ,

$$R_{\mu\nu}(g^{(0)} + h) = R_{\mu\nu}^{(0)} + R_{\mu\nu}^{(1)}(h) + O(h^2). \quad (2.4)$$

Therefore, in the approximation linear in h , the metric $g_{\mu\nu}^{(0)}$ acts as a background metric where a tensor field $h_{\mu\nu}$ propagates.

Note that an infinitesimal coordinate change

$$x^\mu \rightarrow x^\mu + \xi^\mu(x) \quad (2.5)$$

will not affect the condition $|h_{\mu\nu}| \ll 1$. Under such coordinate transformation, the spacetime metric changes as $g \rightarrow g + \mathcal{L}_\xi g$, where \mathcal{L}_ξ is the Lie derivative with respect the vector field generating the coordinate transformation. Thus, the transformation of $h_{\mu\nu}$ under (2.5) is given by

$$h_{\mu\nu} \rightarrow h_{\mu\nu} + \nabla_\mu \xi_\nu + \nabla_\nu \xi_\mu + O(h^2), \quad (2.6)$$

where we have lowered the index of ξ^μ with $g_{\mu\nu}^{(0)}$. Therefore the equation (2.6) gives a gauge freedom for $h_{\mu\nu}$. In particular, we can choose the so-called transverse-traceless gauge,

$$g^{(0)\mu\nu} h_{\mu\nu} = 0, \quad \nabla^{(0)\mu} h_{\mu\nu} = 0. \quad (2.7)$$

The computation of (2.4) is rather long and is beyond the purposes of this Section. In the gauge (2.7) it takes the form [78]

$$R_{\mu\nu} = R_{\mu\nu}^{(0)} - \frac{1}{2} \Delta^{(0)} h_{\mu\nu} + O(h^2). \quad (2.8)$$

where $\Delta^{(0)}$ is the Laplace-Beltrami operator for the background metric. Then, substituting in the Einstein equation, we have

$$\Delta^{(0)} h_{\mu\nu} - g_{\mu\nu}^{(0)} h^{\rho\sigma} R_{\rho\sigma}^{(0)} + h_{\mu\nu} R^{(0)} - 2\Lambda h_{\mu\nu} = -16\pi G_D t_{\alpha\beta}, \quad (2.9)$$

where we have used (2.1) and $t_{\mu\nu}$ is a possible perturbation over the energy-momentum tensor $T_{\mu\nu}^{(0)}$ which sources the weak perturbation $h_{\mu\nu}$ over the background metric $g_{\mu\nu}^{(0)}$ (for example, $t_{\mu\nu}$ could refers to one oscillating mode of a variable star). This is the evolution equation, or wave equation, which we are looking for.

In the special case where the background metric is flat, (2.9) reduces to

$$\Delta^{(0)} h_{\mu\nu} = -16\pi G_D t_{\alpha\beta}. \quad (2.10)$$

This is the equation for the graviton field in linearized gravity. Consider the more special case in which we have a perturbation of the flat vacuum sourced by $t_{uu} = \delta(u)\rho(\vec{x})$, such that the spacetime metric is

$$(\eta_{\mu\nu} + h_{\mu\nu})dx^\mu dx^\nu = -dudv + d\vec{x}^2 + \delta(u)\Phi(\vec{x}) du^2, \quad (2.11)$$

where u and v are lightlike coordinates. Such metric represent an infinitely thin gravitational wave with support at $u = 0$ propagating at the speed of light. The tensor $h_{\mu\nu}$ has only one component $h_{uu} = \Phi(\vec{x})\delta(u)$, and obviously satisfies the gauge (2.7). Then the wave equation (2.10) is reduced to

$$\Delta^{(0)} \Phi(\vec{x}) = -16\pi G_D \rho(\vec{x}). \quad (2.12)$$

Note that, because the distributional nature of $h_{\mu\nu}$, (2.12) is an exact solution to the equations of General Relativity, since quadratic terms in the delta function are identically zero. Thus (2.11) is an exact gravitational wave. In fact, as we will see in the next Section, the gravitational field of a massless particle in flat background is given by a line element of the form (2.11).

2.2 Exact gravitational waves in flat background

The weak gravitational waves we have described in the previous section are not exact gravitational solutions, since they only satisfies the Einstein equation to first order in h . However, as we have already mentioned, we are interested in exact solutions representing a geometrical disturbances in the spacetime that propagate at the speed of light.

2.2.1 Flat pp-waves

A very important type of exact gravitational waves in flat background are the plane-fronted parallel waves or pp-waves. A pp-wave is defined as a spacetime which admits a null vector field k^μ satisfying [81, 82]

$$\nabla_\nu k^\mu = 0, \quad (2.13)$$

that is, it is covariantly constant. In this a way, the integral curves of k^μ can be interpreted as (parallels) rays along which the wave propagates, justifying the name of pp-waves.

The previous definition has the advantage it does not depend on coordinates. However, it is too abstract. Alternatively, a pp-wave spacetime can be defined as the one whose line element takes the form

$$ds^2 = -dudv + d\vec{x}_\perp^2 + H(u, \vec{x}_\perp)du^2, \quad (2.14)$$

in some suitable coordinate system $\{u, v, \vec{x}_\perp\}$, where $\{u, v\}$ are lightlike background coordinates and $(x^i) \equiv \vec{x}_\perp$ span the transverse space to the wave

propagation. Nowadays (2.14) is known as the Brinkmann form of a pp-wave metric². It is interesting to show that the coordinate-dependent definition (2.14) is equivalent to the covariant definition (2.13): the Christoffel symbols for (2.14) are

$$\begin{aligned}\Gamma_{uu}^v &= -\partial_u H, & \Gamma_{ux^i}^v &= -\partial_i H, \\ \Gamma_{uu}^{x^i} &= -\frac{1}{2}\partial_i H,\end{aligned}\tag{2.15}$$

and thus $k_\mu = \partial_\mu u$ is covariantly constant: (2.14) represent the lightlike propagation of a disturbance with amplitude given by $H(u, \vec{x}_\perp)$ and parallel rays of propagation along v direction.

Note that neither the definition (2.13) nor the definition (2.14) make any mention of any field equation. They are entirely independent of Physics. In this sense, a pp-wave is an entirely mathematical notion. For obtaining a wave equation we have to introduce (2.14) in the Einstein field equations. The only no-vanishing component of the Einstein tensor of (2.14) is

$$G_{uu} = -\frac{1}{2} \Delta_\perp H,\tag{2.16}$$

where $\Delta_\perp \equiv \sum_i \partial_i^2$ is the Laplacian in transverse space. Thus the Einstein field equation is reduced to the Poisson equation over the profile wave function $H(u, \vec{x})$:

$$\Delta_\perp H = -16\pi G_D T_{uu}\tag{2.17}$$

The equation (2.17) is a partial differential equation which involves only the transverse coordinates \vec{x}_\perp . Thus any wave packet extension in the null coordinate u can be chosen. In fact, given a family of solutions $H_0(\xi, \vec{x}_\perp)$ to (2.17) and some integrable function $h(\xi, u)$ we can construct a pp-wave as

$$H(u, \vec{x}_\perp) = \int_{-\infty}^{\infty} d\xi h(\xi, u) H_0(\xi, \vec{x}_\perp).\tag{2.18}$$

Physically this means that the lineal superposition of two pp-waves propagating in the same direction is also a pp-wave. Obviously, in the case where the pp-waves propagate in secant trajectories, the result is not true since, as we will see in Section 2.5, the wavefronts will interact in an highly nonlinear way at the collision point [44].

Asymptotically flat solutions to (2.17) are of particular interest. In general, a solution to (2.17) does not have to be asymptotically flat, even in

²Brinkmann was the first in study (2.14) as an exact solution to Einstein equations in 1925.

absence of sources. For example, consider the vacuum solution in $D = 4$ dimensions

$$ds^2 = -dudv + dx^2 + dy^2 + \theta(u)(x^2 + y^2)du^2. \quad (2.19)$$

The uu component has an infinite extension without dumping its strength, and so (2.19) is nonasymptotically flat. In general, any asymptotically flat pp-wave admits a multipolar expansion,

$$H(\vec{x}_\perp) = \sum_n \sum_\Omega U_n(r) Y_\Omega(\theta^i), \quad \lim_{r \rightarrow \infty} U_n(r) = 0 \quad (2.20)$$

where r and θ^i are the usual radial and angular coordinates for the transverse space to the propagation of the pp-wave and $Y_\omega(\theta^i)$ are the spherical harmonics over S^{D-3} . In the special case of an asymptotically flat vacuum solution, this multipolar expansion must satisfy (2.17) for $T_{uu} = 0$. Then, since $U_n(r)$ and $Y_\Omega(\theta^i)$ are linearly independent functions, equation (2.17) splits into radial and angular equations for each component,

$$\begin{aligned} \frac{d}{dr} \left(r^{D-3} \frac{d}{dr} U_n(r) \right) &= n(n + D - 4) r^{D-5} U_n(r), \\ \Delta_{S^{D-3}} Y_\Omega(\theta^i) &= -n(n + D - 4) Y_\Omega(\theta^i). \end{aligned} \quad (2.21)$$

where $n = 0, 1, 2, \dots$. Solution to the radial equation is,

$$U_n(r) = Ar^n + Br^{-(D-5)-n}. \quad (2.22)$$

being A and B integration constants. Since asymptotic flatness implies $U_n(r) \rightarrow 0$ for large enough r , it must be $A = 0$. Thus $B \neq 0$ and there is a singularity at $r = 0$ sourcing the pp-wave. In other words, any asymptotically flat pp-wave must be sourced.

Spacetimes containing pp-waves can be classified according to their symmetries. The most symmetric (no trivial) pp-waves are the plane waves. They are defined as any pp-wave spacetime which admits $D+1$ Killing vector fields, including the covariantly constant field k^μ , or alternatively as the pp-wave spacetime whose curvature tensor components are constant over each wave surface. In the coordinates of (2.14), a pp-wave is a plane wave if and only if $H(u, \vec{x}_\perp)$ depends quadratically in x^i ,

$$ds^2 = -dudv + h_{ij}(u)x^i x^j du^2 + d\vec{x}_\perp^2 \quad (2.23)$$

From this follows that a plane pp-wave cannot be asymptotically flat.

If a pp-wave spacetime has only two Killing vectors, it is said to be an axisymmetric pp-wave. Because of the reduced symmetry with respect to

plane waves, axisymmetric waves admit asymptotic flatness and point-like sources. In Brinkmann form, the metric is

$$ds^2 = -dudv + F(u, r)du^2 + d\vec{x}_\perp^2, \quad (2.24)$$

where r is some radial coordinate in the transverse space to wave propagation. The two Killing fields are the covariantly constant $\vec{k} = \partial_v$, whose integral curves give the propagation rays of the pp-wave, and the generator of rotations around the propagation axis.

2.2.2 Shock waves in flat background

A very special case of axisymmetric pp-waves are the gravitational shock waves in flat background. They are axisymmetric waves for which the function $F(u, r)$ in equation (2.24) depends on u through a delta function,

$$ds^2 = -dudv + \delta(u)\Phi(r)du^2 + d\vec{x}_\perp^2, \quad (2.25)$$

where $r = |\vec{x}_\perp|$. Note that the wave has a zero measure support, $u = 0$, forming an infinitely thin wavefront. Also, before and after the wavefront passes the space time is flat. The function $\Phi(r)$ is called the shock wave profile. Introducing (2.25) in the wave equation for pp-waves (2.17) ($H(u, \vec{x}_\perp) = \delta(u)\Phi(r)$), we find that shock waves are generated by energy-momentum tensors of the form

$$T_{uu} = \rho(r)\delta(u), \quad (2.26)$$

such that the shock wave profile satisfies the Poisson equation

$$\Delta_\perp \Phi(r) = -16\pi G_D \rho(r), \quad (2.27)$$

$\rho(r)$ being some isotropic energy distribution in the transverse space to the wave propagation. Note that this is just the wave equation reproduced in (2.12).

Because of the distributional nature of (2.25), the null geodesics across the wavefront of a gravitational shock wave are discontinuous [83]. To see such jump of the null geodesics rigorously is hard. Here we use a simplified argument which nevertheless gives the right answer. Let us consider a null geodesic with constant lightlike coordinate v_0 intersecting the wavefront located at $u = 0$ with constant values of the transverse coordinates, \vec{x}_\perp_0 . After the geodesics crosses the wavefront it enters again in flat spacetime with constant v'_0 . The question is whether v_0 and v'_0 are or not the same. To see it let us consider the line element across the geodesic just in the intersection with the wavefront,

$$ds^2 = du [-dv + \Phi(r_0)\delta(u)du], \quad (2.28)$$

For a null geodesic $ds^2 = 0$. Thus

$$dv = \Phi(r_0)\delta(u)du. \quad (2.29)$$

Integrating now u between $-\epsilon$ and $+\epsilon$ gives the jump on the v coordinate,

$$\Delta v \equiv v'_0 - v_0 = \Phi(r_0) \int_{-\epsilon}^{\epsilon} du \delta(u) = \Phi(r_0). \quad (2.30)$$

In the case of a generic null geodesic for which \vec{x}_\perp is not constant we find the same result but with r_0 substituted by the value of r when the geodesic crosses the wavefront at $u = 0$.

The discontinuity of the null geodesic through the wavefront may add difficulties to the study of the causal structure of spacetimes containing gravitational shock waves. Thus it would be adequate finding a way in which to avoid this obstacle. As we have seen, the jump in the null geodesics comes from the presence of distributional terms in the metric. Thus a change of coordinates which results in the removal of these distributional terms is the way to proceed. In this way, we define new coordinates, represented by capital letters, as

$$\begin{aligned} u &= U, \\ v &= V + \Phi(\vec{X}_\perp)\theta(U) + \frac{1}{4}U\theta(U) \left[\vec{\nabla}\Phi(\vec{X}_\perp) \right]^2, \\ \vec{x}_\perp &= \vec{X}_\perp + \frac{1}{2}U\theta(U)\vec{\nabla}\Phi(\vec{X}_\perp). \end{aligned} \quad (2.31)$$

Note that for $U < 0$, the new and older coordinates coincide. To carry out the change of coordinates over the metric (2.25) we compute

$$\begin{aligned} du &= dU, \\ dv &= dV + \left[\frac{\delta(U)}{4}\Phi(\vec{\nabla}\Phi)^2 \right] dU + \theta(U) \left[\partial_i\Phi + \frac{U}{2}\partial_j\Phi\partial_i\partial_j\Phi \right] dX^i, \\ dx^i &= dX^i + \frac{\theta(U)}{2}\partial^i\Phi dU + \frac{U}{2}\theta(U)\partial\partial^i\Phi dX^j. \end{aligned} \quad (2.32)$$

On the other hand, because of the properties of the Dirac delta function,

$$\Phi(\vec{x}_\perp) = \Phi \left(\vec{X}_\perp + \frac{1}{2}U\theta(U)\vec{\nabla}\Phi \right) \delta(U) = \Phi(\vec{X}_\perp)\delta(U). \quad (2.33)$$

Then from this equality and (2.32), after a bit of algebra, we find the shock wave metric to be in the new coordinates

$$ds^2 = -dUdV + H_{ik}H_{jk}^d X^i dX^j, \quad (2.34)$$

where summation over repeated indexes are understood, being $H_{ij}(U, \vec{x}_\perp)$ given by,

$$H_{ij}(U, \vec{x}_\perp) = \delta_{ij} + \frac{1}{2}U\theta(U)\partial_i\partial_j\Phi(\vec{x}_\perp). \quad (2.35)$$

The line element (2.34), without distributional terms, but continuous null geodesics crossing the wavefront, is the so called Rosen form of a gravitational shock wave.

2.3 Aichelburg-Sexl boost

In the previous Section we have introduced gravitational shock waves as little more than a mathematical concept, since we have not given any information about what is their physical origin. The delta function appearing in (2.26) reveals that (2.25) is the line element created by a transverse energy density $\rho(r)$ moving at the speed of light in flat background. In [54], Aichelburg and Sexl showed that point-like sourced (that means $\rho(r) \sim \delta(r)$ in (2.26)) shock waves can be obtained from black hole solutions and, in particular, from the Schwarzschild solution, by means of a suitable ultrarelativistic limit. Such mechanism to generate gravitational shock waves will be adapted to an AdS background in the next Chapter. As a warming up exercise, here we are going to briefly reproduce the original Aichelburg-Sexl boost in four-dimensional flat spacetime.

The asymptotically flat Schwarzschild solution is given by,

$$ds^2 = -f(r)dt^2 + f^{-1}(r)dr^2 + r^2d\Omega_2^2, \quad (2.36)$$

where,

$$f(r) = 1 - \frac{2G_4m}{r}, \quad (2.37)$$

m being the mass of the solution. A boost over (2.36) will result in some asymptotically-flat spacetime metric describing a particle with mass m moving at certain velocity. In the infinite boost limit, because of Lorentz contraction, its gravitational field will appear squeezed in the orthogonal plane to movement, forming a gravitational shock wave. However, the limit must be done taking care of a correct scaling of the mass m and the boost velocity to avoid an infinite relativistic energy γm .

Before to perform any boost, we have to change to some isotropic coordinates in which all the spatial components of the line element are treated equally to ensure that no direction is preferred. In this way, we define the isotropic coordinate \bar{r} as [84],

$$r \equiv \bar{r} \left(1 + \frac{G_4m}{\bar{r}} + \frac{G_4^2m^2}{4\bar{r}^2} \right). \quad (2.38)$$

Then,

$$dr^2 = \left(1 - \frac{G_4^2 m^2}{4\bar{r}^2}\right)^2 d\bar{r}^2, \quad (2.39)$$

and the line-element (2.36) after introducing \bar{r} is

$$ds^2 = -f(r(\bar{r})) dt^2 + g(\bar{r}) [d\bar{r}^2 + \bar{r}^2 d\Omega_2^2], \quad (2.40)$$

where

$$g(\bar{r}) = \left(1 + \frac{G_4 m}{\bar{r}} + \frac{G_4^2 m^2}{4\bar{r}^2}\right)^2.$$

Written in this way, (2.40) admits asymptotically Cartesian coordinates $\{x, y, z\}$, defined as

$$\bar{r}^2 = x^2 + y^2 + z^2. \quad (2.41)$$

Once Cartesian coordinates has been defined in an isotropic way, boosts can be performed in any direction since all spatial coordinates are equivalent. For example, boosting in the x direction,

$$\begin{aligned} t &= \gamma(t' + \beta x'), & y &= y', \\ x &= \gamma(\beta t' + x'), & z &= z', \end{aligned} \quad (2.42)$$

the components of (2.40) transform as,

$$\begin{aligned} g_{t't'} &= \gamma^2 [-f(r(\bar{r})) + \beta^2 g(\bar{r})], \\ g_{x'x'} &= \gamma^2 [-\beta f(r(\bar{r})) + g(\bar{r})], \\ g_{t'x'} &= \gamma^2 \beta [-f(r(\bar{r})) + g(\bar{r})], \\ g_{y'y'} &= g(\bar{r}), \\ g_{z'z'} &= g(\bar{r}), \end{aligned} \quad (2.43)$$

\bar{r} being now

$$\bar{r}^2 = \gamma^2 (x' + \beta t')^2 + y'^2 + z'^2. \quad (2.44)$$

Note that the relation between r and \bar{r} gives awkward expressions in (2.43) through $f(r(\bar{r}))$. However, we eventually will perform the $\gamma \rightarrow \infty$ limit, and

$$\lim_{\gamma \rightarrow \infty} r(\bar{r}) = \lim_{\gamma \rightarrow \infty} \bar{r} \left(1 + \frac{G_4 m}{\bar{r}} + \frac{G_4^2 m^2}{4\bar{r}^2}\right) = \lim_{\gamma \rightarrow \infty} \bar{r},$$

so we can substitute $r(\bar{r})$ by \bar{r} in (2.43), providing simplicity *ab initio*. Also, to perform the limit it is advisable to rewrite the components $g_{t't'}$, $g_{x'x'}$ and

$g_{t'x'}$ in terms of light-cone coordinates $u' = t' + x'$ and $v' = t' - x'$:

$$\begin{aligned} g_{u'u'} &= \frac{\gamma^2(1+\beta)^2}{4} [g(\bar{r}) - f(\bar{r})] \\ g_{v'v'} &= \frac{\gamma^2(1-\beta)^2}{4} [g(\bar{r}) - f(\bar{r})] \\ g_{u'v'} &= -\frac{1}{4} [g(\bar{r}) + f(\bar{r})]. \end{aligned} \quad (2.45)$$

The infinite boost for the component $g_{u'v'}$ in (2.45) is easy to compute:

$$\begin{aligned} \lim_{\gamma \rightarrow \infty} g_{u'v'} &= -\frac{1}{4} \lim_{\gamma \rightarrow \infty} \left[2 + \frac{3G_4^2 m^2}{2\bar{r}} + \frac{G_4^3 m^3}{2\bar{r}^3} + \frac{G_4^4 m^4}{16\bar{r}^2} \right] \\ &= -\frac{1}{2}. \end{aligned} \quad (2.46)$$

In a similar way,

$$\lim_{\gamma \rightarrow \infty} g_{y'y'} = 1, \quad \lim_{\gamma \rightarrow \infty} g_{z'z'} = 1.$$

The limit for the components $g_{u'u'}$ and $g_{v'v'}$ is trickier. Naively, since $g_{u'u'}$ and $g_{v'v'}$ both are functions of $\gamma^2(x' + \beta t')^2$ through \bar{r} in (2.44), we can use the relation (A detailed proof can be found in Section C.1 of Appendix C)

$$\lim_{\gamma \rightarrow \infty} \gamma \chi(\gamma^2(x' + \beta t')^2) = \delta(u') \int_{-\infty}^{\infty} dw \chi(w^2) \quad (2.47)$$

to compute the infinite boost limit over the components $g_{u'u'}$ and $g_{v'v'}$. However there are an additional γ factor in (2.45) which diverges. In order to keep finite the limit, we define $\mu \equiv \gamma m$ and take the limit $\gamma \rightarrow \infty$ together with $m \rightarrow 0$ such that μ remains fixed. In other words, we take the limit $\epsilon \rightarrow 0$ with the scaling

$$\gamma \sim \epsilon^{-1}, \quad m \sim \epsilon, \quad (2.48)$$

such that the first order in m in (2.45) gives a finite result, while the $O(m^2)$ terms vanish. Thus, expanding (2.45) as:

$$\begin{aligned} g_{u'u'} &= \gamma(1+\beta)^2 \frac{G_4 \mu}{\bar{r}} + O\left(\frac{\mu^2}{\gamma}\right), \\ g_{v'v'} &= \gamma(1-\beta)^2 \frac{G_4 \mu}{\bar{r}} + O\left(\frac{\mu^2}{\gamma}\right), \end{aligned} \quad (2.49)$$

the limit for the $g_{v'v'}$ component is

$$\lim_{\gamma \rightarrow \infty} g_{v'v'} = \lim_{\gamma \rightarrow \infty} \frac{(1-\beta)^2}{(1+\beta)^2} g_{u'u'} = 0, \quad (2.50)$$

since the factor $(1 - \beta)$ vanishes when $\gamma \rightarrow \infty$, while the limit for the component $g_{u'u'}$ gives

$$\lim_{\gamma \rightarrow \infty} g_{u'u'} = 4G_4\mu\delta(u') \int_{-\infty}^{\infty} \frac{dw}{(w^2 + \rho^2)^{1/2}}, \quad (2.51)$$

where we have defined $\rho^2 = y'^2 + z'^2$.

It remains to compute the explicit form of integral in (2.51). However, $(w^2 + \rho^2)^{-1/2}$ is not integrable in $(-\infty, \infty)$, and thus the integral cannot be formally evaluated. Indeed the relation (2.47) is not even applicable. So we need to compute the limit

$$\lim_{\gamma \rightarrow \infty} \gamma(1 + \beta)^2 \frac{G_4\mu}{\bar{r}} = \lim_{\gamma \rightarrow \infty} \frac{\gamma(1 + \beta)^2 G_4\mu}{[\gamma^2(x' + \beta t')^2 + \rho^2]^{1/2}} \quad (2.52)$$

without the help of the relation (2.47). This problem is solved calculating the limit for a primitive of (2.52) and then differentiating the result [84]. A previous ‘‘renormalization step’’ is necessary, adding and subtracting

$$\gamma(1 + \beta)^2 G_4\mu [\gamma^2(x' + \beta t')^2 + 1]^{-1/2} \quad (2.53)$$

to (2.52). In this way, we compute the limit

$$\begin{aligned} \lim_{\gamma \rightarrow \infty} & \left[\frac{\gamma(1+\beta)^2 G_4\mu}{[\gamma^2(x'+\beta t')^2 + \rho^2]^{1/2}} - \frac{\gamma(1+\beta)^2 G_4\mu}{[\gamma^2(x'+\beta t')^2 + 1]^{1/2}} + \frac{\gamma(1+\beta)^2 G_4\mu}{[\gamma^2(x'+\beta t')^2 + 1]^{1/2}} \right] \\ & = 4G_4\mu \lim_{\gamma \rightarrow \infty} \left[\frac{\gamma}{[\gamma^2(x'+\beta t')^2 + \rho^2]^{1/2}} - \frac{\gamma}{[\gamma^2(x'+\beta t')^2 + 1]^{1/2}} \right] + \frac{4G_4\mu}{|u'|} \end{aligned} \quad (2.54)$$

instead of (2.52). Now, following the previous recipe, we integrate the expression within the brackets in the last line. It yields

$$\begin{aligned} & \int_{-\infty}^{x'} \left[\frac{\gamma}{[\gamma^2(x + \beta t')^2 + \rho^2]^{1/2}} - \frac{\gamma}{[\gamma^2(x + \beta t')^2 + 1]^{1/2}} \right] dx \\ & = \log \left[\frac{\gamma^2(x' + \beta t') + \gamma\sqrt{\gamma^2(x' + \beta t')^2 + \rho^2}}{\gamma^2(x' + \beta t') + \gamma\sqrt{\gamma^2(x' + \beta t')^2 + 1}} \right] \equiv F_\gamma. \end{aligned} \quad (2.55)$$

The $\gamma \rightarrow \infty$ limit for it gives

$$\lim_{\gamma \rightarrow \infty} F_\gamma = \begin{cases} \lim_{\gamma \rightarrow \infty} \log \left[\frac{\gamma^2(x' + \beta t') - \gamma^2(x' + \beta t') - \rho^2/(x' + \beta t')}{\gamma^2(x' + \beta t') - \gamma^2(x' + \beta t') - 1/(x' + \beta t')} \right] \\ \quad = \log \rho^2 & \text{for } x' + t' < 0 \\ \\ \lim_{\gamma \rightarrow \infty} \log \left[\frac{2\gamma^2(x' + \beta t') + \rho^2/(x' + \beta t')}{2\gamma^2(x' + \beta t') + 1/(x' + \beta t')} \right] \\ \quad = \log 1 = 0 & \text{for } x' + t' > 0. \end{cases}$$

Or, in a more compact notation,

$$\lim_{\gamma \rightarrow \infty} F_\gamma = \theta(-u') \log \rho^2. \quad (2.56)$$

Finally, taking the derivative and plugging the result together with (2.52) and (2.54), we obtain

$$\lim_{\gamma \rightarrow \infty} \gamma(1 + \beta)^2 \frac{G_4 \mu}{\bar{r}} = -4G_4 \mu \delta(u') \log \rho^2 + 4 \frac{G_4 \mu}{|u'|}. \quad (2.57)$$

Note that the second term is not integrable, which conflicts with the distributional nature of the first term. Fortunately, the second term can be eliminated from $\lim_{\gamma \rightarrow \infty} g_{u'u'}$ by the transformation

$$du' \rightarrow du' dv' \rightarrow dv' - \frac{4\mu}{|u'|} du', \quad (2.58)$$

solving the inconvenience.

At the end of the day, doing the infinite boost limit with the scaling (2.48) we have obtained the line element

$$ds^2 = -dudv + dy^2 + dz^2 - 4G_4 \mu \delta(u) \log(\rho^2) du^2, \quad (2.59)$$

where we have reverted to unprimed notation for clarity. This is the metric for a gravitational shock wave with wave profile

$$\Phi(\rho) = -4G_4 \mu \log(\rho^2), \quad (2.60)$$

as has been defined in (2.25). We have obtained it as the metric describing a massless particle of energy μ moving in 4-dimensional flat background. The same procedure can be done starting from other flat black hole solution, obtaining the shock wave metric describing massless particles with other parameters besides the relativistic energy μ [84, 85].

2.4 Exact gravitational waves in the AdS space

So far we have studied exact gravitational waves in flat background. Here we generalize them to AdS background and give definitions for AdS pp-waves and, in particular, AdS shock waves. Our interest in this task resides in the holographic connection between AdS spacetime and lower-dimensional conformal field theories.

Before discussing the generalization of pp-waves and, in particular, gravitational shock waves to an AdS background, we have to introduce some coordinate systems in the AdS spacetime. For the reader not familiarized with the AdS space, a more detailed exposition can be found in Appendix A.

2.4.1 Basics on coordinates in the AdS space

The most distinctive feature of the D -dimensional AdS spacetime is that it possesses a timelike conformal boundary, which can be identified with the Minkowski space in $D - 1$ dimensions. This fact turns out to be of great importance to formulate the AdS/CFT correspondence. The timelike nature of the conformal boundary is explicit in the so called Poincaré coordinates $\{z, x^\mu\}$, in which the line element of AdS_D is

$$ds^2 = \frac{L^2}{z^2} (dz^2 + \eta_{\mu\nu} dx^\mu dx^\nu), \quad \mu, \nu = 0, \dots, D - 2. \quad (2.61)$$

The set $\{x^\mu\}$ can be taken as a (flat) coordinate map covering the whole conformal boundary of the AdS spacetime, while z measures the depth towards the interior of the AdS space, such that the conformal boundary is located at $z = 0$. Thus we shall refer to $\{x^\mu\}$ as the boundary coordinates and to z as the depth (or holographic) coordinate. The restriction $z > 0$ defines the Poincaré patch, where gravitational shock waves shall be considered. Note that, in this coordinate system, the AdS space can be obtained from a conformal transformation of the Minkowski space with conformal factor $\Omega^2 = L^2/z^2$, with L fixing the “size” of the AdS space. Moreover, in Poincaré coordinates the line element of the AdS spacetime is explicitly invariant under coordinate rescaling. That is, defining new coordinates

$$z' = kz, \quad x'^\mu = kx^\mu, \quad k \in \mathbb{R}^+ \quad (2.62)$$

the metric (2.61) remains unchanged.

A dimensionless coordinate that will be extremely useful for our purposes is the chordal one, q . From Poincaré coordinates, it is defined as

$$q = \frac{1}{4z_0 z} [(z - z_0)^2 + \eta_{\mu\nu} x^\mu x^\nu], \quad (2.63)$$

where z_0 is an arbitrary positive real number. The usefulness of this coordinate is that it is invariant under the whole Lorentz group $SO(1, D - 2)$ acting on the boundary coordinates $\{x^\mu\}$. Taking angular coordinates to parametrize the spatial sections of the conformal boundary, the metric of AdS_D in terms of the chordal coordinate is

$$ds^2 = -(2q + 1)^2 dt^2 + \frac{L^2}{q(q + 1)} dq^2 + 4L^2 q(q + 1) d\Omega_{D-2}^2. \quad (2.64)$$

The “origin” of the coordinate q is located at $z = z_0 > 0$, $x^\mu = 0$. By means of the scale invariance in Poincaré coordinates (2.62) z_0 can be changed to

any value, and thus it is an arbitrary election. The freedom in choosing z_0 is just the freedom in choosing a depth inside AdS_D to fix the origin of the q coordinate.

The D -dimensional AdS space can also be globally defined from the embedding of the D -dimensional hyperboloid

$$Z_0^2 + Z_D^2 - \sum_{i=1}^{D-1} Z_i^2 = L^2 \quad (2.65)$$

in flat space with line element $ds^2 = -dZ_0^2 - dZ_D^2 + \sum_{i=1}^{D-1} dZ_i^2$. Defining,

$$\begin{aligned} Z^\mu &= \frac{L}{z} x^\mu, \\ Z^{D-1} &= \frac{z}{2} \left[-1 + \frac{L^2 - \eta_{\mu\nu} x^\mu x^\nu}{z^2} \right], \\ Z^D &= \frac{z}{2} \left[1 + \frac{L^2 + \eta_{\mu\nu} x^\mu x^\nu}{z^2} \right], \end{aligned} \quad (2.66)$$

we recover the AdS_D metric in Poincaré coordinates. Although $\{Z^0, \dots, Z^D\}$ are not true coordinates in AdS_D because of the constraint (2.65), we can use them to parametrize tensors in AdS_D . This will be specially useful in Chapter 3. One advantage of viewing AdS_D as a hyperboloid embedded in flat spacetime is that $SO(2, D-1)$ is directly identified as the isometry group of AdS_D , which is not obvious from (2.61) or (2.64).

Eventually we are going to study collisions between gravitational shock waves inside the AdS space, the interaction point being located at $u = t + x^{D-2} = 0$ and $v = t - x^{D-2} = 0$. Therefore the sections $u = v = cte$ of AdS_D become relevant for our work. With the induced metric, these sections coincide with the hyperbolic space in $D-2$ dimensions, \mathbb{H}_{D-2} . Since the components g_{uu} and g_{vv} of the AdS metric are zero, \mathbb{H}_{D-2} is also the transverse space to the propagation of gravitational shock waves in AdS_D . Similar to the AdS space, the hyperbolic space \mathbb{H}_{D-2} can be obtained as the embedding of the hyperboloid

$$-\eta_{AB} Y^A Y^B = L^2, \quad A, B \in \{0, \dots, D-2\} \quad (2.67)$$

in $(D-1)$ -dimensional Minkowski space $ds^2 = \eta_{AB} dY^A dY^B$, such that the

(induced) Poincaré coordinates in \mathbb{H}_{D-2} are related to Y^A as

$$\begin{aligned} Y^0 &= \frac{z}{2} \left[1 + \frac{L^2 + \vec{x}_T^2}{z^2} \right], \\ Y^i &= \frac{L}{z} x^i, \quad i = 1, \dots, D-3, \\ Y^{D-2} &= \frac{z}{2} \left[-1 + \frac{L^2 - \vec{x}_T^2}{z^2} \right], \end{aligned} \quad (2.68)$$

where $\vec{x}_T = (x^1, \dots, x^{D-3})$. Finally, the (induced) chordal coordinate q in \mathbb{H}_{D-2} is given by

$$q = \frac{1}{4zz_0} [(z - z_0)^2 + \vec{x}_T^2], \quad (2.69)$$

being invariant under the group of rotations³ $SO(D-3)$ acting over \vec{x}_T .

2.4.2 Conformal pp-waves

Let us begin with the generalization of pp-waves to the D -dimensional AdS spacetime. Since the metric (2.61) is conformally flat with a conformal factor L^2/z^2 , we generalize the concept of pp-waves in flat background to AdS background in the most intuitive way: such spacetimes whose Brinkmann form of the metric in Poincaré coordinates is given by

$$ds^2 = \frac{L^2}{z^2} [-dudv + dz^2 + d\vec{x}_T + H(u, z, \vec{x}_T)du^2]. \quad (2.70)$$

That is, we generalize the pp-wave concept to an AdS background by just a conformal transformation of (2.14) with a conformal factor L^2/z^2 .

The metric (2.70) represent an exact gravitational wave propagating in the D -dimensional AdS spacetime along the coordinate x^{D-2} , $u = t + x^{D-2}$ and $v = t - x^{D-2}$ being the light-cone coordinates. The transverse space to the propagation of the wave is now spanned by coordinates $\{z, (x^i) \equiv \vec{x}_T\}$. Note that (2.70) is not a pp-wave spacetime as defined in (2.13) since there is not a covariantly constant vector field. In particular the Christoffel symbols for (2.70) are

$$\begin{aligned} \Gamma_{\mu z}^{\mu} &= -\frac{1}{z}, & \Gamma_{u\mu}^v &= -\partial_{\mu}H, & \Gamma_{uz}^v &= -\partial_zH \\ \Gamma_{uu}^{\mu} &= \frac{z^2}{2}\partial_{\mu}\frac{H}{z^2}, & \Gamma_{uu}^z &= \frac{z^2}{2}\partial_z\frac{H}{z^2} \end{aligned} \quad (2.71)$$

³Note that $SO(D-3)$ is just a subgroup of the isometry group $SO(1, D-2)$ of \mathbb{H}_{D-2} , which is explicit in (2.67).

where index a runs here over (z, \vec{x}_T) . Thus $k_\mu = \partial_\mu u$ is not covariantly conserved:

$$(\nabla_u k)_z = -\Gamma_{uz}^u = \frac{1}{z} \neq 0 \quad (2.72)$$

We will refer to any spacetime with line element (2.70) as a conformal pp-wave spacetime.

As in the case of pp-waves in flat spacetime, a wave equation for the function $H(u, z, \vec{x}_T)$ can be obtained introducing (2.70) in the Einstein equation. Only the uu component of the right-hand side of Einstein equation gives a non-vanishing result,

$$R_{uu} - \frac{1}{2}Rg_{uu} + \Lambda g_{uu} = -\frac{L}{2z} \left[\Delta_{\mathbb{H}_{D-2}} - \frac{D-2}{L^2} \right] \bar{H}(u, z, \vec{x}_T), \quad (2.73)$$

where the cosmological constant Λ is related to the AdS $_D$ scale L as

$$\Lambda = -\frac{(D-1)(D-2)}{2L^2}, \quad (2.74)$$

$\Delta_{\mathbb{H}_{D-2}}$ is the Beltrami-Laplace operator in the hyperbolic space \mathbb{H}_{D-2} , and $\bar{H} = \frac{L}{z}H$. Thus the Einstein equation reduces to

$$\left[\Delta_{\mathbb{H}_{D-2}} - \frac{D-2}{L^2} \right] \bar{H}(u, z, \vec{x}_T) = -16\pi G_D \frac{z}{L} T_{uu}. \quad (2.75)$$

where $T_{uu} = \rho(u, z, \vec{x}_T)$ is some energy density which is assumed to be the source of the wave. This is the analog to (2.17). Note that here \mathbb{H}_{D-2} appears as the transverse space to the propagation of the wave.

2.4.3 AdS gravitational shock waves

In a similar way to the extrapolation of flat pp-waves to AdS background, flat gravitational shock waves can be generalized to asymptotically AdS shock waves: naively AdS gravitational shock waves are defined from a conformal transformation over (2.25),

$$ds^2 = \frac{L^2}{z^2} [-dudv + dz^2 + d\vec{x}_T + \phi(z, \vec{x}_T)\delta(u)du^2]. \quad (2.76)$$

In flat background gravitational shock waves are defined as axisymmetric waves. In that follows we will demand axial symmetry for shock waves in AdS background too. This implies that the function $\phi(z, \vec{x}_T)$ must factorize as

$$\phi(z, \vec{x}_T) = \frac{z}{L}\Phi(q), \quad (2.77)$$

where q is the chordal coordinate defined in (2.69). The $\frac{z}{L}$ factor in front of the wave profile function $\Phi(q)$ is introduced to guarantee the invariance of the metric under rotations around the propagation axis. This might be difficult to see, since the isometry group of the AdS space has not an easy realization in Poincaré coordinates. However, from (2.66), we can write $\frac{L}{z}\delta(u)$ in global coordinates,

$$\frac{L}{z}\Phi(q)\delta(u) = \phi(q)\delta(Z^0 + Z^{D-2}), \quad (2.78)$$

showing explicitly the invariance around $x^{D-2} = \frac{L}{z}Z^{D-2}$.

Analogously to gravitational shock waves in flat space, (2.76) physically represents the gravitational field associated to a transverse and isotropic energy distribution traveling at the speed of light. This can be shown substituting $\bar{H}(u, z, \vec{x}_T) = \Phi(q)\delta(u)$ in (2.75), giving a source energy-momentum tensor,

$$T_{uu} = \frac{L}{z}\bar{\rho}(q)\delta(u), \quad (2.79)$$

where $\bar{\rho}(q)\delta(u) = u^a \xi^b T_{ab}$ stands for the transverse energy density as measured by a static observer $u^a = \xi^a / (-\xi^b \xi_b)^{1/2}|_P$ located at the shock wave event P , $\vec{\xi} = \partial_t$ being the timelike Killing vector of the AdS spacetime. In AdS background this is different⁴ from the transverse energy density as it was measured by an observer at the conformal boundary of the spacetime, $\rho(z, \vec{x}_T)\delta(u) = \xi^a \xi^b T_{ab}$. Since $\bar{\rho}(q)$ has $O(D-2)$ symmetry around $q=0$ (note that $\rho(z, \vec{x}_T)$ has not such symmetry in general), (2.76) gives the gravitational field of some lightlike energy distribution traveling at depth $z = z_0$ inside the AdS space.

As in the case of gravitational shock waves in flat background, the null geodesics are not continuous at the wavefront. Following a similar construction that the one to derive (2.30), we can see that crossing the wavefront, located at $u=0$, causes a shift Δv in any null geodesic given by

$$\Delta v = \frac{z_p}{L}\Phi(q_p) \int_{-\epsilon}^{\epsilon} du \delta(u) = \frac{z_p}{L}\Phi(q_p), \quad (2.80)$$

(z_p, q_p) being the point where the geodesic intersects the wavefront. This jump of the null geodesics is a consequence of the distributional term appearing in (2.76). Following the example of flat space, we define ‘‘capital’’

⁴ The energy densities $\bar{\rho}$ and ρ coincide in flat background since the redshift factor is 1 in flat spacetime.

coordinates $\{U, V, Z, \vec{X}_T\}$ to avoid this shift:

$$\begin{aligned} u &= U, \\ v &= V + \phi(\vec{X}_T)\theta(U) + \frac{1}{4}U\theta(U) \left[\vec{\nabla}\phi(\vec{X}_T) \right]^2, \\ z &= Z + \frac{1}{2}U\theta(U)\partial_Z\phi(Z, \vec{X}_T), \\ \vec{x}_T &= \vec{X}_T + \frac{1}{2}U\theta(U)\vec{\nabla}\phi(\vec{X}_T), \end{aligned} \tag{2.81}$$

where ϕ stands for $\frac{z}{L}\Phi$. After the change of coordinates, the metric results in

$$ds^2 = L^2 \frac{-dUdV + \mathcal{H}_{ik}\mathcal{H}_{jk}dX^i dX^j}{\left[Z + \frac{1}{2}U\theta(U)\partial_Z\phi \right]^2} \tag{2.82}$$

where

$$H_{ij} = \delta_{ij} + \frac{1}{2}U\theta(U)\partial_i\partial_j\phi(Z, \vec{X}_T). \tag{2.83}$$

This line element is the Rosen form for a gravitational shock wave propagating in the AdS_D spacetime.

2.5 Colliding gravitational shock waves in AdS background

In general, spacetimes containing more than one gravitational shock wave are awkward to study because the nonlinearity inherent to the Einstein equations. For the special case of two colliding gravitational shock waves, which propagate in opposite direction, the line element in the spacetime region before the collision takes place can be written as a sort of linear superposition of the lines element for each shock wave. However, the challenge is to unraveling the causal structure after the collision happens and, in particular, to study the possibility of generate some kind of horizon in the collision. From now on we shall restrict our attention to colliding shock waves propagating in opposite direction.

The collision of gravitational shock waves in flat background have been thoroughly considered in scientific literature in order to compute, for example, the scattering cross section to generate back holes [42, 44, 50, 56, 61, 84, 85, 86]. However, here we shall focus our attention on the collision in AdS background [45, 51, 52]. From a mathematical point of view, the interest to study gravitational collisions in the AdS spacetime resides in the challenge of extrapolating the GR phenomenology from asymptotically flat to nonasymptotically spacetimes and understand the differences. On the other hand, from

a physical point of view, our interest lies in the holographic connection between gravitational physics in AdS background and conformal field theories in a lower dimensional flat spacetime. This will be the subject of Chapter 4.

2.5.1 Setup

Consider two general shock waves propagating in opposite directions inside AdS_D , the first having support at $u = 0$ and propagating from $v \rightarrow -\infty$, while the wavefront of the second wave is located at $v = 0$ and propagates from $u \rightarrow \infty$. Both collide at $u = v = 0$, defining a $(D - 2)$ -dimensional achronal set which we will call from now on the collision surface. With the induced metric, the collision surface identifies with the hyperbolic space \mathbb{H}_{D-2} briefly exposed in Section 2.4.1.

According to its causal relation with the collision surface, the spacetime is divided in a natural way into four regions by the hypersurfaces $u = 0$ and $v = 0$, as it is sketched in fig. 2.1:

- **Regions I and III:** They are the set of all events such that there is no causal connection between them and the collision, that is, the events satisfying $u < 0, v > 0$ (region I) and $u > 0, v < 0$ (region III).
- **Region II:** It is the chronological past of the collision surface, i.e. for each event in region II there exist at least one timelike future-directed curve which connect it to the collision surface. It is given by the events satisfying $u < 0, v < 0$.
- **Region IV:** It is the chronological future of the collision surface. That is, each event in region IV can be reached from the collision surface following a timelike future-directed curve. It is given by the events satisfying $u > 0, v > 0$.

2.5.2 Regions I, II and III

Since gravitational waves propagate at the speed of light, the two shock waves can not see each other until the collision happens. That is, there is no interaction between the shock waves in regions I, II and III. Therefore the metric in Poincaré coordinates is obtained from the simple linear superposition of two line elements like the one written in (2.76),

$$ds^2 = \frac{L^2}{z^2} \left[-dudv + dz^2 + (d\vec{x}_T)^2 + \frac{z}{L} \Phi_+(q_+) \delta(u) du^2 + \frac{z}{L} \Phi_-(q_-) \delta(v) dv^2 \right] \quad (2.84)$$

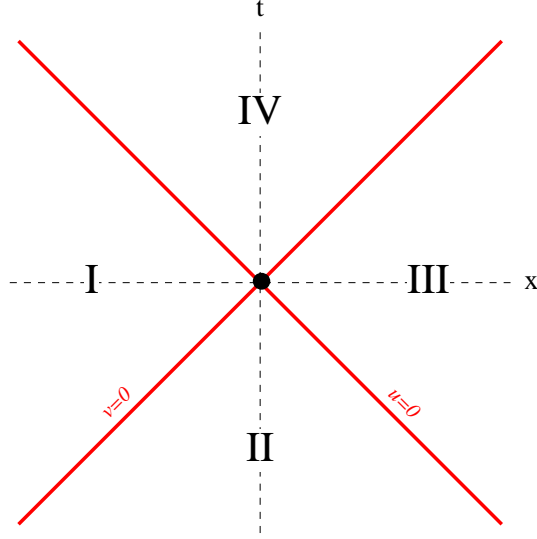


Figure 2.1: An spacetime containing two colliding shock waves. It is divided into four regions by the hypersurfaces $u = 0$ and $v = 0$ (red lines). The black point in the center corresponds to the $(D - 2)$ -dimensional collision surface, whose geometry is that of the hyperbolic space \mathbb{H}_{D-2} . The region IV ($u, v > 0$) is just the future of the collision.

where

$$q_{\pm} = \frac{1}{4zz_{\pm}} \left[(z - z_{\pm})^2 + \left(\vec{x}_T \pm \frac{\vec{b}}{2} \right)^2 \right], \quad (2.85)$$

are the chordal coordinate (2.63) measured from the propagation axis of the shock waves, being \vec{b} the impact parameter parallel to the AdS_D boundary, and $\Delta z = |z_+ - z_-|$ the impact parameter directed along the z coordinate (see fig. 2.2).

Our final goal is to study the causal structure of the whole spacetime containing the two shock waves. Therefore it is convenient to write (2.84) in its Rosen form. This is achieved by just applying the coordinate change to “capital” coordinates (2.81) simultaneously for the two profile functions Φ_{\pm} ,

$$\begin{aligned} u &= U + \phi_-(Z, \vec{X}_T)\theta(V) + \frac{1}{4}V\theta(V) \left[\vec{\nabla}\phi_-(Z, \vec{X}_T) \right]^2, \\ v &= V + \phi_+(Z, \vec{X}_T)\theta(U) + \frac{1}{4}U\theta(U) \left[\vec{\nabla}\phi_+(Z, \vec{X}_T) \right]^2, \\ z &= Z + \frac{1}{2}U\theta(U)\partial_Z\phi_+(Z, \vec{X}_T) + \frac{1}{2}V\theta(V)\partial_Z\phi_-(Z, \vec{X}_T), \\ \vec{x}_T &= \vec{X}_T + \frac{1}{2}U\theta(U)\vec{\nabla}\phi_+(Z, \vec{X}_T) + \frac{1}{2}V\theta(V)\vec{\nabla}\phi_-(Z, \vec{X}_T), \end{aligned} \quad (2.86)$$

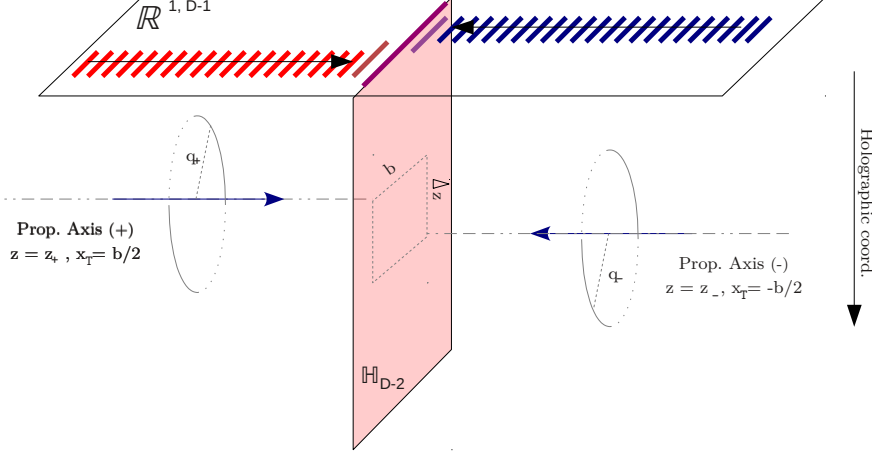


Figure 2.2: Schematic picture for two colliding gravitational shock waves in the AdS space with impact parameters $\Delta z = |z_+ - z_-|$ (measured to the interior of the AdS space) and \vec{b} (parallel to the boundary of AdS space).

where ϕ^\pm stands for $\frac{z}{L}\Phi^\pm$. The Rosen form of the metric (2.84) is then given by

$$ds^2 = L^2 \frac{-dUdV + [\mathcal{H}_{ik}^+ \mathcal{H}_{jk}^+ + \mathcal{H}_{ik}^- \mathcal{H}_{jk}^- - \delta_{ij}] dX^i dX^j}{[Z + \frac{1}{2}U\theta(U)\partial_Z\phi^+ + \frac{1}{2}V\theta(V)\partial_Z\phi^-]^2} \quad (2.87)$$

where

$$\begin{aligned} H_{ij}^+ &= \delta_{ij} + \frac{1}{2}U\theta(U)\partial_i\partial_j\phi^+(Z, \vec{X}_T), \\ H_{ij}^- &= \delta_{ij} + \frac{1}{2}V\theta(V)\partial_i\partial_j\phi^-(Z, \vec{X}_T). \end{aligned} \quad (2.88)$$

Note that in regions I, II and III, outside of the wavefronts, the spacetime is AdS_D . Of course this is not true in region IV, where the two shock waves interact among them after the collision takes place, giving rise to an interesting causal structure.

2.5.3 Region IV

Solving the causal structure of region IV from the line element (2.84) is an extremely hard task. In fact an exact solution remains elusive up to date⁵.

⁵For important progress in this way, see for example [45], where a perturbative approach for short times after the collision has been proposed.

Here we are going to try to shed some light into region IV through the brief study of a collision in flat background between simpler gravitational waves which is known to admit an exact solution in region IV.

Basically, the causal structure after the collision of two gravitational shock waves is hard to compute because, even in flat background, shock waves have not enough symmetry to allow an analytical solution be found in region IV. With this idea in mind, instead of the colliding shock waves given by (2.84), we consider the collision between two plane pp-waves in $D = 4$ dimensions with line element,

$$ds^2 = -dudv + dx^2 + dy^2 + \delta(u)(x^2 - y^2)du^2 + \delta(v)(x^2 - y^2)dv^2, \quad (2.89)$$

in regions I, II and III. The symmetry of this collision (plane symmetry) is noticeably enhanced respect to the one of (2.84) (axial symmetry) and, indeed, it admits an analytical solution in region IV.

Before writing down the metric in region IV, we have to avoid the distributional terms in (2.89) by changing to the Rosen form: defining new coordinates,

$$\begin{aligned} u &= U + \theta(V)(X^2 - Y^2) + V\theta(V)(X^2 + Y^2), \\ v &= V + \theta(U)(X^2 - Y^2) + U\theta(U)(X^2 + Y^2), \\ x &= X + U\theta(U)X + V\theta(V)X, \\ y &= Y - U\theta(U)Y - V\theta(V)Y, \end{aligned} \quad (2.90)$$

the metric in regions I, II and III becomes

$$\begin{aligned} U < 0, V > 0 & : \quad ds^2 = -dUdV + (1 + V)^2dX^2 + (1 - V)^2dY^2, \\ U < 0, V < 0 & : \quad ds^2 = -dUdV + dX^2 + dY^2, \\ U > 0, V < 0 & : \quad ds^2 = -dUdV + (1 + U)^2dX^2 + (1 - U)^2dY^2, \end{aligned} \quad (2.91)$$

Note that the metric is singular in the hypersurfaces $V = 1$ (region I) and $U = 1$ (region III). Actually these are not curvature singularities, since the curvature tensor on them is zero, but they are more than merely coordinate singularities because of null geodesics focalize over them. Indeed no analytic continuation of null geodesics can be done through them. In [44] they are referred as “fold” singularities.

In region IV, the line element is given by the so called Khan-Penrose

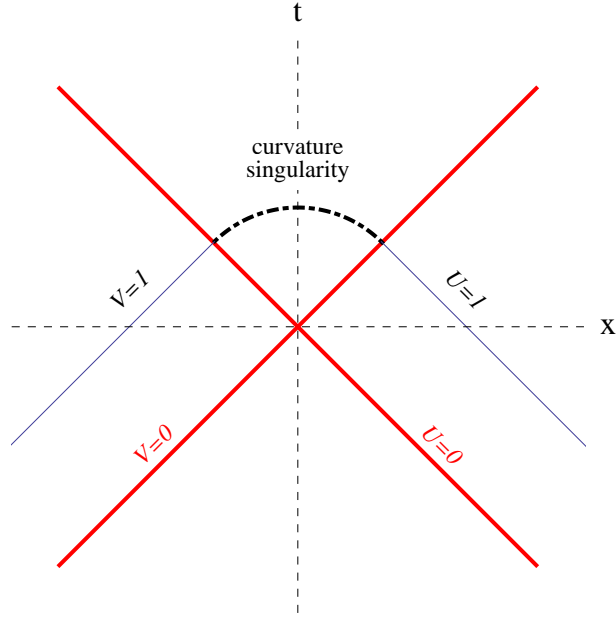


Figure 2.3: Sketch for Khan-Penrose solution (2.92). In region IV a curvature singularity appears in $U^2 + V^2 = 1$. It matches with the fold singularities $U = 1$ and $V = 1$ in regions I and III (blue lines).

solution [86]:

$$\begin{aligned}
 ds^2 = & - \frac{(1 - U^2 - V^2)^{3/2}}{\sqrt{1 - U^2}\sqrt{1 - V^2} (UV + \sqrt{1 - U^2}\sqrt{1 - V^2})^2} dU dV \\
 & + (1 - U^2 - V^2) \left[\frac{1 + U\sqrt{1 - V^2} + V\sqrt{1 - U^2}}{1 - U\sqrt{1 - V^2} - V\sqrt{1 - U^2}} dX^2 \right. \\
 & \left. + \frac{1 - U\sqrt{1 - V^2} - V\sqrt{1 - U^2}}{1 + U\sqrt{1 - V^2} + V\sqrt{1 - U^2}} dY^2 \right]. \tag{2.92}
 \end{aligned}$$

Added to the fold singularities $U = 1$ and $V = 1$, we now have a singularity at $U^2 + V^2 = 1$ too: all components of the metric become unbounded over this hypersurface. In this case it is a true curvature singularity, which joins with the fold singularities in regions I and III. This is shown in fig. 2.3.

The Khan-Penrose solution shows a case in which a curvature singularity appears after the collision. That is a curvature singularity that eventually “happens” to the observer at the collision point. After the curvature singularity appears there is no event horizon, and it seems that an observer could go around the collision event, enter into region IV after the $U^2 + V^2 = 1$ hypersurface, and see a naked singularity, just breaking down the cosmic censorship. However, such observer would have to cross one of the fold singularities at $U = 1$ and $V = 1$, which prevents this type of spacetime trajectory.

The structure of the Khan-Penrose solution is common to most colliding plane pp-waves: in almost all cases a curvature singularity develops in region IV⁶. Roughly speaking, each wave surface focuses the null geodesics crossing it, and thus the waves mutually focus each other until a singularity happens. Also the topological fold singularities in regions I and III are a general feature of all colliding plane waves, preventing in this way the existence of any observer which could see a naked singularity after the collision. The following step is to inquire whether or not the symmetry of colliding waves is a decisive factor for this phenomenology.

We are specially interested in collisions between gravitational waves without plane symmetry. In general terms, one would expect that the focusing of congruences happens in some way whatever the symmetry of the colliding waves is. That is, curvature singularities are possible after collisions even between no-plane pp-waves. In addition, the lack of symmetry respect to plane waves could affect drastically the formation of fold singularities protecting the existence of naked singularities, and then the development of an event horizon after the collision would be necessary. Therefore, it seems plausible to assume that collisions between pp-waves without plane symmetry could lead to the formation of an event horizon in region IV.

Note that the later is an heuristic reasoning, and the development of an event horizon after some collision will depend specifically on the characteristic of the colliding waves and the collision configuration. For example, in the collision of axisymmetric waves, like shock waves, because of the presence of sources, we have to take into account the dependence of the collision on physical magnitudes like impact parameter and energy. One could expect that the horizon production in axisymmetric collisions, if it really takes place, depends on such magnitudes. In particular, critical behavior with respects to these parameters could appear. Concerning colliding gravitational shock waves in anti-de Sitter space, given that they are constructed from its flat cousins through conformal transformations, it is expected that a similar causal dynamics appears in AdS space.

2.5.4 Penrose trapped surface

As we have exposed in the last section, to solve the spacetime structure in region IV from (2.84) is hard because of the lack of symmetry. An alternative approach for studying the horizon appearance after collision is to look for the formation of the Penrose trapped surface before the collision takes place. That is a marginally outer trapped surface (a spacelike $D - 2$ surface whose

⁶ There is a set of exceptional solutions in which the singularity is replaced by a Cauchy horizon.

outer null normals have zero convergence) located, in the coordinates (2.86), at $U = 0$, $V \leq 0$ and $U \leq 0$, $V = 0$, i.e. inside the support of the two shock waves before the collision [46]. Actually there is not any result which links the trapped surface formation before the collision to eventual appearance of horizons in region IV. However, as was already exposed in the introduction chapter, it is a reasonable assumption from a physical point of view. Taking this premise as our starting-point, we could look for Penrose trapped surface production as an indicative for eventual horizon formation in region IV.

In [50] an analytical procedure is developed to compute Penrose trapped surface in flat background. We reproduce it here for the AdS colliding gravitational shock waves (2.84) [51, 53, 57]. First let us split the trapped surface \mathcal{S} we are looking for into two pieces, \mathcal{S}_+ and \mathcal{S}_- , defined as

$$\begin{aligned}\mathcal{S}_+ &= \left\{ (U, V, Z, \vec{X}_T) : U = 0, V + \psi_+(Z, \vec{X}_T) = 0, \psi_+(Z, \vec{X}_T) \geq 0 \right\}, \\ \mathcal{S}_- &= \left\{ (U, V, Z, \vec{X}_T) : U + \psi_-(Z, \vec{X}_T) = 0, V = 0, \psi_-(Z, \vec{X}_T) \geq 0 \right\},\end{aligned}$$

where $\vec{X}_T = (X^1, \dots, X^{D-3})$. The functions $\psi_{\pm}(Z, \vec{X}_T)$ parametrize the trapped surface. The intersection $\mathcal{C} = \mathcal{S}_+ \cap \mathcal{S}_-$, with equation $U = V = 0$, is a $(D - 3)$ -submanifold of the transverse space to collision, \mathbb{H}_{D-2} . By construction the functions $\psi_{\pm}(Z, \vec{X}_T)$ in \mathcal{C} must satisfy

$$\psi_{\pm}(Z, \vec{X}_T) \Big|_{\mathcal{C}} = 0. \quad (2.93)$$

Our goal is to find a vanishing outer normal null vector field to \mathcal{S}_{\pm} . We begin writing two vectors $\left(n_a^{(\pm)} \right) \equiv (n_U^{(\pm)}, n_V^{(\pm)}, n_Z^{(\pm)}, \vec{n}_T^{(\pm)})$ and $\left(m_a^{(\pm)} \right) \equiv (m_U^{(\pm)}, m_V^{(\pm)}, m_Z^{(\pm)}, \vec{m}_T^{(\pm)})$ spanning the orthogonal space to \mathcal{S}_{\pm} :

$$\begin{aligned}\left(n_a^{(+)} \right) &= \begin{pmatrix} 1 \\ 0 \\ 0 \\ 0 \end{pmatrix}, & \left(m_a^{(+)} \right) &= \begin{pmatrix} 0 \\ 1 \\ \partial_Z \psi_+ \\ \vec{\nabla}_T \psi_+ \end{pmatrix} \\ \left(n_a^{(-)} \right) &= \begin{pmatrix} 0 \\ 1 \\ 0 \\ 0 \end{pmatrix}, & \left(m_a^{(-)} \right) &= \begin{pmatrix} 1 \\ 0 \\ \partial_Z \psi_- \\ \vec{\nabla}_T \psi_- \end{pmatrix}\end{aligned} \quad (2.94)$$

Thus, in general, a normal field $N_a^{(\pm)}$ to S_{\pm} is given by

$$\left(N_a^{(+)} \right) = \begin{pmatrix} \alpha \\ \beta \\ \beta \partial_Z \psi_{\pm} \\ \beta \vec{\nabla}_T \psi_{\pm} \end{pmatrix}, \quad \left(N_a^{(-)} \right) = \begin{pmatrix} \beta \\ \alpha \\ \beta \partial_Z \psi_{\pm} \\ \beta \vec{\nabla}_T \psi_{\pm} \end{pmatrix}, \quad (2.95)$$

where α, β are some constants. We now impose the null condition, i.e. $g^{ab}N_a^{(\pm)}N_b^{(\pm)} = 0$, with g_{ab} the metric (2.87) (in the hypersurfaces $U = 0$ and $V = 0$). It results in the equation

$$4\alpha\beta - \beta^2 \left[(\partial_Z\psi_{\pm})^2 + (\vec{\nabla}_T\psi_{\pm})^2 \right] = 0, \quad (2.96)$$

which has two solutions:

$$\begin{aligned} 4\alpha &= \beta \left[(\partial_Z\psi_{\pm})^2 + (\vec{\nabla}_T\psi_{\pm})^2 \right], \\ \beta &= 0 \end{aligned} \quad (2.97)$$

In correspondence with these two solutions there are two null vector fields, N_{\pm}^a and $M^{\pm a}$, orthogonal to each piece of \mathcal{S}_{\pm} . For \mathcal{S}_+ these vector fields are

$$\begin{aligned} (M_+^a) &= \alpha \frac{Z^2}{L^2} \begin{pmatrix} 0 \\ -2 \\ 0 \\ \vec{0} \end{pmatrix}, \\ (N_+^a) &= \beta \frac{Z^2}{L^2} \begin{pmatrix} -2 \\ -\frac{1}{2} \left[(\partial_Z\psi_+)^2 + (\vec{\nabla}_T\psi_+)^2 \right] \\ \partial_Z\psi_+ \\ \vec{\nabla}_T\psi_+ \end{pmatrix}. \end{aligned} \quad (2.98)$$

Where we have raised indexes using the metric (2.87). For \mathcal{S}_- the null vectors are

$$\begin{aligned} (M_-^a) &= \alpha \frac{Z^2}{L^2} \begin{pmatrix} -2 \\ 0 \\ 0 \\ \vec{0} \end{pmatrix}, \\ (N_-^a) &= \beta \frac{Z^2}{L^2} \begin{pmatrix} -\frac{1}{2} \left[(\partial_Z\psi_-)^2 + (\vec{\nabla}_T\psi_-)^2 \right] \\ -2 \\ \partial_Z\psi_- \\ \vec{\nabla}_T\psi_- \end{pmatrix}. \end{aligned} \quad (2.99)$$

Finally we need to impose both vector fields are future directed. It implies that α and β should be negative. In particular, we choose

$$\alpha = -\frac{L^2}{2Z^2}, \quad \beta = -1, \quad (2.100)$$

to have the normalization $N_{\pm}^a M_{\pm}^b g_{ab} = -1$.

The next step is to impose that vector fields (2.98) and (2.99) with normalization (2.100) have zero expansion. It is obvious the expansion θ_{\pm} of the vector fields M_{\pm}^a vanishes. For vector fields N_{\pm}^a we obtain after a bit of algebra,

$$\theta_{\pm} = \nabla_a N_{\pm}^a = \left[\frac{Z^2}{L^2} \Delta_T + \frac{Z^2}{L^2} \partial_Z^2 - \frac{D-2}{L} \frac{Z}{L} \partial_Z \right] \left(\frac{Z}{L} \Phi_{\pm} - \psi_{\pm} \right), \quad (2.101)$$

where Δ_T is the flat Laplacian in the coordinates $\{X^1, \dots, X^{D-3}\}$. Defining now Ψ_{\pm} as

$$\Psi_{\pm}(Z, \vec{X}_T) \equiv \frac{Z}{L} \psi_{\pm}(Z, \vec{X}_T), \quad (2.102)$$

we can reassemble the equation (2.101) as

$$\theta_{\pm} = \left(\Delta_{\mathbb{H}_{D-2}} - \frac{D-2}{L^2} \right) (\Phi_{\pm} - \Psi_{\pm}), \quad (2.103)$$

where $\Delta_{\mathbb{H}_{D-2}}$ is the Beltrami-Laplace operator in \mathbb{H}_{D-2} . So $\mathcal{S} = \mathcal{S}_+ \cup \mathcal{S}_-$ is a surface with zero null expansion if the functions Ψ_{\pm} satisfy

$$\left(\Delta_{\mathbb{H}_{D-2}} - \frac{D-2}{L^2} \right) (\Phi_{\pm} - \Psi_{\pm}) = 0. \quad (2.104)$$

It remains to study the match between the outer normals N_+^a and N_-^a in $\mathcal{C} = \mathcal{S}_+ \cap \mathcal{S}_-$. From (2.98) and (2.99) we get the necessary conditions:

$$\begin{aligned} \left[(\partial_Z \psi_{\pm})^2 + (\vec{\nabla}_T \psi_{\pm})^2 \right] \Big|_{\mathcal{C}} &= 4, \\ \partial_Z \psi_+ \Big|_{\mathcal{C}} &= \partial_Z \psi_- \Big|_{\mathcal{C}}, \\ \vec{\nabla}_T \psi_+ \Big|_{\mathcal{C}} &= \vec{\nabla}_T \psi_- \Big|_{\mathcal{C}}. \end{aligned} \quad (2.105)$$

In terms of Ψ_{\pm} we can write them in the more compact form

$$\begin{aligned} g^{ab} \partial_a \Psi_{\pm} \partial_b \Psi_{\pm} \Big|_{\mathcal{C}} &= 4, \\ \partial_a \Psi_+ \Big|_{\mathcal{C}} &= \partial_a \Psi_- \Big|_{\mathcal{C}}. \end{aligned} \quad (2.106)$$

These equations imply the necessary condition over \mathcal{C}

$$g^{ab} \partial_a \Psi_+ \partial_b \Psi_- \Big|_{\mathcal{C}} = 4, \quad (2.107)$$

which is also a sufficient condition to ensure (2.105) and, therefore, the match between the two vectors N_{\pm}^a in \mathcal{C} .

Summarizing, a Penrose trapped surface is produced in shock wave collisions if and only if exist a $(D-3)$ -submanifold of \mathcal{C} in \mathbb{H}_{D-2} and two (positive)

functions Ψ_{\pm} (which we shall call Penrose functions from now on) inside \mathcal{C} such that the unusual boundary problem

$$\begin{aligned} \left(\nabla_{\mathbb{H}_{D-2}}^2 - \frac{D-2}{L^2} \right) (\Phi_{\pm} - \Psi_{\pm}) &= 0 \\ g^{ab} \partial_a \Psi_+ \partial_b \Psi_- |_{\mathcal{C}} &= 4, \\ \Psi_{\pm} |_{\mathcal{C}} &= 0. \end{aligned} \tag{2.108}$$

is satisfied.

The solution of (2.108) can become an extremely hard task for general collisions. In fact, it has been possible to find an analytical solution only for central collisions, where $\Phi_+ = \Phi_-$, of certain kind of gravitational shock waves [51]. In general, numerical techniques are required to solve it, as we will see in Chapter 4.

Chapter 3

Reissner-Nordström and Fat shock waves in AdS_D

In the previous chapter we have introduced the concept of gravitational waves and, in particular, we have focused on gravitational shock waves in both flat and AdS backgrounds. In flat background we showed how certain type of gravitational shock waves can be obtained from a suitable boost of the Schwarzschild solution. Following the way paved by Aichelburg and Sexl, several authors have directed their efforts to find other gravitational shock waves in flat background boosting asymptotically flat GR solutions other than the Schwarzschild one (see [84, 85] for some examples).

We can distinguish between two different ways of constructing gravitational shock waves: boosting a previously known GR solution, as in Section 2.3, or introducing by hand an arbitrary energy density in the wave equation (2.27) (flat background) or (2.75) (AdS background). The main difference between the two paths is that the first results in shock waves which we can interpret physically as the contracted gravitational field generated by certain objects boosted infinitely, while the second results in shock waves whose physical interpretation depends on one existing for the source chosen. Indeed, the source of an arbitrary “handmade” gravitational shock wave could not be physically acceptable in the sense that the energy-momentum tensor could not be obtained from any solution to the matter equations of the theory. This is specially of importance in supersymmetric theories where the matter content is entirely fixed.

In this chapter we are going to define and compute Reissner-Norstrom and fat gravitational shock waves in AdS_D . The first ones, which we denote as AdS-RN waves, are obtained adapting the original Aichelburg Sexl boost to the Reissner-Norstrom solution in AdS background [59]. The second ones follow from any point-like gravitational shock wave in AdS spacetime by

spreading the source [57], and they are handmade gravitational shock waves in the sense previously mentioned. We will call these latter type of waves “fat shock waves”.

The chapter is divided into three sections. The first Section 3.1 is dedicated to compute the geometry and energy-momentum tensor of the AdS-RN shock waves, while Section 3.2 introduces and discusses the gravitational fat shock waves. Because the AdS/CFT correspondence, colliding AdS shock waves can be regarded as the gravitational dual for colliding energy lumps in the boundary field theory. This connection is studied in detail in Section 3.3, including a comparison with the boosted Woods-Saxon potential which is supposed describes the energy profile of ultrarelativist heavy ions. The reader not familiarized with the AdS-RN solution can find a brief review of the issue in Appendix B.

3.1 AdS-RN shock waves

We are interested in both the line element of the gravitational shock wave resulting from boosting the AdS-RN metric, and the energy-momentum tensor which sources the shock wave. Naively, since the AdS-RN solution describes an spherically symmetric configuration of coupled gravitational and electric fields, it is expected that, once boosted the AdS-RN line element, the gravitational shock wave describes a sort of lightlike particle with certain energy coming from the mass and electric charge of the AdS-RN solution. Computing the boosted energy-momentum tensor will help us to enlighten this point.

3.1.1 Shock wave metric computation

In AdS-spherical coordinates, the AdS-RN solution is given by

$$ds^2 = -f(r)d\tau^2 + f^{-1}(r)dr^2 + r^2d\Omega_{D-2}^2, \quad (3.1)$$

with

$$f(r) = 1 + \frac{r^2}{L^2} - \frac{2M}{r^{D-3}} + \frac{Q^2}{r^{2(D-3)}}. \quad (3.2)$$

The only nonvanishing component of the gauge potential is

$$A_\tau = \sqrt{\frac{D-2}{2(D-3)}} \frac{Q}{r^{D-3}}. \quad (3.3)$$

This solution describes the gravitational field generated by a charged particle with mass m and charge \mathfrak{q}

$$m = \frac{(D-2)\Omega_{D-2}}{8\pi G_D} M, \quad \mathfrak{q}^2 = \frac{(D-2)(D-3)}{8\pi G_D} Q^2. \quad (3.4)$$

To obtain a shock wave from the AdS-RN solution we are going to proceed in the same way than in Section 2.3: first we do a boost and after it we will take the the appropriate infinite-boost limit. Remember that in the original Aichelburg-Sexl boost over the Schwarzschild black hole we had to take the ultrarelativistic limit following a suitable scaling relation between the Schwarzschild mass m and the boost parameter γ to get a finite result. Here we will be forced to take a similar scaling relating M , Q^2 and γ to guarantee a finite result after doing the infinite boost limit.

Eventually we are going to send M and Q^2 to zero. Thus it is convenient to begin doing a series expansion of the AdS-RN metric in M and Q^2 , keeping only the leading order:

$$ds^2 = ds_0^2 + ds_p^2 + O(M^2) + O(Q^4) \quad (3.5)$$

where

$$ds_p^2 = \left(\frac{2M}{r^{D-3}} - \frac{Q^2}{r^{2(D-3)}} \right) dt^2 + \frac{1}{1+r^2/L^2} \left(\frac{2M}{r^{D-3}} - \frac{Q^2}{r^{2(D-3)}} \right) dr^2, \quad (3.6)$$

and ds_0^2 stands for the metric of AdS_D. We perform a boost over Poincaré coordinates $\{t, z, x^i\}$,

$$\begin{aligned} t &= \gamma \left(t' + \beta x^{D-2'} \right), & z &= z' \\ x^{D-2} &= \gamma \left(\beta t' + x^{D-2'} \right), & \vec{x}_T &= \vec{x}'_T, \end{aligned} \quad (3.7)$$

where \vec{x}_T stands for the remaining coordinates besides t , z and x^{D-2} . Under this transformation, ds_0^2 does not change, so we only have to worry about how ds_p^2 does. Of course we could choose any other coordinates. However, note that a boost over Poincaré coordinates describes a boost in the conformal boundary. Thus it is the appropriate coordinate system to boost since the goal is to describe relativistic energy lumps in the field theory at the boundary of AdS_D.

The line element (3.6) takes a very cumbersome form in Poincaré coordinates and, as a consequence, performing the boost (3.7) over it results technically involved. To circumvent the difficulty notice that, from (2.66), the

boost (3.7) is equivalent to¹

$$\begin{aligned} Z_0 &= \gamma(Z_0' + \beta Z_{D-2}') , & Z_i &= Z_i' , & i &= 1, \dots, D-3, \\ Z_{D-2} &= \gamma(\beta Z_0' + Z_{D-2}') , \end{aligned} \quad (3.8)$$

Given that it is easier to write ds_p^2 in the embedding space coordinates $\{Z^0, Z^i, Z^{D-2}\}$ than in Poincaré ones, we will apply (3.8) instead of (3.7).

Using the inverse relation of (A.9),

$$\begin{aligned} r &= \sqrt{Z_0^2 + Z_D^2 - L^2}, \\ \tau &= L \arctan\left(\frac{Z_0}{Z_D}\right), \end{aligned} \quad (3.9)$$

dr and dt are expressed in terms of the coordinates $\{Z^0, Z^i, Z^{D-2}\}$ as

$$\begin{aligned} dr &= \frac{1}{(Z_0^2 + Z_D^2 - L^2)^{1/2}} [Z_0 dZ_0 + Z_D dZ_D], \\ d\tau &= \frac{L}{Z_0^2 + Z_D^2} [Z_D dZ_0 - Z_0 dZ_D]. \end{aligned} \quad (3.10)$$

Thus we have for $ds_p^2 = G_{AB} dZ^A dZ^B$,

$$ds_p^2 = G_{00} dZ_0^2 + G_{DD} dZ_D^2 + 2G_{0D} dZ_0 dZ_D, \quad (3.11)$$

where $G_{AB} = \zeta(Z_0^2 + Z_D^2, M, Q^2) h_{AB}$, with

$$\begin{aligned} h_{00} &= Z_D^2 (Z_0^2 + Z_D^2 - L^2) + L^2 Z_0^2, \\ h_{0D} &= -Z_0 Z_D (Z_0^2 + Z_D^2 - 2L^2), \\ h_{DD} &= Z_0^2 (Z_0^2 + Z_D^2 - L^2) + L^2 Z_D^2, \end{aligned} \quad (3.12)$$

and $\zeta(Z_0^2 + Z_D^2, M, Q^2)$ is the function

$$\begin{aligned} \zeta(Z_0^2 + Z_D^2, M, Q^2) &= \frac{L^2}{(Z_0^2 + Z_D^2)^2} \\ &\times \left[\frac{2M}{(Z_0^2 + Z_D^2 - L^2)^{(D-1)/2}} - \frac{Q^2}{(Z_0^2 + Z_D^2 - L^2)^{(D-2)}} \right]. \end{aligned} \quad (3.13)$$

¹In order to avoid a heavy notation, here and in the next we will lower the coordinate index in the coordinates $\{Z^0, Z^i, Z^{D-2}\}$, i.e. $Z^A \rightarrow Z_A$. But note that we are not using any metric to do it. Is just for getting a nicer reading of the equations whenever it will be necessary.

After the boost (3.8) we get the components,

$$\begin{aligned} G_{Z'_0 Z'_0} &= \gamma^2 G_{00}, & G_{Z'_0 Z'_{D-2}} &= \gamma^2 \beta G_{00}, \\ G_{Z'_0 Z'_D} &= \gamma G_{0D}, & G_{Z'_{D-2} Z'_{D-2}} &= \gamma^2 \beta^2 G_{00}, \\ G_{Z'_{D-2} Z'_D} &= \gamma \beta G_{0D}, & G_{Z'_D Z'_D} &= G_{DD}. \end{aligned} \quad (3.14)$$

In light-cone coordinates $U' = Z'_0 + Z'_{D-2}$ and $V' = Z'_0 - Z'_{D-2}$,

$$\begin{aligned} G_{U'U'} &= \frac{1}{4} \gamma^2 (1 + \beta)^2 G_{00}, & G_{U'V'} &= \frac{1}{4} \gamma^2 (\beta^2 - 1) G_{00} \\ G_{V'V'} &= \frac{1}{4} \gamma^2 (1 - \beta)^2 G_{00}. \end{aligned} \quad (3.15)$$

As in the original Aichelburg-Sexl boost explained in Section 2.3, we are forced to take the infinite boost limit of (3.15) with care in order to get a finite result. Keeping this in mind, we introduce two new parameters, p_M and p_Q , defined as,

$$p_M \equiv \gamma M, \quad p_Q^2 \equiv \gamma Q^2, \quad (3.16)$$

and take the limit such that p_M and p_Q^2 remain finite. Note that this implies sending M and Q^2 to zero while $\gamma \rightarrow \infty$, which legitimizes keeping only the leading order in (3.5). Once we have introduced these parameters in $G_{U'U'}$,

$$\begin{aligned} G_{U'U'} &= \frac{(1 + \beta)^2}{4} \gamma \zeta \left(\gamma^2 (Z'_0 + \beta Z'_{D-2})^2, Z'^2_D, p_M, p_Q^2 \right) \\ &\times \left[Z'^2_D \left(\gamma^2 (Z'_0 + \beta Z'_{D-2})^2 + Z'^2_D - L^2 \right) + L^2 \gamma^2 (Z'_0 + \beta Z'_{D-2})^2 \right], \end{aligned} \quad (3.17)$$

we can compute the infinite boost limit using the equation demonstrated in Section C.1 of Appendix C,

$$\lim_{\gamma \rightarrow \infty} \gamma \chi \left(\gamma^2 (Z'_0 + \beta Z'_{D-2}) \right) = \delta(U') \int_{-\infty}^{\infty} \chi(w^2) dw, \quad (3.18)$$

In this way, the limit (3.17) results in the integral expression

$$\begin{aligned} \lim_{\gamma \rightarrow \infty} G_{U'U'} &= 2p_M L^2 \delta(U') \int_{-\infty}^{\infty} dx \frac{Z'^2_D (x^2 + Z'^2_D - L^2) + x^2 L^2}{(x^2 + Z'^2_D - L^2)^{(D-1)/2} (Z'^2_D + x^2)^2} \\ &- p_Q^2 L^2 \delta(U') \int_{-\infty}^{\infty} dx \frac{Z'^2_D (x^2 + Z'^2_D - L^2) + x^2 L^2}{(x^2 + Z'^2_D - L^2)^{D-2} (Z'^2_D + x^2)^2}. \end{aligned} \quad (3.19)$$

These integrals are computed in detail in Section C.2 of Appendix C. They result in Gauss hypergeometric functions,

$$\begin{aligned} \int_{-\infty}^{\infty} dx \frac{Z'^2_D (x^2 + Z'^2_D - L^2) + x^2 L^2}{(x^2 + Z'^2_D - L^2)^B (Z'^2_D + x^2)^2} &= \frac{\Gamma(3/2) \Gamma(B + 1/2)}{\Gamma(B + 1)} \times \\ &\frac{2^{2(1-B)}}{(Lq)^{2B-1}} {}_2F_1(2B - 1, B + 1/2; 2B + 1; -1/q), \end{aligned} \quad (3.20)$$

where q is the chordal coordinate defined in (2.63). Substituting in (3.19) we get

$$\begin{aligned} \lim_{\gamma \rightarrow \infty} G_{U'U'} &= 2p_M \delta(U') \frac{\Gamma(\frac{3}{2})\Gamma(\frac{D}{2})}{\Gamma(\frac{D+1}{2})} \frac{2^{3-D}}{L^{D-4}q^{D-2}} {}_2F_1\left(D-2, \frac{D}{2}; D; -\frac{1}{q}\right) \\ &- p_Q^2 \delta(U') \frac{\Gamma(\frac{3}{2})\Gamma(\frac{2D-3}{2})}{\Gamma(D-1)} \frac{2^{2(3-D)}}{L^{2D-7}q^{2D-5}} {}_2F_1\left(2D-5, \frac{2D-3}{2}; 2D-3; -\frac{1}{q}\right). \end{aligned}$$

In a similar way we can compute the infinite-boost limit for $G_{V'V'}$ and $G_{U'V'}$ in (3.15). However, since they are proportional to $(1-\beta)^2$ and (β^2-1) , both result in zero,

$$\begin{aligned} \lim_{\gamma \rightarrow \infty} G_{V'V'} &= (\dots) \times \lim_{\beta \rightarrow 1} (1-\beta)^2 = 0, \\ \lim_{\gamma \rightarrow \infty} G_{U'V'} &= (\dots) \times \lim_{\beta \rightarrow 1} (\beta^2-1) = 0. \end{aligned} \quad (3.21)$$

At the end of the day, after the infinite-boost limit is taken, we have obtained that ds_p^2 in (3.5) only retains the $U'U'$ component. Defining

$$\Phi^{(RN)}(p_M, p_Q^2; q) = \lim_{\gamma \rightarrow \infty} G_{U'U'}, \quad (3.22)$$

the metric after the infinite boost takes the form

$$ds^2 = ds_0^2 + \Phi^{(RN)}(p_M, p_Q^2; q) \delta(U') dU'^2, \quad (3.23)$$

In Poincaré coordinates, $U' = \frac{L}{z}(t' + x') = \frac{L}{z}u'$. Therefore,

$$\delta(U') dU'^2 = \frac{z}{L} \delta(u') \left(\frac{L}{z} du' - \frac{L}{z^2} u dz \right)^2 = \frac{L}{z} \delta(u') du'^2. \quad (3.24)$$

So we finally arrive at the line element of the AdS-RN shock wave spacetime in Poincaré coordinates to be,

$$ds^2 = \frac{L^2}{z^2} \left(-dudv + dz^2 + d\vec{x}_T^2 + \frac{z}{L} \Phi^{(RN)}(p_M, p_Q^2; q) \delta(u) du^2 \right), \quad (3.25)$$

where we have changed the primed coordinates by unprimed ones for clarity, and

$$\begin{aligned} \Phi^{(RN)}(p_M, p_Q^2; q) &= \\ &2p_M \frac{\Gamma(\frac{3}{2})\Gamma(\frac{D}{2})}{\Gamma(\frac{D+1}{2})} \frac{2^{3-D}}{L^{D-4}q^{D-2}} {}_2F_1\left(D-2, \frac{D}{2}; D; -\frac{1}{q}\right) \\ &- p_Q^2 \frac{\Gamma(\frac{3}{2})\Gamma(\frac{2D-3}{2})}{(D-2)!} \frac{2^{2(3-D)}}{L^{2D-7}q^{2D-5}} {}_2F_1\left(2D-5, D-\frac{3}{2}; 2D-3; -\frac{1}{q}\right). \end{aligned} \quad (3.26)$$

An important remark must be done here. Notice that the dependence in dimension of the second term of (3.26) is the same as for the first term but with an effective value of the dimension $2D - 3$. That is, the electromagnetic contribution to the shock wave (3.25) in D dimensions is equal to the one for a particle in dimension $D' = 2D - 3$ and weighted by $\frac{p_Q^2}{2p_M}$. This observation is the starting point in [59] to compute the line element of the AdS-RN shock wave without explicitly computing the integral (3.20).

3.1.2 Electromagnetic field and energy-momentum tensor

The shock wave (2.59) obtained from the original Aichelburg-Sexl boost can be seen as the gravitational field of a massless particle in flat spacetime. Naively we could interpret (3.25) as the gravitational field sourced by some sort of “charged” massless particle traveling in AdS spacetime at the speed of light. However, note that the wave profile (3.26) depends on two parameters, p_M and p_Q , in contrast with (2.59), which only depends on one parameter, μ . Thus, it is not clear the kind of lightlike source which generates an AdS-RN gravitational shock wave. In particular, it is not clear how we can identify the relativistic energy of the AdS-RN shock wave spacetime, as well as the role of charge after the ultrarelativistic boost is done.

Before the boost, the AdS-RN spacetime has a singularity at $r = 0$, which corresponds to the position of a charged particle sourcing the gravitational and electromagnetic field. In Poincaré coordinates such charged particle is located at

$$z = z_0 \sqrt{1 + \left(\frac{t}{z_0}\right)^2}, \quad \vec{x} = 0, \quad (3.27)$$

where we have defined $z_0 = L/k$ for $k > 0$ arbitrary to take into account the scale invariance of the spacetime² (2.62). For an asymptotic observer at the boundary of the AdS-RN spacetime the singularity undergoes some sort of motion approaching and leaving the spacetime boundary. However, after the infinite-boost limit, such approaching-and-leaving motion is frozen: from

² Actually the scale invariance (2.62) is not a symmetry of the AdS-RN spacetime, but of the empty AdS spacetime. However we are interested in symmetry transformations of the conformal boundary of the spacetime. From this point of view, the scale transformations (2.62) could be viewed as a technique to generate solutions, such that we are working with a entire family of spacetimes obtained from AdS-RN by means of the symmetry transformations of the conformal boundary.

(3.7),

$$z' = z_0 \sqrt{1 + \left(\frac{t'}{\gamma z_0}\right)^2}, \quad x^{D-2'} = -t', \quad \vec{x}'_T = 0. \quad (3.28)$$

which approaches z_0 when $\gamma \rightarrow \infty$. Therefore after the infinite boost limit, the particle-like singularity sourcing the AdS-RN gravitational shock wave follows a lightlike trajectory along the x^{D-2} coordinate and at constant depth $z = z_0$ inside the AdS spacetime. Note that the depth of the trajectory can be chosen freely since z_0 in (2.66) is a free parameter.

The functional action for the AdS-RN solution is the one given in (B.4) of Appendix B. That is Einstein gravity coupled to Maxwell field plus a cosmological term $\Lambda = -(D-1)(D-2)/(2L^2)$. It also will be the action for the AdS-RN gravitational shock wave (3.25). However, since switching off the electromagnetic field the AdS-RN shock wave spacetime would correspond to the gravitational field sourced by a lightlike particle, we have to add a lightlike particle term to the action (B.4) to describe the physics of the AdS-RN gravitational shock wave. Such term is given by

$$S_P = \int d^D x \int d\eta \frac{1}{2e} \frac{dx^a}{d\eta} \frac{dx^b}{d\eta} g_{ab} \delta^{(D)}(x - x(\eta)), \quad (3.29)$$

$x(\eta)$ being the worldline of the particle after the boost and e the *einbein* over it. Therefore the energy-momentum tensor sourcing the AdS-RN gravitational shock wave have two contributions, $T_{ab} = T_{ab}^{EM} + T_{ab}^P$, the first one coming from the electromagnetic field and the second one coming from the particle contribution (3.29),

$$\begin{aligned} T_{ab}^{EM} &= \frac{1}{4\pi G_D} \lim_{\gamma \rightarrow \infty} \left[F_{ac} F_b{}^c - \frac{1}{4} g_{ab} F_{cd} F^{cd} \right], \\ T_{ab}^P &= \int d\eta \frac{1}{e\sqrt{-g}} \frac{dx_a}{d\eta} \frac{dx_b}{d\eta} \delta^{(D)}(x - x(\eta)). \end{aligned} \quad (3.30)$$

We are going to compute this two pieces separately: first we will compute the electromagnetic contribution for the AdS-RN solution, without boost, and then the infinite boost limit over it. Second, we will evaluate the lightlike particle piece, without the necessity of any subsequent boost.

From (3.30), the no-vanishing components of the energy-momentum tensor of the AdS-RN solution are

$$\begin{aligned} T_{tt}^{EM} &= \frac{1}{8\pi G_D} \frac{(D-2)(D-3)}{2} \frac{Q^2}{r^{2(D-2)}} f(r), \\ T_{rr}^{EM} &= -\frac{1}{8\pi G_D} \frac{(D-2)(D-3)}{2} \frac{Q^2}{r^{2(D-2)}} f^{-1}(r), \\ T_{\theta_i \theta_i}^{EM} &= \frac{1}{8\pi G_D} \frac{(D-2)(D-3)}{2} \frac{Q^2}{r^{2(D-2)}} g_{\theta_i \theta_i}, \end{aligned} \quad (3.31)$$

where $g_{\theta_i\theta_i}$ stands for the angular components of the metric in (3.1). Note that the function $f(r)$ defined in (3.2) contains a term proportional to Q^2 . After the infinite boost limit is taken, only the terms linear in Q^2 will survive because of the scaling taken in order to give a finite line element describing the gravitational shock wave in (3.25). Thus, to gain simplicity, it is convenient to perform a series expansion of (3.31) in $\frac{Q^2}{r^{2(D-2)}}$ keeping only the leading order,

$$\begin{aligned} T_{tt}^{EM} &= \frac{1}{8\pi G_D} \frac{(D-2)(D-3)}{2} \frac{Q^2}{r^{2(D-2)}} \left(1 + \frac{r^2}{L^2}\right), \\ T_{rr}^{EM} &= -\frac{1}{8\pi G_D} \frac{(D-2)(D-3)}{2} \frac{Q^2}{r^{2(D-2)}} \frac{L^2}{L^2 + r^2}, \\ T_{\theta_i\theta_i}^{EM} &= \frac{1}{8\pi G_D} \frac{(D-2)(D-3)}{2} \frac{Q^2}{r^{2(D-2)}} g_{\theta_i\theta_i}. \end{aligned} \quad (3.32)$$

From (A.9) of Appendix A we can parametrize (3.32) in terms of $\{Z_0, Z_i, Z_D\}$ as $T_{AB}^{EM} = \xi(Z_0^2 + Z_D^2; Q^2) t_{AB}$, $\xi(Z_0^2 + Z_D^2; Q^2)$ being the function

$$\xi(Z_0^2 + Z_D^2; Q^2) = \frac{1}{8\pi G_D} \frac{(D-2)(D-3)}{2} \frac{Q^2}{(Z_0^2 + Z_D^2 - L^2)^{D-1}}. \quad (3.33)$$

In light-cone coordinates $U = Z_0 + Z_{D-2}$ and $V = Z_0 - Z_{D-2}$, the non vanishing components of t_{AB} are

$$\begin{aligned} t_{UU} &= \frac{1}{2} (Z_D^2 - L^2), & t_{UD} &= -Z_0 Z_D, \\ t_{VV} &= \frac{1}{2} (Z_D^2 - L^2), & t_{VD} &= Z_0 Z_D, \\ t_{UV} &= -\frac{Z_0^2}{2}, & t_{Z_l Z_l} &= Z_0^2 + Z_D^2 - L^2, \end{aligned} \quad (3.34)$$

where $l = 1, \dots, D-3, D-1$.

The boost (3.8) in coordinates U, V takes the form

$$U = \gamma(1 + \beta)U', \quad V = \gamma(1 - \beta)V'. \quad (3.35)$$

Thus, after the boost, we have the following components of t_{AB} ,

$$\begin{aligned} t_{U'U'} &= \gamma^2(1 + \beta)^2 t_{UU}, & t_{U'Z'_D} &= \gamma(1 + \beta) t_{UZ_D}, \\ t_{V'V'} &= \gamma^2(1 - \beta)^2 t_{VV}, & t_{V'Z'_D} &= \gamma(1 - \beta) t_{VZ_D}, \\ t_{U'V'} &= t_{UV}, & t_{Z'_D Z'_D} &= t_{Z_D Z_D}, \\ t_{Z'_l Z'_l} &= t_{Z_l Z_l}. \end{aligned} \quad (3.36)$$

The infinite-boost limit for any component only results in something different form zero if the component is linear in γ^2 , since we need a power in γ to define $p_Q^2 = \gamma Q^2$ and another to perform the limit over $\gamma \xi(Z_0^2 + Z_D^2; p_Q^2)$. Also, the components which have a factor $(1 - \beta)$ give a vanishing limit. Therefore only the component $T_{U'U'}^{EM}$ yields to a non vanishing result: using equation (3.18), we have

$$\begin{aligned} \lim_{\gamma \rightarrow \infty} T_{U'U'}^{EM} &= \lim_{\gamma \rightarrow \infty} \frac{(1 + \beta)^2}{2} \gamma \xi \left(\gamma^2 (Z_0' + \beta Z_1')^2 + Z_D'^2; p_Q^2 \right) \\ &\times \left(Z_D'^2 - L^2 \right) = p_Q^2 \frac{(D-2)(D-3)}{8\pi G_D} \left(Z_D'^2 - L^2 \right) \delta(U') \\ &\times \int_{-\infty}^{\infty} \frac{dx}{[x^2 + Z_D'^2 - L^2]^{D-1}}. \end{aligned} \quad (3.37)$$

The improper integral is computed in Section C.2 of Appendix C. It results in

$$\lim_{\gamma \rightarrow \infty} T_{U'U'}^{EM} = p_Q^2 \frac{\Gamma(D-3/2)\sqrt{\pi}}{8\pi G_D(D-4)!} \frac{\delta(U')}{(Z_D'^2 - L^2)^{D-5/2}}. \quad (3.38)$$

In Poincaré coordinates we would get *a priori* components $T_{u'u'}^{EM}$, $T_{u'z'}^{EM}$ and $T_{z'z'}^{EM}$, since $U' = \frac{L}{z}u'$, but the latter two are linear in u' and thus they are zero because the $\delta(u')$ factor. Thus, in Poincaré coordinates, the $u'u'$ component is the only no-vanishing term of the energy-momentum tensor after the infinite boost limit,

$$\lim_{\gamma \rightarrow \infty} T_{u'u'}^{EM} = p_Q^2 \frac{\Gamma(D-3/2)\sqrt{\pi} L (2qL)^{5-2d} \delta(u')}{8\pi G_D(D-4)! z \left(1 + \frac{1}{q}\right)^{D-5/2}}, \quad (3.39)$$

where q is the chordal coordinate (2.63).

The particle contribution is simpler to compute than the electromagnetic one, since the particle piece in (3.30) is applicable to a lightlike particle, and thus the computation can be done directly without taking any infinite boost limit. First note that, choosing $v = t - x^{D-2}$ to parametrize the particle worldline and integrating in (3.30), the Lagrangian describing the particle dynamics is

$$L = \frac{1}{2e} \dot{x}^a(v) \dot{x}^b(v) g_{ab}, \quad (3.40)$$

where dot denotes derivative of the worldline coordinates with respect to v . Thus the particle momentum is given by

$$p_a = \frac{\partial L}{\partial \dot{x}_a(v)} = \frac{1}{e} g_{ab} \dot{x}^b(v), \quad (3.41)$$

Substituting it in (3.30) the particle energy-momentum tensor takes the form

$$T_{ab}^P = \frac{e}{\sqrt{-g}} \delta^{(D-1)}(x - x(v)) p_a p_b. \quad (3.42)$$

On the other hand, the worldline equations in Poincaré coordinates are

$$u = 0, \quad z = z_0, \quad \vec{x}_T = 0. \quad (3.43)$$

Thus the particle momentum p_a only has the component p_u different from zero. Defining $\bar{\mu}$ as the energy of the massless particle measured by and static observer located “next to” the particle³, such component takes the form

$$p_u = -\frac{L}{z_0} \bar{\mu}. \quad (3.44)$$

Thus, from (3.41), the *einbein* is

$$e = \frac{L}{2\bar{\mu}z_0}. \quad (3.45)$$

Substituting in (3.42), only the T_{uu}^P component is different from zero,

$$T_{uu}^P = \bar{\mu} \left(\frac{z_0}{L}\right)^{D-3} \delta(u) \delta^{(D-3)}(\vec{x}_T) \delta(z - z_0). \quad (3.46)$$

Putting (3.39) and (3.46) together we get finally the energy-momentum tensor which sources the AdS-RN gravitational shock wave,

$$\begin{aligned} T_{uu} = & \bar{\mu} \left(\frac{z_0}{L}\right)^{D-3} \delta(u) \delta^{(D-3)}(\vec{x}_T) \delta(z - z_0) \\ & + p_Q^2 \frac{\Gamma(D - 3/2) \sqrt{\pi} L (2qL)^{5-2d} \delta(u)}{8\pi G_D (D - 4)! z \left(1 + \frac{1}{q}\right)^{D-5/2}}. \end{aligned} \quad (3.47)$$

From the point of view of a static observer, $\vec{u} = \vec{\xi}/(-\xi^a \xi_a)^{1/2}$ with $\vec{\xi} = \partial_t$ the timelike Killing vector field of the AdS background, that energy-momentum tensor corresponds to an isotropic transverse energy density $\bar{\rho}(q) = u^a \xi^b T_{ab}$ which decomposes into two pieces, $\bar{\rho}(q) = \bar{\rho}^P(q) + \bar{\rho}^{EM}(q)$, corresponding to the particle and electromagnetic contributions,

$$\begin{aligned} \bar{\rho}^P(q) &= \bar{\mu} \left(\frac{z_0}{L}\right)^{D-2} \delta(u) \delta^{(D-3)}(\vec{x}_T) \delta(z - z_0) \\ \bar{\rho}^{EM}(q) &= p_Q^2 \frac{\Gamma(D - 3/2) \sqrt{\pi} (2qL)^{5-2D} \delta(u)}{8\pi G_D (D - 4)! \left(1 + \frac{1}{q}\right)^{D-5/2}}. \end{aligned} \quad (3.48)$$

³For a static observer at an event P , $\vec{u} = \vec{\xi}/V(p)$, with $V = (-\xi^a \xi_a)^{1/2}$ the redshift factor and $\vec{\xi}$ the timelike Killing vector field of the spacetime. Then $\bar{\mu} = -u^a p_a|_P$ is the energy of a particle with momentum p_a as determined by the observer \vec{u} who is present at the event P on the worldline of the particle at which the energy is measured.

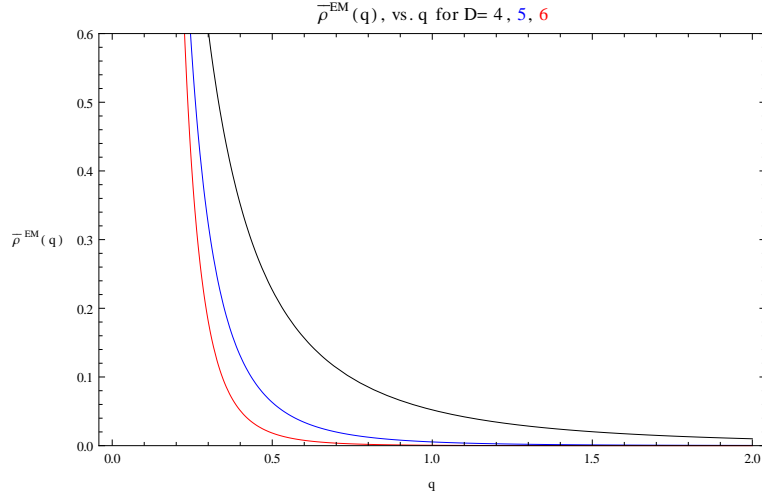


Figure 3.1: Graph for the electromagnetic contribution to the energy $\bar{\rho}^{EM}$ density versus the chordal coordinate q for dimensions $D = 4$ (black), $D = 5$ (blue) and $D = 6$ (red). This contribution forms an energetic halo around the solid particle-like nucleus, located at $q = 0$. Note that $\bar{\rho}^{EM}(q)$ diverges at the origin, such that the contribution of $\bar{\rho}^{EM}(q)$ to the total energy of the shock wave’s source is infinite.

As we see, the electromagnetic energy-momentum tensor of the AdS-RN solution contains, after the infinite boost limit, a halo of energy weighted by p_Q^2 . Thus the source of the AdS-RN shock wave computed here is a sort of energetic halo surrounding a relativistic massless “nucleus” of energy $\bar{\mu}$. In addition, although the energetic halo vanishes for $q \rightarrow \infty$, its contribution to the total energy of the shock wave’s source is infinite,

$$\int_0^\infty dq \bar{\rho}^{EM}(q) \rightarrow \infty, \quad (3.49)$$

because of $\bar{\rho}^{EM}(q)$ diverges at $q \rightarrow 0$ as q^{5-2D} (see fig. 3.1).

3.1.3 Some remarks

The wave profile of the AdS-RN shock wave computed here, equation (3.25), depends on two parameters p_M and p_Q^2 related respectively to the mass and charge of the AdS-RN solution. However we have not related them to physical observables.

The physical meaning of p_M^2 can be elucidated by fixing $p_Q^2 = 0$ and substituting the wave profile (3.25) and energy-momentum tensor (3.47) in the wave equation (2.75) ($\bar{H}(u, z, \vec{x}_T) = \Phi^{(RN)}(p_M, p_Q^2; q)\delta(u)$). After a bit of

algebra we obtain the equation

$$\bar{\mu} = \frac{2(D-2)\pi^{\frac{D-1}{2}}}{8\pi G_D \Gamma\left(\frac{D-1}{2}\right)} p_M. \quad (3.50)$$

Through (3.4), this is equivalent to $\bar{\mu} = \gamma m$, being m the mass of the AdS-RN solution, in such a way that $\bar{\mu}$ remains fixed while the infinite boost limit is taken. This enforced the definition of $\bar{\mu}$ given in (3.44) as the relativistic mass of the particle contribution to the AdS-RN shock wave measured by a static observer present at the worldline followed by the massless nucleus of (3.48). It is also interesting to introduce the relativistic energy μ as measured from the conformal boundary of AdS_D,

$$\mu = \xi^a p_a = \frac{L}{z_0} \bar{\mu}. \quad (3.51)$$

This can be also viewed as the energy measured respect to the coordinate time t of the background, while $\bar{\mu}$ is the energy as measured with respect to the proper time of a static observer at the particle worldline. This is the energy defined and used in [45, 51, 53, 55, 60] and related works as the energy of AdS gravitational shock waves. Once we have established its physical meaning by relating it to $\bar{\mu}$, we shall use μ instead of $\bar{\mu}$ in the subsequent equations.

By analogy with (3.50), from the charge parameter p_Q^2 we can define a sort of electrostatic energy e^2 as

$$e^2 = \frac{(D-2)(D-3)}{8\pi G_D} p_Q^2. \quad (3.52)$$

However, although p_Q^2 derives from the charge of the AdS-RN solution, e^2 is no more associated to any charge. Indeed, the source of the AdS-RN shock wave have not any charge. We can see it from computing the infinite boost limit over the Maxwell field of the AdS-RN solution. Note that the electromagnetic field is computed as usual, i.e. $F_{ab} = \partial_a A_b - \partial_b A_a$, since $F = dA$ and thus the connection does not influence in its computation. Then, from (3.1), we have only one component,

$$F_{rr} = \left(\frac{(D-2)(D-3)}{2} \right)^{1/2} \frac{Q}{r^{D-2}}. \quad (3.53)$$

In coordinates $\{Z^0, Z^i, Z^D\}$ this is

$$F_{0D} = \left(\frac{(D-2)(D-3)}{2} \right)^{1/2} \frac{Q}{Lr^{D-3}}. \quad (3.54)$$

It results in an expression linear in Q and without possibility to include positive powers of γ after doing a boost. Thus, according to the scaling taken for the shock wave metric computation, the electromagnetic strength tensor vanishes after the infinite boost limit. In other words, the AdS-RN shock wave does not act as source for any electromagnetic field [61, 84]. Although e^2 is related to the electrostatic charge of the AdS-RN solution, it has not any electromagnetic nature. We conclude that (3.39) is just a residual energetic contribution inherited from the original electromagnetic nature of the AdS-RN solution which is not associated to any electromagnetic charge. This contribution to the energy-momentum tensor appears because it depends quadratically in the electromagnetic field strength F and thus quadratically in Q . In addition, such contribution spreads the energy sourcing the AdS-RN shock wave.

In terms of μ and e^2 , the wave equation (2.70) takes the form

$$\begin{aligned} \left[\Delta_{\mathbb{H}_{D-2}} - \frac{D-2}{L^2} \right] \Phi^{(RN)}(q) = \\ - 16\pi \left(\frac{G_D \mu}{L^{D-3}} \right) \frac{z_0^{D-1}}{L^2} \delta(z - z_0) \delta^{(D-3)}(\vec{x}_\perp) \\ - 16\pi \frac{\Gamma(D-3/2)\sqrt{\pi}}{2^{2D-5}(D-2)!} \left(\frac{G_D e^2}{L^{2(D-3)}} \right) \frac{L}{(q^2 + q)^{D-5/2}}, \end{aligned} \quad (3.55)$$

where $G_D \mu / L^{D-3}$ and $G_D e^2 / L^{2(D-3)}$ are dimensionless parameters. The solution to this equation is given by equation (3.26),

$$\begin{aligned} \Phi^{(RN)}(\mu, e^2; q) = 16\pi \frac{\Gamma\left(\frac{D-2}{2}\right)}{2^{D-1}(D-1)\pi^{\frac{D-2}{2}}} \left(\frac{G_D \mu}{L^{D-3}} \right) \frac{z_0}{q^{D-2}} \\ \times {}_2F_1\left(D-2, \frac{D}{2}; D; -1/q\right) - 16\pi \frac{2^{2(2-D)}\sqrt{\pi}\Gamma\left(\frac{2D-3}{2}\right)}{(D-2)^2(D-3)!} \left(\frac{G_D e^2}{L^{2(D-3)}} \right) \\ \times \frac{L}{q^{2D-5}} {}_2F_1\left(2D-5, \frac{2D-3}{2}; 2D-3; -1/q\right). \end{aligned} \quad (3.56)$$

Note that for $e = 0$ we have the gravitational shock wave obtained from the AdS-Schwarzschild solution by means of the infinite boost limit done here, which we call AdS-Sch shock waves, with wave profile

$$\Phi^{(Sch)}(\mu; q) = \Phi^{(RN)}(\mu, e^2 = 0; q). \quad (3.57)$$

Until now we have not specified anything about the relation between the charge and mass of the AdS-RN we started with. That is, whether it should be extremal ($M = Q$), subextremal ($M > Q$) or superextremal ($M < Q$)

(see Appendix B), i.e. we have not established any difference in the final gravitational shock wave depending on performing the infinite boost limit over a AdS-RN black hole or over a naked singularity. In fact, the character of the initial black hole is immaterial. Note that we have taken the limit with the scaling

$$\gamma \sim 1/\epsilon^2, \quad M \sim \epsilon^2, \quad Q \sim \epsilon, \quad \text{with } \epsilon \rightarrow 0, \quad (3.58)$$

such that $p_M = \gamma M$ and $p_Q^2 = \gamma Q^2$ (or equivalently μ and e^2) remain fixed while the infinite boost limit is taken. On the other hand, for large enough Q^2 with respect to M^2 the AdS-RN solution becomes super-extremal. This condition, whatever the initial values of M and Q^2 are, is reached after a large enough boost taken with the scaling (3.58). Thus the gravitational shock wave (3.56) always arises from a super-extremal AdS-RN solution whatever the values of μ and e^2 are.

3.2 Fat gravitational shock waves

The AdS-RN shock waves are generated by a point-like source of energy μ surrounded by an energetic halo weighted by e^2 . Being ambitious, we can generalize them by spreading the source. That is, by considering gravitational shock waves generated from a no point-like transverse energy density traveling at the speed of light in AdS spacetime. We shall refer to these gravitational shock waves as fat shock waves [57].

Because we are interested in preserve the $O(D-2)$ symmetry of the shock waves, we restrict to energy densities (as measured by an static observer, see discussion about equation (2.79)) depending only in the chordal coordinate q . Since $T_{uu} = \frac{L}{z}\bar{\rho}(q)\delta(u)$, the Einstein equations for the shock wave (2.75) is reduced to the ordinary differential equation

$$q(q+1)\Phi''(q) + \frac{D-2}{2}(2q+1)\Phi'(q) - (D-2)\Phi(q) = -16\pi G_D L^2 \bar{\rho}(q), \quad (3.59)$$

where we have used that (see metric (A.26))

$$\Delta_{\mathbb{H}_{D-2}} = \frac{q(q+1)}{L^2}\partial_q^2 + \frac{(D-2)(2q+1)}{2L^2}\partial_q + \frac{1}{4L^2q(q+1)}\Delta_{S^{D-3}} \quad (3.60)$$

in chordal coordinate, and $\bar{H}(u, z, \vec{x}_T) = \Phi(q)\delta(u)$. Solving $\Phi(q)$ is not any trivial task, even though the axial symmetry allows to reduce the wave equation to a one-dimensional linear differential equation.

The general solution to the latter differential equation is given in terms of the Green's function⁴ of the differential operator $\Delta_{\mathbb{H}_{D-2}} - (D-2)/L^2$ with $O(D-2)$ symmetry,

$$\begin{aligned}\Phi(q) &= \int dq' \sqrt{|g|_{q'}} G(q, q') (-16\pi G_D L^2 \bar{\rho}(q')) \\ &= \int_0^\infty dq' [q'(q'+1)]^{\frac{D-4}{2}} \bar{G}(q, q') \bar{\rho}(q'),\end{aligned}\quad (3.61)$$

where we have integrated out the angular coordinates over the sphere S^{D-3} and include them in $\bar{G}(q, q') = -8\pi G_D L^2 (2L)^{D-2} \Omega_{D-3} G(q, q')$, such that $\bar{G}(q, q')$ satisfies

$$\begin{aligned}q(q+1)\bar{G}''(q, q') + \frac{D-2}{2}(2q+1)\bar{G}'(q, q') - (D-2)\bar{G}(q, q') \\ = -16\pi G_D L^2 \frac{\delta(q-q')}{[q(q+1)]^{\frac{D-4}{2}}}.\end{aligned}\quad (3.62)$$

To find the function $\bar{G}(q, q')$ we follow the construction of [51, 57]. We begin solving the associated homogeneous equation. It has two linearly independent solutions, $f_1(q)$ and $f_2(q)$, which are divergent at $q \rightarrow 0$ and $q \rightarrow \infty$ respectively,

$$f_1(q) = \frac{1}{q^{D-2}} {}_2F_1\left(D-2, \frac{D}{2}; D; -\frac{1}{q}\right), \quad f_2(q) = 2q+1. \quad (3.63)$$

Then we choose for $\bar{G}(q, q')$ a linear combination of $f_1(q)$ and $f_2(q)$ weighted by Heaviside step functions to integrate the delta function. Since $f_1(q)$ diverges at $q \rightarrow 0$, it must be weighted by $\theta(q-q')$, while $f_2(q)$ must be weighted by $\theta(q'-q)$. Thus we propose the ansatz

$$\bar{G}(q, q') = C_1(q') f_1(q) \theta(q-q') + C_2(q') f_2(q) \theta(q'-q), \quad (3.64)$$

for unknown functions of q' , $C_1(q')$ and $C_2(q')$. However, since the Green's function must be symmetric under the interchange between q and q' ,

$$C_1(q') f_1(q) = C_2(q) f_2(q') \quad \forall q, q' \in (0, \infty). \quad (3.65)$$

Thus $C_1(q') = \alpha f_2(q')$ and $C_2(q') = \alpha f_1(q')$, and

$$\bar{G}(q, q') = \alpha [f_2(q') f_1(q) \theta(q-q') + f_1(q') f_2(q) \theta(q'-q)], \quad (3.66)$$

⁴Given some differential equation $\hat{D}F(x^a) = f(x^a)$, where \hat{D} is any differential operator in a d -dimensional smooth Riemannian manifold (M, g) , the solution is given by $F(x^a) = \int d^d x' \sqrt{|g|_{x'}} G(x^a, x'^a) f(x'^a)$, being $G(x^a, x'^a)$ the Green's function for \hat{D} , i.e. $\hat{D}G(x^a, x'^a) = \frac{1}{\sqrt{|g|}} \delta^{(d)}(x^a - x'^a)$.

being $\alpha \in \mathbb{R}$ some constant to be determined by substituting in the differential equation (3.62). Since

$$\begin{aligned} \bar{G}'(q, q') = & \alpha [f_2(q')f_1'(q)\theta(q - q') + f_1(q')f_2'(q)\theta(q' - q)] \\ & + \alpha [f_2(q')f_1(q) - f_1(q')f_2(q)] \delta(q - q') \end{aligned} \quad (3.67)$$

and, deriving a second time⁵,

$$\begin{aligned} \bar{G}''(q, q') = & \alpha [f_2(q')f_1''(q)\theta(q - q') + f_1(q')f_2''(q)\theta(q' - q)] \\ & + \alpha [f_2(q')f_1'(q) - f_1(q')f_2'(q)] \delta(q - q'), \end{aligned} \quad (3.68)$$

the differential equation (3.62) gives an algebraic equation for α ,

$$\begin{aligned} \alpha q(q+1) [f_2(q')f_1'(q) - f_1(q')f_2'(q)] \delta(q - q') + \alpha \frac{D-2}{2} (2q+1) \\ \times [f_2(q')f_1(q) - f_1(q')f_2(q)] \delta(q - q') = \frac{-16\pi G_D L^2}{[q(q+1)]^{\frac{D-4}{2}}}. \end{aligned} \quad (3.69)$$

Then, integrating over q both sides and substituting $f_2(q) = 2q + 1$,

$$\alpha [2f_1(q') - (2q' + 1)f_1'(q')] = \frac{16\pi G_D L^2}{[q'(q' + 1)]^{\frac{D-2}{2}}}. \quad (3.70)$$

Because of the difficulty inherent to compute with the Gauss hypergeometric function, evaluation of the right-hand side of this equation requires the use of the hypergeometric differential equation. Then, it follows that $W(q') = 2f_1(q') - (2q' + 1)f_1'(q')$ satisfies the differential equation

$$\frac{q'(q' + 1)}{2q' + 1} W'(q') = -\frac{D-2}{2} W(q'), \quad (3.71)$$

which solution is $W(q') = C[q(q+1)]^{D-2}$. Since at large q' we have $f_1(q') \sim q'^{2-D}$ and, moreover,

$$W(q') = 2f_1(q') - (2q' + 1)f_1'(q') \sim 2(D-1)q'^{2-D}, \quad (3.72)$$

the integration constant must be $C = 2(D-1)$. This fixes the value of α in equation (3.70) to be

$$\alpha = \frac{8\pi G_D L^2}{D-1}, \quad (3.73)$$

⁵The derivative in a distributional sense of the Dirac delta is defined as $\int dx \delta'(x - x_0)f(x) = -\int dx \delta(x - x_0)f'(x) = -f'(x_0)$. Therefore $\delta'(x - x_0)f(x) \equiv -\delta(x - x_0)f'(x)$

and thus

$$\bar{G}(q, q') = \frac{8\pi G_D L^2}{D-1} \begin{cases} \frac{2q+1}{q'^{D-2}} {}_2F_1(D-2, D/2; D; -1/q') & q < q', \\ \frac{2q'+1}{q^{D-2}} {}_2F_1(D-2, D/2; D; -1/q) & q > q'. \end{cases} \quad (3.74)$$

The knowledge of the Green's function lets us to determine the large q behavior of the fat shock waves profile $\Phi(q)$ when the transverse density $\bar{\rho}(q)$ has compact support. Since $q \gg q'$, from (3.61) $\Phi(q)$ only receives contribution from the piece of $\bar{G}(q, q')$ for $q > q'$. Thus the large q behavior of $\Phi(q)$ is given by

$$\Phi(q) \sim \frac{8\pi G_D L^2}{D-1} f_1(q) \int_0^\infty dq' (2q' + 1) [q'(q' + 1)]^{\frac{D-4}{2}} \bar{\rho}(q'), \quad (3.75)$$

where the compactness of the support of $\bar{\rho}(q)$ let us extend the integral to $q' \rightarrow \infty$. Since (see (A.19))

$$\begin{aligned} & \int d^{D-2} x \sqrt{g|_{\mathbb{H}_{D-2}}} (2q + 1) \\ &= \frac{1}{2} (2L)^{D-2} \Omega_{D-3} \int_0^\infty dq [q(q+1)]^{\frac{D-4}{2}} (2q+1), \end{aligned} \quad (3.76)$$

we can rewrite (3.75) as

$$\begin{aligned} \Phi(q) &\sim \frac{16\pi G_D}{2^{D-2} L^{D-4} (D-1) \Omega_{D-3}} f_1(q) \int d^{D-2} x' \sqrt{g|_{\mathbb{H}_{D-2}}} (2q' + 1) \bar{\rho}(q') \\ &= \frac{16\pi}{2^{D-2} (D-1) \Omega_{D-3}} \left(\frac{G_D \bar{E}}{L^{D-3}} \right) L f_1(q), \end{aligned} \quad (3.77)$$

where

$$\bar{E} = \int d^{D-2} x' \sqrt{g|_{\mathbb{H}_{D-2}}} (2q' + 1) \bar{\rho}(q') \quad (3.78)$$

could be understood as the total energy of the transverse distribution sourcing the fat shock wave as measured by a set of static observers located along the wavefront. Indeed, substituting here the energy distribution which sources an AdS-Sch shock wave, expressed in chordal coordinate as

$$\bar{\rho}(q) = \frac{2\bar{\mu}}{(2L)^{D-2} \Omega_{D-3}} \frac{\delta(q)}{[q(q+1)]^{\frac{D-4}{2}}}, \quad (3.79)$$

we obtain $\bar{E} = \bar{\mu} = \frac{z_0}{L} \mu$, and

$$\Phi(q) \sim 16\pi \frac{\Gamma\left(\frac{D-2}{2}\right)}{2^{D-1} (D-1) \pi^{\frac{D-2}{2}}} \left(\frac{G_D \bar{\mu}}{L^{D-3}} \right) L f_1(q) = \Phi^{(Sch)}(\bar{\mu}; q) \quad (3.80)$$

as it was expected. Here we have used the volume of the n -sphere,

$$\Omega_n = \frac{2\pi^{\frac{n+1}{2}}}{\Gamma\left(\frac{n+1}{2}\right)}. \quad (3.81)$$

In what follow, we are interested in describing the gravitational shock wave sourced by a (extremely) boosted extended source. That is equivalent to consider transverse energy densities for which \bar{E} is finite. Thus we restrict fat shock waves to those with transverse density [57]

$$\bar{\rho}(q) = \frac{2\bar{E}}{(2L)^{D-2}\Omega_{D-3}} \frac{F(\omega, q)}{[q(q+1)]^{\frac{D-4}{2}}}, \quad (3.82)$$

with ω being a parameter which measures the width of the energy density, i.e. how much the energy density is spread, and the shape function $F(\omega, q)$ satisfies the normalization condition

$$\int_0^\infty dq(2q+1)F(\omega, q) = 1 \quad (3.83)$$

for all ω . Note that $F(\omega, q)$ has not necessarily compact support. However, equation (3.77) remains valid as long as $F(\omega, q)$ goes to zero quickly enough, which is forced by this condition.

Fat waves are interesting because they arise from widespread sources and thus, in fat waves collisions, the width of sources is an additional element we have to take into account. It could play some role in the formation of the Penrose surface. Indeed, the authors of [57] showed that there is a critical behavior with the size of the source for the production of the Penrose trapped surface. In addition, although this must be analyzed for each case in particular, i.e. for each shape function $F(\omega, q)$ in equation (3.82), this critical behavior depends strongly with the background dimension. For the general case of shape functions regularizing a delta function, i.e. satisfying⁶

$$\lim_{\omega \rightarrow 0^+} F(\omega, q) = \delta(q), \quad (3.84)$$

in [57] it was found that for $D = 4$ and $D = 5$ dimensions, the formation of the Penrose trapped surface exhibits a critical behavior with ω . For $D = 4$, the collision below the critical situation results in two Penrose surfaces, one inside the other, and we consider only the outermost surface. As counterpoint, for

⁶In particular, this implies $F(\omega, q = 0) \neq 0$. In some sense we are doing a rude expansion of the point-like sources of the AdS-Sch shock waves, being ω a kind of diluting parameter.

$D = 5$ we have only a trapped surface below the critical point. Near the critical value, the size q_0 of the trapped surface decreases as ω approaches ω_c following laws

$$q_0 - q_c \sim (\omega_c - \omega)^{\gamma_D}, \quad (3.85)$$

where the critical exponents are $\gamma_4 = 1/2$ and $\gamma_5 = 1$, and q_c is the size of the Penrose surface at the critical point. For $D = 5$, $q_c = 0$, while for $D = 4$ it has a finite value. Finally, for $D > 6$ there is no critical behavior and the Penrose surface always appears.

3.3 Holography for AdS-RN and fat gravitational shock waves

As we have already discussed in the introduction, the AdS/CFT conjecture builds a bridge between (super)gravity inside the AdS space and a strongly coupled gauge theory in the conformal boundary of AdS. In the framework of this correspondence, colliding gravitational shock waves in AdS are the gravitational dual for colliding energy lumps in the boundary theory. Here we discuss in some detail this issue and, in particular, compute the energy density of the holographic lumps corresponding to AdS-RN and fat shock waves.

3.3.1 Holographic stress tensor

In accordance with the holographic principle, the gravitational dynamics in the AdS space must contain the information to determine the energy-momentum vacuum expectation value of the boundary theory. From a series expansion of the Dirac-Born-Infeld action for the D3-brane it can be shown that gravitons in the bulk with polarizations parallel to the brane couple to the world-volume stress tensor [87, 88]. Thus the vacuum expectation value of the holographic energy-momentum tensor must be encoded in some way inside the metric giving the gravitational field in the AdS background. There are different approaches for extracting the holographic stress tensor from the line element [89]. Here we choose to compute it from the quasilocal gravitational energy defined by Brown and York [90].

In [91], Brown and York gave a construction (based on a Hamilton-Jacobi analysis) which allows to define a lower-dimensional energy-momentum tensor including both gravitational and matter dynamics inside a bounded region of spacetime. For indices μ, ν on the timelike⁷ boundary B of the spacetime

⁷Brown and York define a surface stress tensor in both timelike and spacelike bound-

region being considered, the surface stress tensor at B of York and Brown is given by

$$\tau_{\mu\nu} = \frac{2}{\sqrt{-\gamma}} (\pi_{\mu\nu}^{(sol)} - \pi_{\mu\nu}^{(0)}), \quad (3.86)$$

where $\gamma_{\mu\nu}$ is the induced metric at B , and $\pi_{\mu\nu}$ is the gravitational momentum conjugated to the surface metric,

$$\pi_{\mu\nu} = \frac{1}{16\pi G_D} \sqrt{-\gamma} (K_{\mu\nu} - K\gamma_{\mu\nu}), \quad (3.87)$$

with $K_{\mu\nu}$ the extrinsic curvature of B . The labels (sol) and (0) in (3.86) refer to the background geometry respect to which the gravitational momentum is computed: (sol) stands for the gravitational momentum computed from the extrinsic curvature of B as embedded in the spacetime that is been considered, while (0) stands for the gravitational momentum as if the boundary B was embedded in a reference spacetime such that the metric at B coincides with the induced metric $\gamma_{\mu\nu}$. Such reference spacetime is included in order to get a finite result when B encloses the entire spacetime (see [90] for a detailed discussion).

For our purposes, the spacetime region to be considered lies inside some (asymptotically AdS) spacetime. The spacetime metric in Poincaré coordinates is

$$ds^2 = \frac{L^2}{z^2} [dz^2 + g_{\mu\nu}(z, x)dx^\mu dx^\nu], \quad (3.88)$$

such that $g_{\mu\nu}(z, x)$ admits a series expansion⁸ in powers of z ,

$$g_{\mu\nu}(x, z) = \eta_{\mu\nu} + g_{\mu\nu}^{(D-1)}(x)z^{D-1} + \dots \quad (3.89)$$

We choose the region bounded by the hypersurface of constant Poincaré coordinate z , i.e. $B = \{(t, z, \vec{x}) / z = z_0 \in \mathbb{R}^+\}$. Note that, in this way, the limit $z_0 \rightarrow 0$ encloses the entire spacetime and gives the Brown-York stress tensor of all the spacetime. The normalized vector field orthogonal to the hypersurface $z = z_0$ is

$$n_\mu dx^\mu = \frac{L}{z} dz, \quad (3.90)$$

being the induced metric in B

$$\gamma_{\mu\nu} = \frac{L^2}{z^2} (\eta_{\mu\nu} + g^{(D-1)}z^{D-1} + \dots) \quad (3.91)$$

aries. However, for our purposes it shall be enough to consider the case of a timelike boundary.

⁸ Lower orders in z in the series expansion (3.89) will introduce additional terms to (3.98) related to conformal anomalies of the boundary field theory [92].

Then, a straightforward computation of the second fundamental form yields to

$$K_{\mu\nu}^{(sol)} = -\frac{L}{z_0}\eta_{\mu\nu} + \frac{D-3}{2}Lg_{\mu\nu}^{(D-1)}z_0^{D-3} + \dots, \quad K^{(sol)} = -\frac{D-1}{L} + \dots \quad (3.92)$$

where the ellipsis stands for higher order terms in z_0 which are not relevant for the calculation we are developing here, and $K^{(sol)} \equiv \gamma^{\mu\nu} K_{\mu\nu}^{(sol)}$. Substituting in (3.86), the contribution from the spacetime geometry to the surface stress tensor at B is

$$\tau_{\mu\nu}^{(sol)} = \frac{1}{8\pi G_D} \left[\frac{(D-2)L}{z_0^2}\eta_{\mu\nu} + \frac{(3D-5)L}{2}z_0^{D-3}g_{\mu\nu}^{(D-1)} + \dots \right]. \quad (3.93)$$

Notice that there is a negative power of z_0 which gives a divergent behavior at the spacetime boundary. We must choose the reference geometry such that its contribution to (3.86) cancels this term. With this in mind, we choose this reference spacetime to be

$$(ds^2)_{(0)} = \frac{L^2}{z^2} [dz^2 + (\eta_{\mu\nu} + g_{\mu\nu}^{(D-1)}z_0^{D-1}) dx^\mu dx^\nu]. \quad (3.94)$$

For this reference geometry we have,

$$K_{\mu\nu}^{(0)} = -\frac{L}{z_0^2}\eta_{\mu\nu} - Lg_{\mu\nu}^{(D-1)}z_0^{D-3}, \quad K^{(0)} = -\frac{D-1}{L}. \quad (3.95)$$

Thus, its contribution to the Brown-York stress tensor is

$$\tau_{\mu\nu}^{(0)} = \frac{(D-2)L}{z_0^2}\eta_{\mu\nu} + (D-2)Lg_{\mu\nu}^{(D-1)}z_0^{D-3}. \quad (3.96)$$

Subtracting equation (3.93) and the latter we get finally the ‘‘renormalized’’ stress tensor, i.e. without negative power in z_0 and, therefore, finite at $z_0 \rightarrow 0$,

$$\tau_{\mu\nu} = \tau_{\mu\nu}^{(sol)} - \tau_{\mu\nu}^{(0)} = \frac{(D-1)L}{16\pi G_D}g_{\mu\nu}^{(0)}z_0^{D-3} + \dots \quad (3.97)$$

It remains to compute the vacuum expectation value of the holographic energy-momentum tensor. Naively we could be tempted to think that, in the spirit of the holographic principle in general and the AdS/CFT connection in particular, it is the Brown-York surface stress tensor at the boundary of the entire spacetime, i.e. taking the limit $z_0 \rightarrow 0$ in the last equation. However, although the subtraction respect to the reference geometry has removed the negative power in z_0 appearing at (3.93), the resultant ‘‘renormalized’’ Brown-York stress tensor is zero for $z_0 \rightarrow 0$. The reason for this

discordance is that the holographic field theory lives in the *conformal* boundary of AdS_D, not at the boundary of AdS_D, and that means we have to kill the conformal dependence of (3.97) before to take the $z_0 \rightarrow 0$ limit. In order to do it, from the definition of $\tau_{\mu\nu}$, note that $\sqrt{-\gamma}\gamma^{\mu\nu}\tau_{\mu\nu}$ is invariant under a rescaling of z_0 . Thus, an additional factor $(L/z_0)^{D-3}$ needs to be introduced before taking the $z_0 \rightarrow 0$ limit. In this way, the holographic energy tensor is finally founded to be

$$\begin{aligned}\langle T_{\mu\nu} \rangle_{CFT} &= \lim_{z_0 \rightarrow 0} \left(\frac{L}{z_0} \right)^{D-3} \left[\frac{(D-1)L}{16\pi G_D} g_{\mu\nu}^{(D-1)} z_0^{D-3} + \dots \right] \\ &= \frac{(D-1)L^{D-2}}{16\pi G_D} g_{\mu\nu}^{(D-1)}.\end{aligned}\quad (3.98)$$

It is interesting to realize that only the $(D-1)$ order in the series expansion of $g_{\mu\nu}(z, x)$ contributes to the holographic energy-momentum tensor.

The expression we have obtained can be applied to any asymptotically AdS spacetime of the form (3.88) as the recipe to extract the vacuum expectation value of the holographic stress tensor. In particular it can be applied to AdS gravitational shock waves. Since the chordal coordinate q near the boundary of the hyperbolic space \mathbb{H}_{D-2} scales with z as

$$q = \frac{1}{4zz_0} [(z - z_0^2) + (\vec{x}_T)^2] \implies q \simeq \frac{z_0^2 + \vec{x}_T^2}{4z_0} \frac{1}{z}, \quad (3.99)$$

for a gravitational shock wave in AdS background, $ds^2 = L^2/z^2[-dudv + dz^2 + d\vec{x}_T^2 + \frac{z}{L}\Phi(q)\delta(u)du^2]$, we find

$$g_{uu}^{(D-1)} = \frac{\delta(u)}{L} \Phi(q)|_{z^{D-2}}, \quad (3.100)$$

where

$$\Phi(q)|_{z^{D-2}} = \frac{1}{(D-2)!} \left(\frac{4z_0}{z_0^2 + \vec{x}_T^2} \right)^{D-2} \frac{d^{D-2}}{dw^{D-2}} \Phi(w^{-1}) \Big|_{w \rightarrow 0} \quad (3.101)$$

is the $D-2$ order in a series expansion of $\Phi(q)$ in powers of the depth coordinate z . Applied to the case of two colliding gravitational shock waves with impact parameter ($\Delta z = |z_+ - z_-|, \vec{b}$), line element (2.84), the expectation value of the holographic stress tensor results in

$$\begin{aligned}\langle T_{uu} \rangle_{CFT} &= \frac{(D-1)L^{D-3}}{16\pi G_D} \delta(u) \Phi_+(q_+)|_{z^{D-2}}, \\ \langle T_{vv} \rangle_{CFT} &= \frac{(D-1)L^{D-3}}{16\pi G_D} \delta(v) \Phi_-(q_-)|_{z^{D-2}},\end{aligned}\quad (3.102)$$

with all the other components vanishing. That corresponds with two colliding ultrarelativistic energy lumps with energy distributions given by the $D - 2$ order in z of the wave profiles $\Phi_{\pm}(q_{\pm})$. Thus colliding AdS shock waves are the gravitational dual for colliding energy lumps at the boundary field theory.

3.3.2 Holographic dual for colliding shock waves

Naively, we would expect that differently sourced AdS gravitational shock waves result in different energy distributions of the colliding energy lumps in the holographic theory. Therefore, we would be able construct improved configurations to model thermalized sQGP production from high energy heavy ion collisions by tuning in an suitable way the energy distribution $\bar{\rho}(q)$ in (2.79). However, as we shall see now, both AdS-RN shock waves and AdS-Sch or fat shock waves give rise to the same holographic energy distributions.

Let us begin considering AdS-RN shock waves. Then, equation (3.101) gives

$$\Phi_{\pm}^{(RN)}(q_{\pm}) \Big|_{z^{D-2}} = \frac{2^{5-D} \Gamma\left(\frac{D-2}{2}\right)}{(D-1)\pi^{\frac{D-4}{2}}} \left(\frac{G_D \mu}{L^{D-3}}\right) z_{\pm} \left[\frac{4z_{\pm}}{z_{\pm}^2 + \left(\vec{x}_T \pm \frac{\vec{b}}{2}\right)^2} \right]^{D-2} \quad (3.103)$$

where we have used the definition of the hypergeometric function as a power series,

$$\begin{aligned} {}_2F_1(a, b; c; w) &= \frac{\Gamma(c)}{\Gamma(a)\Gamma(b)} \sum_{n=0}^{\infty} \frac{\Gamma(a+n)\Gamma(b+n)}{\Gamma(c+n)} \frac{w^n}{n!} \\ \implies \frac{d}{dw} {}_2F_1(a, b; c; w) &= \frac{ab}{c} {}_2F_1(a+1, b+1; c+1; w). \end{aligned} \quad (3.104)$$

Thus the holographic stress tensor for two (identical) colliding AdS-RN shock waves is

$$\begin{aligned} \langle T_{uu} \rangle_{CFT} &= \mu \frac{2^{D-3} \Gamma\left(\frac{D-2}{2}\right)}{\pi^{\frac{D-2}{2}}} \frac{z_+^{D-1}}{\left[z_+^2 + \left(\vec{x}_T - \frac{\vec{b}}{2}\right)^2 \right]^{D-2}} \delta(u), \\ \langle T_{vv} \rangle_{CFT} &= \mu \frac{2^{D-3} \Gamma\left(\frac{D-2}{2}\right)}{\pi^{\frac{D-2}{2}}} \frac{z_-^{D-1}}{\left[z_-^2 + \left(\vec{x}_T - \frac{\vec{b}}{2}\right)^2 \right]^{D-2}} \delta(v), \end{aligned} \quad (3.105)$$

This corresponds to two colliding energy lumps with transverse energy den-

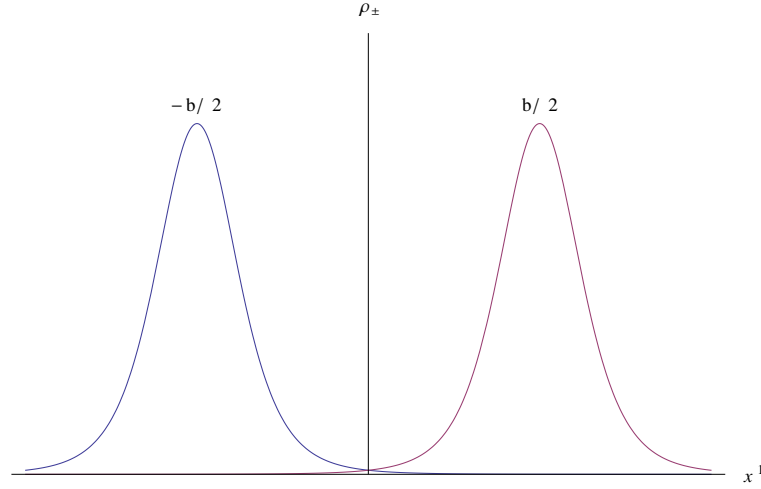


Figure 3.2: Plot for the energy densities (3.106) for $z_+ = z_-$ versus the x^1 coordinate, which we choose along the impact parameter parallel to the boundary of the AdS spacetime, \vec{b} . The maximums are located at $x^1 = \pm b/2$.

sities

$$\rho_{\pm} \left(\vec{x}_T \pm \frac{\vec{b}}{2} \right) = \mu \frac{2^{D-3} \Gamma \left(\frac{D-2}{2} \right)}{\pi^{\frac{D-2}{2}}} \frac{z_{\pm}^{D-1}}{\left[z_{\pm}^2 + \left(\vec{x}_T \pm \frac{\vec{b}}{2} \right)^2 \right]^{D-2}}, \quad (3.106)$$

confined to the transverse space to the direction of propagation because of the Lorentz contraction. Note that these energy densities have polynomial fall-offs, approaching 0 at $(\vec{x}_T \pm \vec{b}/2)^2 \rightarrow \infty$. In addition, they have maximum at $\vec{x}_T = \pm \vec{b}/2$ (see fig. 3.2)). Thus, the impact parameter parallel to the boundary of the AdS spacetime, \vec{b} , translates into the holographic theory as the impact parameter in the collision between the energy lumps, while the impact parameter along the holographic coordinate, $\Delta z = |z_+ - z_-|$, is not observable in this sense. Instead of that, z_{\pm} appears as the parameter controlling the width of the energy profiles of the lumps. In addition, notice that the parameter e^2 , related to the charge of the AdS-RN solution, does not appear in (3.106) and the energy densities of the lumps depend only on the energy (as measured from the boundary) μ of the colliding waves. Therefore, from the point of view of the holographic field theory, *before the collision* there are no difference between colliding AdS-RN shock waves or the more simple AdS-Sch shock waves (3.57).

The previous analysis can be also extended to fat shock waves. Since $q \sim 1/z$, $q \rightarrow \infty$ near the spacetime boundary. Thus, in the case we have a

fat shock wave with compact support, $q \in (0, q_0)$, equation (3.75) gives

$$\begin{aligned} \Phi(q)|_{z^{D-2}} &= \frac{8\pi G_D L^2}{(D-1)!} \left(\frac{4z_0}{z_0^2 + \vec{x}_T^2} \right)^{D-2} \frac{d^{D-2}}{dw^{D-2}} f_1(w^{-1}) \Big|_{w \rightarrow 0} \\ &\quad \times \int_0^{q_0} dq' (2q' + 1) [q'(q' + 1)]^{\frac{D-4}{2}} \bar{\rho}(q') \\ &= \frac{2^{5-D} \Gamma\left(\frac{D-2}{2}\right)}{(D-1)\pi^{\frac{D-4}{2}}} \left(\frac{G_D \bar{E}}{L^{D-3}} \right) L \left(\frac{4z_0}{z_0^2 + \vec{x}_T^2} \right)^{D-2} \end{aligned} \quad (3.107)$$

which coincides with (3.103) for $z_0 = z_{\pm}$, $\vec{b} = 0$ and $\mu = L/z_0 \bar{E}$. Thus, from the point of view of the holographic stress tensor, fat shock waves with compact support are indistinguishable from AdS-Sch shock waves. This is counter-intuitive since one would expect that an extended gravitational source had caused some change in the shape or width of the holographic stress tensor. Naively we could think that this surprise is because of the compactness of the energy density sourcing the fat shock wave, since the gravitational field of fat shock waves with compact support behaves in the same way than the gravitational field of AdS-Sch shock waves when the spacetime's boundary is reached. However the situation does not change notably if we consider fat shock waves sourced by a transverse energy density with no compact support. In this case we have an additional contribution to $\Phi(q)|_{z^{D-2}}$ coming from the piece of the Green's function (3.74) for $q < q'$. Defining

$$\begin{aligned} \xi(q) &= f_2(q) \int_q^\infty dq' [q'(q' + 1)]^{\frac{D-4}{2}} f_1(q') \bar{\rho}(q') \\ &= q^{\frac{D-2}{2}} f_2(q) \int_1^\infty dv [v(qv + 1)]^{\frac{D-4}{2}} f_1(qv) \bar{\rho}(qv), \end{aligned} \quad (3.108)$$

being $f_1(q)$ and $f_2(q)$ the functions of (3.63), the contribution to $\Phi(q)|_{z^{D-2}}$ for $q < q'$ is given by

$$\begin{aligned} \frac{8\pi G_D L^2}{(D-1)} \xi(q)|_{z^{D-2}} &= \frac{8\pi G_D L^2}{(D-1)!} \left(\frac{4z_0}{z_0^2 + \vec{x}_T^2} \right)^{D-2} \frac{d^{D-2}}{dw^{D-2}} \xi(w^{-1}) \Big|_{w \rightarrow 0} \\ &= \frac{2^{5-D} \Gamma\left(\frac{D-2}{2}\right)}{(D-1)! \pi^{\frac{D-4}{2}}} \left(\frac{G_D \bar{E}}{L^{D-3}} \right) L \left(\frac{4z_0}{z_0^2 + \vec{x}_T^2} \right)^{D-2} \frac{d^{D-2}}{dw^{D-2}} \left[\frac{2+w}{w^2} \right. \\ &\quad \left. \times \int_1^\infty dv f_1\left(\frac{v}{w}\right) F\left(u, \frac{v}{w}\right) \right] \Big|_{w \rightarrow 0}, \end{aligned} \quad (3.109)$$

where we have used the parametrization of the energy density $\bar{\rho}(q)$ showed in (3.82). Since

$$f_1(v/w) \sim \left(\frac{w}{v}\right)^{D-2} + \dots \quad (3.110)$$

near $w \rightarrow 0$, the $(D - 2)$ -th derivative of the previous expression would be zero if and only if

$$F(u, v/w) \sim F_0(u) \left(\frac{w}{v}\right)^2 + \dots \quad (3.111)$$

when $w \rightarrow 0$. Then

$$\begin{aligned} \frac{8\pi G_D L^2}{(D-1)} \xi(q)|_{z^{D-2}} &= \frac{2^{5-D} \Gamma\left(\frac{D-2}{2}\right)}{(D-1)! \pi^{\frac{D-4}{2}}} \left(\frac{G_D \bar{E}}{L^{D-3}}\right) L \left(\frac{4z_0}{z_0^2 + \bar{x}_T^2}\right)^{D-2} \\ &\times F_0(u) \frac{d^{D-2}}{dw^{D-2}} \left[2w^{D-2} \int_1^\infty \frac{dv}{v^{D-2}} + O(w^{D-1}) \right] \Big|_{w \rightarrow 0} \\ &= \frac{2^{6-D} \Gamma\left(\frac{D-2}{2}\right)}{(D-1) \pi^{\frac{D-4}{2}}} \left(\frac{G_D \bar{E}}{L^{D-3}}\right) \frac{L F_0(u)}{D-3} \left(\frac{4z_0}{z_0^2 + \bar{x}_T^2}\right)^{D-2}. \end{aligned} \quad (3.112)$$

Thus, when this condition is satisfied, the additional contribution coming from values $q < q'$ resumes in a redefinition of \bar{E} in (3.107) given by

$$\bar{E} \rightarrow \bar{E} + \frac{2F_0(u)}{D-3} \bar{E}. \quad (3.113)$$

However, note that the scaling (3.111) contradicts the finite-energy condition (3.83).

We conclude that, before any collision, the size of the holographic energy lumps does not depend on the width of the gravitational shock waves propagating in the AdS spacetime, but only on the value of the holographic coordinate of the center of the source. Moreover, the shape of the holographic energy lumps, i.e. how they decay with the transverse coordinates from the center of each lump, can not be tuned in any way (they are always of Lorentzian type). Note that the functional dependence $\sim [z_0/(z_0^2 + \bar{x}_T^2)]^{D-2}$ is a consequence of the exclusive q dependence of the shock waves, which is fixed by the $O(D-2)$ symmetry of the solution. This means that we would have to sacrifice the $O(D-2)$ symmetry of the shock waves if we want to obtain changes in the shape of the holographic energy lumps. However, although the width of two colliding shock waves does not have any consequence in the shape of the energy lumps before the collision, this does not mean that it does not have observable consequences when the collision takes place. As we shall see in the next chapter, the trapped surface formation in the gravitational collision (and thus the thermalization of the plasma produced after the energy lump collision) is drastically affected by the charge parameter e^2 in the case of Reissner-Nordström shock wave collisions [60] or the width of the waves in the more general case of fat shock waves collision [57]. That is not any intricate jigsaw puzzle, since it indicates the dependence of the holographic collision with the expectation vacuum value of some boundary field which has not been specified.

3.3.3 Comparison with boosted Woods-Saxon potential

Our final motivation to study AdS shock wave collisions is modeling thermalization in heavy-ion collisions via the gauge/gravity connection. Obviously, the more precise the holographic energy-momentum tensor describing a boosted heavy-ion is, the more accurate the model will be. That means we should tune μ and $z_0 = z_{\pm}$ in (3.106) such that the holographic energy lumps resemble as much as possible highly boosted heavy nuclei.

For a heavy nucleus at rest, the energy density can be read off the Woods-Saxon number density [51], and thus the energy-momentum tensor is

$$\langle T_{00} \rangle_{WS}(r) = \frac{\rho_0}{1 + e^{\frac{r-R}{a}}}, \quad (3.114)$$

where a is a length scale measuring the “surface thickness” of the nucleus, and $R = r_0 A^{1/3}$ is the nuclear radius, with $r_0 = 1.25 fm$ and A the mass number. After a boost $x \rightarrow \gamma(x + \beta t)$, the stress tensor components describing a heavy nucleus are

$$\langle T_{uu} \rangle_{WS} = \frac{\gamma^2(1 + \beta)^2}{4} \langle T_{00} \rangle_{WS}(r'), \quad \langle T_{vv} \rangle_{WS} = \frac{\gamma^2(1 - \beta)^2}{4} \langle T_{00} \rangle_{WS}(r'), \quad (3.115)$$

where $r' = \gamma^2(x + \beta t)^2 + \vec{x}_T^2$. Keeping $\bar{\rho}_0 \equiv \gamma\rho_0$ fixed we can take the infinite boost limit. Then, using the lemma (2.47), the vv component vanishes, whereas the uu components results in a transverse energy density,

$$\langle T_{uu} \rangle_{WS} = \rho_{WS}(\vec{x}_T) \delta(u), \quad (3.116)$$

where

$$\rho_{WS}(\vec{x}_T) = 2\bar{\rho}_0 \int_0^{\infty} \frac{d\omega}{1 + e^{\frac{\sqrt{\omega^2 + \vec{x}_T^2} - R}{a}}}. \quad (3.117)$$

Unfortunately, this expression cannot be integrated. We can recast it in an integral expression with finite limits instead,

$$\rho_{WS}(\vec{x}_T) = 2\bar{\rho}_0 |\vec{x}_T| \int_0^{\pi/2} \frac{d\theta}{\cos^2 \theta \left(1 + e^{\frac{|\vec{x}_T|}{a \cos \theta} - \frac{R}{a}} \right)}, \quad (3.118)$$

which is more suitable for numerical computations.

There are two quantities we can use to characterize an energy density, which, by means of direct comparison with the infinitely boosted nuclei we have obtained, can be used to tune μ and z_0 in (3.106). Such quantities

are the expectation value of the energy, $\langle E \rangle_{ws}$, and the transverse energy-weighted mean squared size, $\langle \vec{x}_T^2 \rangle_{ws}$. For the energy density of a boosted nucleus (3.117), the first one is given by

$$\langle E \rangle_{ws} = \bar{\rho}_0 \int_{-\infty}^{\infty} \int_{\mathbb{R}^{D-3}} \frac{d\omega d^{D-3}x_T}{1 + e^{\frac{\sqrt{\omega^2 + \vec{x}_T^2} - R}{a}}}. \quad (3.119)$$

Note that $\{\omega, \vec{x}_T\}$ covers the entire Euclidean space \mathbb{R}^{D-2} . Defining $u^2 = (\omega^2 + \vec{x}_T^2)/a^2$ and integrating over the volume of the $(D-3)$ -sphere,

$$\begin{aligned} \langle E \rangle_{ws} &= \bar{\rho}_0 a^{D-2} \Omega_{D-3} \int_0^{\infty} \frac{u^{D-3} du}{1 + e^{u - \frac{R}{a}}} \\ &= \bar{\rho}_0 a^{D-2} \Omega_{D-3} \Gamma(D-2) F_{D-3} \left(\frac{R}{a} \right), \end{aligned} \quad (3.120)$$

where $F_s(x)$ is the complete Fermi-Dirac integral,

$$F_s(x) = \frac{1}{\Gamma(s+1)} \int_0^{\infty} \frac{t^s}{1 + e^{t-x}}, \quad (3.121)$$

related to the polylogarithm by $F_s(x) = -Li_{s+1}(-e^x)$. Therefore, for a boosted heavy ion in $D-1$ flat dimensions,

$$\langle E \rangle_{ws} = -\rho_0 a^{D-2} \frac{2\pi^{\frac{D-2}{2}} \Gamma(D-2)}{\Gamma(\frac{D-2}{2})} Li_{D-2} \left(-e^{\frac{R}{a}} \right). \quad (3.122)$$

In a similar way, we can compute the transverse energy-weighted mean squared size $\langle \vec{x}_T^2 \rangle_{ws}$. Note that transverse lengths are not affected by the boost. Thus we can compute $\langle \vec{x}_T^2 \rangle_{ws}$ directly from (3.114). It is given by

$$\langle \vec{x}_T^2 \rangle_{ws} = \frac{D-3}{D-2} \langle r^2 \rangle_{ws} = \frac{D-3}{D-2} \frac{\int d^{D-2}x \frac{r^2}{1 + e^{\frac{r-R}{a}}}}{\int d^{D-2}x \frac{1}{1 + e^{\frac{r-R}{a}}}}, \quad (3.123)$$

since, supposing heavy ions at rest are isotropic, $\langle r^2 \rangle_{ws} = (D-2) \langle x_i^2 \rangle_{ws}$ for any coordinate x_i . Integrating over the angular coordinates, we are left with

$$\langle \vec{x}_T^2 \rangle_{ws} = a^2 \frac{D-3}{D-2} \frac{\int_0^{\infty} \frac{u^{D-1} du}{1 + e^{u - R/a}}}{\int_0^{\infty} \frac{u^{D-3} du}{1 + e^{u - R/a}}} = a^2 \frac{(D-3)\Gamma(D)}{\Gamma(D-1)} \frac{F_{D-1}(\frac{R}{a})}{F_{D-3}(\frac{R}{a})}. \quad (3.124)$$

In terms of polylogarithms, that is

$$\langle \vec{x}_T^2 \rangle_{WS} = a^2(D-1)(D-3) \frac{Li_D\left(-e^{\frac{R}{a}}\right)}{Li_{D-2}\left(-e^{\frac{R}{a}}\right)}. \quad (3.125)$$

Equations (3.122) and (3.125) characterize physically the transverse energy density describing an infinitely boosted heavy nuclei.

The same computation can be carried out for the holographic energy lumps (3.106). Omitting the impact parameter b and defining $z_0 = z_{\pm}$, the expectation value $\langle E \rangle_{CFT}$ is

$$\langle E \rangle_{CFT} = \int d^{D-3}x_T \rho_{CFT}(\vec{x}_T), \quad (3.126)$$

where

$$\rho_{CFT}(\vec{x}_T) = \mu \frac{2^{D-3} \Gamma\left(\frac{D-2}{2}\right)}{\pi^{\frac{D-2}{2}}} \frac{z_0^{D-1}}{(z_0^2 + \vec{x}_T^2)^{D-2}}. \quad (3.127)$$

Integrating over the volume of the $(D-4)$ -sphere,

$$\langle E \rangle_{CFT} = \mu \frac{2^{D-2} \Gamma\left(\frac{D-2}{2}\right)}{\pi^{1/2} \Gamma\left(\frac{D-3}{2}\right)} \int_0^\infty \frac{u^{D-4} du}{(1+u^2)^{D-2}}. \quad (3.128)$$

This integral results in Gaussian hypergeometric functions,

$$\begin{aligned} \int_0^\infty \frac{u^{D-4} du}{(1+u^2)^{D-2}} &= \lim_{u \rightarrow \infty} \left[\frac{u^{D-3}}{(D-3)} {}_2F_1\left(\frac{D-3}{2}, D; \frac{D-1}{2}; -u^2\right) \right. \\ &\quad + \frac{2u^{D-1}}{(D-1)} {}_2F_1\left(\frac{D-1}{2}, D; \frac{D+1}{2}; -u^2\right) \\ &\quad \left. + \frac{u^{D+1}}{(D+1)} {}_2F_1\left(\frac{D+1}{2}, D; \frac{D+3}{2}; -u^2\right) \right]. \end{aligned} \quad (3.129)$$

After a bit of algebra and using the first Pfaff transformation for hypergeometric functions to compute the limit (see equation (C.26) of Appendix C), the result is

$$\int_0^\infty \frac{u^{D-4} du}{(1+u^2)^{D-2}} = \frac{\Gamma\left(\frac{D-3}{2}\right) \Gamma\left(\frac{D-1}{2}\right)}{2(D-3)!}. \quad (3.130)$$

Thus, substituting in (3.128)

$$\langle E \rangle_{CFT} = \mu. \quad (3.131)$$

Therefore, the energy of the gravitational shock waves, as measured from the boundary of the AdS spacetime, corresponds in the boundary conformal field

theory to the expectation value of the energy of the lumps. In addition, notice that the result does not depend on the dimension where the gravitational model is constructed. In a similar way, the energy-weighted mean squared size $\langle \vec{x}_T^2 \rangle_{CFT}$ for each energy lump is given by

$$\begin{aligned} \langle \vec{x}_T^2 \rangle_{CFT} &= \frac{\int d^{D-3} x_T \vec{x}_T^2 \rho_{CFT}}{\int d^{D-3} x_T \rho_{CFT}} \\ &= \frac{z_0^2}{\langle E \rangle_{CFT}} \frac{2^{D-2} \Gamma\left(\frac{D-2}{2}\right)}{\pi^{1/2} \Gamma\left(\frac{D-3}{2}\right)} \int_0^\infty \frac{u^{D-2} du}{(1+u^2)^{D-2}}. \end{aligned} \quad (3.132)$$

The integral here results, once more, in hypergeometric functions, such that

$$\begin{aligned} \int_0^\infty \frac{u^{D-2} du}{(1+u^2)^{D-2}} &= \frac{4(D-2)}{(D-1)(D-3)} \lim_{u \rightarrow \infty} \frac{u^{D-1}}{(1+u^2)^{D-1}} \\ &\quad \times {}_2F_1\left(\frac{1-D}{2}, 1; \frac{D+1}{2}; -u^2\right). \end{aligned} \quad (3.133)$$

After applying the first Pfaff transformation and a bit of algebra, we get

$$\int_0^\infty \frac{u^{D-2} du}{(1+u^2)^{D-2}} = \frac{2(D-2)}{D-3} \frac{\Gamma\left(\frac{D-1}{2}\right) \Gamma\left(\frac{D+1}{2}\right)}{\Gamma(D)}. \quad (3.134)$$

Substituting in (3.132) we have finally,

$$\langle \vec{x}_T^2 \rangle_{CFT} = z_0^2. \quad (3.135)$$

Therefore the value of the holographic coordinate of the source of the shock waves inside the AdS fixes the energy-weighted size of the holographic lumps.

Matching the expectation values of energy and energy-weighted transverse size for both boosted heavy nuclei and holographic energy lumps, we can tune μ and z_0 in (3.106). Fixing $D = 5$ in (3.122) and (3.125),

$$\begin{aligned} \langle E \rangle_{WS} &= -8\pi \rho_0 a^3 Li_3\left(-e^{\frac{R}{a}}\right), \\ \langle \vec{x}_T^2 \rangle_{WS} &= 8a^2 \frac{Li_5\left(-e^{\frac{R}{a}}\right)}{Li_3\left(-e^{\frac{R}{a}}\right)}. \end{aligned} \quad (3.136)$$

Then, assuming a nucleus with $A \simeq 197$ (Gold) and a nuclear surface thickness $a \simeq 0.535$ fm (typical value),

$$\langle \vec{x}_T^2 \rangle_{WS} \simeq 23.80 \text{ fm}^2 \quad (3.137)$$

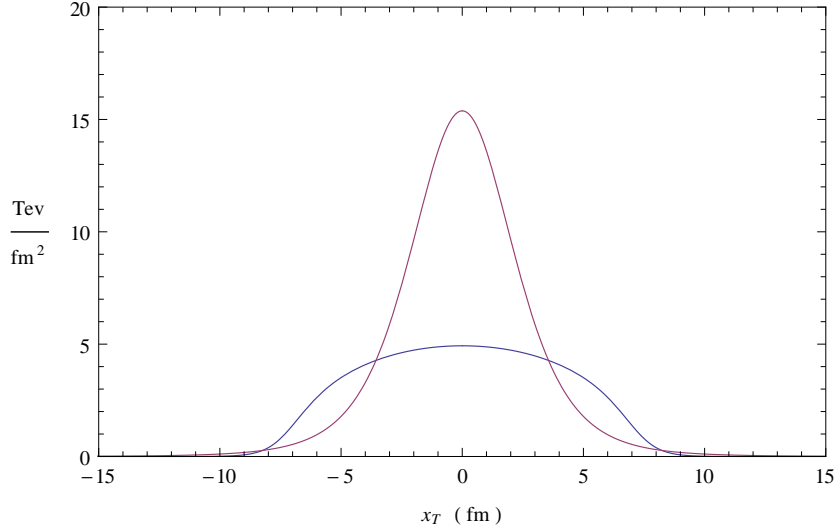


Figure 3.3: Plot for the energy densities (3.117) (blue) and (3.127) (red) with the values of z_0 , $\bar{\rho}_0$ and μ estimated in (3.138), (3.139) and (3.140). The plot for (3.117) has been done using a Montecarlo method for numerically calculating the integral expression (3.118).

and the equality $\langle \vec{x}_T^2 \rangle_{CFT} = \langle \vec{x}_T^2 \rangle_{WS}$ gives

$$z_0 \simeq 4.88 \text{ fm}. \quad (3.138)$$

The value for the energy density $\langle E \rangle_{WS}$ can be estimated from heavy ion collisions at the LHC. Thus, taking a center of mass energy 1150 TeV for heavy-ion collisions, $\langle E \rangle_{WS} \simeq 575 \text{ TeV}$, which leads to

$$\bar{\rho}_0 \simeq 0.34 \text{ TeV}/\text{fm}^3, \quad (3.139)$$

and, from $\langle E \rangle_{CFT} = \langle E \rangle_{WS}$,

$$\mu \simeq 575 \text{ TeV} \quad (3.140)$$

In fig. 3.3 the two transverse energy densities, equation (3.127) and equation (3.117), are showed with these values for z_0 and μ . As we see, whereas the transverse energy density obtained from the Woods-Saxon potential flattens, the transverse density of the holographic energy lumps has a definite peak, with a higher central density, such that it is not possible to tune the free parameters in the holographic theory to fit in any way the energy distribution of boosted heavy ions. However, that does not mean the results obtained from modeling the heavy-ion high-energy collision with holographic energy-lumps from gravitational colliding shock waves in the AdS spacetime cannot be interpreted as describing some features of the collisions of heavy ions, at least qualitatively.

Chapter 4

Critical phenomena in collisions of AdS gravitational shock waves

In the previous chapter we have computed the line element for AdS-RN and fat shock waves, as well as the energy-momentum tensor sourcing them, and showed that they are the gravitational dual for energy lumps propagating in the boundary field theory proposed by the AdS/CFT conjecture. In this chapter we go one step beyond and study the formation of Penrose trapped surfaces in the collisions of AdS-Sch and AdS-RN shock waves. As we argued in the introductory chapter, the formation of the Penrose trapped surface could be taken as signaling an eventual horizon formation after the collision and, therefore, as an indicative for plasma thermalization in the holographic boundary theory.

As it was expected, the formation of a Penrose trapped surface in a collision depends on the parameters determining the collision (energy, impact parameter, size, dimension, . . .), such that for each set of collision parameters there is a critical energy below of that there is no possibility to produce any Penrose trapped surface after the collision. That translates in the holographic theory as a critical behavior for strongly coupled plasma thermalization depending on the collision parameters as well as some vacuum expectation values [51, 55, 57, 60]. That can be taken as a first approximation model to sQGP production in high-energy heavy-ion collisions [52, 53].

Besides its physical interest because of the holographic connection between Penrose trapped surface formation and boundary plasma thermalization, the study of the critical formation of Penrose trapped surface has also a great mathematical interest. On one side, to analyze the purely mathematical problem in flat backgrounds teaches us more about how causal structure could evolve in asymptotically flat spacetimes [50, 56, 61]. On the other hand, the mathematical challenge of generalizing to spaces which are not

asymptotically flat, dS or AdS [45, 59, 93], would show where the difference between flat and nonflat backgrounds is respect to causal structure evolution.

This chapter is divided into three section. In the Section 4.1 we study the collision between AdS-Sch gravitational shock waves with nonzero impact parameter parallel to the boundary of the AdS background by means of numerical techniques. The case in which the AdS-Sch shock waves collision takes place with an impact parameter directed along the holographic coordinate, $\Delta z = |z_+ - z_-|$, is considered in Section 4.2. Because the connection between the value of the holographic coordinate inside AdS spacetime and energy redshift in the boundary, both cases have different holographic interpretations. Finally in Section 4.3 we examine the formation of the critical Penrose trapped surface for AdS-RN shock waves collision.

4.1 AdS-Sch shock wave collision

Let us begin with a brief and clear exposition of the setup. We have two AdS-Sch shock waves which propagate in opposite directions, i.e. they have support in $u = 0$ and $v = 0$ respectively. Both waves are supposed to have the same energy μ_0 as it was measured from the boundary. They are disposed such that they collide with some impact parameter \vec{b} parallel to the boundary of the spacetime and zero impact parameter in the holographic coordinate. As discussed in Section 2.5.1, the line element before the collision is

$$ds^2 = \frac{L^2}{z^2} \left(-dudv + dz^2 + d\vec{x}_T^2 + \frac{z}{L} \Phi_+^{(Sch)}(q_+) \delta(u) du^2 + \frac{z}{L} \Phi_-^{(Sch)}(q_-) \delta(v) dv^2 \right), \quad (4.1)$$

where the wave profiles $\Phi_{\pm}^{(Sch)}(q_{\pm}) \equiv \Phi_{\pm}^{(RN)}(\mu_0, e^2 = 0; q_{\pm})$ are solutions to the partial differential equation

$$\left[\Delta_{\mathbb{H}_{D-2}} - \frac{D-2}{L^2} \right] \Phi^{(Sch)}(q_{\pm}) = -16\pi \left(\frac{G_D \mu_{\pm}}{L^{D-3}} \right) \frac{z_0^{D-1}}{L^2} \delta(z - z_0) \delta^{(D-3)} \left(\vec{x}_T \pm \frac{\vec{b}}{2} \right), \quad (4.2)$$

with boundary condition $\lim_{q_{\pm} \rightarrow \infty} \Phi_{\pm} = 0$ and $\mu_{\pm} = \mu_0$. Without lost of generality, we take the impact parameter \vec{b} directed along the $x \equiv x^1$ coordinate, and

$$q_{\pm} = \frac{1}{4z z_0} \left[(z - z_0)^2 + \left(x \pm \frac{b}{2} \right)^2 + y^2 \right], \quad (4.3)$$

where $\vec{x}_T = (x, \vec{y})$. The result of the collision will be independent of this election because of the $SO(D-3)$ symmetry of the $\{x^1, \dots, x^{D-3}\}$ coordinates. The head-on collision corresponds to $b = 0$. The energy-momentum tensor sourcing the two waves is given by the particle contribution (3.46), having one component for each incoming shock wave,

$$\begin{aligned} T_{uu} &= \mu_0 \left(\frac{z}{L}\right)^{D-2} \delta(u) \delta^{(D-4)}(\vec{y}) \delta\left(x + \frac{b}{2}\right) \delta(z - z_0), \\ T_{vv} &= \mu_0 \left(\frac{z}{L}\right)^{D-2} \delta(v) \delta^{(D-4)}(\vec{y}) \delta\left(x - \frac{b}{2}\right) \delta(z - z_0), \end{aligned} \quad (4.4)$$

Finding the Penrose trapped surface supposes to solve an unusual boundary problem in \mathbb{H}_{D-2} , introduced in Section 2.5.4,

$$\begin{aligned} \left(\nabla_{\mathbb{H}_{D-2}}^2 - \frac{D-2}{L^2}\right) \left(\Phi_{\pm}^{(Sch)}(q_{\pm}) - \Psi_{\pm}(q_{\pm})\right) &= 0 \\ g^{ab} \partial_a \Psi_+(q_+) \partial_b \Psi_-(q_-) \Big|_{\mathcal{C}} &= 4, \\ \Psi_{\pm}(q_{\pm}) \Big|_{\mathcal{C}} &= 0. \end{aligned} \quad (4.5)$$

\mathcal{C} being the intersection of the Penrose trapped surface with \mathbb{H}_{D-2} . Solving this boundary problem is not exclusively reduced to compute the Penrose functions Ψ_{\pm} , but also the submanifold \mathcal{C} must be found. Since the energy-momentum tensor is the one for two colliding particles of certain energy without any other characteristic, we shall assume a topology S^{D-3} for \mathcal{C} .

4.1.1 head-on collision

Despite the complexity of (4.5), the boundary problem simplifies for head-on collisions enough to allow an analytical approach [51].

Since $b = 0$ for head-on collisions and the two sources in (4.4) have the same relativistic energy μ_0 ,

$$q_+ = q_- = q, \quad \implies \quad \Phi_{\pm}^{(Sch)}(q) \equiv \Phi^{(Sch)}(q), \quad \Psi_{\pm}(q) \equiv \Psi(q). \quad (4.6)$$

So the number of involved functions in (4.5) is drastically reduced¹. Moreover, the whole system depends only on q and thus the collision symmetry $SO(D-3)$ of (4.1) enhances to $SO(D-2)$ rotation symmetry around the propagation axis of the shock waves. As a consequence the submanifold \mathcal{C} must be a sphere determined by some chordal radius q_0 .

¹As we will see in next section, $b = 0$ also implies $z_0 = L$.

Writing the metric of \mathbb{H}_{D-2} in chordal coordinate q plus some angular coordinates in S^{D-3} (see Appendix A),

$$ds_{\mathbb{H}_{D-2}}^2 = \frac{L^2}{q(q+1)} dq^2 + 4L^2 q(q+1) d\Omega_{D-3}^2, \quad (4.7)$$

the boundary conditions in (4.5) are reduced to

$$q_0(q_0+1)(\Psi'(q_0))^2 = 4L^2, \quad \Psi(q_0) = 0. \quad (4.8)$$

Since $\Psi(q) > 0$ inside \mathcal{C} implies $\Psi'(q_0) \leq 0$, the first order differential condition can be simplified even more taking the negative branch of its square root,

$$\Psi'(q_0) = -\frac{2L}{\sqrt{q_0(q_0+1)}}. \quad (4.9)$$

On the other hand, $\Phi^{(Sch)}(q)$ satisfies the equation (4.2). The homogeneous partial differential equation associated to (4.2) coincides with the one satisfied by $\Phi^{(Sch)}(q) - \Psi(q)$ in the boundary problem. Thus the Penrose function $\Psi(q)$ must obey also the wave equation of the AdS-Sch shock waves. Computing the Beltrami-Laplace operator $\Delta_{\mathbb{H}_{D-2}}$ from (4.7),

$$\begin{aligned} \Delta_{\mathbb{H}_{D-2}} &= \frac{1}{\sqrt{g}} \partial_a (\sqrt{g} g^{ab} \partial_b) \\ &= \frac{q(q+1)}{L^2} \partial_q^2 + \frac{D-2}{2L^2} (2q+1) \partial_q + \frac{1}{4L^2 q(q+1)} \Delta_{S^{D-3}}, \end{aligned} \quad (4.10)$$

the differential equation satisfied by the Penrose function is

$$\begin{aligned} \frac{q(q+1)}{L^2} \Psi''(q) + \frac{D-2}{2L^2} (2q+1) \Psi'(q) - \frac{D-2}{L^2} \Psi(q) = \\ -16\pi \left(\frac{G_D \mu_0}{L^{D-3}} \right) \frac{2^{3-D} z_0}{L^2 [q(q+1)]^{\frac{D-4}{2}} \Omega_{D-3}} \delta(q), \end{aligned} \quad (4.11)$$

where Ω_{D-3} is the volume of S^{D-3} and we have used the identity

$$\delta(z - z_0) \delta^{(D-3)}(\vec{x}_T) = \left(\frac{L}{z_0} \right)^{D-2} \frac{2^{3-D} \delta(q)}{L^{D-2} [q(q+1)]^{\frac{D-4}{2}} \Omega_{D-3}} \quad (4.12)$$

to write the right-hand side in function of q . At this point, finding the Penrose trapped surface is reduced from computing two Penrose functions $\Psi_{\pm}(q_{\pm})$ and the shape of \mathcal{C} satisfying (4.5) to find only one Penrose function $\Psi(q)$ and a value of the chordal radius q_0 satisfying the ordinary differential

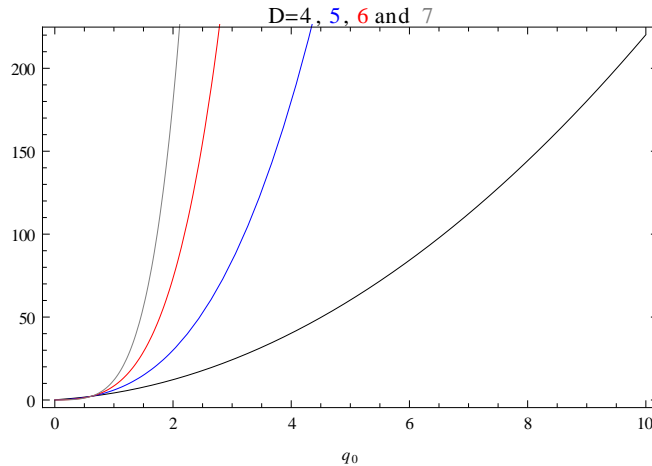


Figure 4.1: Left-hand side of (4.17) for $D = 4$ (black), $D = 5$ (blue), $D = 6$ (Red) and $D = 7$ (grey).

equation (4.11) with boundary conditions (4.8). In addition we will require that the Penrose function is regular at $q = 0$ for $\mu_0 = 0$ (i.e. when we have no source).

The solution to the differential equation (4.11) is given by the sum of a particular solution and the general solution to the associated homogeneous equation. The wave profile function $\Phi^{(Sch)}(q)$ can be taken as the particular solution, whereas the general solution to the associated homogeneous equation is $C_1 f_1(q) + C_2 f_2(q)$, where $C_{1,2}$ are some arbitrary constants and $f_{1,2}(q)$ are given in (3.63). Thus, the solution to (4.11) can be written as

$$\Psi(q) = \Phi^{(Sch)}(q) + C_1 f_1(q) + C_2 f_2(q). \quad (4.13)$$

The constants $C_{1,2}$ are then fixed by the initial conditions (4.8). The constant C_1 must be taken equal to zero since we have fixed the regularity of $\Psi(q)$ at $q = 0$ for $\mu_0 = 0$ as a requirement and $f_1(q)$ does not satisfy it. Thus, since $f_2(q) = 2q + 1$, C_2 is determined from the second condition in (4.8) to be

$$C_2 = -\frac{\Phi^{(Sch)}(q_0)}{2q_0 + 1}. \quad (4.14)$$

Substituting in (4.13), we have for the Penrose function

$$\Psi(q) = \Phi^{(Sch)}(q) - \Phi^{(Sch)}(q_0) \frac{2q + 1}{2q_0 + 1}. \quad (4.15)$$

It remains to compute q_0 in order to complete the solution to (4.5) for head-on collisions. This is done by substituting (4.15) in (4.9). In this way

we obtain an algebraic equation for q_0 ,

$$\Phi'^{(Sch)}(q_0) - \Phi^{(Sch)}(q_0) \frac{2}{2q_0 + 1} = -\frac{2L}{\sqrt{q_0(q_0 + 1)}}, \quad (4.16)$$

which, after substituting the expression for $\Phi^{(Sch)}(q)$ and doing some manipulations, is reduced to

$$\frac{16\pi}{2^{D-2}\Omega_{D-3}} \left(\frac{G_D\mu_0}{L^{D-3}} \right) = (2q_0 + 1) [q_0(q_0 + 1)]^{\frac{D-3}{2}}. \quad (4.17)$$

As long as this equation has a solution for some q_0 , we find that a Penrose trapped surface has been formed in the head-on collision. Notice that the right-hand side of this equation is a monotonically increasing function of q_0 in $[0, \infty)$, being zero for $q_0 = 0$, and thus the equation has always one unique solution (see fig. 4.1 and 4.2). In other words, a Penrose trapped surface is always formed in a head-on collision of two AdS-Sch gravitational shock waves, being unique and with chordal radius q_0 such that $q_0 = 0$ for $\mu_0 = 0$. For practical purposes, the transcendental equation (4.17) must be solved numerically by means of some algorithm as, for example, the Newton–Raphson method. In fig. 4.2 the solution for q_0 is showed for some values of D and $G_D\mu_0/L^{D-3}$.

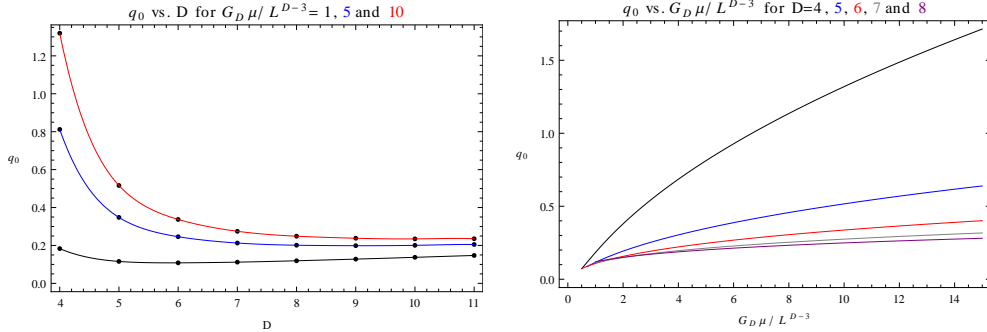


Figure 4.2: Numerical solution to (4.17). *Left panel.* q_0 versus D for energies $G_D\mu_0/L^{D-3} = 1$ (black), $G_D\mu_0/L^{D-3} = 5$ (blue) and $G_D\mu_0/L^{D-3} = 10$ (red). *Right panel.* q_0 versus $G_D\mu_0/L^{D-3}$ for dimensions $D = 4$ (black), $D = 5$, (blue), $D = 6$ (red), $D = 7$ (gray) and $D = 8$ (purple).

4.1.2 Off-center collision

Whereas the head-on collision admits an analytical approach to solve the shape of the submanifold \mathcal{C} and the Penrose trapped surface, the case with

nonzero impact parameter requires numerical techniques to face with the unusual boundary problem (4.5). The off-center collision for $D = 5$ is considered in [52] by means of a spectral method to solve for \mathcal{C} . On the other hand, we have solved the problem for $D = 4, 5, 6, 7$ and 8 in [55] using the finite difference discretization that we reproduce here. In both studies a critical value of the impact parameter depending on the energy of the sources has been found, such that no Penrose trapped surface is created beyond this critical value. Criticality in the impact parameter has also been observed in collisions in flat spacetime [56]. In addition, in [55] we found a scaling of the critical impact parameter with the energy depending on the dimension of the background.

Symmetries for off-center collisions are reduced respect to head-on collisions from $SO(D - 2)$ to $SO(D - 3)$, since only rotations keeping fixed the direction along the impact parameter are allowed. We define spherical coordinates in \mathbb{H}_{D-2} as (see Appendix A)

$$\begin{aligned} Y^0 &= \sqrt{r^2 + L^2}, & Y^1 &= r \cos \theta, \\ Y^i &= r \vartheta^i \sin \theta, & \sum_{i=2}^{D-2} (\vartheta^i)^2 &= 1, \end{aligned} \tag{4.18}$$

The angular coordinates are chosen such that the sources (4.4) are located at

$$r_0 = \frac{Lb}{2z_0}, \quad \theta_+ = 0, \quad \theta_- = \pi, \tag{4.19}$$

or equivalently, at $Y_{\pm}^0 = L(1 + \beta^2)^{1/2}$, $Y_{\pm}^1 = \pm L\beta$ and $Y_{\pm}^i = 0$ for $i = 2, \dots, D - 2$, where $\beta = r_0/L$. As a consequence of the way we have defined the angular coordinates, and the requirement $Y_{\pm}^{D-2} = 0$, the holographic coordinate of the sources and the impact parameter are not independent from one another. They are related by

$$z_0 = \frac{L}{(1 + \beta^2)^{\frac{1}{2}}}, \quad b = \frac{2L\beta}{(1 + \beta^2)^{\frac{1}{2}}}. \tag{4.20}$$

This corresponds to colliding shock waves whose holographic coordinate changes with its impact parameter, which is not a desirable property. Fortunately, since scale transformations are isometries of both AdS and hyperbolic spaces, we can use them to fix z_0 independent of b . Redefining Poincaré coordinates as

$$z \rightarrow \frac{z}{(1 + \beta^2)^{\frac{1}{2}}}, \quad x^\mu \rightarrow \frac{x^\mu}{(1 + \beta^2)^{\frac{1}{2}}}. \tag{4.21}$$

the collision happens at $z_0 = L$, with impact parameter $b = 2\beta L$. Also $r_0 = b/2$, keeping $Y_{\pm}^1 = \pm b/2$ and $Y_{\pm}^{D-2} = 0$. However, this transformation

changes the right-hand side of the partial differential equation for the wave profiles, equation (4.2). To keep its form we have to scale also the energy of the incoming waves μ_0 to a new value μ given by

$$\mu = \frac{\mu_0}{(1 + \beta^2)^{\frac{1}{2}}}. \quad (4.22)$$

In this way, we conserve the boundary problem for the Penrose surface up to scale transformations in the sense that the differential equations in (4.5) are the same before and after scale transformations. That is, to solve the Penrose surface for a collision with energy μ_0 and sources at $z_0 = L/(1+\beta^2)^{1/2}$ is equivalent to solve it for a collision at depth L and energy μ . Therefore, if the Penrose surface exists for the first, it also does for the second. Since collisions at a fixed holographic coordinate L are easier to analyze, we shall consider it to solve the Penrose trapped surface. Thus, in the following,

$$q_{\pm} = \frac{1}{4zL} [(z - L)^2 + (x^1 \pm b/2)^2 + \vec{y}^2]. \quad (4.23)$$

The metric of the \mathbb{H}_{D-2} space in spherical coordinates is

$$ds_{\mathbb{H}_{D-2}}^2 = \frac{L^2}{L^2 + r^2} dr^2 + r^2 d\theta^2 + r^2 \sin^2 \theta d\Omega_{D-4}^2. \quad (4.24)$$

The symmetry under $SO(D-3)$ transformations is explicit in this coordinates, leaving invariant the unitary sphere S^{D-4} . Thus the boundary problem we have to solve must only involve coordinates $\{r, \theta\}$. That is,

$$\Phi_{\pm}^{(Sch)}(q_{\pm}) = \Phi_{\pm}^{(Sch)}(r, \theta), \quad \Psi_{\pm}(q_{\pm}) = \Psi_{\pm}(r, \theta). \quad (4.25)$$

In addition, the coordinate θ can be used to parametrize \mathcal{C} as the set of points satisfying

$$r = LG(\theta), \quad (4.26)$$

for some function $G(\theta)$ under the condition $G(0) = G(2\pi)$. At this point we have transformed (4.5) in a two-dimensional boundary problem in the plane Y^1 - Y^{D-2} with $\{r, \theta\}$ the polar coordinates at this plane. In addition, the invariance with respect to rotations around the Y^1 axis implies reflexion symmetry respect to Y^1 . Thus,

$$\begin{aligned} \Phi_{\pm}^{(Sch)}(r, \theta) &= \Phi_{\pm}^{(Sch)}(r, -\theta), & G(\theta) &= G(-\theta), \\ \Psi_{\pm}(r, \theta) &= \Psi_{\pm}(r, -\theta). \end{aligned} \quad (4.27)$$

Also, because of the sources having the same energy μ , we have an additional reflexion symmetry respect to the Y^{D-2} axis,

$$\begin{aligned} \Phi_{\pm}^{(Sch)}(r, \theta) &= \Phi_{\mp}^{(Sch)}(r, \pi - \theta), & G(\theta) &= G(\pi - \theta), \\ \Psi_{\pm}(r, \theta) &= \Psi_{\mp}(r, \pi - \theta). \end{aligned} \quad (4.28)$$

Thanks to this symmetry it is only necessary to solve for one of the functions Ψ_{\pm} , and only one of the profile functions $\Phi_{\pm}^{(Sch)}$ must be taken into account. In this way, we halve the number of functions implied in the unusual problem we have to solve. Furthermore, (4.27) allows us solving only for $\theta \in [0, \pi]$, since the periodicity of $G(\theta)$ is lowered from 2π to π . These simplifications leads to a drastic simplification of the original problem, that now can be handled by numerical methods.

From the metric (4.24), the Beltrami-Laplace operator in \mathbb{H}_{D-2} in spherical coordinates is

$$\begin{aligned} \Delta_{\mathbb{H}_{D-2}} &= \frac{1}{\sqrt{g}} \partial_a (\sqrt{g} g^{ab} \partial_b) = \left(1 + \frac{r^2}{L^2}\right) \partial_r^2 + \frac{1}{r^2} \partial_\theta^2 \\ &+ \frac{(D-3)L^2 + (D-2)r^2}{rL^2} \partial_r + \frac{(D-4)}{r^2 \tan \theta} \partial_\theta + \frac{1}{r^2 \sin^2 \theta} \Delta_{S^{D-4}}. \end{aligned} \quad (4.29)$$

Defining $H(r, \theta) = \Phi_+(r, \theta) - \Psi_+(r, \theta)$, the partial differential equation in (4.5) reads now

$$\begin{aligned} &\left[\left(1 + \frac{r^2}{L^2}\right) \partial_r^2 + \frac{(D-3)L^2 + (D-2)r^2}{rL^2} \partial_r + \frac{1}{r^2} \partial_\theta^2 \right. \\ &\quad \left. + \frac{D-4}{r^2 \tan \theta} \partial_\theta - \frac{D-2}{L^2} \right] H = 0, \end{aligned} \quad (4.30)$$

where we have omitted the equation for Ψ_- according to the previous discussion. This two-dimensional partial differential equation has to be solved inside the contour $r = LG(\theta)$ with the boundary conditions specified in (4.5). However, $G(\theta)$ is unknown and, from a technical point of view, it is tremendously difficult to built an algorithm solving a partial differential equation inside an unknown boundary. At this point, we define a new radial coordinate ρ as

$$\rho = \frac{r}{LG(\theta)}. \quad (4.31)$$

In terms of this new radial coordinate, the submanifold \mathcal{C} in the plane Y^1 - Y^{D-2} is given by the curve $\rho = 1$, i.e. a circumference with radius 1, whatever the explicit form of $G(\theta)$ is, avoiding the technical difficulty of solving an equation inside an unknown boundary by numerical methods. In coordinates

$\{\rho, \theta\}$, the differential equation (4.30) is

$$\left\{ \left[1 + G^2 \rho^2 + \left(\frac{G'}{G} \right)^2 \right] \partial_\rho^2 + \frac{1}{\rho^2} \partial_\theta^2 - \frac{2G'}{\rho G} \partial_\rho \partial_\theta + \frac{1}{\rho} \left[2 \left(\frac{G'}{G} \right)^2 - \frac{G''}{G} - \frac{D-4}{\tan \theta} \left(\frac{G''}{G} \right) + (D-3) + (D-2)G^2 \rho^2 \right] \partial_\rho + \frac{D-4}{\rho^2 \tan \theta} \partial_\theta - (D-2)G^2 \right\} H(\rho, \theta) = 0, \quad (4.32)$$

which now can be solved numerically inside the circumference $\rho = 1$.

The boundary conditions for the last differential equations are the ones in (4.5). In coordinates $\{\rho, \theta\}$, they read

$$H(\rho = 1, \theta) = \Phi_+(r = LG(\theta), \theta) \quad (4.33)$$

$$\left[1 + \frac{G'}{G} + G^2 \right] \partial_\rho \Psi_+(\rho = 1, \theta) \partial_\rho \Psi_+(\rho = 1, \pi - \theta) = 4G(\theta). \quad (4.34)$$

where we have taken into account that $\Psi_-(r, \theta) = \Psi_+(r, \pi - \theta)$ and the fact that, from $\Psi_\pm|_{\mathcal{C}} = 0$,

$$\partial_\theta \Psi_\pm(\rho = 1, \theta) = 0. \quad (4.35)$$

The equation (4.33) is a Dirichlet boundary condition for H over the circumference $\rho = 1$. However, as we have discussed previously, it is not necessary to solve the problem in the whole circle, being enough to do it inside the half circle $\rho = 1$, $\theta \in [0, \pi]$. This requires an additional boundary condition over the $\theta = 0, \pi$ diameter (see fig. 4.3). This can be read from (4.27):

$$\partial_\theta H|_{\theta=0} = 0, \quad \partial_\theta H|_{\theta=\pi} = 0, \quad (4.36)$$

which is a Neumann boundary condition for H over the $\theta = 0, \pi$ diameter.

To tackle numerically the problem we use a finite difference method combined with a trial-and-correction loop [55, 56] as follow: Given values for the energy μ and the impact parameter b , we begin with some arbitrary ansatz $G_0(\theta)$ for the shape of \mathcal{C} and solve (4.32) inside $\rho = 1$, $\theta \in [0, \pi]$ with the Dirichlet condition (4.33) over $\rho = 1$ and the Neumann boundary condition over the $\theta = 0, \pi$ diameter. To do it we use a finite difference method over a 50×100 (angular \times radial) lattice and solve until a precision $\delta \sim 10^{-4}$ is reached. Then, from the solution obtained in this way, $(\Psi_+)_0 = H_0 + \Psi_+^{(Sch)}$, we compute

$$T_0(\theta) \equiv \left[1 + \frac{G'_0}{G_0} + G_0^2 \right] \partial_\rho (\Psi_+)_0(\rho = 1, \theta) \partial_\rho (\Psi_+)_0(\rho = 1, \pi - \theta) - 4G_0(\theta). \quad (4.37)$$

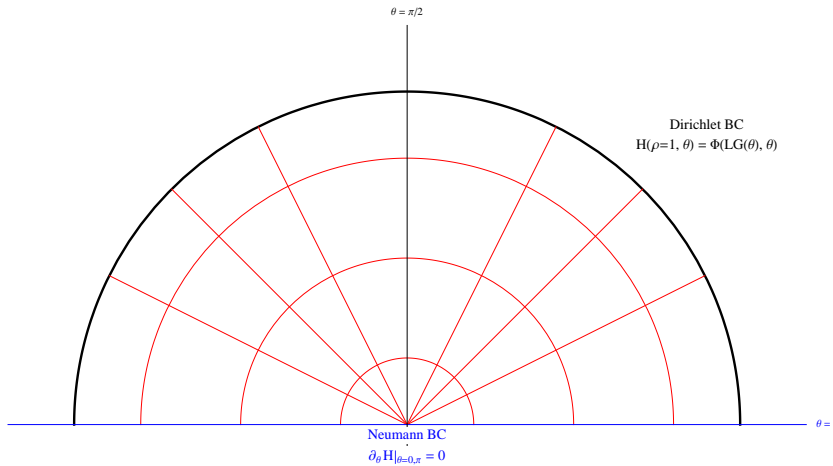


Figure 4.3: Region where (4.32) has to be solved, with boundary conditions (4.33) and (4.36). We construct a lattice inside it (red lines) and solve numerically using a finite difference method.

The function $T_0(\theta)$ measures the deviation of $G_0(\theta)$ to satisfy the boundary condition (4.34). From it we construct a new sampling shape for \mathcal{C} , $G_1(\theta)$, as

$$G_1(\theta) = G_0(\theta) + \epsilon T_0(\theta), \quad (4.38)$$

where $\epsilon \ll 1$, and repeat the procedure, computing a corrected solution H_1 , computing a new correction function $T_1(\theta)$ and so on. After a sufficient number of iterations (typically 10^5 with $\epsilon \cong 10^{-4}$), the correction function $T_i(\theta)$ converges to zero with the desired precision and the corrected function $G_i(\theta)$, approaches the shape of \mathcal{C} which is the exact solution to (4.5) for the given energy μ and impact parameter b . In the case the method described here does not converge, it is supposed there is no Penrose trapped surface for the values of the impact parameter and energy chosen. That is detected when the minimal value of the function $T_i(\theta)$ begins to oscillate at random. Usually this implies that the iteration of the code exceed 10^7 times, since convergence normally happens below 10^6 iterations. In fig. 4.4 and simplified scheme of the code is showed.

The solutions for \mathcal{C} with the previous algorithm for several impact parameters and energy $G_D \mu / L^{D-3} = 1$ in dimensions $D = 4, 5, 6, 7$ and 8 are showed in fig. 4.5. The most internal curve in each graph corresponds to the solution for a critical value of the impact parameter depending on the energy, $b_c(\mu)$, such that no any Penrose trapped surface is formed for impact parameters above this value [52, 55]. Our results show that for large enough impact parameter at fixed energy, both shock waves collide without enough interaction to create any Penrose trapped surface. A more detailed and exhaustive

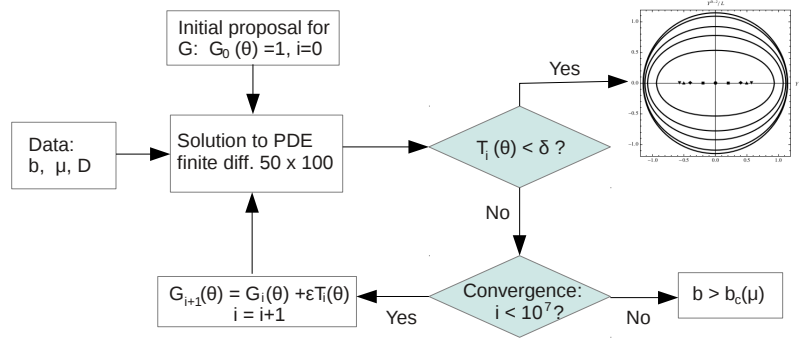


Figure 4.4: Simplified flux diagram for the code solving numerically the unusual boundary problem (4.32), (4.33) and (4.34). We apply this scheme in a sequential way from zero impact parameter until the critical value is reached. The initial function $G_0(\theta)$ is equaled to one when we are at low impact parameter. However, to get a quicker code, when we are close to the critical impact parameter we use the solution of the previous case solved to propose the initial $G_0(\theta)$.

numerical analysis in [55] shows that critical impact parameter grows with energy following the law

$$\frac{b_c(\mu)}{L} \sim \left(\frac{G_D \mu}{L^{D-3}} \right)^{\frac{1}{D-2}}, \quad (4.39)$$

where the proportionality constant is of order one. In fig. 4.6 it is shown the numerical data are well fitted by this scaling.

The scaling (4.39) is measured with respect to the AdS radius L . That is because the collision we have solved numerically is at a value $z = L$ of the holographic coordinate, and the value of z determines, as we saw in Section 3.3, the size of the energy lumps in the boundary theory. Thus the scaling (4.39) gives the dependence with energy of the critical impact parameter measured in units of the size of the energy lumps. That seems physically reasonable since it is expected that the critical impact parameter depends on the size of the colliding energy lumps. Indeed, since scale transformations can bring us from collisions at $z = L$ to collisions at any other value of z , we

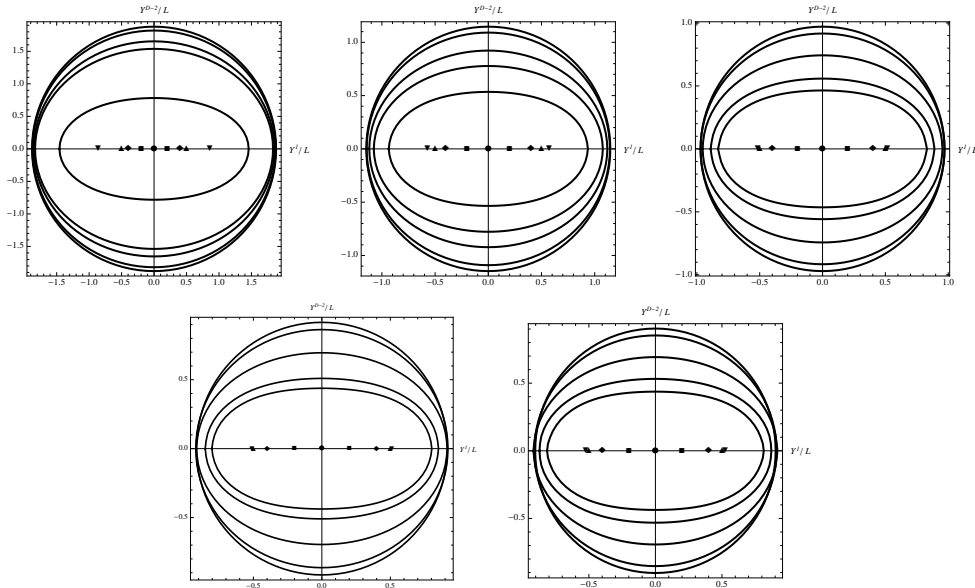


Figure 4.5: Numerical solutions for the shape of the submanifold \mathcal{C} in the plane Y^1 - Y^{D-2} for various values of the impact parameter b , energy $\frac{EG_N}{L^{D-3}} = 1$ and dimensions $D = 4, 5, 6, 7$ and 8 (from left to right, from top to bottom). The outer curve corresponds to the head-on collision, while the inner one corresponds to the critical impact parameter. The successive points over the Y^1 axis mark the location of the shock wave sources at the collision moment.

can rewrite the previous scaling for arbitrary size of the energy lumps: from (4.21) and (4.22),

$$\frac{b_c(\mu_0)}{z_0} \sim \left(\frac{G_D \mu_0}{z_0^{D-3}} \right)^{\frac{1}{D-2}}. \quad (4.40)$$

One consequence of scaling (4.39) is that the dependence of the critical impact parameter with the energy flattens when the dimensions increases. In the limit $D \rightarrow \infty$ this seems to indicate that the critical behavior with impact parameter decouples from the energy. This scaling is valid when $G_D \mu / L^{D-3} \gtrsim 1$. In this case the physics is sensitive to the large-scale geometry of AdS_D . On the other hand, when $G_D \mu / L^{D-3} \ll 1$ the collision effectively sees a flat space. Thus in this region (not plotted in the graphs presented here) the flat space behavior is recovered. On dimensional grounds, the scaling in flat background must be

$$b_c \sim \mu^{\frac{1}{D-3}}. \quad (4.41)$$

Thus we should see a soft transition from scaling (4.39) to scaling (4.41) for $G_D \mu / L^{D-3} \ll 1$. Finally, in [53] the off-center collision in AdS_5 has

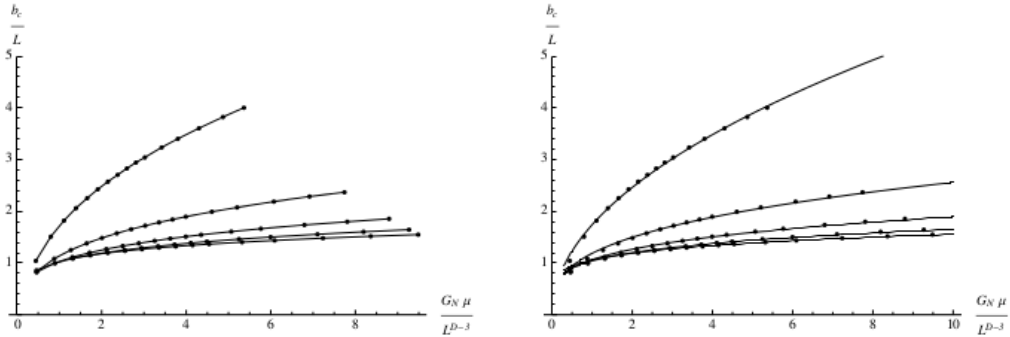


Figure 4.6: Plot for the critical impact parameter $\frac{b_c}{L}$ as a function of $\frac{G_D \mu}{L^{D-3}}$. The points corresponds to the numerical results. The plot of the right correspond to the fit of the results using scaling (4.39). The curves correspond, from top to bottom, to $D = 4, 5, 6, 7$ and 8 .

also been studied, but this time in a perturbative way, without finding any critical value of the critical impact parameter for the formation of the Penrose trapped surface. However, the authors of this reference works in a regime where $G_D \mu / L^{D-3} \gg 1$ while keeping fixed the impact parameter. As a consequence, the results of [53] are always in a regime where the impact parameter is much smaller than the critical value given by scaling (4.39), and a critical behavior of the Penrose trapped surface with the impact parameter cannot be detected.

4.1.3 Holographic interpretation

From the energy densities (3.106), the line element of two colliding AdS-Sch shock waves is the gravitational dual for two energy lumps which collide with impact parameter b and relativistic energy μ . After the collision happens, it is physically acceptable to suppose that the formation of the Penrose trapped surface evolves into an event horizon. Then, the holographic connection between horizons and finite temperature plasmas in the boundary field theory can be used to fix the formation of the Penrose trapped surface as indicative that a plasma thermalization has happened in the boundary theory after the collision of the relativistic energy lumps. Thus, in this framework, our numerical computation shows that:

- The head-on collision of extremely boosted energy lumps always results in a thermalized plasma. This coincides with the phenomena observed in [56] for collisions of shock waves in flat space and [52] for collisions in AdS_5 .

- For off-center collisions, the result depends on the impact parameter as well as on the energy collision in such a way that plasma thermalization does not happen for too high impact parameter. This seems to be in accordance with naive expectations.

From the boundary field theory point of view, the scaling (4.39) shows how the critical impact parameter grows with the energy of the lumps that collide in flat $(D - 1)$ -dimensional spacetime. Note that, since on the gravity side of the duality we are in a regime where gravity is still classic (i.e. it obey classic GR), the thermalized plasma produced at the boundary is strongly coupled. Therefore, for $D = 5$, colliding AdS-Sch shock waves could be understood as a gravitational toy model for sQGP production in high energy collisions of heavy ions at laboratory. Regarding this, it is important to take into account two important points of disagree:

- Even in the case in which the characteristics of the collision prevent the formation of the Penrose trapped surface, it does not mean that no event horizon is formed in the future light-cone. Other trapped surfaces different from the Penrose one could appear and evolve eventually into a horizon. For example, in [61] it was showed the formation of a trapped surface over the future light-cone in flat RN shock wave collision, while in [60] we showed that charge prevents the formation of any trapped surface over the past light-cone.
- The holographic energy density (3.106) does not reproduce the energy distribution of a extremely boosted heavy ion given in (3.114). This does not means that the existence of a critical impact parameter for thermalization is void, but perhaps the scaling (4.39) must include some kind of form factor correction.

In any case, these are technical difficulties in the sense that improved models could correct them. For example, the use of gravitational shock waves without $SO(D - 2)$ symmetry could help to achieve more accurate energy densities for describing extremely boosted heavy ions.

In addition to the previous technical issues, we have to add the fact that QCD is not a conformal theory but, however, the boundary theory is. Thus the boundary theory has not a confined phase and we are not colliding hadrons to form sQGP, but “drops” of sQGP to form a thermalized sQGP. An improved model must break in some way conformal symmetry to give a more realistic description of sQGP creation in heavy ion collisions [53]. While this limitation can affect aspects of the model related to the number of degrees of freedom, as entropy production, it seem reasonably to expect that

AdS/CFT does not introduce severe departures with the conditions to thermalization in nonconformal scenarios. From this point of view, the existence of a critical impact parameter, and maybe also the scaling (4.39), should be approximately valid for nonconformal theories as QCD.

4.2 Gravitational dual of nonequal sized energy lumps

In Section 3.3 of the previous chapter we showed that the energy-weighted size of the colliding holographic energy lumps corresponds to the the value of the holographic coordinate z_0 of the colliding gravitational shock waves in the AdS spacetime. Thus, by considering the collision of two shock waves propagating at z_+ and z_- ($z_+ \neq z_-$) we have a gravitational dual to study collisions between non-equal sized energy lumps in the boundary theory. Naively we shall expect some kind of critical behavior for the formation of the Penrose trapped surface on $\Delta z = |z_+ - z_-|$ since it seems physically acceptable that enough different sized energy lumps may not thermalize.

Since we are interested in analyzing the effects of relative size, we collide pure AdS-Sch gravitational waves. For zero impact parameter parallel to the boundary, \vec{b} , and a nonvanishing holographic impact parameter Δz , the components of the stress tensor before the collision are

$$\begin{aligned} T_{uu} &= \mu_+ \left(\frac{z}{L}\right)^{D-2} \delta(u) \delta^{(D-3)}(\vec{x}_T) \delta(z - z_+), \\ T_{vv} &= \mu_- \left(\frac{z}{L}\right)^{D-2} \delta(v) \delta^{(D-3)}(\vec{x}_T) \delta(z - z_-). \end{aligned} \quad (4.42)$$

and the chordal coordinates relative to each source are

$$q_{\pm} = \frac{1}{4zz_{\pm}} [(z - z_{\pm})^2 + \vec{x}_T^2]. \quad (4.43)$$

In addition, to gain generality we shall not suppose the energies μ_{\pm} sourcing each shock wave are equal.

To find the Penrose trapped surface for this collision by solving again the boundary problem (4.5) become, at least, repetitive and boring. One more time it requires to run the numeric method exposed in the previous section, this time for $\Delta z \neq 0$ and $\vec{b} = 0$, and it means a long computing time. On the other hand, we are interested mainly in analyzing the possible existence of a critical behavior for thermalization depending on the difference in the sizes of the colliding lumps, not the Penrose surface itself. Fortunately the isometries of the AdS spacetime can be exploited satisfactorily to link the

collision numerically analyzed in the previous section ($\Delta z = 0$, $\vec{b} \neq 0$) with the one we want to solve now, $\Delta z \neq 0$ and $\vec{b} = 0$, avoiding the numerical work [55]. As in Section 4.1.2, we choose \vec{b} directed along the $x^1 \equiv x$ coordinate, and \vec{x}_T splitting as $\vec{x}_T = (x, \vec{y})$.

In the analysis of the off-center collision of the previous section, we chose spherical coordinates in \mathbb{H}_{D-2} such that the sources of the colliding waves were located at some $r_0 = L\beta$ and $\theta_{\pm} = 0, \pi$, with $\beta > 0$. In this way the collision problem was reduced to the plane Y^1 - Y^{D-2} where $\{r, \theta\}$ played the role of ordinary polar coordinates. In the present case, there are not impact parameter parallel to the spacetime boundary and therefore $Y_{\pm}^1 = 0$. In addition, we choose $Y_{\pm}^i = 0$ for $i = 2, \dots, D-3$. Thus $Y_{\pm}^{D-2} = \pm r_0$, and the sources are located at

$$r_0 = L\beta, \quad \beta > 0 \quad \theta_{\pm} = \pm \frac{\pi}{2}. \quad (4.44)$$

Since, from (2.68), $z = L^2/(Y^0 + Y^{D-2})$ and $x \equiv x^1 = Y^1 L/z$,

$$z_{\pm} = \frac{L}{(1 + \beta^2)^{1/2} \pm \beta}, \quad x_{\pm} = 0, \quad (4.45)$$

and

$$\Delta z = |z_+ - z_-| = 2\beta L, \quad b = |x_+ - x_-| = 0. \quad (4.46)$$

The problem is one more time effectively restricted to the plane Y^1 - Y^{D-2} , with $\{r, \theta\}$ polar coordinates again. Thus a rotation $\theta \rightarrow \theta + \pi/2$ in this plane should relate this situation with the one numerically solved in the previous section, where $b = 2\beta L$ and $\Delta z = 0$ (see fig. 4.7). That corresponds to the action of the $SO(2)$ subgroup of the group $SO(D-2)$ of isometries of \mathbb{H}_{D-2} ,

$$\begin{aligned} Y'^1 &= Y^1 \cos \alpha + Y^{D-2} \sin \alpha \\ Y'^{D-2} &= -Y^1 \sin \alpha + Y^{D-2} \cos \alpha \end{aligned} \quad (4.47)$$

for $\alpha = \pi/2$. Under this rotation, z_{\pm} and x_{\pm} transform as,

$$z'_{\pm}(\alpha) = \frac{L}{(1 + \beta^2)^{1/2} \pm \beta \cos \alpha}, \quad x'_{\pm} = \pm \frac{L\beta \sin \alpha}{(1 + \beta^2)^{1/2} \pm \beta \cos \alpha}. \quad (4.48)$$

Thus, after the rotation, the impact parameters are

$$\Delta z' = \frac{2L\beta \cos \alpha}{1 + \beta^2 \sin^2 \alpha}, \quad b'(\alpha) = \frac{2L\beta(1 + \beta^2)^{1/2} \sin \alpha}{1 + \beta^2 \sin^2 \alpha}. \quad (4.49)$$

Because of the presence of sources in the collision problem, the action of the subgroup $SO(2)$ which rotates the plane Y^1 - Y^{D-2} is no longer a symmetry of the solution. This becomes explicit when we carry on the transformation of the partial differential equation for the shock wave profiles under

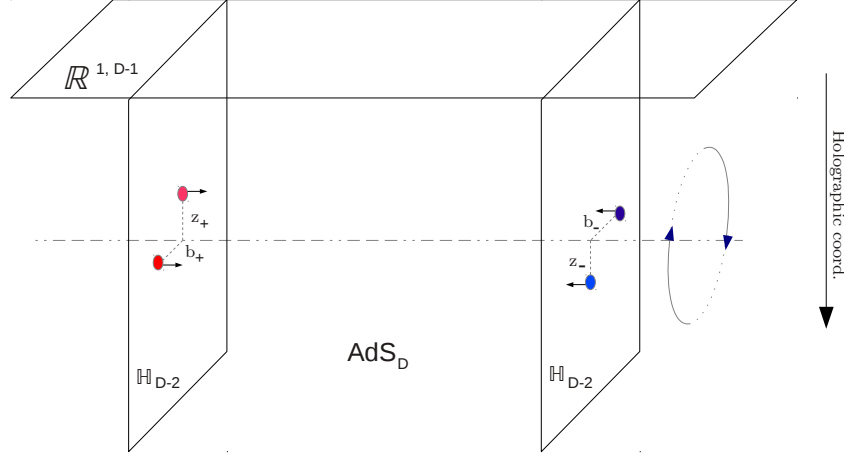


Figure 4.7: Schematic representation of the $O(2)$ rotation over \mathbb{H}_{D-2} to bring a collision with impact parameter only in the holographic coordinate ($b = 0$, $\Delta z \neq 0$) into a collision with purely boundary impact parameter ($b' \neq 0$, $\Delta z' = 0$).

(4.47). The left-hand side remains unchanged, whereas the transformation of the right-hand side implies the energies of the sources are not preserved. They change as²

$$\mu'_{\pm}(\alpha) = \mu_{\pm} \frac{(1 + \beta^2)^{1/2} \pm \beta \cos \alpha}{(1 + \beta^2)^{1/2} \pm \beta}. \quad (4.50)$$

Providing this energy transformation, the line element before the collision is preserved. From this point of view we are using the $SO(2)$ underlying symmetry as a solution generating technique, since the transformation of a solution to the Einstein equations -the collision with impact parameter directed along z - is again a solution but with other orientation of the impact parameter and different energies.

Using the transformation discussed above, we have mapped the collision problem with impact parameter along the holographic coordinate z into a collision with impact parameter but where both sources have the same value of z . However we have paid the price of transforming the energies of the shock waves, in a way that one increases the energy whereas the second one decreases it. This is a simple consequence of the UV/IR connection of the

²Note that the measure $\frac{1}{\sqrt{|g|}} \delta^D(x^\mu)$ in any D-dimensional metric manifold remains invariant under isometries.

AdS/CFT correspondence [94, 95]. The two energies can be balanced by means of a longitudinal boost,

$$\bar{u} = \lambda u', \quad \bar{v} = \lambda^{-1} v', \quad \lambda > 0 \quad (4.51)$$

which belong to the group of isometries $SO(2, D-1)$ of the AdS_D spacetime. However, the entire line element of the spacetime is not preserved under longitudinal boost, since the g_{uu} and g_{vv} components of the metric in (4.1) include a $\lambda^{\pm 1}$ factor after longitudinal boosts. This is compensated by a simultaneous rescaling of the wave profiles by

$$\bar{\Phi}_{\pm}^{(Sch)}(q'_{\pm}) = \lambda^{\mp 1} \Phi_{\pm}^{(Sch)}(q_{\pm}). \quad (4.52)$$

This is understood as a change of the shock-waves energies,

$$\bar{\mu}_{\pm}(\alpha) = \lambda^{\mp 1} \mu'_{\pm}(\alpha) \quad (4.53)$$

Equivalently, the transformation of the stress-energy tensor (4.42) under a longitudinal boost gives (4.53). For our purposes, we take

$$\lambda^2(\alpha) = \left(\frac{\mu_+}{\mu_-} \right) \left(\frac{(1 + \beta^2)^{1/2} - \beta}{(1 + \beta^2)^{1/2} + \beta} \right) \left(\frac{(1 + \beta^2)^{1/2} + \beta \cos \alpha}{(1 + \beta^2)^{1/2} - \beta \cos \alpha} \right). \quad (4.54)$$

Then, the energy $\bar{\mu}(\alpha)$ of the shock waves after this longitudinal boost is

$$\bar{\mu}(\alpha) = [\mu_+ \mu_- (1 + \beta^2 \sin^2 \alpha)]^{1/2}. \quad (4.55)$$

By applying the $SO(2)$ -rotation previously discussed for $\alpha = \pi/2$ followed by the longitudinal boost we arrive at a collision symmetric in energies, which happens at a constant value of the holographic coordinate and nonvanishing impact parameter given by

$$z_0 = z'_{\pm}(\alpha = \pi/2) = \frac{L}{(1 + \beta^2)^{1/2}}, \quad b'(\alpha = \pi/2) = \frac{2L\beta}{(1 + \beta^2)^{1/2}} \quad (4.56)$$

At this point we are with the off-center collision (4.20) for an energy

$$\mu_0 = \sqrt{\mu_+ \mu_- (1 + \beta^2)}. \quad (4.57)$$

In addition, the scaling transformation (4.21) leave us with a collision which happens at depth $z'' = L$, impact parameter $b'' = 2L\beta$ and energy $\mu'' = \sqrt{\mu_+ \mu_-}$. Of course, the transformations can be applied in reverse order and so the path we have traced is bijective. Thus we have constructed a link between the off-center collisions analyzed in the previous section, which

project as collisions with impact parameter in the CFT, and collisions having holographic impact parameter, corresponding to collisions between nonequal sized lumps in the CFT.

The consecutive application of the transformations previously described can be used to construct a map to obtain the Penrose trapped surfaces for the problem at hand from the Penrose trapped surfaces previously computed by means of numerical techniques for off-center collision. In terms of the Poincaré coordinates in \mathbb{H}_{D-2} , the inverse transformations are:

- Inverse $SO(2)$ rotation:

$$\begin{aligned} z(\alpha) &= \frac{L^2 z'}{L^2 \cos^2 \frac{\alpha}{2} + (z'^2 + \vec{x}'_T{}^2) \sin^2 \frac{\alpha}{2} + Lx' \sin \alpha}, \\ x(\alpha) &= \frac{2L^2 x' \cos(\alpha) - L \left(L^2 - z'^2 - \vec{x}'_T{}^2 \right) \sin(\alpha)}{2L^2 \cos^2 \frac{\alpha}{2} + 2(z'^2 + \vec{x}'_T{}^2) \sin^2 \frac{\alpha}{2} + 2Lx' \sin(\alpha)}, \\ \vec{y}(\alpha) &= \frac{L^2 \vec{y}'}{L^2 \cos^2 \frac{\alpha}{2} + (z'^2 + \vec{x}'_T{}^2) \sin^2 \frac{\alpha}{2} + Lx' \sin(\alpha)} \end{aligned} \quad (4.58)$$

and we take $\alpha = \pi/2$.

- Inverse longitudinal boost: the longitudinal boost (4.51) does not affect to the Poincaré coordinates in \mathbb{H}_{D-2} .
- Inverse rescaling:

$$z' = \frac{z''}{(1 + \beta^2)^{1/2}}, \quad \vec{x}'_T = \frac{\vec{x}''_T}{(1 + \beta^2)^{1/2}}. \quad (4.59)$$

The Penrose trapped surfaces obtained from the numerical results for off-center collisions by applying these inverse transformations are showed in fig. 4.2.

Since the off-center collision shows the existence of a critical value of the impact parameter, $b''_c = 2L\beta_c$, that means the collision with impact parameter directed along the z coordinate also shows such a critical behavior, i.e. beyond a critical value $(\Delta z)_c = 2L\beta_c$ the Penrose surface does not appear at the collision. From (4.40),

$$\frac{(\Delta z)_c}{L} \sim \left(\frac{G_D \sqrt{\mu_+ \mu_-}}{L^{D-3}} \right)^{\frac{1}{D-2}} \quad (4.60)$$

This leads to the conclusion that there is a critical value for the size difference $|z_+ - z_-|$ in the CFT below which no trapped surface is formed. Physically

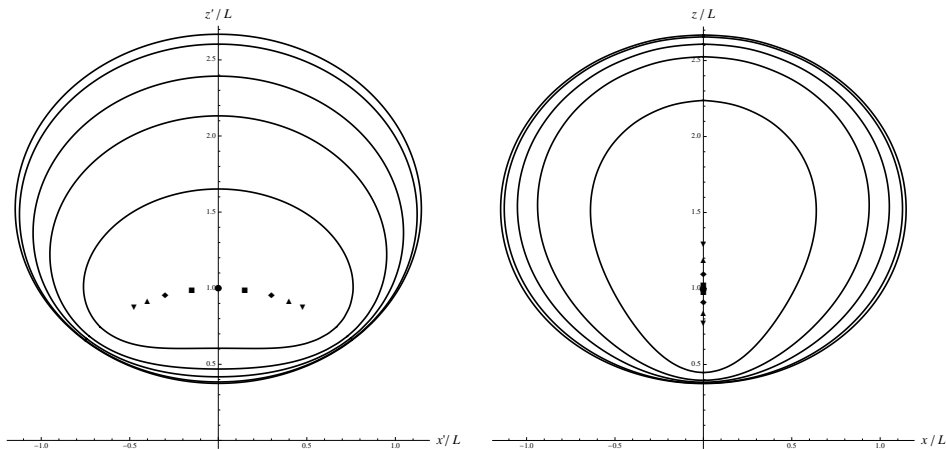


Figure 4.8: *Left panel.* Sections of the Penrose trapped surfaces in Poincaré coordinates $\{x', z'\}$ of equation (4.59). From outer inwards, the curves correspond to the $b/L = 0.0$, $b/L = 0.3$, $b/L = 0.6$, $b/L = 0.8$ and the critical value b_c/L , with energy $G_D \mu_0 / L^{D-3} = 1$ and $D = 5$. *Right panel.* Section of the same Penrose surfaces after the inverse rotation (4.58) for $\alpha = \pi/2$. In both plot, the horizontal axis $z' = z = 0$ represents the boundary of \mathbb{H}_3 .

this can be interpreted as indicating that, at a fixed energy, a too small energy lump does not have enough degrees of freedom to induce thermalization after a collision with a big one. In $D = 5$ and large size difference, the collision of the lumps in the CFT could be used as a model to thermalization of sQGP in hadron-nucleus collisions. Note that here we have considered the case of head-on scattering but, however, we can get collisions with both *spatial* and holographic impact parameter by an arbitrary angle $0 < \alpha < \pi/2$ in (4.48), which corresponds to collisions of unequal objects with nonvanishing impact parameter in the boundary theory. In this case note that, in the gravitational dual, the quantities

$$\begin{aligned} \mathcal{Q}_0 &= \mu'_+(\alpha) \mu'_-(\alpha) z'_+(\alpha) z'_-(\alpha) = \mu_+ \mu_-, \\ \mathcal{Q}_\pm &= \mu'_\pm(\alpha) \left[1 + \frac{z'_\pm(\alpha)^2 + x'_\pm(\alpha)^2}{L^2} \right] = 2\mu_\pm L \frac{(1 + \beta^2)^{1/2}}{(1 + \beta^2)^{1/2} \pm \beta}, \end{aligned} \quad (4.61)$$

are independent of the angle α and thus invariant under the $SO(2)$ rotations. It would be interesting to see if these invariants have any relevance in the phenomenological description of hadron-nucleus collisions at strong coupling.

4.3 Improving the model: Colliding AdS-RN shock waves

AdS-Sch shock waves are the simplest we can collide to develop a model for the the formation of thermalized plasmas in the boundary theory using the AdS/CFT connection. This is a first step towards a concrete holographic model of the sQGP production in heavy-ion high energy collisions. However it has the problem that we can play with a limited set of parameters. Thus it seems acceptable that the next step is to collide shock waves with a richer structure, as for example fat shock waves or AdS-RN shock waves, such that we have extra parameters to tune in order to get accurate models to reality.

As exposed in 3.2, in [57] the collision of fat shock waves was studied showing that, in four and five dimensions, the formation of the Penrose trapped surface depends on the diluting parameter ω . However there is no way to understand this critical behavior from the boundary theory since the diluting parameter ω has no influence over the expectation value of the holographic stress tensor. This could be because the fat shock waves does not correspond to any SUGRA solution or because the extension of the wave couples to the vacuum expectation value of some unknown field in the boundary field theory.

Unlike fat shock waves, AdS-RN shock waves come from a boost over a well known GR solution, the Reissner-Nordström black hole. In [96] it was showed that the Reissner-Nordström solution is indeed re-interpretable as a solution to complete SUGRA IIB equations, whose holographic dual is discussed in [97, 98]. Thus, AdS-RN sock waves can be extended to full SUGRA solutions without the potential pitfalls mentioned in the case of fat waves. By this reason we choose to study the collision of AdS-RN shock waves to get an improved holographic model to plasma thermalization.

A simple computation shows that the size of the Reissner-Nordström black hole horizon decreases with charge. In general terms, the horizon of the Reissner-Nordström solution is located where

$$f(r) = 1 + \frac{r^2}{L^2} - \frac{2M}{r^{D-3}} + \frac{Q^2}{r^{2(D-3)}} = 0. \quad (4.62)$$

Since the charge term is always positive that means that, for fixed mass, there is a maximum charge which cannot be exceeded in order to avoid a naked singularity. In some sense it seems that electrical charge works against the formation of horizons (for a more elaborated discussion see Section B.2). The physical picture behind such behavior is not fully understood up to date beyond the mathematical formalism, but one could think naively that it is a consequence of the repulsive feature of electrical forces. As we will show later,

colliding AdS-RN shock waves indicate that this, at least from the point of view of the Penrose trapped surface, is not a good explanation.

This being said, here we are going to search for both Penrose surfaces with topologies S^{D-2} and $S^1 \times S^{D-3}$ [60]. The reason for the second one is that the Penrose function $\Psi(q)$ solving the differential equation with S^{D-2} topology shows a zero inside the integration region \mathcal{C} . On the other hand, a torus topology could isolate the harmful effects of the electromagnetic energy density to form horizons. That idea is partly supported by the computation at [61], where a trapped surface with internal and external radii was found for colliding RN-shock waves in flat background.

Setting aside collisions with nonzero impact parameter, which would drag out the analysis, we are going to center the study over head-on collisions. The discussion must be particularized for each topology of the Penrose surface:

S^{D-2} topology. Because of the $SO(D-2)$ symmetry of the head-on collision, the intersection of the Penrose surface with the colliding surface, $\mathcal{C} \subseteq \mathbb{H}_{D-2}$, have constant chordal coordinate q_0 . Following the procedure at Section 4.1, the differential equation satisfied by the Penrose surface is (see equation (4.7) et sqq.),

$$\left[q(q+1) \frac{d^2}{dq^2} + \frac{D-2}{2} (2q+1) \frac{d}{dq} - (D-2) \right] [\Phi - \Psi^{(RN)}] = 0, \quad (4.63)$$

being the solution

$$\Psi(q) = \Phi^{(RN)}(q) + C_1 f_1(q) + C_2 f_2(q), \quad (4.64)$$

where $f_{1,2}(q)$ are the functions given at (3.63). Since the function $f_1(q)$ diverges at $q=0$ and $\Psi(q)$ must be finite inside \mathcal{C} , we fix $C_1=0$. In addition, the solution must satisfy the boundary conditions

$$\Psi(q_0) = 0, \quad \Psi'(q_0) = -\frac{2L}{\sqrt{q_0(q_0+1)}}. \quad (4.65)$$

From the first one,

$$\Psi(q) = \Phi^{(RN)}(q) - \frac{2q+1}{2q_0+1} \Psi^{(RN)}(q_0). \quad (4.66)$$

Finally, the second boundary condition introduced in (4.64) gives the consistency equation for q_0 ,

$$\Phi^{(RN)'}(q_0) - \frac{2}{2q_0+1} \Phi^{(RN)}(q_0) + \frac{2L}{\sqrt{q_0(q_0+1)}} = 0. \quad (4.67)$$

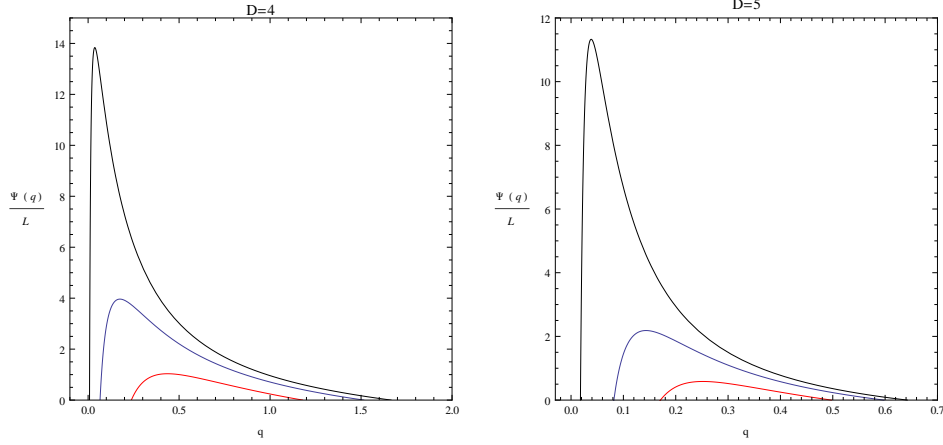


Figure 4.9: Plot of the function $\Psi(q)$ for $D = 4$ (left panel) and $D = 5$ (right panel) for head-on collisions with energy $G_D \mu / L^{D-3} = 5$. From top to bottom, the curves corresponds to charge parameters $\sqrt{G_D e} / L^{D-3} = 0.5, 0.75$ and 1.0 .

This algebraic equation cannot be solved analytically, and a numerical approach is necessary to obtain the size of the Penrose surface, q_0 , for each value of the parameters μ and e^2 , and dimension D .

The obstruction to the existence of trapped surfaces of the Penrose type with topology S^{D-2} becomes clear when we fix our attention on (4.66). The charge-dependent term in $\Phi^{(RN)}(q)$ in (3.56) diverges to minus infinity as $q \rightarrow 0^+$. Thus the function $\Psi^{(RN)}(q)$ in (4.66) has a zero below q_0 , which contradicts the assumed S^{D-2} topology. This is showed in fig. 4.3 in $D = 4, 5$ dimensions. The conclusions is that there are no trapped surfaces of the Penrose type with topology S^{D-2} produced in the head-on collision of two RN-AdS shock waves.

$S^1 \times S^{D-3}$ **topology.** The zero of $\Psi(q)$ inside \mathcal{C} in equation (4.66) strongly suggest to search for a toroidal topology of the Penrose surface.

For a toroidal topology, \mathcal{C} splits into two pieces,

$$\mathcal{C} = \mathcal{C}_{in} \cup \mathcal{C}_{out}. \quad (4.68)$$

Because of the $O(D - 2)$ symmetry, both components \mathcal{C}_{in} and \mathcal{C}_{out} are S^{D-3} spheres defined by constant chordal coordinates $q = q_{in}$ and $q = q_{out}$. As a consequence, the equation (4.63) must be solved this time in the region $q_{in} \leq q \leq q_{out}$, and the boundary conditions in (4.65) are duplicated. The first boundary condition splits into

$$\Psi(q_{in}) = 0, \quad \Psi(q_{out}) = 0. \quad (4.69)$$

while for the second one in (2.108) we have

$$\begin{aligned}\Psi'(q_{in}) &= \frac{2L}{\sqrt{q_{in}(q_{in} + 1)}}, \\ \Psi'(q_{out}) &= -\frac{2L}{\sqrt{q_{out}(q_{out} + 1)}}.\end{aligned}\tag{4.70}$$

Note that the first equation have positive sign since $\Psi(q)$ grows from 0 when q increases from q_{in} .

The solution to (4.63) with the previous boundary conditions is still given by (4.64), but now, because of $q = 0$ is not inside \mathcal{C} , the function $f_1(q)$, which is singular at the origin, enters in the solution. Thus $C_1 \neq 0$, and both C_1 and C_2 are determined by the boundary conditions (4.69),

$$\begin{aligned}C_1 f_1(q_{in}) + C_2 f_2(q_{in}) &= -\Phi^{(RN)}(q_{in}), \\ C_1 f_1(q_{out}) + C_2 f_2(q_{out}) &= -\Phi^{(RN)}(q_{out}).\end{aligned}\tag{4.71}$$

Once these constants are solved in terms of q_{in} and q_{out} , we impose the conditions at (4.70). This provides two algebraic equations that, in principle, are enough to determine the values of q_{in} and q_{out} . However, as can be seen in fig. 4.3, there is no simultaneous solution to the two equations at (4.70) once the constants C_1 and C_2 have been fixed in function of q_{in} and q_{out} . Thus we conclude that there is no Penrose surface formation with toroidal topology.

Summarizing, although AdS-RN shock waves seemed to be promising because of their relation to a well known SUGRA IIB solution, the collision does not produce any Penrose surface. This does not mean that other trapped surface could form after the collision happens but, in any way, is a negative indication against the horizon formation in the collision. Considering the CFT dual to Einstein- Maxwell theory, this indicate that thermalization after head-on collision of energy lumps could not be possible. The physical reason for that is not fully clear: the AdS-RN solution corresponds to the grand canonical ensemble of the boundary CFT with the electromagnetic potential a chemical potential coupled to the charge as measured from the boundary [97, 98]. However, after the infinite boost limit to obtain the AdS-RN shock waves there is no direct physical interpretation. In any case, the absence of the Penrose surface in collisions of AdS-RN shock waves that we probe here corrects the error in [59] where these trapped surfaces were computed despite the function $\Psi(q)$ takes negative values.

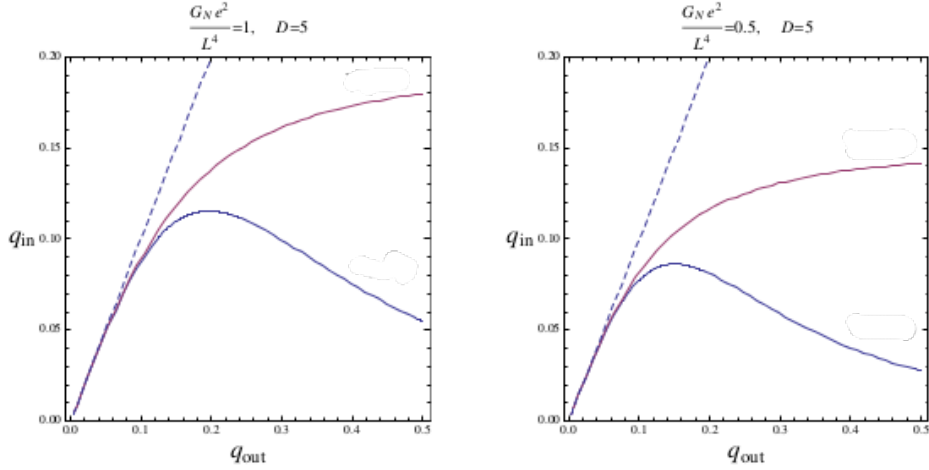


Figure 4.10: Locus of the points in the plane (q_{out}, q_{in}) - $D = 5$ and $G_D e^2/L^4 = 1$ (left panel), $G_D e^2/L^4 = 0.5$ (right panel)- where the equations (4.70) are satisfied once the constants C_1 and C_2 are fixed solving (4.71). The red curve corresponds to the first boundary condition in (4.70), while the blue curve corresponds to the second one. The curves approach each other near the origin, but never cross. The dashed lines indicates the points where $q_{in} = q_{out}$, showing that the curves always are in the region where $q_{in} < q_{out}$.

The absence of the Penrose trapped surface, beyond its holographic interpretation, seems to be in accordance with the idea that charge prevents the formation of horizons, which follows from the solution to (4.62). However, this idea must be revised since, although it seems physically acceptable, the charge of the AdS-RN shock waves is zero, the same as the electromagnetic field, as we discussed at the end of Section 3.1.

Chapter 5

Gauge symmetries in noncommutative geometry

In this chapter we will deal with the second topic contained in the Thesis: field theories on noncommutative spacetimes.

There are several reasons to be interested in noncommutative field theories or NCFTs. The first one is that, near Planck scale, the spacetime structure may be something like a foam of black holes, and it is expected that below the Planck energy this situation can be effectively described by means of noncommutative geometries, where locality is lost because of the uncertainty relations between coordinates. Also NCFTs arise as a certain low-energy limit of string theory, reinforcing the idea of NCFTs as a good framework to develop effective theories of quantum gravity halfway between string theory and classical Einstein gravity. Finally, NCFT can be viewed from a purely mathematical point of view as a noncommutative deformation of ordinary field theory, being interesting to study the mathematical behavior resulting from incorporate a noncommutative feature to the spacetime.

In the contemporary Physics, gauge symmetries are one of the cornerstones of the standard model, which is constructed as a local field theory. Thus, seeing NCFTs either as a possible framework to go beyond standard model or as a purely mathematical deformation of the ordinary theory, searching for a formulation of Yang-Mills symmetries in NCFTs is an interesting task.

In this chapter we discuss a new type of gauge-like invariances that can be defined in noncommutative gauge theories. Section 5.1 is dedicated to a brief introduction to NCFT. In sections Section 5.2 and Section 5.3 we introduce two different ways in which gauge invariance can be defined in noncommutative spaces: star-gauge invariance and twist-gauge invariance. In Section 5.4 we discuss about the physical relevance of these invariances,

i.e. the possibility to obtain conserved currents from them. Finally, in Section 5.5 we define an infinite family of star-twisted gauge invariances interpolating continuously between star-gauge and twist-gauge invariances.

5.1 Basics on noncommutative field theory

The goal of this section is to provide the basics tools on noncommutative field theories to understand the followings sections, not to give a complete exposition of the subject. The reader really interested in NCFT can find detailed reviews in [8, 62, 63, 64, 65].

5.1.1 Noncommutative geometry and noncommutative flat space

As it was sketched in the introductory chapter (Section 1.4), a noncommutative space is a space with noncommutative coordinates instead of commutative ones. More precisely, a noncommutative space is a manifold \mathcal{M} endowed with a set of noncommutative coordinates, which can be represented as a set of self-adjoint operators, $\{\hat{x}^1, \hat{x}^2 \dots \hat{x}^n\}$, over some Hilbert space \mathcal{H} . We call $\{\hat{x}^1, \hat{x}^2 \dots \hat{x}^n\}$ the coordinate operators in \mathcal{M} .

Taking into account that coordinates in any space \mathcal{M} are the generators of the algebra of continuous complex functions over the space, noncommutative spaces correspond to noncommutative algebras of continuous functions over them. Strictly speaking, the connection between algebras of functions and (Hausdorff) topological spaces is established by the Gel'fand-Naimark theorem. It states the equivalence between commutative spaces and commutative algebras, in such a way that to any Hausdorff topological space locally compact \mathcal{M} corresponds a commutative algebra \mathcal{C} , being the connection a one-to-one map and $\mathcal{C} \simeq \mathcal{C}_0(\mathcal{M})$, the algebra of complex continuous functions on \mathcal{M} vanishing at infinity¹. Extending the theorem to noncommutative algebras gives the definition of noncommutative spaces as those in one-to-one correspondence with noncommutative algebras, isomorphic to the noncommutative algebras of continuous complex functions vanishing at infinity,

$$\begin{array}{ccc} \text{noncommutative} & \longleftrightarrow & \text{noncommutative} \\ \text{space } \mathcal{M} & & \text{algebra } \simeq \mathcal{C}_0(\mathcal{M}) \end{array} \quad (5.1)$$

¹The restriction to functions vanishing at infinity is only necessary for locally compact but no compact spaces. The algebras corresponding to compact spaces can include functions with finite values at their boundaries. At the end, this traduces in the fact that compact spaces are related to unitary algebras, whereas no compact spaces corresponds to no unitary algebras.

Summarizing, defining a noncommutative space \mathcal{M} is equivalent to specifying the noncommutative algebra of continuous complex functions over it vanishing at infinity, $\mathcal{C}_0(\mathcal{M})$, which is completely determined by means of the commutation relations between the generators of the algebra, that is, the commutation relations between the coordinate operators $\{\hat{x}^1, \hat{x}^2 \dots \hat{x}^n\}$.

A simple example of noncommutative space is the fuzzy sphere of radius R . It is defined as the noncommutative space with coordinate operators $\{\hat{x}_1, \hat{x}_2, \hat{x}_3\}$ satisfying

$$\hat{x}_1^2 + \hat{x}_2^2 + \hat{x}_3^2 = R^2 \mathcal{I}, \quad (5.2)$$

\mathcal{I} being the identity in the noncommutative algebra generated by $\{\hat{x}_i\}$. A solution to equation (5.2) is given by

$$\hat{x}_i = \frac{R}{\sqrt{j(j+1)}} J_i, \quad i = 1, 2, 3 \quad (5.3)$$

being J_i the generators of the Lie algebra of $SU(2)$ in a irreducible representation of spin j , with spectrum $\{-j, -j+1 \dots j-1, j\}$. Thus the coordinate operators $\{\hat{x}_i\}$ generate the algebra

$$[\hat{x}_i, \hat{x}_j] = \frac{iR}{\sqrt{j(j+1)}} \sum_{k=1}^3 \epsilon_{ijk} \hat{x}_k, \quad (5.4)$$

which determines completely the fuzzy sphere of radius R .

From now on we shall work in the noncommutative space \mathbb{R}_θ^d , defined as the noncommutative space with coordinate operators $\{\hat{x}^\mu\}_{\mu=0}^d$ satisfying the noncommutative algebra $\mathcal{A}_\theta \simeq \mathcal{C}_0(\mathbb{R}_\theta^d)$ given by,

$$[\hat{x}^\mu, \hat{x}^\nu] = i\theta^{\mu\nu}, \quad (5.5)$$

where $\theta^{\mu\nu}$ is an antisymmetric $d \times d$ matrix of real numbers and rank p not necessarily² equals to d . In addition, each coordinate operator has spectrum \mathbb{R} . Note that, from a purely mathematical point of view, \mathbb{R}_θ^d is the simplest noncommutative generalization of the commutative space \mathbb{R}^d .

5.1.2 Weyl correspondence and Moyal product

Fields over \mathbb{R}_θ^d are elements of the abstract algebra \mathcal{A}_θ . For later use, it is convenient to construct a representation of \mathcal{A}_θ in the Hilbert space of continuous complex functions vanishing at infinity over \mathbb{R}^d . That means defining a

²Indeed, unitarity of any quantum field theory over \mathbb{R}_θ^d requires $\theta^{0i} = 0$, where 0 labels the temporal direction and i the spatial ones [99].

noncommutative product \star between functions in \mathbb{R}^d and an isomorphism of algebras W such that [62, 63, 100]

$$W[\hat{f}\hat{g}](x) = W[\hat{f}](x) \star W[\hat{g}](x), \quad (5.6)$$

for any two elements \hat{f}, \hat{g} of \mathcal{A}_θ .

Given a basis³ $\{\hat{O}_{k_\mu}\}$ of \mathcal{A}_θ , for any complex function $f(x) \in \mathcal{C}_0(\mathbb{R}^d)$ and its Fourier transform $\tilde{f}(k_\mu)$, we define the symbol of $f(x)$ in the basis $\{\hat{O}_{k_\mu}\}$ as the element of \mathcal{A}_θ given by

$$\hat{f}_{\hat{O}} \equiv \int \frac{d^d k}{(2\pi)^d} \tilde{f}(k_\mu) \hat{O}_{k_\mu}. \quad (5.7)$$

Any element of \mathcal{A}_θ can be obtained as the symbol of some function $f(x^\mu) \in \mathcal{C}_0(\mathbb{R}^d)$. Furthermore, if $\{\hat{O}_{k_\mu}\}$ is an orthonormal basis, in the sense that

$$\text{Tr} \left(\hat{O}_{k_\mu} \hat{O}_{q_\mu} \right) = \delta^{(d)}(k_\mu + q_\mu), \quad (5.8)$$

$\text{Tr}()$ being the trace operator in \mathcal{A}_θ , equation (5.7) can be inverted,

$$\tilde{f}(k_\mu) \equiv \text{Tr} \left(\hat{O}_{k_\mu} \hat{f}_{\hat{O}} \right). \quad (5.9)$$

In this way we associate to any element \hat{a} of the abstract algebra \mathcal{A}_θ the Fourier transform of some function $f(x) \in \mathcal{C}_0(\mathbb{R}^d)$, such that $\hat{a} = \hat{f}_{\hat{O}}$, the symbol of $f(x)$ in the basis $\{\hat{O}_{k_\mu}\}$ of \mathcal{A}_θ . This defines a map in the sense explained in the previous paragraph.

To particularize the map given by (5.9), we need to specify a basis of \mathcal{A}_θ . A specially useful basis is the one given by the set $\{e^{ik_\mu \hat{x}^\mu} \ \forall k_\mu \in \mathbb{R}^d\}$, where $e^{ik_\mu \hat{x}^\mu}$ are the elements of \mathcal{A}_θ defined by the formal series

$$e^{ik_\mu \hat{x}^\mu} \equiv \sum_{n=0}^{\infty} \frac{1}{n!} (ik_\mu \hat{x}^\mu)^n. \quad (5.10)$$

Normalizing the trace in \mathcal{A}_θ such that

$$\text{Tr} \left(e^{ik_\mu \hat{x}^\mu} \right) = \delta^{(d)}(k_\mu), \quad (5.11)$$

this basis is orthonormal in the sense of (5.8), and the equation (5.9) takes the specially simple form,

$$\tilde{f}(k_\mu) = \text{Tr} \left(e^{ik_\mu \hat{x}^\mu} \hat{f} \right). \quad (5.12)$$

³Since the spectrum of the coordinate operators \hat{x}^μ is \mathbb{R}^d , each element of a basis of \mathcal{A}_θ must be labeled by a parameter $k_\mu \in \mathbb{R}^d$.

Then, the inverse Fourier transform of $\tilde{f}(k_\mu)$ defines the bijective map given by (5.9) in the basis $\{e^{ik_\mu \hat{x}^\mu}\}$. In the notation of (5.6),

$$W[\hat{f}](x) \equiv \int d^d k \operatorname{Tr} \left(e^{ik_\mu(x^\mu - \hat{x}^\mu)} \hat{f} \right) = f(x). \quad (5.13)$$

This one-to-one map between functions of $\mathcal{C}_0(\mathbb{R}^d)$ and elements of \mathcal{A}_θ is called the Weyl correspondence or Weyl map [63].

From the definition (5.13) we can compute the noncommutative product appearing in (5.6) so that the Weyl correspondence be an isomorphism. First, note that, by construction of the Weyl map, plane waves are in correspondence with “noncommutative plane waves”. That is,

$$W \left[e^{ip_\mu \hat{x}^\mu} \right] (x) = e^{ip_\mu x^\mu}. \quad (5.14)$$

On the other hand,

$$e^{ip_\mu \hat{x}^\mu} e^{-iq_\mu \hat{x}^\mu} = e^{\frac{i}{2} p \times q} e^{i(p_\mu - q_\mu) \hat{x}^\mu}, \quad (5.15)$$

where we have used the Baker-Campbell-Hausdorff formula and

$$p \times q = p_\mu q_\nu \theta^{\mu\nu}. \quad (5.16)$$

Therefore, from the property (5.14), the noncommutative product between functions of $\mathcal{C}_0(\mathbb{R}^d)$ must be such that, for two plane waves,

$$W[e^{ip_\mu \hat{x}^\mu} e^{-iq_\mu \hat{x}^\mu}] \equiv e^{ip_\mu \hat{x}^\mu} \star e^{-iq_\mu \hat{x}^\mu} = e^{\frac{i}{2} p \times q} e^{i(p_\mu - q_\mu) \hat{x}^\mu}. \quad (5.17)$$

From this equation, the explicit form for the noncommutative product of two functions $f(x), g(x) \in \mathcal{C}_0(\mathbb{R}^d)$ is found using the Fourier transform of each them. It results in

$$f(x) \star g(x) \equiv f(x) e^{\frac{i}{2} \overleftarrow{\partial}_\mu \theta^{\mu\nu} \overrightarrow{\partial}_\nu} g(x), \quad (5.18)$$

where the arrows over the partial derivatives stand for derivation over previous (back arrow, \leftarrow) or later (forward arrow, \rightarrow) functions in the equation, i.e., expanding the exponential function in a power series,

$$f(x) \star g(x) = \sum_{n=0}^{\infty} \frac{(i/2)^n}{n!} \theta^{\mu_1 \nu_1} \dots \theta^{\mu_n \nu_n} (\partial_{\mu_1} \dots \partial_{\mu_n} f) (\partial_{\nu_1} \dots \partial_{\nu_n} g). \quad (5.19)$$

This differential representation of the noncommutative product between ordinary functions corresponding to the Weyl map is called the Moyal product

or star product [62]. With it, the Weyl map is an isomorphism between the algebras \mathcal{A}_θ and $(\mathcal{C}_0(\mathbb{R}^d), \star)$ as specified by (5.6).

Note that the Moyal product can be seen as a smooth deformation of the ordinary commutative product between functions: in the limit $\theta^{\mu\nu} \rightarrow 0$, equation (5.19) reduces to the usual product between functions, being this limit smooth in the sense that it involves positive powers of $\theta^{\mu\nu}$. From this point of view, the space \mathbb{R}_θ^d is just a smooth noncommutative deformation of the commutative space \mathbb{R}^d , constructed substituting the ordinary product between functions by the Moyal product. Another important feature of the Moyal product is its highly nonlocal nature since it involves an infinite number of partial derivatives.

An relevant property of the Moyal product is that, inside an integral, it is always possible to substitute one Moyal product by one ordinary product without change the value of the integral,

$$\int d^d x f(x) \star g(x) = \int d^d x f(x) g(x). \quad (5.20)$$

This property can be seen substituting each function in the right-hand side by its Fourier transform,

$$\int d^d x f(x) \star g(x) = \int d^d x \int d^d p \int d^d q \tilde{f}(p) \tilde{g}(q) e^{-\frac{i}{2} p \times q} e^{i(p+q)_\mu x^\mu} \quad (5.21)$$

The integration with respect to x^μ of the factor $e^{i(p+q)_\mu x^\mu}$ gives a Dirac delta $\delta^{(d)}(p+q)$. Using the the convolution theorem we arrive at

$$\begin{aligned} \int d^d x f(x) \star g(x) &= \int d^d x \int d^d p \int d^d q \tilde{f}(p) \tilde{g}(q) e^{i(p+q)_\mu x^\mu} \\ &= \int d^d x f(x) g(x). \end{aligned} \quad (5.22)$$

As a corollary, the Moyal product inside an integral have the cyclic property,

$$\begin{aligned} \int d^d x f(x) \star g(x) \star h(x) &= \int d^d x g(x) \star h(x) \star f(x) = \\ &= \int d^d x h(x) \star f(x) \star g(x). \end{aligned} \quad (5.23)$$

These two properties will be used profusely in the next subsection.

5.1.3 Non-commutative functional actions

Defining field theories on noncommutative geometries reduces to construct action functionals over such geometries. Then the field equations are obtained

in the usual way as the conditions for the extremalization of the action we are considering.

Action functionals for field theories over \mathbb{R}_θ^d are constructed using the Weyl correspondence. Since fields over \mathbb{R}_θ^d are elements of the algebra \mathcal{A}_θ , for each field theory over the commutative space \mathbb{R}^d with action $S[\varphi]$ we can construct at least one functional action over \mathbb{R}_θ^d , $S_\star[\varphi]$, substituting commutative products by star products in the commutative action $S[\varphi]$. For example, the noncommutative version of the $\lambda\Phi^4$ theory over \mathbb{R}_θ^d is given by the functional action

$$S_\star[\Phi] = \int d^d x \left(\frac{1}{2} \partial_\mu \Phi \star \partial^\mu \Phi - \frac{1}{2} m^2 \Phi \star \Phi - \frac{\lambda}{4!} \Phi \star \Phi \star \Phi \star \Phi \right). \quad (5.24)$$

Constructed in this fashion, noncommutative field theories are smooth deformations of the commutative ones at the classical level, so that ordinary theories are recovered smoothly in the commutative limit $\theta^{\mu\nu} \rightarrow 0$. However, note that noncommutative field theories constructed in this way are not in one-to-one correspondence with commutative theories. It may exist order ambiguities which leads to different noncommutative actions from the same commutative theory. For example, for an interaction term $\varphi^i \varphi_i \varphi^j \varphi_j$ in the commutative action, we have two not equivalent noncommutative possibilities:

$$\int d^d x \varphi^i \varphi_i \varphi^j \varphi_j \implies \begin{cases} \int d^d x \varphi^i \star \varphi_i \star \varphi^j \star \varphi_j \\ \int d^d x \varphi_i \star \varphi_j \star \varphi^i \star \varphi^j \end{cases} \quad (5.25)$$

Thus, several not equivalent noncommutative field theories can have the same commutative limit $\theta^{\mu\nu} \rightarrow 0$.

Given some noncommutative action, the field equations follow from it by searching for the solution which extremizes the action. As an example, let us consider a variation of the field Φ for the $\lambda\Phi^4$ theory,

$$\Phi \rightarrow \Phi + \delta\Phi, \quad (5.26)$$

which satisfies the Leibniz rule with respect to the Moyal product of fields,

$$\delta(\Phi_1 \star \Phi_2) = (\delta\Phi_1) \star \Phi_2 + \Phi_1 \star (\delta\Phi_2). \quad (5.27)$$

Then, the variation of the noncommutative action (5.24) induced by (5.26) is

$$\begin{aligned} \delta S_\star = \int d^d x \left[\frac{1}{2} (\partial_\mu \Phi \star \partial^\mu \delta\Phi + \partial_\mu \delta\Phi \star \partial^\mu \Phi) \right. \\ \left. - \frac{1}{2} m^2 (\delta\Phi \star \Phi + \Phi \star \delta\Phi) - \frac{\lambda}{4!} (\delta\Phi \star \Phi \star \Phi \star \Phi \right. \\ \left. + \Phi \star \delta\Phi \star \Phi \star \Phi + \Phi \star \Phi \star \delta\Phi \star \Phi + \Phi \star \Phi \star \Phi \star \delta\Phi) \right]. \end{aligned} \quad (5.28)$$

Using the cyclicity of the Moyal product under the integral symbol, this can be written in the shorter form

$$\delta S_\star = \int d^d x \left(-\partial_\mu \partial^\mu \Phi - m^2 \Phi - \frac{\lambda}{3!} \Phi \star \Phi \star \Phi \right) \star \delta \Phi + \text{Boundary Terms}, \quad (5.29)$$

where we have also integrated out total derivatives. If the variation in (5.26) vanish at infinity, the equations of motion associated with the action (5.24) is

$$\partial_\mu \partial^\mu \Phi + m^2 \Phi + \frac{\lambda}{3!} \Phi \star \Phi \star \Phi = 0. \quad (5.30)$$

In general, this procedure cannot be generalized to arbitrary noncommutative Lagrangian densities in order to obtain the noncommutative version to the Euler-Lagrange equations. Naively, the noncommutative alter ego of the Euler-Lagrange equations for a noncommutative Lagrangian density $\mathcal{L}_\star(\varphi_i, \partial_\mu \varphi_i, x^\mu)$ should be

$$\frac{\partial \mathcal{L}_\star}{\partial \varphi_i} - \partial_\mu \left(\frac{\partial \mathcal{L}_\star}{\partial (\partial_\mu \varphi_i)} \right) = 0. \quad (5.31)$$

However, the derivative of the star product of fields is not defined *a priori*. Therefore, for each action functional the field equations must be obtained by hand: computing the variation of the action and looking for a field solution giving zero variation.

Because of one Moyal product can be removed inside an integral, quadratic terms in noncommutative actions are formally equivalent to the ones of in ordinary fields theories. Thus the kinetic and mass terms are identical to those in the corresponding commutative one. In particular, they preserve Lorentz invariance. However, interaction terms involve more that one star product, and not all star products can be integrated out. Due to the presence of $\theta^{\mu\nu}$ in the interaction terms, only the subgroup of the Lorentz group leaving invariant $\theta^{\mu\nu}$ remains a symmetry for terms with $n > 2$ fields. In other words, Lorentz symmetry is broken in interacting noncommutative theories. For example, in four dimensions, for a noncommutativity given by

$$(\theta^{\mu\nu}) = \begin{pmatrix} 0 & 0 & 0 & 0 \\ 0 & 0 & 0 & 0 \\ 0 & 0 & 0 & \theta \\ 0 & 0 & -\theta & 0 \end{pmatrix} \quad (5.32)$$

the Lorentz symmetry is broken in $SO(1,1) \times SO(2) \subseteq SO(1,3)$ for any interacting theory.

Besides the break of Lorentz symmetry at the classical level, another feature of noncommutative field theories is the mixing of scales in the perturbative quantum dynamics because of noncommutativity [65, 101]. Naively, it is expected that the ultraviolet behavior of quantum field theories in noncommutative spaces be better than in commutative ones, since noncommutativity implies Heisenberg inequalities between coordinates,

$$\Delta x^\mu \Delta x^\nu \geq \frac{1}{2} |\theta^{\mu\nu}|, \quad (5.33)$$

and thus $|\theta^{\mu\nu}|^{1/2}$ seems to be a natural ultraviolet cut-off rendering the theory finite. However, against intuition, planar diagrams in perturbative quantum dynamics do not see the noncommutativity of space, while nonplanar diagrams substitute the ultraviolet divergences by infrared divergences. In this way, noncommutativity introduces UV/IR mixing phenomena in quantum perturbative dynamics, which is at the origin of interesting physical effects [102, 103].

5.1.4 Non-commutative Yang-Mills theories

Following the prescription given in the previous subsection, the noncommutative Yang-Mills Lagrangian density over \mathbb{R}_θ^d follows from the commutative one substituting dot products by star products,

$$\mathcal{L}_{NCYM} = i\bar{\psi} \star \not{D}\psi - m\bar{\psi} \star \psi - \frac{1}{2} \text{Tr} (F_{\mu\nu} \star F^{\mu\nu}), \quad (5.34)$$

where we have coupled to a Dirac field ψ , with

$$D_\mu = \partial_\mu - i\lambda A_\mu \star \quad (5.35)$$

the covariant derivative and λ the gauge coupling constant. In addition, the field strength tensor $F_{\mu\nu}$ is defined as

$$F_{\mu\nu} = \frac{i}{\lambda} [D_\mu, D_\nu]_\star = \partial_\mu A_\nu - \partial_\nu A_\mu - i\lambda [A_\mu, A_\nu]_\star, \quad (5.36)$$

where $[A, B]_\star = A \star B - B \star A$. Note that the last equation goes one step beyond the naive recipe given in the previous subsection to construct noncommutative actions, since we also use the Moyal product to construct the field strength tensor from the covariant derivative [14, 103]. As a consequence, $F_{\mu\nu}$ cannot be Lie algebra valued since, expanding (5.36),

$$F_{\mu\nu} = \partial_\mu A_\nu - \partial_\nu A_\mu - \frac{i\lambda}{2} \{A_\mu^a, A_\nu^b\}_\star [T_a, T_b] - \frac{i\lambda}{2} [A_\mu^a, A_\nu^b]_\star \{T_a, T_b\}, \quad (5.37)$$

being T_a (with $a \in \{1, 2, \dots, \dim_{\mathbb{R}} G\}$) the generators of the gauge group \mathcal{G} . We see that there is an extra term proportional to $\{T_a, T_b\}$ because of the noncommutativity of the star product, which forces us to consider that the field strength $F_{\mu\nu}$ takes values in the universal enveloping algebra of the Lie algebra of G ,

$$F_{\mu\nu} = F_{\mu\nu}^{(0)}\mathbb{1} + F_{\mu\nu}^a T_a + F_{\mu\nu}^{a_1 a_2} T_{a_1} T_{a_2} + F_{\mu\nu}^{a_1 a_2 a_3} T_{a_1} T_{a_2} T_{a_3} + \dots \quad (5.38)$$

with $\mathbb{1}$ the unity in the universal enveloping algebra. We shall denote by \mathfrak{g} the Lie algebra of the gauge group \mathcal{G} , and $U(\mathfrak{g})$ its universal enveloping algebra.

The field equations for (5.34) are obtained by imposing zero variation of the functional action under variations of the fields over extremal solutions. For a pure Yang-Mills theory (without Dirac field), the field equations result in,

$$\partial_\mu F^{\mu\nu} - i\lambda[A_\mu, F^{\mu\nu}]_\star = 0, \quad (5.39)$$

as we had naively expected from the prescription of changing dot products by Moyal products. Since the field strength $F_{\mu\nu}$ takes values in the universal enveloping algebra $U(\mathfrak{g})$ and not in the Lie algebra \mathfrak{g} , this field equation forces us to consider also that the gauge field A_μ takes values in $U(\mathfrak{g})$. Thus consistency of the field equation yields to consider an infinite number of gauge bosons $A_\mu^{(0)}$, A_μ^a , $A_\mu^{a_1 a_2}$, $A_\mu^{a_1 a_2 a_3}$, \dots associated with the infinite generators of $U(\mathfrak{g})$,

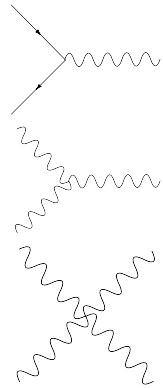
$$A_{\mu\nu} = A_\mu^{(0)}\mathbf{1} + \mathbf{A}_\mu^a \mathbf{T}_a + \mathbf{A}_\mu^{a_1 a_2} \mathbf{T}_{a_1} \mathbf{T}_{a_2} + \mathbf{A}_\mu^{a_1 a_2 a_3} \mathbf{T}_{a_1} \mathbf{T}_{a_2} \mathbf{T}_{a_3} + \dots \quad (5.40)$$

So, it seems that noncommutative Yang-Mills theories has infinite gauge degrees of freedom. However, this may not be true at all: in [71] it has been proposed the existence of a map between commutative and noncommutative Yang-Mills theories in a way that commutative and noncommutative gauge orbits are in one-to-one correspondence. In this way, the so called Seiberg-Witten map allows to relate gauge degrees of freedom of the commutative and noncommutative worlds. Thus, from this point of view, the number of gauge degrees of freedom of any noncommutative Yang-Mills theory may be finite, since the infinite sequence of gauge fields appearing in (5.40) could be expressed, in principle⁴, in terms of the finite gauge fields of the commutative theory though the Seiberg-Witten map. Indeed, for unitary but not special gauge groups, $U(N)$, the anticommutator of any two generators of the group

⁴Up to date, there is no any exact analytical solution to the Seiberg-Witten map. It has been explicitly computed only perturbatively in powers of $\theta^{\mu\nu}$ at low orders. Thus the possibility of relate the apparently infinite gauge degrees of freedom of a noncommutative Yang-Mills theory with the finite gauge degrees of freedom in the commutative limit is, nowadays, only a conjecture.

is inside the Lie algebra of the gauge group (taken as a vectorial space), $u(N)$, and thus the gauge degrees of freedom are finite for $U(N)$ gauge groups without any need to make use of the Seiberg-Witten map.

Beyond the fact that the gauge fields of noncommutative Yang-Mills theories take values in $U(\mathfrak{g})$, noncommutativity introduces a richer dynamics than the one in commutative theories. This is specially glaring in noncommutative QED. In this case, in spite of the gauge group being Abelian, there are interaction terms between (noncommutative) photons because of the star-commutator in (5.36). In this way, quantum noncommutative QED includes vertices with three and four photons depending on $\theta^{\mu\nu}$,



$$\lambda \bar{\psi} \star \gamma^\mu A_\mu \star \psi \quad \sim 1,$$

$$\lambda^2 \partial_\mu A_\nu \star [A^\mu, A^\nu]_\star \quad \sim \sin \theta,$$

$$\lambda^2 [A_\mu, A_\nu]_\star \star [A^\mu, A^\nu]_\star \quad \sim \sin^2 \theta,$$

with θ the noncommutative parameter as in (5.32). In a similar way, vertices in nonAbelian Yang Mills theories in \mathbb{R}_θ^d present a more complicated dynamics than in their commutative limit. Obviously, this new dynamics does not appear in nature, neither for QED nor weak and strong interactions. Together with the breaking of Lorentz invariance and the UV/IR phenomena discussed in the previous subsection, this not observed new dynamics yields to an extremely poor phenomenological perspective for noncommutative field theories and, in particular, for noncommutative Yang-Mills theories⁵.

From a purely conceptual point of view, the main problem of noncommutative Yang-Mills theories is that they are not invariant under ordinary gauge transformations. This can be seen even for the quadratic term $\bar{\psi} \star \psi$: given some local element of the gauge group \mathcal{G} in the fundamental representation,

$$U(x) = e^{i\omega^a(x)T_a}, \tag{5.41}$$

⁵Strictly speaking the absence of vertices with three and four photons in the experimental data obtained up to date only establishes an upper bound for the noncommutativity scale of flat spacetime in accordance with observations. On the other hand, the UV/IR mixing can be kept under control by including a cut-off Λ in the theory. Then the UV range is completed with a supersymmetric theory as $\mathcal{N} = 4$ SYM. However this leads to photons with mass and birefringence. Keeping these new phenomena under the experimental bound requires a specific fine tuning of the breaking of supersymmetry [103].

with T_a the generators of G in the fundamental representation and $\omega^a(x)$ real functions, the associated gauge transformation of $\bar{\psi} \star \psi$ is

$$\bar{\psi}(x) \star \psi(x) \rightarrow (\bar{\psi}(x)U^\dagger(x)) \star (U(x)\psi(x)) \neq \bar{\psi}(x) \star \psi(x), \quad (5.42)$$

since the star product also acts over the dependence on x of the gauge transformation, and therefore the Lagrangian density (5.34) is not invariant under ordinary gauge transformations. In physical terms, the local nature of gauge transformations is *a priori* incompatible with the highly nonlocal nature of the Moyal product. In this way, noncommutative Yang-Mills theories lose the ordinary gauge invariance as the symmetry which justifies them: in commutative theories, invariance under local gauge transformations yields to the introduction of gauge fields but, however, we lose this construction in noncommutative geometries and thus (5.34) has no mathematical justification. Although conceptual, this is a serious problem, since now we have not a symmetry fixing the dynamics of noncommutative Yang-Mills theories.

Note that the not invariance of (5.42) is based on two assumption:

- The gauge group locally acts in the usual way (through the standard product) over fields. That is, we suppose that, even in noncommutative geometry, local gauge transformation of a field in a representation R of the gauge group \mathcal{G} is given by

$$\Psi^R \rightarrow U^R \Psi^R. \quad (5.43)$$

- It acts over the star product of fields in an ordinary way. That is, transformation of the first field star-times the transformation of the second field,

$$\Psi^{R_1} \star \Psi^{R_2} \rightarrow (U^{R_1} \Psi^{R_1}) \star (U^{R_2} \Psi^{R_2}). \quad (5.44)$$

Equations (5.43) and (5.44) define the standard way in which the gauge group locally acts over the field algebra. While the action defined in this way results in an invariance of the Yang-Mills theory for $\theta^{\mu\nu} \rightarrow 0$, it is not for a finite value of $\theta^{\mu\nu}$. Changing one of these two equations (or the two at the same time) can help us to define adapted local gauge transformations to a noncommutative geometry in a way that the action associated with (5.34) be invariant under them. In other words, we have to redefine the way in which the gauge group acts over the field algebra in order to define an invariance for finite $\theta^{\mu\nu}$. Thus, noncommutative geometry does not only change the product of the field algebra, but also deforms the way in which the local symmetries act over such algebra. In the following sections we see how.

5.2 Star-gauge invariance

Star-gauge transformations arise when we deform the ordinary group action over the fields (5.43) by replacing the ordinary product by the Moyal one. In this way we construct “star”-representations of the gauge group which are compatible with the highly nonlocal feature of the field algebra over \mathbb{R}_θ^d and, as a consequence, the noncommutative Yang-Mills Lagrangian density remains invariant under the so called star-gauge transformations [10, 71].

Let us begin defining the infinitesimal star-gauge transformation of a field Ψ^R in some representation R of the gauge group \mathcal{G} as

$$\delta_\omega^\star \Psi^R(x) = i\omega^a(x)T_a \star \Psi^R(x), \quad (5.45)$$

T_a being the generators of \mathcal{G} in the representation R . The difference with the ordinary infinitesimal gauge transformations is the inclusion of the star product before the field Ψ^R . This infinitesimal “star-action” of the gauge group extends to the algebra of fields by means of the ordinary Leibniz rule,

$$\delta_\omega^\star (\Psi^{R_1} \star \Psi^{R_2}) = \delta_\omega^\star (\Psi^{R_1}) \star \Psi^{R_2} + \Psi^{R_1} \star \delta_\omega^\star (\Psi^{R_2}), \quad (5.46)$$

for any two fields Ψ^{R_1} and Ψ^{R_2} transforming in representations R_1 and R_2 of \mathcal{G} . Finite transformations are obtained by exponentiation of (5.45) and (5.46),

$$\begin{aligned} \Psi^R(x) &\longrightarrow U_\star^R(x) \star \Psi^R(x) \\ \Psi^{R_1} \star \Psi^{R_2} &\longrightarrow (U_\star^{R_1} \star \Psi^{R_1}) \star (U_\star^{R_2} \star \Psi^{R_2}), \end{aligned} \quad (5.47)$$

where

$$U_\star^R(x) = \sum_{n=0}^{\infty} \frac{i^n}{n!} \omega^{a_1}(x) \star \dots \star \omega^{a_n}(x) T_{a_1} \dots T_{a_n}. \quad (5.48)$$

Defined in this way, the operators $U_\star^R(x)$ satisfy the group law with respect to the star product. In particular, for a star-gauge transformation in the fundamental representation, $U_\star(x)$,

$$U_\star \star U_\star^\dagger = U_\star^\dagger \star U_\star = 1, \quad (5.49)$$

where we have assumed the existence of unitary representations for the gauge group \mathcal{G} (that is always true for $U(N)$). This leads directly to the star-gauge invariance of the quadratic term,

$$\bar{\psi} \star \psi \longrightarrow \bar{\psi} \star U_\star^\dagger \star U_\star \star \psi = \bar{\psi} \star \psi. \quad (5.50)$$

In general, the Moyal product of any two objects transforming in the anti-fundamental and fundamental representation of the gauge group is invariant under star-gauge transformations.

Since $\bar{\psi} \star \psi$ does not change under star-gauge transformations, the whole noncommutative Yang-Mills action can become invariant under star-gauge transformations if we give a suitable transformation law for the gauge field A_μ . For this, the gauge group \mathcal{G} must act over A_μ such that $D_\mu \psi$ transforms covariantly in the fundamental representation,

$$D_\mu \psi \longrightarrow U_\star \star D_\mu \psi. \quad (5.51)$$

In this way, we would get the invariance of the term $i\bar{\psi} \star \not{D}\psi$. This is done by imposing the following transformation of A_μ :

$$A_\mu \longrightarrow U_\star \star A_\mu \star U_\star^\dagger - \frac{i}{\lambda} (\partial_\mu U_\star) \star U_\star^\dagger. \quad (5.52)$$

Note that this is essentially the ordinary gauge transformation of A_μ substituting ordinary products by star ones. Finally it remains to check the invariance of the trace term in (5.34) to prove the invariance of the whole noncommutative Yang-Mills action under star-gauge transformations. From the previous transformation of A_μ and the definition of $F_{\mu\nu}$ in (5.36),

$$F_{\mu\nu} \longrightarrow U_\star \star F_{\mu\nu} \star U_\star^\dagger. \quad (5.53)$$

Then, by the cyclicity of the Moyal product under the integral symbol (5.23),

$$\begin{aligned} \int d^d x \text{Tr} (F_{\mu\nu} \star F^{\mu\nu}) &\longrightarrow \int d^d x \text{Tr} (U_\star \star F_{\mu\nu} \star F^{\mu\nu} \star U_\star^\dagger) \\ &= \int d^d x \text{Tr} (F_{\mu\nu} \star F^{\mu\nu}), \end{aligned} \quad (5.54)$$

which, together with (5.50) and (5.51), proves the invariance of the noncommutative Yang-Mills action under star-gauge transformations. Notice that in the case of noncommutative QED, the field strength is not gauge invariant, but transforms in the “star-adjoint representation” (see below) of $U(1)$, which is nontrivial.

Until now we have worked with matter fields in the fundamental and antifundamental representation of the gauge group \mathcal{G} . Naively we could expect the star-gauge invariance to be compatible with matter fields in any other representation of \mathcal{G} , as it occurs in ordinary field theory. Unfortunately, this is only possible for fields in the trivial, fundamental, antifundamental and adjoint representations [104, 105]. The reason is that only for fields in

these representations we can construct covariant derivatives under star-gauge transformations, i.e. such that

$$D_\mu^R \Psi^R \longrightarrow U_\star^R \star D_\mu^R \Psi^R. \quad (5.55)$$

Explicitly, these covariant derivatives are,

$$\begin{aligned} \text{Singlet:} & \quad D_\mu^0 \phi = \partial_\mu \phi, \\ \text{Fundamental:} & \quad D_\mu \psi = \partial_\mu \psi - i\lambda A_\mu \star \psi, \\ \text{Antifund. :} & \quad D_\mu \bar{\psi} = \partial_\mu \bar{\psi} + i\lambda \bar{\psi} \star A_\mu, \\ \text{Adjoint:} & \quad D_\mu^{(Adj)} \Phi = \partial_\mu \Phi - i\lambda [A_\mu, \Phi]_\star. \end{aligned} \quad (5.56)$$

This restrict drastically the models we can build with star-gauge invariance.

An important feature of star-gauge invariance is that the transformation of the gauge field goes outside the Lie algebra \mathfrak{g} of the gauge group \mathcal{G} : for an infinitesimal star-gauge transformation, we have

$$\delta_\omega^\star A_\mu = i[\omega^a T_a, A_\mu]_\star + \frac{1}{\lambda} \partial_\mu \omega^a T_a. \quad (5.57)$$

This can be expanded as

$$\delta_\omega^\star A_\mu = \frac{i}{2} \{\omega^a, A_\mu^b\}_\star [T_a, T_b] + \frac{i}{2} [\omega^a, A_\mu^b]_\star \{T_a, T_b\} + \frac{1}{\lambda} \partial_\mu \omega^a T_a, \quad (5.58)$$

and the anticommutator $\{T_a, T_b\}$ is, in general, outside the Lie algebra \mathfrak{g} . Therefore we have to consider enveloped valued gauge fields or, alternatively, restrict our attention to $U(N)$ gauge groups [10, 11]. However, remember that we found this same constrain when we considered the field equations for noncommutative Yang-Mills theories (see Section 5.1.4). Thus, strictly speaking, star-gauge transformations do not impose any additional condition in this sense.

5.3 Twist-gauge invariance

A manifest shortcoming of star-gauge invariance from the point of view of model building is that it cannot be implemented for gauge groups different from $U(N)$ and for fields in arbitrary representations of the gauge group. Luckily, we can formulate gauge transformations in \mathbb{R}_θ^d by either deforming the way in which the gauge group locally acts on the fields (star-gauge transformations) or deforming the action of the gauge group on the Moyal product of fields. Since this last option does not modify the ordinary local action of

the gauge groups over the fields, but over their Moyal product, it allows matter fields in any representation of the gauge group. These are the so called twist-gauge transformations [13, 14, 68].

In the end, infinitesimal gauge transformations are given by the action of the Lie algebra \mathfrak{g} of the gauge group \mathcal{G} over the algebra of fields or, being pragmatic, the action of the universal enveloped algebra of \mathfrak{g} , $U(\mathfrak{g})$, over the field algebra. In order to define the infinitesimal transformation of the product of fields, the enveloped algebra must be equipped with a coproduct⁶ $\Delta : U(\mathfrak{g}) \longrightarrow U(\mathfrak{g}) \otimes U(\mathfrak{g})$. For example, in the case of commutative Yang-Mills theory and ordinary gauge transformations, the coproduct is

$$\Delta(\omega) = \omega \otimes \mathbf{1} + \mathbf{1} \otimes \omega, \quad (5.59)$$

for all $\omega \in U(\mathfrak{g})$, and the infinitesimal gauge transformation of any product of fields is defined as⁷

$$\delta_\omega(\Psi^{R_1} \Psi^{R_2}) \equiv \mu [i\Delta^{R_1 \times R_2}(\omega)(\Psi^{R_1} \otimes \Psi^{R_2})], \quad (5.60)$$

with $\mu(a \otimes b) = ab$ the (commutative) product in the field algebra. Acting with the the coproduct on the fields this gives the Leibniz rule for infinitesimal gauge transformations,

$$\delta_\omega(\Psi^{R_1} \Psi^{R_2}) = (\delta_\omega \Psi^{R_1}) \Psi^{R_2} + \Psi^{R_1} (\delta_\omega \Psi^{R_2}). \quad (5.61)$$

Finally, by exponentiation we get the ordinary finite gauge transformation of the product of fields,

$$\Psi^{R_1} \Psi^{R_2} \longrightarrow (U^{R_1} \Psi^{R_1}) (U^{R_2} \Psi^{R_2}). \quad (5.62)$$

In mathematical terms, the coproduct give us the rule to transform elements in the product (Kronecker) representation $R_1 \times R_2$ from the transformation of elements in the representations R_1 and R_2 of the gauge group.

In the case of the noncommutative field theory over \mathbb{R}_θ^d , the Moyal product can be written in the previous notation as

$$\Psi_1 \star \Psi_2 = \mu (\mathcal{F}^{-1} \Psi_1 \otimes \Psi_2), \quad (5.63)$$

with \mathcal{F} the twist operator, defined as the bilinear operator

$$\mathcal{F} = \sum_{n=0}^{\infty} \frac{-i/2}{n!} \theta^{\mu_1 \nu_1} \dots \theta^{\mu_n \nu_n} \partial_{\mu_1} \dots \partial_{\mu_n} \otimes \partial_{\nu_1} \dots \partial_{\nu_n} = e^{\frac{-i}{2} \theta^{\mu\nu} \partial_\mu \otimes \partial_\nu}. \quad (5.64)$$

⁶For a general overview of Hopf algebras see [106] and Appendix A of [70].

⁷We define $\Delta^R(\omega)$ as the coproduct of $\omega \in U(\mathfrak{g})$ acting over fields in the representation R of the gauge group \mathcal{G} .

Then, we define the twist-gauge transformations as the ones which act in the ordinary way over individual fields,

$$\delta_\omega^t \Psi^R \equiv i\omega^a T_a \Psi^R, \quad (5.65)$$

but such that the infinitesimal transformation of the Moyal product of two fields is

$$\delta_\omega^t (\Psi^{R_1} \star \Psi^{R_2}) \equiv \mu [i\Delta^{R_1 \times R_2}(\omega) \mathcal{F}^{-1} \Psi^{R_1} \otimes \Psi^{R_2}], \quad (5.66)$$

with μ the ordinary (commutative) product and $\Delta(\omega)$ the ordinary coproduct (5.59).

However, we can as well use a “twisted” coproduct

$$\Delta_{\mathcal{F}}(\omega) \equiv \mathcal{F} \Delta(\omega) \mathcal{F}^{-1}, \quad (5.67)$$

such that

$$\delta_\omega^t (\Psi^{R_1} \star \Psi^{R_2}) \equiv \mu [\mathcal{F}^{-1} i\Delta_{\mathcal{F}}^{R_1 \times R_2}(\omega) \Psi^{R_1} \otimes \Psi^{R_2}], \quad (5.68)$$

which, taking as a reference (5.60), can be identified as a modified Leibniz rule for the star-product, thus twisting the ordinary coproduct (5.59) by the twist operator (5.64). Finally, by exponentiation of (5.66) we get the finite twist-gauge transformation of a star-product of fields,

$$\Psi^{R_1} \star \Psi^{R_2} \rightarrow \mu [(U^{R_1} \otimes U^{R_2}) \mathcal{F}^{-1} \Psi^{R_1} \otimes \Psi^{R_2}]. \quad (5.69)$$

Manipulating (5.66), the modified Leibniz rule for twist-gauge transformations takes the form

$$\begin{aligned} \delta_\omega^t (\Psi^{R_1} \star \Psi^{R_2}) &= \mu [i\Delta(\omega) \mathcal{F}^{-1} \Psi^{R_1} \otimes \Psi^{R_2}] \\ &= i \sum_{n=0}^{\infty} \frac{(i/2)^n}{n!} \theta^{\mu_1 \nu_1} \dots \theta^{\mu_n \nu_n} \mu [\Delta(\omega) \partial_{\mu_1} \dots \partial_{\mu_n} \Psi^{R_1} \otimes \partial_{\nu_1} \dots \partial_{\nu_n} \Psi^{R_2}] \\ &= i \sum_{n=0}^{\infty} \frac{(i/2)^n}{n!} \theta^{\mu_1 \nu_1} \dots \theta^{\mu_n \nu_n} \mu [\omega^a T_a \partial_{\mu_1} \dots \partial_{\mu_n} \Psi^{R_1} \otimes \partial_{\nu_1} \dots \partial_{\nu_n} \Psi^{R_2} \\ &\quad + \partial_{\mu_1} \dots \partial_{\mu_n} \Psi^{R_1} \otimes \omega^a T_a \partial_{\nu_1} \dots \partial_{\nu_n} \Psi^{R_2}], \end{aligned} \quad (5.70)$$

which, taking into account the definition of the Moyal product (5.19) can be recast into the more compact equation

$$\delta_\omega^t (\Psi^{R_1} \star \Psi^{R_2}) = i\omega^a [(T_a \Psi^{R_1}) \star \Psi^{R_2} + \Psi^{R_1} \star (T_a \Psi^{R_2})]. \quad (5.71)$$

This last equation can be used to show the star-product of fields in the fundamental and antifundamental representations of \mathcal{G} is invariant under twist-gauge transformations,

$$\delta_\omega^t(\bar{\psi} \star \psi) = i\omega^a [- (\bar{\psi} T_a) \star \psi + \bar{\psi} \star (T_a \psi)] = 0 \quad (5.72)$$

In a similar way, the star-product $\text{Tr}(F_{\mu\nu} \star F^{\mu\nu})$ is invariant under twist-gauge transformations. In this case, for an adjoint field Φ we have,

$$\delta_\omega^t \Phi = i\omega^a [T_a, \Phi], \quad (5.73)$$

with T_a the generators of the gauge group acting over the fundamental representation. Thus, the star-product $F_{\mu\nu} \star F^{\mu\nu}$ transforms as

$$\begin{aligned} \delta_\omega^t (F_{\mu\nu} \star F^{\mu\nu}) &= i\omega^a ([T_a, F_{\mu\nu}] \star F^{\mu\nu} + F_{\mu\nu} \star [T_a, F^{\mu\nu}]) \\ &= i\omega^a [T_a, F_{\mu\nu} \star F^{\mu\nu}]. \end{aligned} \quad (5.74)$$

Therefore $\text{Tr}(F_{\mu\nu} \star F^{\mu\nu})$ is invariant under twist-gauge transformations,

$$\delta_\omega^t \text{Tr}(F_{\mu\nu} \star F^{\mu\nu}) = \text{Tr} [\delta_\omega^t (F_{\mu\nu} \star F^{\mu\nu})] = 0. \quad (5.75)$$

Equations (5.72) and (5.75) prove the invariance under twist-gauge transformations of the fermion mass and F^2 terms of the noncommutative Yang-Mills Lagrangian (5.34). For the term including the covariant derivative, we have

$$\delta_\omega^t (D_\mu \psi) = \partial_\mu \delta_\omega^t \psi - i\lambda \delta_\omega^t (A_\mu \star \psi). \quad (5.76)$$

Using the notation of [107], we define

$$\begin{aligned} \mathbf{A}_\mu &= \begin{pmatrix} A_\mu \\ 1 \end{pmatrix}, \\ R(\omega^a) &= \begin{pmatrix} \omega^a & -\frac{i}{\lambda} \partial_\mu \omega^a \\ 0 & 0 \end{pmatrix}, \\ R(T^a) &= \begin{pmatrix} \text{Adj } T^a & 0 \\ 0 & T^a \end{pmatrix}, \end{aligned} \quad (5.77)$$

the infinitesimal gauge transformation of A_μ , $\delta_\omega^t = i\omega^a [T_a, A_\mu] + \frac{1}{\lambda} \partial_\mu \omega^a T_a$, can be written as

$$\delta_\omega^t \mathbf{A}_\mu = iR(\omega^a) R(T_a) \mathbf{A}_\mu, \quad (5.78)$$

with $(\text{Adj } T_a) A_\mu = [T_a, A_\mu]$. Written in this way, \mathbf{A}_μ seems to transform in some ‘‘representation’’ of the gauge group. Thus, from (5.71), the variation of $\mathbf{A}_\mu \star \psi$ must be given by

$$\delta_\omega^t (\mathbf{A}_\mu \star \psi) = iR(\omega^a) [R(T_a) \mathbf{A}_\mu \star \psi] + i\omega^a [\mathbf{A}_\mu \star (T_a \psi)]. \quad (5.79)$$

The first component of this equation gives us the transformation of the star-product $(A_\mu \star \psi)$,

$$\delta_\omega^t(A_\mu \star \psi) = i\omega^a T_a(A_\mu \star \psi) + \frac{1}{\lambda}(\partial_\mu \omega^a) T_a \psi. \quad (5.80)$$

Substituting in (5.76), we get finally the transformation of the covariant derivative $D_\mu \psi$,

$$\begin{aligned} \delta_\omega^t(D_\mu \psi) &= \partial_\mu(i\omega^a T_a \psi) + \lambda\omega^a T_a(A_\mu \star \psi) - i(\partial_\mu \omega^a) T_a \psi \\ &= i\omega^a T_a D_\mu \psi, \end{aligned} \quad (5.81)$$

i.e., $D_\mu \psi$ transform as a field in the fundamental representation of the gauge group. Thus $\delta_\omega^t(\bar{\psi} \star \not{D}\psi) = 0$, and the term of the covariant derivative in (5.34) remains unchanged under twist-gauge transformations. Together with equations (5.72) and (5.75) this proves the invariance of the whole noncommutative Yang-Mills Lagrangian (5.34) under twist-gauge transformations.

5.4 Star- and twist-gauge invariances as true symmetries

So far we have considered star- and twist-gauge transformations as invariances of the noncommutative Yang-Mills theory without elevating them to the category of true physical symmetries, this means, associated with conserved currents.

Mathematically, the extra terms appearing in the twisted Leibniz rule for twist-gauge transformations can be understood as due to a transformation of the star-product itself under gauge transformations [70] and thus, from this point of view, they are not standard, bona-fide transformations since they involve not only the transformation of fields but of the product operation as well. This prevents the standard procedures to obtain Noether currents and Ward identities from the twist-gauge invariance. On the other hand, any theory with twist-gauge invariance is also invariant under the corresponding star-gauge transformations. The latter can be considered a standard invariance of the theory in the sense that it acts only on fields. In this way, in [70] it was argued that star-gauge transformations play a custodial rôle in guaranteeing the existence of conserved current and Ward identities, and thus the invariance under star-gauge transformations is the true symmetry of the theory. This point of view was further supported in [69], where it was argued that the consistency of the twisted gauge theory requires the presence of the custodian star-gauge symmetry.

Let us begin considering twist-gauge transformations. Note that we can write equation (5.69) in the form

$$\Psi^{R_1} \star \Psi^{R_2} \rightarrow \mu \left[(U^{R_1} \otimes U^{R_2}) \mathcal{F}^{-1} (U^{R_1^{-1}} \otimes U^{R_2^{-1}}) (U^{R_1} \Psi^{R_1} \otimes U^{R_2} \Psi^{R_2}) \right]. \quad (5.82)$$

This could be interpreted as some ordinary gauge transformation where the twist operator \mathcal{F} also transforms,

$$\mathcal{F} \rightarrow (U^{R_1} \otimes U^{R_2}) \mathcal{F}^{-1} (U^{R_1^{-1}} \otimes U^{R_2^{-1}}). \quad (5.83)$$

This can be interpreted as a transformation of the star product itself with respect to gauge transformations [70, 72]. Infinitesimally, from (5.83), such transformation are given by

$$\Psi^{R_1} (\delta_\omega^t \star) \Psi^{R_2} \equiv \mu \left[(\delta_\omega^t \mathcal{F}^{-1}) \Psi^{R_1} \otimes \Psi^{R_2} \right], \quad (5.84)$$

where

$$\delta_\omega^t \mathcal{F}^{-1} = e^{\frac{i}{2} [(\delta_\omega^t \partial_\mu) \otimes \partial_\nu + \partial_\mu \otimes (\delta_\omega^t \partial_\nu)]} \Big|_\omega, \quad (5.85)$$

with $\delta_\omega^t \partial_\mu$ the linear term in $U^R \partial_\mu U^{R^{-1}}$ when we expand in powers of $\omega \equiv \omega^a T_a$,

$$\begin{aligned} (e^{i\omega} \partial_\mu e^{-i\omega}) \Psi^R &= (\partial_\mu + i\omega \partial_\mu - i\partial_\mu \omega + \dots) \Psi^R \\ &\implies \delta_\omega^t \partial_\mu = -[\partial_\mu, \omega]. \end{aligned} \quad (5.86)$$

Substituting in (5.85),

$$\begin{aligned} \delta_\omega^t \mathcal{F}^{-1} &= \\ \mathcal{F}^{-1} i \sum_{n=1}^{\infty} \frac{(-i/2)^n}{n!} \theta^{\mu_1 \nu_1} \dots \theta^{\mu_n \nu_n} \{ &[\partial_{\mu_1}, [\dots, [\partial_{\mu_n}, \omega] \dots]] \otimes \partial_{\nu_1} \dots \partial_{\nu_n} \\ &+ \partial_{\mu_1} \dots \partial_{\mu_n} \otimes [\partial_{\nu_1}, [\dots, [\partial_{\nu_n}, \omega] \dots]] \} \end{aligned} \quad (5.87)$$

where we have used the standard Leibniz rule over the tensorial product $\theta^{\mu\nu} \partial_\mu \otimes \partial_\nu$,

$$\delta_\omega^t (\theta^{\mu\nu} \partial_\mu \otimes \partial_\nu) = -\theta^{\mu\nu} ([\partial_\mu, \omega] \otimes \partial_\nu + \partial_\mu \otimes [\partial_\nu, \omega]), \quad (5.88)$$

together with the well-known formula

$$e^{A+\delta A} \Big|_{\delta A} = e^A \sum_{n=1}^{\infty} \frac{(-1)^n}{n!} [A, [A, \dots [A, \delta A] \dots]]. \quad (5.89)$$

In this way, from (5.87), we get an analytical expression for (5.84),

$$\begin{aligned} \Psi^{R_1}(\delta_\omega^t \star) \Psi^{R_2} &= \\ &= i \sum_{n=1}^{\infty} \frac{(-i/2)^n}{n!} \theta^{\mu_1 \nu_1} \dots \theta^{\mu_n \nu_n} \{ [\partial_{\mu_1}, [\dots, [\partial_{\mu_n}, \omega] \dots]] \Psi^{R_1} \\ &\quad \star \partial_{\nu_1} \dots \partial_{\nu_n} \Psi^{R_2} + \partial_{\mu_1} \dots \partial_{\mu_n} \Psi^{R_1} \star [\partial_{\nu_1}, [\dots, [\partial_{\nu_n}, \omega] \dots]] \Psi^{R_2} \}. \end{aligned} \quad (5.90)$$

On the other hand, using the Hadamard formula,

$$e^A B e^{-A} = B + \sum_{n=1}^{\infty} \frac{1}{n!} [A, [A, \dots [A, B] \dots]], \quad (5.91)$$

the twisted coproduct we defined in (5.67) can be expanded as

$$\begin{aligned} \Delta_{\mathcal{F}}(\omega) &= \Delta(\omega) \\ &+ \sum_{n=1}^{\infty} \frac{(-i/2)^n}{n!} \theta^{\mu_1 \nu_1} \dots \theta^{\mu_n \nu_n} \{ [\partial_{\mu_1}, [\dots, [\partial_{\mu_n}, \omega] \dots]] \\ &\quad \otimes \partial_{\nu_1} \dots \partial_{\nu_n} + \partial_{\mu_1} \dots \partial_{\mu_n} \otimes [\partial_{\nu_1}, [\dots, [\partial_{\nu_n}, \omega] \dots]] \}, \end{aligned} \quad (5.92)$$

which, once we substitute into equation (5.68), gives

$$\begin{aligned} \delta_\omega^t(\Psi^{R_1} \star \Psi^{R_2}) &= (\delta_\omega^t \Psi^{R_1}) \star \Psi^{R_2} + \Psi^{R_1} \star (\delta_\omega^t \Psi^{R_2}) \\ &+ i \sum_{n=1}^{\infty} \frac{(-i/2)^n}{n!} \theta^{\mu_1 \nu_1} \dots \theta^{\mu_n \nu_n} \{ [\partial_{\mu_1}, [\dots, [\partial_{\mu_n}, \omega] \dots]] \Psi^{R_1} \\ &\quad \star \partial_{\nu_1} \dots \partial_{\nu_n} \Psi^{R_2} + \partial_{\mu_1} \dots \partial_{\mu_n} \Psi^{R_1} \star [\partial_{\nu_1}, [\dots, [\partial_{\nu_n}, \omega] \dots]] \Psi^{R_2} \}. \end{aligned} \quad (5.93)$$

The last term in this equation coincides with (5.90). Therefore, assuming the transformation of the Moyal product itself given in (5.84), we can write the infinitesimal change under twist-gauge transformations of the star-product of fields in a extremely compact form:

$$\delta_\omega^t(\Psi^{R_1} \star \Psi^{R_2}) = (\delta_\omega^t \Psi^{R_1}) \star \Psi^{R_2} + \Psi^{R_1} \star (\delta_\omega^t \Psi^{R_2}) + \Psi^{R_1}(\delta_\omega^t \star) \Psi^{R_2}. \quad (5.94)$$

That is, the modified Leibniz rule for twist-gauge transformations we define in the previous section can be viewed as an ordinary Leibniz rule where the Moyal product also transforms itself [70]. In some sense this is a weird result, since the Moyal product is a feature of the theory related with its underlying geometrical structure which, *a priori*, is no related to the gauge degrees of freedom of the theory. Thus, this could be regarded as a first indication that twist-gauge invariance cannot be consider as the true gauge symmetry in noncommutative Yang-Mills theories.

In principle, since star-gauge invariance does not imply modifying the coproduct in the enveloping universal algebra of the gauge group, it is a better candidate to true gauge symmetry than twist-gauge invariance. Indeed, following the standard Noether construction, star-gauge invariance leads to conserved currents: let us consider a point-to-point “global” star-gauge transformation⁸ over a solution to the gauge field equations,

$$\delta_{\omega}^{(*)} A_{\mu} \equiv i[\omega, A_{\mu}]_{\star}. \quad (5.95)$$

Since ω depends on the coordinates, there are terms depending on derivatives of ω in the variation of the strength field $F_{\mu\nu}$ under this transformation,

$$\begin{aligned} \delta_{\omega}^{(*)} F_{\mu\nu} &= \partial_{\mu} \delta_{\omega}^{(*)} A_{\nu} - \partial_{\nu} \delta_{\omega}^{(*)} A_{\mu} - i\lambda[\delta_{\omega}^{(*)} A_{\mu}, A_{\nu}] - i\lambda[A_{\mu}, \delta_{\omega}^{(*)} A_{\nu}] \\ &= i[\omega, F_{\mu\nu}]_{\star} + i\{[\partial_{\mu}\omega, A_{\nu}]_{\star} - [\partial_{\nu}\omega, A_{\mu}]_{\star}\}. \end{aligned} \quad (5.96)$$

Considering a pure Yang-Mills theory (i.e. without matter fields), the additional terms depending on $\partial_{\mu}\omega$ generate a variation of the action functional given by

$$\delta_{\omega}^{(*)} S = -2i \int d^d x \text{Tr} [(A_{\nu} \star F_{\mu\nu} - F^{\mu\nu} \star A_{\nu}) \star \partial_{\mu}\omega]. \quad (5.97)$$

Integrating by parts and dropping global derivatives, we finally obtain

$$\delta_{\omega}^{(*)} S = 2i \int d^d x \text{Tr} \{ \partial_{\mu} [A_{\nu}, F^{\mu\nu}]_{\star} T_a \} \star \omega^a + \text{Boundary Terms}. \quad (5.98)$$

Since (5.95) is a variation over a solution to field equations, we must have $\delta_{\omega}^{(*)} S = 0$, which leads to a conserved current j^{μ} given by [70]

$$j^{\mu} = [A_{\nu}, F^{\mu\nu}]_{\star}. \quad (5.99)$$

Thus star-gauge invariance leads to a conserved current in noncommutative Yang-Mills theory. We could try to develop the same procedure from equations (5.95) to (5.99) for twist-gauge invariance. However, the existence of a term in the modified Leibniz rule (5.94) for the transformation of the star-product itself under twist-gauge transformations would introduce terms in (5.96) depending on the variation of the star-product which would prevent eliminating the boundary terms in (5.98), so a conserved current does not result. This fact, together with the unusual and, in some sense, weird variation of the star-product itself with twist-gauge transformations, seems to indicate that the star-gauge invariance is the true gauge symmetry, the one physically relevant for noncommutative Yang-Mills in \mathbb{R}_{θ}^d , twist-gauge transformations being just an accidental invariance.

⁸That means a global transformation such that ω depends in coordinates. Note that this is different from local star-gauge transformation, for which we have $\delta_{\omega}^{*} A_{\mu} = i[\omega, A_{\mu}]_{\star} + 1/\lambda \partial_{\mu}\omega$.

5.5 Star-twisted gauge invariances

We have discussed in detail how gauge invariance admits two deformations on noncommutative spacetimes: either by means of a star-action of the gauge group over the field algebra (star-gauge) or a modification of the Leibniz rule (twist-gauge), showing that the first method seems to give the true gauge symmetry in noncommutative geometry. In addition to this, we will show how there is a third possibility consisting of a simultaneous star-action and a twisted-gauge transformation with different deformation parameters. These we call star-twisted gauge transformations, and define an infinite family of invariances interpolating continuously between star-gauge and twist-gauge invariance [72].

The key ingredient of twist-gauge transformations is the use of a product for the action of the gauge group (the commutative one) different from the Moyal product operating in the field algebra. Star-twisted transformations generalize this idea considering that the gauge group acts through a star-product with a noncommutativity parameter $\theta'^{\mu\nu}$ different from the noncommutativity parameter $\theta^{\mu\nu}$ operating in the field algebra. That is, the infinitesimal gauge transformation of a field Ψ^R in a representation R of the gauge group is given by

$$\delta_\omega^{\theta'} \Psi^R \equiv i\omega \star_{\theta'} \Psi^R, \quad (5.100)$$

where $\omega = \omega^a(x)T_a$ and $\star_{\theta'}$ states for the star-product with noncommutativity parameter $\theta'^{\mu\nu}$,

$$A \star_{\theta'} B \equiv \mu(\mathcal{F}_{\theta'}^{-1} A \otimes B). \quad (5.101)$$

Here, \mathcal{F}_θ is the twist operator with noncommutativity parameter $\theta^{\mu\nu}$,

$$\mathcal{F}_\theta = \sum_{n=0}^{\infty} \frac{-i/2}{n!} \theta^{\mu_1\nu_1} \dots \theta^{\mu_n\nu_n} \partial_{\mu_1} \dots \partial_{\mu_n} \otimes \partial_{\nu_1} \dots \partial_{\nu_n} = e^{-\frac{i}{2}\theta^{\mu\nu}\partial_\mu \otimes \partial_\nu}. \quad (5.102)$$

Note that, defined in this way, twist operators with different noncommutativity parameters satisfy,

$$\mathcal{F}_\theta \mathcal{F}_{\theta'} = \mathcal{F}_{\theta+\theta'}, \quad \mathcal{F}_\theta^{-1} = \mathcal{F}_{-\theta}. \quad (5.103)$$

Simultaneously to the star-prime action (5.100), star-twisted gauge transformation include a twist in the Leibniz rule depending on the difference $(\theta - \theta')^{\mu\nu}$ to guarantee the compatibility with the underlying noncommutativity with parameter $\theta^{\mu\nu}$. In the notation of (5.66), this new Leibniz rule is

$$\delta_\omega^{\theta'} (\Psi^{R_1} \star_\theta \Psi^{R_2}) \equiv \mu \left[\mathcal{F}_\theta^{-1} \mathcal{F}_{\theta-\theta'} \Delta(\delta_\omega^{\theta'}) \mathcal{F}_{\theta-\theta'}^{-1} \Psi^{R_1} \otimes \Psi^{R_2} \right]. \quad (5.104)$$

which is a direct generalization of (5.68) with a coproduct twisted with respect to the difference between the two star-product that we have now in the theory,

$$\delta_{\omega}^{\theta'}(\Psi^{R_1} \star_{\theta} \Psi^{R_2}) = \mu \left[\mathcal{F}_{\theta}^{-1} \Delta_{\theta-\theta'}(\delta_{\omega}^{\theta'}) \Psi^{R_1} \otimes \Psi^{R_2} \right], \quad (5.105)$$

with

$$\Delta_{\theta-\theta'}(\omega) = \mathcal{F}_{\theta-\theta'} \Delta(\omega) \mathcal{F}_{\theta-\theta'}^{-1}. \quad (5.106)$$

Using the law (5.103) we find $\mathcal{F}_{\theta}^{-1} \mathcal{F}_{\theta-\theta'} \Delta(\omega) \mathcal{F}_{\theta-\theta'}^{-1} = \mathcal{F}_{\theta'}^{-1} \Delta_{\omega} \mathcal{F}_{\theta-\theta'}^{-1}$. Then, expanding the last twist operator, we obtain

$$\begin{aligned} \delta_{\omega}^{\theta'}(\Psi^{R_1} \star_{\theta} \Psi^{R_2}) &= \sum_{n=0}^{\infty} \frac{(-i/2)^n}{n!} (\theta - \theta')^{\mu_1 \nu_1} \dots (\theta - \theta')^{\mu_n \nu_n} \\ &\times \left\{ \left(\delta_{\omega}^{\theta'} \partial_{\mu_1} \dots \partial_{\mu_n} \Psi^{R_1} \right) \star_{\theta'} (\partial_{\nu_1} \dots \partial_{\nu_n} \Psi^{R_2}) \right. \\ &\quad \left. + (\partial_{\mu_1} \dots \partial_{\mu_n} \Psi^{R_1}) \star_{\theta'} \left(\delta_{\omega}^{\theta'} \partial_{\nu_1} \dots \partial_{\nu_n} \Psi^{R_2} \right) \right\}, \end{aligned} \quad (5.107)$$

which is a generalization of equation (5.70). Written in this way, we see that star-twisted transformations are in a sense halfway between star- and twist-gauge transformations, such that twist-gauge transformations are recovered for $\theta'^{\mu\nu} = 0$ (equation (5.71)), while star-gauge transformations are recovered for $\theta'^{\mu\nu} = \theta^{\mu\nu}$ (equation (5.46)). From this point of view, $\theta'^{\mu\nu}$ is a parameter interpolating from star-gauge to twist-gauge transformations.

Following the the same reasoning that for twist-gauge transformations, the Leibniz rule for star-twisted transformations can be seen as an ordinary Leibniz rule where the Moyal product is also transformed. Using equation (5.92) we can expand the coproduct $\Delta_{\theta-\theta'}(\omega)$ in (5.105) to give

$$\begin{aligned} \delta_{\omega}^{\theta'}(\Psi^{R_1} \star_{\theta} \Psi^{R_2}) &= (\delta_{\omega}^{\theta'} \Psi^{R_1}) \star_{\theta} \Psi^{R_2} + \Psi^{R_1} \star_{\theta} (\delta_{\omega}^{\theta'} \Psi^{R_2}) \\ &+ \sum_{n=1}^{\infty} \frac{(-i/2)^n}{n!} (\theta - \theta')^{\mu_1 \nu_1} \dots (\theta - \theta')^{\mu_n \nu_n} \\ &\times \left\{ \left([\partial_{\mu_1}, \dots [\partial_{\mu_n}, \delta_{\omega}^{\theta'}] \dots] \Psi^{R_1} \right) \star_{\theta} (\partial_{\nu_1} \dots \partial_{\nu_n} \Psi^{R_2}) \right. \\ &\quad \left. + (\partial_{\mu_1} \dots \partial_{\mu_n} \Psi^{R_1}) \star_{\theta} \left([\partial_{\nu_1}, \dots [\partial_{\nu_n}, \delta_{\omega}^{\theta'}] \dots] \Psi^{R_2} \right) \right\}. \end{aligned} \quad (5.108)$$

The last term, similar to (5.90), can be reinterpreted as the θ' -gauge variation of the θ -star product, $\Psi^{R_1}(\delta_{\omega}^{\theta'} \star_{\theta}) \Psi^{R_2}$, to write

$$\delta_{\omega}^{\theta'}(\Psi^{R_1} \star_{\theta} \Psi^{R_2}) = (\delta_{\omega}^{\theta'} \Psi^{R_1}) \star_{\theta} \Psi^{R_2} + \Psi^{R_1} \star_{\theta} (\delta_{\omega}^{\theta'} \Psi^{R_2}) + \Psi^{R_1} (\delta_{\omega}^{\theta'} \star_{\theta}) \Psi^{R_2}. \quad (5.109)$$

Obviously the last term vanishes for $\theta'^{\mu\nu} = \theta^{\mu\nu}$, that is, for star-gauge transformations. This seems to indicate that any twist of the gauge action inevitably leads to a variation of the star-product under gauge transformations, operating from the shadows of the theory.

Surprisingly, the same as star-gauge and twist-gauge transformations are invariances of the noncommutative Yang-Mills action, star-twisted transformation are too. From equation (5.107) we can check the invariance of the quadratic term $\bar{\psi} \star_{\theta} \psi$. Since

$$\delta_{\omega}^{\theta'} \psi = i\omega^a \star_{\theta'} (T_a \psi), \quad (5.110)$$

and

$$\delta_{\omega}^{\theta'} \bar{\psi} = -i(\bar{\psi} T_a) \star_{\theta'} \omega^a, \quad (5.111)$$

with T_a the generators of the gauge algebra in the fundamental representation,

$$\begin{aligned} \delta_{\omega}^{\theta'} (\bar{\psi} \star_{\theta} \psi) &= i \sum_{n=0}^{\infty} \frac{(-i/2)^n}{n!} (\theta - \theta')^{\mu_1 \nu_1} \dots (\theta - \theta')^{\mu_n \nu_n} \\ &\times \left\{ -(\partial_{\mu_1} \dots \partial_{\mu_n} \bar{\psi} T_a) \star_{\theta'} \omega^a \star_{\theta'} (\partial_{\nu_1} \dots \partial_{\nu_n} \psi) \right. \\ &\left. + (\partial_{\mu_1} \dots \partial_{\mu_n} \bar{\psi}) \star_{\theta'} \omega^a \star_{\theta'} (T_a \partial_{\nu_1} \dots \partial_{\nu_n} \psi) \right\} = 0. \end{aligned} \quad (5.112)$$

In a similar way, we can check that the covariant derivative $D_{\mu} \psi$ transforms in the fundamental representation of the gauge group, i.e.

$$\delta_{\omega}^{\theta'} D_{\mu} \psi = i\omega^a T_a \star_{\theta'} D_{\mu} \psi. \quad (5.113)$$

In this case, we have

$$\delta_{\omega}^{\theta'} (D_{\mu} \psi) = i\partial_{\mu} [\omega^a \star_{\theta'} (T_a \psi)] - i\lambda \delta_{\omega}^{\theta'} (A_{\mu} \star_{\theta} \psi). \quad (5.114)$$

For the last terms, following the notation of (5.79), we find

$$\begin{aligned} \delta_{\omega}^{\theta'} (\mathbf{A}_{\mu} \star_{\theta} \psi) &= i \sum_{n=0}^{\infty} \frac{(-i/2)^n}{n!} (\theta - \theta')^{\mu_1 \nu_1} \dots (\theta - \theta')^{\mu_n \nu_n} \\ &\times \left\{ R(\omega) \star_{\theta'} \partial_{\mu_1} \dots \partial_{\mu_n} \mathbf{A}_{\mu} \star_{\theta'} (\partial_{\nu_1} \dots \partial_{\nu_n} \psi) \right. \\ &\left. + (\partial_{\mu_1} \dots \partial_{\mu_n} \mathbf{A}_{\mu}) \star_{\theta'} \omega^a \star_{\theta'} (T_a \partial_{\nu_1} \dots \partial_{\nu_n} \psi) \right\}. \end{aligned} \quad (5.115)$$

Then, the first component of this equation gives

$$\begin{aligned} \delta_{\omega}^{\theta'} (A_{\mu} \star_{\theta} \psi) &= \frac{1}{\lambda} \partial_{\mu} \omega^a \star_{\theta'} (T_a \psi) \\ &+ i \sum_{n=0}^{\infty} \frac{(-i/2)^n}{n!} (\theta - \theta')^{\mu_1 \nu_1} \dots (\theta - \theta')^{\mu_n \nu_n} \\ &\times \omega^a \star_{\theta'} (T_a \partial_{\mu_1} \dots \partial_{\mu_n} A_{\mu}) \star_{\theta'} (\partial_{\nu_1} \dots \partial_{\nu_n} \psi). \end{aligned} \quad (5.116)$$

Using the formula

$$f \star_{\theta} g = \sum_{n=0}^{\infty} \frac{(-i/2)^n}{n!} (\theta'^{\mu_1 \nu_1} - \theta^{\mu_1 \nu_1}) \dots (\theta'^{\mu_n \nu_n} - \theta^{\mu_n \nu_n}) \times (\partial_{\mu_1} \dots \partial_{\mu_n} f) \star_{\theta'} (\partial_{\nu_1} \dots \partial_{\nu_n} g), \quad (5.117)$$

valid for all functions f and g , (5.116) can be finally simplified to

$$\delta_{\omega}^{\theta'} (A_{\mu} \star_{\theta} \psi) = \frac{1}{\lambda} \partial_{\mu} \omega^a \star_{\theta'} (T_a \psi) + i \omega^a T_a \star_{\theta'} (A_{\mu} \star_{\theta} \psi), \quad (5.118)$$

and thus, substituting in (5.114),

$$\delta_{\omega}^{\theta'} D_{\mu} \psi = i \omega^a T_a \star_{\theta'} D_{\mu} \psi. \quad (5.119)$$

Finally it rests to prove the invariance of the F^2 term in (5.34). Form the definition of the gauge field strength tensor,

$$\begin{aligned} \delta_{\omega}^{\theta'} F_{\mu\nu} &= i[\omega, \partial_{\mu} A_{\nu} - \partial_{\nu} A_{\mu}]_{\theta'} + i[\partial_{\mu} \omega, A_{\nu}]_{\theta'} \\ &\quad - i[\partial_{\nu} \omega, A_{\mu}]_{\theta'} - i\lambda \delta_{\omega}^{\theta'} (A_{\mu} \star_{\theta} A_{\nu} - A_{\nu} \star_{\theta} A_{\mu}). \end{aligned} \quad (5.120)$$

To compute the last term, we carry out similar algebraic manipulations to the ones used in the computation of (5.118). It results in

$$\delta_{\omega}^{\theta'} (A_{\mu} \star_{\theta} A_{\nu}) = i[\omega, A_{\mu} \star_{\theta} A_{\nu}]_{\theta'} + (\partial_{\mu} \omega) \star_{\theta'} A_{\nu} + A_{\mu} \star_{\theta'} (\partial_{\nu} \omega). \quad (5.121)$$

Thus, substituting in (5.120),

$$\delta_{\omega}^{\theta'} F_{\mu\nu} = [i\omega, \partial_{\mu} A_{\nu} - \partial_{\nu} A_{\mu} - i\lambda [A_{\mu}, A_{\nu}]_{\theta}]_{\theta'} = [i\omega, F_{\mu\nu}]_{\theta'}, \quad (5.122)$$

and we conclude that $F_{\mu\nu}$ transforms in the adjoint representation of the gauge group. The same happens when we compute $\delta_{\omega}^{\theta'} (F_{\mu\nu} \star_{\theta} F^{\mu\nu})$. In this case, from (5.108) we have

$$\begin{aligned} \delta_{\omega}^{\theta'} (F_{\alpha\beta} \star_{\theta} F^{\alpha\beta}) &= \sum_{n=0}^{\infty} \frac{(-i/2)^n}{n!} (\theta - \theta')^{\mu_1 \nu_1} \dots (\theta - \theta')^{\mu_n \nu_n} \\ &\quad \times \left\{ \left([\partial_{\mu_1}, \dots, [\partial_{\mu_n}, \delta_{\omega}^{\theta'}] \dots] F_{\alpha\beta} \right) \star_{\theta} (\partial_{\nu_1} \dots \partial_{\nu_n} F^{\alpha\beta}) \right. \\ &\quad \left. + (\partial_{\mu_1} \dots \partial_{\mu_n} F_{\alpha\beta}) \star_{\theta} \left([\partial_{\nu_1}, \dots, [\partial_{\nu_n}, \delta_{\omega}^{\theta'}] \dots] F^{\alpha\beta} \right) \right\}. \end{aligned} \quad (5.123)$$

Using manipulations similar to the ones applied above, this can be recast into

$$\delta_{\omega}^{\theta'} (F_{\mu\nu} \star_{\theta} F^{\mu\nu}) = [i\omega, F_{\mu\nu} \star_{\theta} F^{\mu\nu}]_{\theta'}. \quad (5.124)$$

Thus $F_{\mu\nu} \star_{\theta} F^{\mu\nu}$ transforms in the adjoint representation of the gauge group too. Therefore, the pure Yang-Mills action satisfies,

$$\delta_{\omega}^{\theta'} S = -\frac{1}{2} \int d^d x \text{Tr} [i\omega \star_{\theta'} (F_{\mu\nu} \star_{\theta} F^{\mu\nu}) - i(F_{\mu\nu} \star_{\theta} F^{\mu\nu}) \star_{\theta'} \omega] = 0, \quad (5.125)$$

where we have used the cyclicity property of the Moyal product under the integral symbol. Together with equations (5.112) and (5.119), this proves the invariance of the entire Yang-Mills action under star-twisted gauge transformations.

Star-twisted gauge transformations form a continuous family of invariances of the Yang-Mills action at which ends the star-gauge and twist-gauge are [72]. Since in all cases we have a modified Leibniz rule except for star-gauge invariance, following the reasoning of the previous section (impossibility to obtain Noether currents from a modified Leibniz rule) we can conclude that all the twisted invariances are not true symmetries, but accidental invariances. On the other hand, from star-gauge invariance we can obtain Noether currents. In this sense, star-gauge symmetry seems to be the true symmetry of the theory, fixing the gauge coupling to fields in the Lagrangian, and thus any other twisted gauge invariance comes from it accidentally. In other words, star-gauge symmetry has a custodial role over the entire family of star-twisted gauge invariances.

Chapter 6

Conclusions and outlook

In this Thesis we have exposed two different topics: in one side, we have studied the generation of the Penrose trapped surface in collisions of gravitational shock waves in AdS_D , proposing this phenomenon as a signal of thermalization in the boundary theory after a collision of two energy lumps. On the other hand, we have faced the construction of gauge invariances for noncommutative Yang-Mills theories, defining a continuous family of twisted gauge invariances. This final chapter collects the results and discuss them in some detail.

6.1 Collisions of gravitational shock waves and plasma thermalization

The use of the collision of gravitational shock waves as a gravitational dual for colliding energy lumps lies in the fact that the expectation value of the holographic stress tensor corresponding to a gravitational shock wave, propagating at constant holographic coordinate z_0 , is the one describing an energy lump traveling through the boundary of AdS at the speed of light. In this picture, z_0 translates into the boundary theory as the energy-weighted size of the lump, while the energy μ of the shock wave as measured from the boundary coincides with the energy of the lump at the boundary. In this way, colliding gravitational shock waves correspond to colliding energy lumps, whose energy and size can be tuned. The appearance of the Penrose trapped surface in the collision has been taken as a signal for event horizon formation after collision and thus, in the spirit of the AdS/CFT connection, for thermal equilibrium in the boundary theory.

The first collision we have analyzed is the one of two AdS-Sch shock waves. The search of the Penrose trapped surface has shown that it always appears

when the collision has no impact parameter. i.e. for head-on collisions. However, when the collision happens with a nonvanishing impact parameter, the formation of the Penrose trapped surface depends strongly in the value of this impact parameter for a fixed energy. In particular, beyond a critical value, for a given energy there is no possible formation of the Penrose trapped surface [55]. For the case of an impact parameter b parallel to the AdS boundary, our numerical work has shown the scaling

$$\frac{b_c}{z_0} \sim \left(\frac{G_D \mu_0}{L^{D-3}} \right)^{\frac{1}{D-2}} \quad (6.1)$$

of the critical impact parameter b_c with the energy μ of the colliding waves and the dimension D of the AdS background. From the boundary theory point of view, since in this case both waves collide with the same holographic coordinate, this corresponds to the collision of two energy lumps of the same size with certain impact parameter b . Thus the existence of this critical value is taken as an indicative that thermalization in the boundary after the collision does not happen for large enough impact parameter.

The case where the impact parameter is directed along the holographic coordinate z has been considered apart because its different holographic interpretation. This time, since both shock waves collide at different values of the holographic coordinate, z_+ and z_- , they corresponds to the head-on collision of two energy lumps of different sizes. Fortunately, it is not necessary to carry out a separate numerical analysis of this case, since the isometries of the AdS space-time can be combined in a suitable way to relate collisions with purely holographic impact parameter $\Delta z = |z_+ - z_-|$ to collisions with impact parameter parallel to the AdS boundary b . In this way, we have obtained a critical value of the holographic impact parameter $(\Delta z)_c$ beyond of which no Penrose trapped surface is produced. The scaling for the critical value of the holographic impact parameter is given by

$$\frac{(\Delta z)_c}{L} \sim \left(\frac{G_D \sqrt{\mu_+ \mu_-}}{L^{D-3}} \right)^{\frac{1}{D-2}}, \quad (6.2)$$

with μ_{\pm} the energy of the shock waves as measured from the boundary. The existence of this critical behavior in the creation of the Penrose trapped surface indicates that for enough difference in size, the head-on collision of two energy lumps in the boundary theory could not thermalize.

In $D = 5$ these results can be used as a first model to thermalization of sQGP in off-center collisions and frontal collisions between unequal sized objects. In addition, our approach can be generalized to the case in which we have both impact parameter and unequal objects by $O(2)$ rotations. In

this case we have showed that there are two quantities invariant under $O(2)$ rotations inside the AdS space, and thus they have the same value for a large class of related collisions. These are

$$\begin{aligned} \mathcal{Q}_0 &= \mu'_+(\alpha)\mu'_-(\alpha)z'_+(\alpha)z'_-(\alpha) = \mu_+\mu_-, \\ \mathcal{Q}_\pm &= \mu'_\pm(\alpha) \left[1 + \frac{z'_\pm(\alpha)^2 + x'_\pm(\alpha)^2}{L^2} \right] = 2\mu_\pm L \frac{(1 + \beta^2)^{1/2}}{(1 + \beta^2)^{1/2} \pm \beta}. \end{aligned} \quad (6.3)$$

Whereas off-center collisions in $D = 5$ are physically interpretable as heavy-ion collisions with nonvanishing impact parameter, the frontal collision of two gauge theory energy lumps with large size difference could be used as a model for head-on hadron-nucleus collisions at strong coupling. Off-center hadron-nucleus collisions can be studied as well by performing $O(2)$ rotations over the numerical solutions we have obtained. In this case, it would be interesting to see if the invariants (6.3) have any relevance in the phenomenological description of this type of collisions.

The model we have constructed based on collisions of AdS-Sch shock waves is a first approximation to the real problem of sQGP production. Although the results are physically acceptable (mainly the existence of critical values for impact parameter, difference of sizes and their growth with energy seem to go in the right direction), obviously it would be desirable to develop more elaborate models to get a more accurate descriptions of real high-energy collisions. In this sense, there are three paths we can follow to progress:

- Breakdown of conformal invariance. Quantum field dynamics arising from gravitational physics in AdS spacetime is, necessarily, conformal. However real QCD are far away to be conformal. Although the confined-deconfined phase transition in QCD seems to be related mainly to the non-Abelian nature of $SU(3)$ instead of the running of the coupling constant with the energy scale, conformal invariance could have a significant effect in the scaling of the critical values of the impact parameters we have observed. Therefore, collisions of gravitational shock waves in non-AdS spacetimes would be more appropriate gravitational duals for sQGP formation in high-energy collisions.
- Search of other trapped surfaces. Strictly speaking, thermalization in the boundary field theory is related to the formation of an event horizon after the collision, in region IV in fig. 2.1. We have used the formation of the Penrose trapped surface, which lies over the past light cone, as the signal for an eventual horizon after the collision. Although this assumption seems in accordance with the laws of physics, up to date

there is no hard proof of it. For example, it could be that, in a collision where the Penrose surface was not found, other trapped surface appeared, guaranteeing the existence of an event horizon after the collision. In this sense, the search for other trapped surfaces besides the Penrose surface could improve the estimation for plasma thermalization, maybe even beyond critical configurations. A first example can be found in [61], where a trapped surface over the future light cone is computed for collisions between RN shock waves in flat background. In addition, the lost of energy by gravitational radiation after the collision could have implications in the eventual formation of an event horizon [108, 109, 110, 111].

- Collision of shock waves with richer structure. AdS-Sch shock waves have no physical parameters apart from their energy, in the sense that the energies of the sources are the only free quantities, together with impact parameters, that we can tune in a collision of two AdS-Sch shock waves. Since the holographic energy distribution comes from the shock wave profiles, we have no room to incorporate new features to the holographic lumps, and to get, in this way, a more realistic description for extremely boosted heavy-ions. It would be interesting to search for new critical behavior respect to other magnitudes than energy and impact parameter/difference of size, even in head-on collisions.

The last point has lead us to consider collisions between fat and AdS-RN shock waves. The first ones, studied in [57], yields to a dependence of the Penrose trapped surface with the diluting parameter ω , such that, in $D = 4$ and $D = 5$ dimensions, there is a critical value ω_c for the formation of the Penrose surface. However the absence of any trail of the diluting parameter in the vacuum expectation value of the holographic stress tensor has as consequence a poor understanding of the holographic dual for the collision of these shock waves. One reason for this result could be that fat waves couple to some unknown boundary field or, even, they can not be considered as a SUGRA IIB solution.

The AdS-RN shock waves do not suffer from the doubt about their validity as SUGRA IIB phenomena since the AdS-RN solution can be reinterpreted as a complete SUGRA IIB solution. Thus they are a good candidate to improve the model constructed over AdS-Sch shock waves. Naively we expected that the addition of an extra parameter (the chrage parameter e^2) to the collision problem could help to get an accurate description of real sQGP production in heavy-ion collisions at high energy. However, as we have show, the effect of the charge parameter, even for small values, prevents totally the formation of a Penrose surface in the collision [60]. This result holds for both S^{D-2}

and $S^1 \times S^{D-3}$ topologies of the Penrose trapped surface. The reason to search for the second topology is that the solution to the function $\Psi(q)$ which parametrizes the Penrose surface with S^{D-2} topology takes negative values (this is the reason because the Penrose surface is not possible), thus indicating a nontrivial topology of the marginal surface.

The holographic consequences of the absence of the Penrose trapped surface for colliding AdS-RN shock waves are not clear. First, although the holographic dual of the AdS-RN solution is fully understood, the one for AdS-RN has no direct interpretation. The reason is that in the AdS-RN solution, charge corresponds to a chemical potential in the boundary theory [97, 98], describing a grand canonical ensemble, although the charge and the electromagnetic field vanish after the infinite boost limit that leads to the AdS-RN shock waves.

Finally we have shown that, independently of the gravitational nature, i.e. AdS-Sch, AdS-RN or fat shock waves, all the gravitational shock waves give rise to the same holographic stress tensor. That suggests that the form of the holographic potential is related to the $O(D-2)$ symmetry of the colliding waves and not to the concrete mathematical form of their profile functions. In addition, the boosted Woods-Saxon energy distribution is not well fitted by the vacuum expectation value of the holographic stress-tensor. Therefore collision of fat and AdS-RN shock waves will not help to get better approximations to the energy distribution of real extremely boosted heavy-ions. Shock waves with a reduced symmetry could give better energy distribution for fitting the boosted Wood-Saxon potential. However this does not mean the effort of studying collision of fat and AdS-RN shock waves is futile. For example, estimations as entropy production from the area of the Penrose surface could be improved [51, 53].

6.2 Gauge invariances in noncommutative Yang-Mills theories

In the Chapter 5 we have discussed the construction of gauge invariances in noncommutative Yang-Mills theories. Typically, in the scientific literature there existed two ways to define the action of the gauge group over a non-commutative algebra of fields constructed with the Moyal product:

- Star-gauge transformations. These transformations use a star-action to acts over fields. That is, the gauge transformation includes the Moyal product while the Leibniz rule remains in its standard form [10, 71].
- Twist-gauge transformations. This time the gauge group acts over fields

1426.2. Gauge invariances in noncommutative Yang-Mills theories

using the standard commutative product, but the Leibniz rule becomes twisted to force a transformation law compatible with the star product of fields [13, 14, 68].

These two transformations are invariances of the noncommutative Yang-Mills action, although their implementations force to consider only unitary gauge groups, or gauge fields taking values over the universal enveloping algebra of the gauge group.

The coincidence of two radically different invariances for the noncommutative Yang-Mills action gives rise to the question of what of them is the true symmetry of the theory. Because of the twist-gauge transformations operate through a twisted Leibniz rule, the derivation of Noether currents and/or Ward identities is not possible from the twist-gauge invariance. On the other hand, star-gauge invariance, with a standard Leibniz rule, does not have this problem. In this way star-gauge invariance is taken as the true symmetry of the theory, playing a custodial role over twist-gauge invariance, which appears accidentally. In addition, the Leibniz rule can be reinterpreted as an unhealthy variation of the star product under gauge transformations [70, 72].

In this Thesis we have shown that a third class of star-twisted invariances of the noncommutative Yang-Mills action can be constructed. In this case the gauge group acts through a star product over the fields algebra but with a noncommutative parameter $\theta'^{\mu\nu}$ different for the one operating in the fields algebra, $\theta^{\mu\nu}$. As a consequence, the Leibniz rule has to be twisted. In this way we have constructed a continuous family of twisted invariances, depending on the noncommutative parameter $\theta'^{\mu\nu}$, which interpolates between star-gauge symmetry ($\theta'^{\mu\nu} = \theta^{\mu\nu}$) and twist-gauge invariance ($\theta'^{\mu\nu} = 0$). The direct consequence of the existence of this family of invariance is that twist-gauge invariance is no more a particular twisted invariance, but it is part of a large family of invariances with a twisted Leibniz rule.

The loss of any special status by the twist-gauge invariance in the sense here explained reinforces itself the idea of the twist as a mechanism giving accidental invariances and not true symmetries as well. Another point in favour of this statement is the fact that for $\theta^{\mu\nu} = 0$ and $\theta'^{\mu\nu} \neq 0$ we have a twisted gauge invariance for the ordinary Yang-Mills action which, obviously, does not play any physical role in the standard theory [72].

Appendix A

Anti-de Sitter space

This Appendix is written to those reader which are not familiarized with the Anti-de Sitter space and/or coordinates on it. Here we introduce the Anti-de Sitter spacetime and develop in detail the different coordinate system that are used along the main text.

From a purely mathematical point of view, D -dimensional Anti-de Sitter space, AdS_D , is defined as the maximally symmetric space with negative constant curvature and Lorentz signature. Maximally symmetric (in D dimensions) means it admits $D(D + 1)/2$ Killing vectors. Equivalently, the metric $g_{\mu\nu}$ of any maximally symmetric space satisfies,

$$R_{\mu\nu\rho\sigma} = K(g_{\mu\rho}g_{\nu\sigma} - g_{\mu\sigma}g_{\nu\rho}), \quad (\text{A.1})$$

where greek letters here run from 1 to D , with the constant K the curvature of the space and $R_{\mu\nu\rho\sigma}$ the Riemann curvature tensor. AdS_D is the space which satisfies (A.1) with $K < 0$ and Lorentz signature [78, 79, 80, 81, 82, 112].

The definition of AdS space given above is not very useful for physical purposes. Alternatively, AdS_D can be defined as the embedding of the D -dimensional hyperboloid with equation

$$(Z^0)^2 + (Z^D)^2 - \sum_{i=1}^{D-1} (Z^i)^2 = L^2, \quad (\text{A.2})$$

in the $(D + 1)$ -dimensional flat space with metric

$$ds^2 = -(dZ^0)^2 - (dZ^D)^2 + \sum_{i=1}^{D-1} (dZ^i)^2. \quad (\text{A.3})$$

Note that (A.3) has two timelike coordinates, Z^0 and Z^D . The constant L fixes the scale of AdS_D , and is related to the curvature K in (A.1) by $K =$

$-1/L^2$. Defined in this way, AdS_D is explicitly invariant under $SO(2, D - 1)$, the isometry group of the hyperboloid (A.2). This is generated by the $D(D + 1)/2$ Killing vector fields required by a maximally symmetric space.

Of course, since the AdS space has Lorentz signature, it is a solution of GR. Indeed it can be shown that AdS_D arises as the (conformally flat) vacuum solution to Einstein equations with negative cosmological constant Λ related to the AdS scale L as

$$\Lambda = -\frac{(D - 1)(D - 2)}{2L^2}. \quad (\text{A.4})$$

A section of AdS_4 is obtained as a solution to the Friedman equation for vanishing density, negative spatial curvature and negative cosmological constant. In any case, cosmological observations show the existence of a positive cosmological constant, so AdS is of little cosmological interest.

Concerning coordinates in AdS_D , obviously we can use the set $\{Z^0, \dots, Z^D\}$ as a sort of “overdetermined” coordinates. This is specially useful in Chapter 3, where we computed the Aichelburg-Sexl boost over the Reissner-Nordström solution in AdS space from these coordinates. Leaving them aside, other set of global coordinates covering the whole hyperboloid (A.2) can be also defined. A useful set of global coordinates $\{T, R, \varphi_i\}$ is defined from $\{Z^0, \dots, Z^D\}$ as

$$\begin{aligned} Z^0 &= L \cosh R \sin \frac{T}{L}, \\ Z^i &= L \varphi^i \sinh R, \\ Z^D &= L \sinh R \sin \frac{T}{L}, \end{aligned} \quad (\text{A.5})$$

where $R \in [0, \infty)$, $T \in [0, 2\pi)$ and φ^i are angular coordinates satisfying $\sum_{i=1}^{D-1} (\varphi^i)^2 = 1$. The AdS_D metric in these coordinates is

$$ds^2 = -\cosh^2 R dT^2 + L^2 (dR^2 + \sinh^2 R d\Omega_{D-2}^2). \quad (\text{A.6})$$

Note that, for constant R , the temporal coordinates Z^0 and Z^D are parametrized by a single time coordinate T which is periodic. Thus, in these coordinates we see explicitly the AdS space has topology $S^1 \times \mathbb{R}^3$ with closed timelike curves. For overcoming this unphysical feature, it is usual to work with the universal covering space of the AdS space by taking $T \in (-\infty, \infty)$ and unwrapping S^1 to \mathbb{R} . In the picture of the AdS space as an embedded hyperboloid in flat space, this corresponds to an infinite number of turns around the hyperboloid.

This set of coordinates is useful to study the causal structure of AdS space. A conformal coordinate χ can be introduced by setting

$$\tan \chi = \sinh R. \quad (\text{A.7})$$

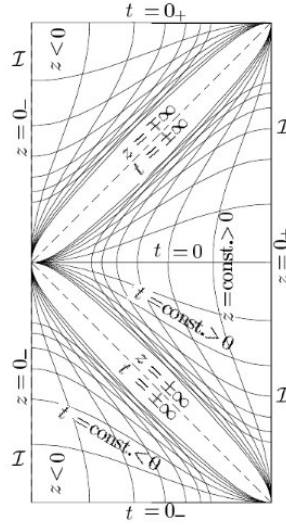


Figure A.1: Penrose diagram for the whole anti-de Sitter space (taken from [112]). Space-like ($t = \text{const.}$) and timelike ($z = \text{const.}$) geodesics in Poincaré coordinates are also drawn. The diagram is divided into three regions depending on the sign of z , each of them separated from the others by Cauchy horizons (dashed lines). Thus AdS_D has not global hyperbolicity. The Poincaré patch corresponds to the region with $z > 0$.

Defining also $\psi = T/L$, the metric takes the form

$$ds^2 = \frac{L^2}{\cos^2 \chi} (-d\psi^2 + d\chi^2 + \sin^2 \chi d\Omega_{D-2}^2). \quad (\text{A.8})$$

Thus the whole AdS space is conformal to the region $\chi \in [0, \pi/2)$ of the Einstein static universe with conformal factor $L/\cos \chi$ and radius L . The conformal boundary of the AdS space is reached at $\chi = \pi/2$, when the conformal factor diverges. In addition, it is timelike with topology $\mathbb{R} \times S^{D-2}$.

Drawing the region $0 \leq \chi < \pi/2$ of the Einstein static universe we get the Penrose conformal diagram of the whole AdS space, sketched in fig. A.1. In contrast to Minkowski space, there is only one conformal infinity \mathcal{I} , where null geodesics end, which also coincides with the spatial infinity i^0 and the boundary of the space. Note that no timelike geodesic can reach \mathcal{I} . In addition, \mathcal{I} is timelike. As a consequence, there exists no complete Cauchy surface in AdS_D since any initial data in the boundary \mathcal{I} would propagate inside AdS space. Thus the anti-de Sitter space has no global hyperbolicity: no initial data set over a spacelike hypersurface exists such that it determines the evolution of physical phenomena inside AdS_D . In this sense, the whole anti-de Sitter space is unphysical.

Another set of global coordinates $\{\tau, r, \theta^i\}$ in AdS_D is the one given from

$\{Z^0, \dots, Z^D\}$ as

$$\begin{aligned} Z^0 &= \sqrt{r^2 + L^2} \sin \frac{\tau}{L}, \\ Z^i &= r\theta^i, \\ Z^D &= \sqrt{r^2 + L^2} \cos \frac{\tau}{L}, \end{aligned} \tag{A.9}$$

where $\tau \in (0, 2\pi)$, $r \in (0, \infty)$ and $\sum_{i=1}^{D-1} (\theta^i)^2 = 1$. Similarly to (A.5), demanding τ to take values in $(-\infty, \infty)$ we have the universal covering space of AdS_D . We will refer to these global coordinates as the AdS-spherical ones. The reason for the nomenclature is that, in these coordinates, the line element of AdS_D is

$$ds^2 = - \left(1 + \frac{r^2}{L^2}\right) d\tau^2 + \left(1 + \frac{r^2}{L^2}\right)^{-1} dr^2 + r^2 d\Omega_{D-2}^2. \tag{A.10}$$

which, when $L \rightarrow \infty$, reduces to the flat metric in the usual spherical coordinates.

Other very useful coordinates in AdS_D are the Poincaré ones. From $\{Z^0, \dots, Z^D\}$, Poincaré coordinates $\{z, t \equiv x^0, x^1, \dots, x^{D-2}\}$ are defined by

$$\begin{aligned} Z^\mu &= \frac{L}{z} x^\mu, \quad \mu = 0, \dots, D-2, \\ Z^{D-1} &= \frac{z}{2} \left[-1 + \frac{L^2 + t^2 - \vec{x}^2}{z^2} \right], \\ Z^D &= \frac{z}{2} \left[1 + \frac{L^2 - t^2 + \vec{x}^2}{z^2} \right]. \end{aligned} \tag{A.11}$$

where \vec{x}^2 stands for $\sum_{i=1}^{D-2} (x^i)^2$. The line element of AdS spacetime is specially simple in Poincaré coordinates,

$$ds^2 = \frac{L^2}{z^2} (dz^2 + \eta_{\mu\nu} dx^\mu dx^\nu), \tag{A.12}$$

The main feature of Poincaré coordinates is that they show explicitly the scale invariance of the AdS spacetime, since the line element remains unchanged under

$$t \rightarrow kt, \quad z \rightarrow kz, \quad x^i \rightarrow kx^i. \tag{A.13}$$

for $k > 0$ arbitrary. This explicit invariance was specially useful in Chapter 4.

Poincaré coordinates divide the AdS space into three regions according to the sign of z , such that each of these regions are separated from the others

by Cauchy horizons. The region corresponding to $z > 0$, where there are not closed timelike curves and global hyperbolicity is recovered, is called the Poincaré patch. Usually the physics in the AdS space is restricted to the Poincaré patch since causal structure is nice in this region¹ (see fig. A.1). On the other hand, the conformal boundary of AdS_D is located at $z \rightarrow 0$. Note that the flatness of the conformal boundary and, in general, of any hypersurface $z = \text{constant}$ is explicit in Poincaré coordinates. The set $\{x^\mu\}$ are Cartesian coordinates in the hypersurfaces of z constant, while z is a coordinate labeling these flat hypersurfaces, running until it reaches the conformal boundary at $z \rightarrow 0$. As a consequence, in the context of the AdS/CFT correspondence, we refer to $\{x^\mu\}$ as the boundary coordinates, and to z as the holographic or Poincaré coordinate. Finally, the AdS metric in Poincaré coordinates is manifestly conformally flat with conformal factor L/z . Indeed, defining a new coordinate \bar{z} as

$$\bar{z} = z - L, \quad (\text{A.14})$$

and taking the limit $L \rightarrow \infty$, $z \rightarrow \infty$ such that $\bar{z} \ll L$, we recover the flat metric in Cartesian coordinates from the line element (A.12). We shall refer to this connection as the flat limit of the AdS space.

In addition to the coordinates introduced so far, it is possible to define also a dimensionless coordinate q using the chordal distance between a point of the hyperboloid (A.2) to its "top point" $Z^\mu = Z^{D-1} = 0$, $Z^D = L$ measured with the flat metric (A.3). If d stands for this chordal distance, q is defined as

$$q \equiv \frac{d^2}{4L^2} = \frac{1}{4L^2} [-(Z^D - L)^2 + (Z^{D-1})^2 + \eta_{\mu\nu} Z^\mu Z^\nu]. \quad (\text{A.15})$$

We call q the chordal coordinate. Equations (A.11) allow us to relate the chordal coordinate q to Poincaré coordinates as

$$q = \frac{Z^D}{2L} - \frac{1}{2} = \frac{1}{4zL} [(z - L)^2 + \eta_{\mu\nu} x^\mu x^\nu]. \quad (\text{A.16})$$

The origin of the chordal coordinates, i.e. $q = 0$, is located at $z = L$ and $x^\mu = 0$ and thus, from the point of view of Poincaré coordinates, the position of the origin of q is fixed by the scale of the AdS spacetime. However, thanks to the scale invariance (A.13), it is possible to set the origin of chordal coordinates at arbitrary values of the holographic coordinate z_0 ,

$$q = \frac{1}{4zz_0} [(z - z_0)^2 + \eta_{\mu\nu} x^\mu x^\nu] \quad (\text{A.17})$$

¹Indeed the collisions of shock waves studied in this Thesis are restricted to the region $z > 0$.

In addition, translational symmetry under $\vec{x} \rightarrow \vec{x} + \vec{b}$ let us to move the origin point of q to an arbitrary boundary spatial coordinate.

From (A.9) and equation (A.16) or equivalently (A.17) we get a relation between the chordal coordinate q and the spherical coordinate r ,

$$r = 2L\sqrt{q(q+1)}. \quad (\text{A.18})$$

This enables us to write the metric of AdS_D in coordinates $\{q, \theta^i\}$ from (A.10),

$$ds^2 = -(2q+1)^2 dt^2 + \frac{L^2}{q(q+1)} dq^2 + 4L^2 q(q+1) d\Omega_{D-2}^2. \quad (\text{A.19})$$

The chordal coordinate is specially useful in colliding wave scenarios since it is invariant under rotations around the collision axis in head-on collision.

It is convenient to define also the hyperbolic space $\mathbb{H}_{(D-2)}$. In a similar way to AdS_D , it is defined as the embedding of an hyperboloid in flat space. In this case, we have the $(D-2)$ -dimensional hyperboloid

$$(Y^0)^2 - (Y^{D-2})^2 - \sum_{i=1}^{D-3} (Y^i)^2 = L^2, \quad (\text{A.20})$$

embedded in a $(D-1)$ -dimensional space with metric

$$ds^2 = -(dY^0)^2 + (dY^{D-2})^2 + \sum_{i=1}^{D-3} (dY^i)^2. \quad (\text{A.21})$$

As for the AdS space, Poincaré coordinates can be introduced to cover the hyperbolic space \mathbb{H}_{D-2} . We define them as

$$\begin{aligned} Y^0 &= \frac{z}{2} \left[1 + \frac{L^2 + \vec{x}^2}{z^2} \right], \\ Y^i &= \frac{L}{z} x^i, \quad i = 1, \dots, D-3, \\ Y^{D-2} &= \frac{z}{2} \left[-1 + \frac{L^2 - \vec{x}^2}{z^2} \right], \end{aligned} \quad (\text{A.22})$$

where $\vec{x}^2 = \sum_i (x^i)^2$. The metric in Poincaré coordinates takes the form

$$ds^2 = \frac{L^2}{z^2} [dz^2 + d\vec{x}^2]. \quad (\text{A.23})$$

Similarly to the AdS case, these coordinates divide the hyperbolic space according to the sign of z . The condition $z > 0$ restrict us to the region of \mathbb{H}_{D-2} where $Y^0 > 0$, which is the Poincaré patch of \mathbb{H}_{D-2} .

Apart from Poincaré coordinates, spherical (global) coordinates can be defined in \mathbb{H}_{D-2} . Similar to (A.9), we define

$$Y^0 = \sqrt{r^2 + L^2}, \quad Y^i = r\vartheta^i, \quad (\text{A.24})$$

such that $\sum_{i=1}^{D-2} (\vartheta^i)^2 = 1$. In these coordinates, the metric of \mathbb{H}_{D-2} takes the form

$$ds_{\mathbb{H}_{D-2}}^2 = \left(1 + \frac{r^2}{L^2}\right)^{-1} dr^2 + r^2 d\Omega_{D-3}^2. \quad (\text{A.25})$$

Analogously, the metric of \mathbb{H}_{D-2} can be written in terms of the chordal coordinate q ,

$$ds_{\mathbb{H}_{D-2}}^2 = \frac{L^2}{q(q+1)} dq^2 + 4L^2 q(q+1) d\Omega_{D-3}^2, \quad (\text{A.26})$$

which results from (A.24) taking $r = 2L\sqrt{q(q+1)}$.

The hyperbolic space \mathbb{H}_{D-2} can be obtained by slicing AdS_D . By the identification

$$Z^D \equiv Y^0, \quad Z^{D-1} \equiv Y^{D-2}, \quad Z^i \equiv Y^i, \quad (\text{A.27})$$

the hyperbolic space (A.20) arises as the slice $Z^0 = Z^{D-2} = 0$ of AdS_D . In Poincaré coordinates such slicing is $t = x^{D-2} = 0$, or $u, v = 0$ if we take light cone coordinates. This corresponds to the collision surface of (2.84) in the collision scheme presented in Section 2.5, as well as the transverse space to the propagation of the shock waves, since the metric (2.84) is both singular in u and v . This is the reason the hyperbolic space \mathbb{H}_{D-2} appears in equations governing the propagation and collision of gravitational shock waves in AdS_D .

Appendix B

Anti-de Sitter Reissner-Nordström solution

In classical texts of General Relativity, the Reissner-Nordström spacetime is the one static, spherically symmetric and asymptotically flat solving the Einstein equations coupled to the Maxwell electromagnetic field. It describes the spacetime geometry sourced by an electrically charged point-like particle in flat background. The generalization to AdS background is what we call Anti-de Sitter Reissner-Nordström (AdS-RN) solution.

B.1 Line element, equations of motion and action

In the AdS-spherical coordinates defined in (A.9), the AdS-RN metric and electromagnetic potential are

$$ds^2 = -f(r)d\tau^2 + f^{-1}(r)dr^2 + r^2d\Omega_{D-2}^2,$$
$$A_\tau = \sqrt{\frac{D-2}{2(D-3)}} \frac{Q}{r^{D-3}}, \quad (\text{B.1})$$

with

$$f(r) = 1 + \frac{r^2}{L^2} - \frac{2M}{r^{D-3}} + \frac{Q^2}{r^{2(D-3)}}. \quad (\text{B.2})$$

Notice that (B.1) depends in two constants of integration, M and Q . These parameters give the strength of the gravitational and electrostatic fields and thus they must be related in some way to the mass and electric charge of the AdS-RN solution. In addition, (B.2) is singular at $r = 0$ and we recover the AdS Schwarzschild solution by setting $Q = 0$.

The AdS-RN metric solves the Einstein-Maxwell equations with negative cosmological constant $\Lambda = -\frac{(D-1)(D-2)}{2L^2}$,

$$\begin{aligned} R_{ab} - \frac{1}{2}g_{ab}(R - 2\Lambda) &= 8\pi G_D T_{ab}^{(EM)}, \\ \nabla_b F^{ab} &= \alpha j^a, \end{aligned} \quad (\text{B.3})$$

with $j^a = 0$, where α is a constant which depends on the units used, and $T_{ab}^{(EM)}$ the electromagnetic energy-momentum tensor. These equations follow from the Einstein-Hilbert action with cosmological constant term coupled to the Maxwell action,

$$\begin{aligned} S &= \frac{1}{16\pi G_D} \int_M d^D x \sqrt{-g} (R - 2\Lambda - F_{ab}F^{ab} + 4\alpha A_a j^a) \\ &+ \frac{1}{8\pi G_D} \int_{\partial M} d^{D-1} y \sqrt{|\gamma|} \varepsilon (K - K_0). \end{aligned} \quad (\text{B.4})$$

The electromagnetic energy-momentum tensor follows from this action as the variation of the Maxwell part with respect to the metric,

$$T_{ab}^{(EM)} = \frac{2}{\sqrt{-g}} \frac{\delta S_M}{\delta g^{ab}}. \quad (\text{B.5})$$

For zero currents, $j^a = 0$, it is

$$T_{ab}^{(EM)} = \frac{1}{4\pi G_D} \left(F_{ac} F_b{}^c - \frac{1}{4} g_{ab} F_{cd} F^{cd} \right). \quad (\text{B.6})$$

This energy-momentum tensor is the generalization of the Belinfante tensor to curved spaces. In addition, it appears a global factor $1/4\pi G_D$ which depends on the normalization of the charge we use. It appears here because we have chosen to including the $1/16\pi G_D$ factor in the Maxwell action as in the Einstein-Hilbert action we do. From the equations of motions point of view, there are no difference between include or not this factor. However the dimensions in which we measure the electric charge become affected, or equivalently, the constant α is obeyed to include a G_D factor.

Notice that in the action (B.4) we have also included a boundary term proportional to the extrinsic curvature K of the boundary of the spacetime, ∂M , and a function K_0 defined on it. This term is included because the AdS spacetime has a (timelike) boundary and we have to guarantee the vanishing of the variation of the action over the boundary to obtain the Einstein equations in the bulk [113]. In addition, the function K_0 is introduced in order the action over the background spacetime (the AdS spacetime in our case) be finite. It is taken as the extrinsic curvature of the boundary as embedded in a reference spacetime [114].

B.2 Horizons

The AdS-RN solution has an interesting horizon structure. Because of the presence of charge, the equation $f(r) = 0$ can have either more than one solution, one double solution or no solution at all depending on the ratio between M and Q . This way the AdS-RN solution classifies in three phases:

- Sub-extremal phase (AdS-RN black hole): The values of M and Q^2 allow two different solutions r_{\pm} for the equation $f(r) = 0$. This way we have two horizons in this phase: an external event horizon and an internal Cauchy horizon. Solving $f(r) = 0$ for $D = 4$ and large enough L , they are located at

$$r_{\pm} = M \pm \sqrt{M^2 - Q^2} \pm \frac{2M^2 - Q^2 \pm 2M\sqrt{M^2 - Q^2}}{2\sqrt{M^2 - Q^2}} \frac{1}{L^2} + O\left(\frac{1}{L^4}\right). \quad (\text{B.7})$$

- Extremal phase: The values of M and Q^2 allow only one (double) solution to the equation $f(r) = 0$. The two horizons are degenerated forming a unique horizon surface. In the approximation of (B.7) this happens when $M^2 = Q^2$.
- Super-extremal phase: The function $f(r)$ is positive everywhere because of the relative values of M and Q^2 . There are neither event horizon nor Cauchy horizon, and we have a naked singularity. Although there is no analytical solution to $f(r) = 0$, in general $f(r) > 0$ is satisfied everywhere for enough high value of Q^2 with respect to M^2 . Thus the condition $Q^2 \gg M^2$ guarantees we have a super-extremal AdS-RN solution.

For arbitrary dimension D and scale L , we cannot write an analytical solution to the equation $f(r) = 0$. Approximations like (B.7) for particular values of the dimension D , together with numerical methods to solve non-linear algebraic equations, are the only possibilities to face the equation $f(r) = 0$ and describe the phase diagram of the AdS-RN solution. In fig. B.1 the equation $f(r) = 0$ is numerically solved for $D = 5$ for finite L (AdS-RN) and compared with the case for $L = 0$ (flat Reissner-Nordström solution). In general we can conclude that the presence of charge tends to prevent the horizon formation, since for large enough Q^2 with respect to M^2 we enter inside the super-extremal phase.

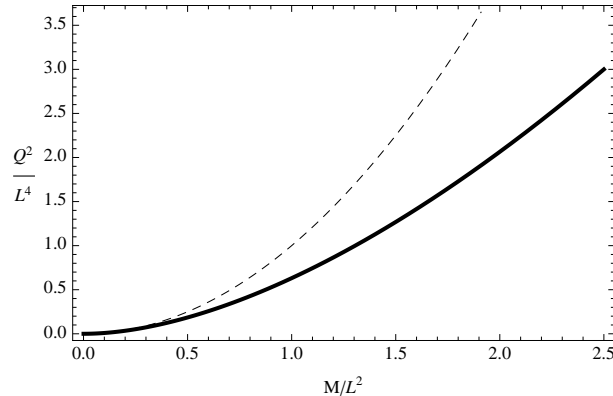


Figure B.1: Phase diagram in $D = 5$ for flat- and AdS-Reissner-Nordström solution. The solid curve represent the extremal, asymptotically AdS₅ solution, whereas dashed curve corresponds to flat extremal solution. In AdS₅ spacetime, above the solid curve we have a naked singularity, and under it there are two values r_+ and r_- solving $f(r) = 0$.

B.3 Mass and charge

We have begun this appendix defining the AdS-RN solution as the only static, spherically symmetric and asymptotically AdS solution to the Einstein-Maxwell equations, and we have argued that the integration constants M and Q in (B.2) must be related to the mass m and charge \mathbf{q} of the spacetime. However we have not computed them yet.

In General Relativity, there are various definitions of mass. In general terms it is understood as the total “gravitational energy” sourcing the spacetime curvature. However there is no well-defined notion of energy density of the gravitational field. Any effort in constructing a gravitational energy-momentum tensor is sterile since no tensor other than the metric itself can be constructed locally from only the metric components and its first derivatives. To circumvent the problem, several definitions of the total mass of a given spacetime have been proposed, avoiding the necessity to define any local gravitational energy density. In the case of asymptotically AdS spacetimes it is convenient to use the Brown and York approach to compute the gravitational mass [91].

Given a timelike hypersurface B bounding a region of some spacetime, (M, g_{ab}) , the Brown and York approach defines a surface energy-momentum tensor $\tau_{\mu\nu}$, where μ, ν runs over coordinates y^μ in B , from a Hamilton-Jacobi analysis of the classical action S_{cl} , i.e. the gravitational action evaluated at the classical solution (M, g_{ab}) . Notice that the classical action depends on the boundary data in B , and thus it can be viewed as a functional of the induced metric $\gamma_{\mu\nu}$ at B . Brown and York define the surface energy-

momentum tensor $\tau_{\mu\nu}$ at B as the variation of the classical action S_{cl} with respect to the induced metric $\gamma_{\mu\nu}$,

$$\tau_{\mu\nu} = \frac{2}{\sqrt{-\gamma}} \frac{\delta S_{sol}}{\delta \gamma^{\mu\nu}} = \frac{2}{\sqrt{-\gamma}} (\pi_{\mu\nu}^{(sol)} - \pi_{\mu\nu}^{(0)}), \quad (\text{B.8})$$

where $\pi_{\mu\nu}$ is the momentum conjugated to $\gamma_{\mu\nu}$ at B ,

$$\pi_{\mu\nu} = \frac{1}{16\pi G_D} \sqrt{-\gamma} (K_{\mu\nu} - K \gamma_{\mu\nu}), \quad (\text{B.9})$$

and $K_{\mu\nu}$ the extrinsic curvature of B . The upper labels (cl) and (0) refer to the metric with respect to the extrinsic curvature of B is computed: the label (cl) means the gravitational momentum is evaluated from the spacetime metric g_{ab} in M with the induced boundary metric in B , $\gamma_{\mu\nu}$, while (0) means the gravitational momentum is evaluated using a reference metric $g_{ab}^{(0)}$ in M such that it makes the classical action finite (last term in (B.4) proportional to K_0) and coincides with the induced boundary metric $\gamma_{\mu\nu}$ at B . Without this term, the surface stress tensor would diverge when the surface B is extended to enclose the whole spacetime (M, g) , i.e. it regularizes the stress tensor of the whole spacetime to a finite value.

From the Einstein equations in (M, g_{ab}) the surface energy-momentum tensor (B.8) satisfies the relationship

$$\mathfrak{D}_\mu \tau^{\mu\nu} = -T^{n\nu}, \quad (\text{B.10})$$

where \mathfrak{D}_μ the induced covariant derivative at B , and

$$T^{n\nu} = T^{\mu\alpha} n_\mu \gamma_\alpha^\nu, \quad (\text{B.11})$$

with n_μ is the normal to B . In the case we are in an empty spacetime or, equivalently, $T^{n\nu}$ vanishes over B , and the spacetime posses a no-vanishing Killing vector field ξ^a at B ,

$$\mathfrak{D}_\mu (\xi_\nu \tau^{\mu\nu}) = 0, \quad (\text{B.12})$$

which defines a conserved surface current associated to ξ^a and B . Now, let B_{t_0} be a closed spacelike hypersurface of B with unitary normal vector field u^μ . Note that u^μ defines a freely falling observer at B with proper time t defined as $u_\mu dy^\mu = dt$ such that B_{t_0} is a hypersurface of B of constant $t = t_0$. Then we can define the conserved surface charge $Q_\xi(t_0)$ associated to the Killing vector field ξ^a and measured by the observer given by u^μ at B and proper time t_0 as

$$Q_\xi(t_0) = \oint_{B_{t_0}} u_\mu \tau^{\mu\nu} \xi_\nu. \quad (\text{B.13})$$

For the case (M, g_{ab}) be some region of a stationary spacetime and ξ^a the associated timelike Killing vector, Q_ξ is independent of t_0 and it is understood as the total gravitational energy enclosed by B as measured by the observer defined by u^μ at B . When B bounds the whole spacetime, Q_ξ is identified with the total gravitational mass of the spacetime.

Equation (B.13) can be particularized for the case of a spherically symmetric and static spacetime with metric

$$ds^2 = -N^2(r)dt^2 + h^2(r)dr^2 + r^2d\Omega_{D-2}^2, \quad (\text{B.14})$$

where the spacetime is not necessarily flat, that is

$$N(r) \simeq N_0(r), \quad h(r) \simeq h_0(r) \quad (\text{B.15})$$

for large enough r . The timelike Killing vector field is entirely directed along t , with $\xi_t = 1$. Taking B as the timelike hypersurface for constant $r = R$, the unit normal vector field at B has only t component, $u_t = N^{-1}(R)$, and B_{t_0} is any $D - 2$ sphere of constant $r = R$ and $t = t_0$ coordinates. Thus, choosing the reference metric $g_{ab}^{(0)}$ as

$$g_{ab}^{(0)} dx^a dx^b = -\frac{N^2(R)}{N_0^2(R)} N_0^2(r) dt^2 + h_0(r) dr^2 + r^2 d\Omega_{D-2}^2, \quad (\text{B.16})$$

the associated conserved surface charge at B (gravitational energy bounded by B_{t_0} as measured by the observer \vec{u} at B) computed from (B.13) is given by

$$E(R) = \frac{(D-2)\Omega_{D-2} R^{D-3} N(R)}{8\pi G_D h_0(R)} \left(1 - \frac{h_0(R)}{h(R)} \right). \quad (\text{B.17})$$

The gravitational mass of a spacetime with metric (B.14) is then $m = \lim_{R \rightarrow \infty} E(R)$. For the special case of the AdS-RN solution,

$$N^2(r) = h^{-2}(r) = 1 + \frac{r^2}{L^2} - \frac{2M}{r^{D-3}} + \frac{Q^2}{r^{2(D-3)}}. \quad (\text{B.18})$$

Substituting in (B.17) and after taking the limit $R \rightarrow \infty$ we get the mass of the AdS-RN solution,

$$m = \frac{(D-2)\Omega_{D-2}}{8\pi G_D} M. \quad (\text{B.19})$$

Surprisingly, it coincides with the mass of the flat Schwarzschild solution, being immune to the AdS scale L .

In [90] an alternative approach is proposed for asymptotically AdS spacetimes. From the AdS/CFT connection, the divergence of the stress tensor

when B is moved to the boundary of the spacetime is identified with the standard ultraviolet divergences of the holographic quantum field theory. Thus it can be removed by adding a finite number of local counterterms to the action depending only in the intrinsic geometry of B . In addition, the counterterms are well defined and can be computed once for all spacetimes. Following this procedure the authors of [90] has found a shift of the mass (B.19) for $D = 5$, given by

$$m_0 = \frac{3\pi L^2}{32G_5}. \quad (\text{B.20})$$

for all asymptotically AdS_5 spacetimes. Surprisingly it does not depends on M and introduces a no vanishing mass for the empty AdS_5 spacetime because of the cosmological constant. This term is not derived form the Brown and York procedure since the reference geometry taken to regularize the stress tensor is also asymptotically AdS. Physically that is full of significance, since m_0 coincides with the Casimir energy of the holographic dual to $\text{AdS}_5 \times S^5$, i.e. $\mathcal{N} = 4$ SYM living at the boundary of AdS_5 , which has topology $\mathbb{R} \times S^3$. In any case, it supposes a shift over the zero energy point, and thus it is not relevant to study gravitational shock wave collisions and their the boundary images. On the other hand, anyone living inside AdS_5 would not see this shift of the mass, just measuring (B.19) for the mass of the AdS-RN black hole, so we can take (B.19) as the physical mass of the AdS-RN black hole. Therefore we shall forget (B.20) conveniently.

The charge of the Reissner-Nordström solution is a much more accessible issue than the mass. In general, given some stationary spacetime, we can define a stationary observer at p as $u^a = \xi^a/V(p)$, where ξ is the timelike Killing vector field of the spacetime and $V(p) = (-\xi_a \xi^a)^{1/2}(p)$ is the redshift factor at p . The existence of a Killing field enables us to do a 3 + 1 decomposition which folliates the spacetime (M, g_{ab}) in a continuous family of spatial hypersurfaces Σ_t . Then the electric and magnetic fields measured by this observer are defined from the Maxwell tensor F_{ab} as

$$E_a = F_{ab}u^b, \quad B_{a_4 \dots a_D} = u \frac{\sqrt{|g|}}{2} \epsilon_{abca_4 \dots a_D} F^{ab} u^c. \quad (\text{B.21})$$

From the definition it follows that both the electric and magnetic field are spacelike, since $u^a E_a = 0 = u^{a_i} B_{a_4 \dots a_D}$. Also E_a and $B_{a_4 \dots a_D}$ collect all the information contained in F_{ab} . In a similar way, the current can be decomposed in charge density ρ and spatial current \mathfrak{J}^a as

$$j^a = \rho u^a + \mathfrak{J}^a, \quad (\text{B.22})$$

such that $\mathfrak{J}^a u_a = 0$. Carrying this same 3+1 decomposition over the Maxwell equation at (B.3) gives an equation for the evolution of the magnetic field

$B_{a_4 \dots a_D}$ (which we are not interested in) plus an equation for the sources of the electric field E_a . The last is given by

$$D_\mu E^\mu + \epsilon_{\mu\nu\mu_3 \dots \mu_{D-1}} \omega^{\mu\nu} B^{\mu_3 \dots \mu_{D-1}} = \alpha \rho, \quad (\text{B.23})$$

where D_μ is the covariant derivative in the hypersurface Σ_{t_0} containing p and $\omega_{\mu\nu} = D_{[\mu} u_{\nu]}$ the vorticity of the congruence u_μ . In the special case of static spacetimes, the congruence u_a is surface forming and thus have zero vorticity. Then, the equation takes the more usually form

$$D_\mu u^\mu = \alpha \rho. \quad (\text{B.24})$$

For the special case of the AdS-RN solution, this equation can be integrated inside a closed hypersurface of constant $r = R$ radius. Then the right-hand side gives the total charge enclosed by the hypersurface, and relates it to the electric field. For an suitable election of the arbitrary constant α we gets

$$q^2 = \frac{(D-2)(D-3)}{8\pi G_D} Q^2, \quad (\text{B.25})$$

which is the charge of the AdS-RN solution. Note that the scale L of the AdS space does not contributes in any way to the measure of the charge.

Appendix C

Mathematical supplement

In this Appendix we collect the details of some calculations that are outlined in the main text.

C.1 A useful lemma

In this section we give the details of the proof of the equation

$$\lim_{\beta \rightarrow 1} \frac{1}{\sqrt{1-\beta^2}} \chi\left(\frac{(x+\beta t)^2}{1-\beta^2}\right) = \delta(x+t) \int_{-\infty}^{\infty} \chi(y^2) dy, \quad (\text{C.1})$$

where $\chi(x^2)$ is an integrable function in \mathbb{R} . This identity has been used in Sections 2.3 and 3.1.

To prove (C.1) we shall proceed by computing a primitive for the left-hand side of the equation, then taking the $\beta \rightarrow 1$ limit and finally arriving at the result after differentiation. Let us begin by computing

$$F_\beta(z) = \int_{-\infty}^z \chi\left(\frac{(x+\beta t)^2}{1-\beta^2}\right) dx. \quad (\text{C.2})$$

Changing variables to $y = \frac{x+\beta t}{\sqrt{1-\beta^2}}$ we have

$$F_\beta(z) = \sqrt{1-\beta^2} \int_{-\infty}^{\frac{z+\beta t}{\sqrt{1-\beta^2}}} \chi(y^2) dy. \quad (\text{C.3})$$

Thus the limit $\beta \rightarrow 1$ of the left-hand side of (C.1) is

$$\lim_{\beta \rightarrow 1} \frac{1}{\sqrt{1-\beta^2}} F_\beta(z) = \lim_{\beta \rightarrow 1} \int_{-\infty}^{\frac{z+\beta t}{\sqrt{1-\beta^2}}} \chi(y^2) dy. \quad (\text{C.4})$$

Now notice that according to the sign of $z + t$ we have:

$$\begin{aligned} z + t < 0 &\implies \lim_{\beta \rightarrow 1} \frac{z + \beta t}{\sqrt{1 - \beta^2}} = -\infty, \\ z + t < 0 &\implies \lim_{\beta \rightarrow 1} \frac{z + \beta t}{\sqrt{1 - \beta^2}} = \infty. \end{aligned} \quad (\text{C.5})$$

Therefore substituting in (C.4),

$$\lim_{\beta \rightarrow 1} \frac{1}{\sqrt{1 - \beta^2}} F_\beta(z) = \theta(z + t) \int_{-\infty}^{\infty} \chi(y^2) dy. \quad (\text{C.6})$$

Finally taking a derivative with respect to z and evaluating in x gives the final result:

$$\begin{aligned} \lim_{\beta \rightarrow 1} \frac{1}{\sqrt{1 - \beta^2}} \chi\left(\frac{(x + \beta t)^2}{1 - \beta^2}\right) &= \left(\frac{d}{dz} \theta(z + t)\right) \Bigg|_{z=x} \int_{-\infty}^{\infty} \chi(y^2) dy \\ &= \delta(x + t) \int_{-\infty}^{\infty} \chi(y^2) dy. \end{aligned} \quad (\text{C.7})$$

C.2 Computation of some improper integrals

This section is dedicated to the detailed computation of the integrals (3.20) and (3.37).

The integral (3.20),

$$\mathfrak{J} \equiv \int_{-\infty}^{\infty} dx \frac{Z_D'^2 (x^2 + Z_D'^2 - L^2) + x^2 L^2}{(x^2 + Z_D'^2 - L^2)^B (Z_D'^2 + x^2)^2}, \quad (\text{C.8})$$

can be solved by hand in terms of the Appell series $\mathfrak{F}(a; b_1, b_2; c, z_1, z_2)$ as

$$\begin{aligned} \mathfrak{J} &= \frac{x}{Z_D^2 (Z_D^2 - L^2)^B} \left[(L^2 + Z_D^2) \mathfrak{F}\left(\frac{1}{2}; B, 1; \frac{3}{2}; \frac{x^2}{L^2 - Z_D^2}, -\frac{x^2}{Z_D^2}\right) \right. \\ &\quad \left. - 2L^2 \mathfrak{F}\left(\frac{1}{2}; 2, B; \frac{3}{2}; -\frac{x^2}{Z_D^2}, \frac{x^2}{L^2 - Z_D^2}\right) \right] \Bigg|_{-\infty}^{\infty}. \end{aligned} \quad (\text{C.9})$$

The Appell series is a two variables generalization of the hypergeometric series. An integral representation is given by

$$\mathfrak{F}(a; b_1, b_2; c, z_1, z_2) = \frac{\Gamma(c)}{\Gamma(a)\Gamma(c-a)} \int_0^1 t^{a-1} (1-t)^{c-a-1} (1-t)^{-b_1} (1-tz_2)^{-b_2} dt.$$

To study its asymptotic behavior we use the linear transformation

$$\begin{aligned} \mathfrak{F}(a; b_1, b_2; c, z_1, z_2) &= (1 - z_2)^{-a} \\ &\times \mathfrak{F}\left(a; b_1, c - b_1 - b_2; c, \frac{z_2 - z_1}{z_2 - 1}, \frac{z_2}{z_2 - 1}\right), \end{aligned} \quad (\text{C.10})$$

togetherwith the following expression in terms of the Gaussian hypergeometric function

$$\mathfrak{F}(a; b_1, b_2; c, z_1, 1) = {}_2F_1(a, b_2; c; 1) {}_2F_1(a, b_1; c - b_2; z_1). \quad (\text{C.11})$$

This enables us to compute the first Appell series in (C.9) for $x^2 \gg Z_D^2$:

$$\begin{aligned} \mathfrak{F}\left(\frac{1}{2}; B, 1; \frac{3}{2}; \frac{x^2}{L^2 - Z_D^2}, -\frac{x^2}{Z_D^2}\right) &\simeq \frac{Z_D}{\sqrt{Z_D^2 + x^2}} \frac{\Gamma(\frac{3}{2})\Gamma(\frac{2B+1}{2})}{\Gamma(B+1)} \\ &\times {}_2F_1\left(\frac{1}{2}, B; B+1; \frac{L^2}{L^2 - Z_D^2}\right), \end{aligned} \quad (\text{C.12})$$

where we have used the value

$${}_2F_1(a, b; c; 1) = \frac{\Gamma(c) \Gamma(c - a - b)}{\Gamma(c - a) \Gamma(c - b)} \quad (\text{C.13})$$

to evaluate the first Gaussian hypergeometric function in (C.11). With a previous use of the reflexivity condition

$$\mathfrak{F}(a; b_1, b_2; c, z_1, z_2) = \mathfrak{F}(a; b_2, b_1; c, z_2, z_1), \quad (\text{C.14})$$

which follows from integral representation (C.10), we can follow the same procedure to compute the asymptotic value for the second Appell series in (C.9) when $x^2 \gg Z_D^2$. It results in

$$\begin{aligned} \mathfrak{F}\left(\frac{1}{2}; 2, B; \frac{3}{2}; -\frac{x^2}{Z_D^2}, \frac{x^2}{L^2 - Z_D^2}\right) &\simeq \frac{Z_D}{\sqrt{Z_D^2 + x^2}} \frac{\Gamma(\frac{3}{2})\Gamma(\frac{2B+3}{2})}{\Gamma(B+2)} \\ &\times {}_2F_1\left(\frac{1}{2}, B; B+2; \frac{L^2}{L^2 - Z_D^2}\right). \end{aligned} \quad (\text{C.15})$$

Substituting (C.12) and (C.15) into (C.9) we express the integral in terms of Gaussian hypergeometric series:

$$\begin{aligned} \mathfrak{J} &= \frac{2}{Z_D \sqrt{Z_D^2 - L^2}} \frac{\Gamma(\frac{3}{2})\Gamma(\frac{2B+1}{2})}{\Gamma(B+1)} \left[(L^2 + Z_D^2) {}_2F_1\left(\frac{1}{2}, B; B+1; \frac{L^2}{L^2 - Z_D^2}\right) \right. \\ &\quad \left. - L^2 \frac{2B+1}{B+1} {}_2F_1\left(\frac{1}{2}, B; B+2; \frac{L^2}{L^2 - Z_D^2}\right) \right]. \end{aligned} \quad (\text{C.16})$$

On the other hand, the chordal coordinate is related to Z_D^2 by $Z_D = L(2q+1)$. Thus

$$\frac{L^2}{L^2 - Z_D^2} = -\frac{1}{q(4q+4)}. \quad (\text{C.17})$$

Then we can use the quadratic transformation of the Gaussian hypergeometric series,

$${}_2F_1(a, b; 2b, u) = (1-u)^{-\frac{a}{2}} {}_2F_1\left(\frac{a}{2}, b - \frac{a}{2}; b + \frac{1}{2}, \frac{u^2}{4u-4}\right), \quad (\text{C.18})$$

with $u = -1/q$, to manipulate the first hypergeometric series in (C.16). It gives

$${}_2F_1\left(\frac{1}{2}, B; B+1; \frac{L^2}{L^2 - Z_D^2}\right) = \left(1 + \frac{1}{q}\right)^{1/2} {}_2F_1\left(1, B + \frac{1}{2}; 2B+1; -\frac{1}{q}\right). \quad (\text{C.19})$$

The second hypergeometric series in (C.16) can not be directly transformed using (C.18). Previously we have to use the contiguous relation,

$${}_2F_1(a, b; c; z) = \frac{c-1}{c-b-1} {}_2F_1(a, b; c-1; z) - \frac{b}{c-b-1} {}_2F_1(a, b+1; c; z). \quad (\text{C.20})$$

In this way,

$$\begin{aligned} {}_2F_1\left(\frac{1}{2}, B; B+2; \frac{L^2}{L^2 - Z_D^2}\right) &= (B+1) {}_2F_1\left(\frac{1}{2}, B; B+1; \frac{L^2}{L^2 - Z_D^2}\right) \\ &\quad - B {}_2F_1\left(\frac{1}{2}, B+1; B+2; \frac{L^2}{L^2 - Z_D^2}\right). \end{aligned} \quad (\text{C.21})$$

After application of (C.18) and the change to chordal coordinate, it reads

$$\begin{aligned} {}_2F_1\left(\frac{1}{2}, B; B+2; \frac{L^2}{L^2 - Z_D^2}\right) &= (B+1)\sqrt{1+\frac{1}{q}} {}_2F_1\left(1, B + \frac{1}{2}; 2B+1; -\frac{1}{q}\right) \\ &\quad - B\sqrt{1+\frac{1}{q}} {}_2F_1\left(1, B + \frac{3}{2}; 2B+3; -\frac{1}{q}\right). \end{aligned} \quad (\text{C.22})$$

Substituting this into (C.16), together with (C.19), we get

$$\begin{aligned} \mathfrak{J} &= \frac{2^{1-2B}}{L^{2B-1}(2q+1)q^{2B}} \frac{\Gamma\left(\frac{3}{2}\right)\Gamma\left(B + \frac{1}{2}\right)}{\Gamma(B+1)} \left(1 + \frac{1}{q}\right)^{\frac{1-2B}{2}} \\ &\quad \times \left\{ \left[4q^2 \left(1 + \frac{1}{q}\right) - (2B-1) \right] {}_2F_1\left(1, B + \frac{1}{2}; 2B+1; -\frac{1}{q}\right) \right. \\ &\quad \left. + \frac{B(2B+1)}{B+1} {}_2F_1\left(1, B + \frac{3}{2}; 2B+3; -\frac{1}{q}\right) \right\}. \end{aligned} \quad (\text{C.23})$$

Finally, consecutive applications of Gauss contiguous relations¹ allows the recast the term inside the brackets in terms of just one hypergeometric series:

$$\mathfrak{J} = \frac{\Gamma(3/2)\Gamma(B+1/2)}{\Gamma(B+1)} \frac{2^{2(1-B)}}{(Lq)^{2B-1}} {}_2F_1(2B-1, B+1/2; 2B+1; -1/q), \quad (\text{C.24})$$

which gives (3.20).

The improper integral appearing in (3.37) can be expressed as

$$\mathfrak{J} \equiv \int_{-\infty}^{\infty} \frac{dy}{[y^2 + \rho^2]^B} = \frac{y}{\rho^{2B}} {}_2F_1\left(\frac{1}{2}, B; \frac{3}{2}; -\frac{y^2}{\rho^2}\right) \Big|_{-\infty}^{\infty}. \quad (\text{C.25})$$

To evaluate the limits over the hypergeometric function we use the first Pfaff transformation, which states that

$${}_2F_1(a, b; c; z) = (1-z)^{-a} {}_2F_1\left(a, c-b; c; \frac{z}{z-1}\right). \quad (\text{C.26})$$

Thus

$$\begin{aligned} \lim_{y \rightarrow \pm\infty} x {}_2F_1\left(\frac{1}{2}, B; \frac{3}{2}; -\frac{y^2}{\rho^2}\right) &= {}_2F_1\left(\frac{1}{2}, \frac{3}{2} - B; \frac{3}{2}; 1\right) \\ &\times \lim_{x \rightarrow \pm\infty} x \left(1 + \frac{x^2}{\rho^2}\right)^{-\frac{1}{2}} = \pm \rho \frac{\sqrt{\pi} \Gamma(B - \frac{1}{2})}{2 \Gamma(B)}, \end{aligned} \quad (\text{C.27})$$

where we have applied (C.13). Substituting in (C.25) we finally get

$$\mathfrak{J} = \frac{1}{\rho^{2B-1}} \sqrt{\pi} \frac{\Gamma(B - \frac{1}{2})}{2 \Gamma(B)}, \quad (\text{C.28})$$

which is the result quoted in (3.38).

¹A complete list can be found in page 558 of [115].

Bibliography

- [1] U. W. Heinz and M. Jacob, *Evidence for a new state of matter: An Assessment of the results from the CERN lead beam program*, [nucl-th/0002042](#).
- [2] H. van Hees, V. Greco, and R. Rapp, *Heavy-quark probes of the quark-gluon plasma at RHIC*, *Phys.Rev.* **C73** (2006) 034913, [[nucl-th/0508055](#)].
- [3] Y. Kohsuke, Y. Tetsuo, and Y.M.Hatsuda, *Quark-Gluon Plasma: From Big Bang to Little Bang*. Cambridge University Press, 2010.
- [4] U. W. Heinz, *The Strongly coupled quark-gluon plasma created at RHIC*, *J.Phys.* **A42** (2009) 214003, [[arXiv:0810.5529](#)].
- [5] J. M. Maldacena, *The Large N limit of superconformal field theories and supergravity*, *Adv.Theor.Math.Phys.* **2** (1998) 231–252, [[hep-th/9711200](#)].
- [6] O. Aharony, S. S. Gubser, J. M. Maldacena, H. Ooguri, and Y. Oz, *Large N field theories, string theory and gravity*, *Phys.Rept.* **323** (2000) 183–386, [[hep-th/9905111](#)].
- [7] E. Witten, *Anti-de Sitter space and holography*, *Adv.Theor.Math.Phys.* **2** (1998) 253–291, [[hep-th/9802150](#)].
- [8] G. Landi, *An Introduction to noncommutative spaces and their geometry*, [hep-th/9701078](#).
- [9] E. Witten, *Noncommutative Geometry and String Field Theory*, *Nucl.Phys.* **B268** (1986) 253.
- [10] B. Jurco, S. Schraml, P. Schupp, and J. Wess, *Enveloping algebra valued gauge transformations for nonAbelian gauge groups on noncommutative spaces*, *Eur.Phys.J.* **C17** (2000) 521–526, [[hep-th/0006246](#)].

-
- [11] S. Schraml, *Enveloping algebra-valued gauge transformations on noncommutative spaces*, *Mod.Phys.Lett.* **A16** (2001) 337–341.
- [12] L. Bonora, M. Schnabl, M. Sheikh-Jabbari, and A. Tomasiello, *Noncommutative $SO(n)$ and $Sp(n)$ gauge theories*, *Nucl.Phys.* **B589** (2000) 461–474, [[hep-th/0006091](#)].
- [13] P. Aschieri, M. Dimitrijevic, F. Meyer, S. Schraml, and J. Wess, *Twisted gauge theories*, *Lett.Math.Phys.* **78** (2006) 61–71, [[hep-th/0603024](#)].
- [14] J. Wess, *Deformed gauge theories*, *J.Phys.Conf.Ser.* **53** (2006) 752–763, [[hep-th/0608135](#)].
- [15] H. Fritzsch, M. Gell-Mann, and H. Leutwyler, *Advantages of the Color Octet Gluon Picture*, *Phys.Lett.* **B47** (1973) 365–368.
- [16] M. E. Peskin and D. V. Schroeder, *An introduction to Quantum Field Theory*. Perseus Books Publishing, L. L. C., 1995.
- [17] K. G. Wilson, *Confinement of Quarks*, *Phys.Rev.* **D10** (1974) 2445–2459.
- [18] V. Schon and M. Thies, *2-D Model Field Theories at Finite Temperature and Density*, [[hep-th/0008175](#)].
- [19] I. Zakout, C. Greiner, and J. Schaffner-Bielich, *The Order, shape and critical point for the quark-gluon plasma phase transition*, *Nucl.Phys.* **A781** (2007) 150–200, [[nucl-th/0605052](#)].
- [20] F. Karsch, *The Phase transition to the quark gluon plasma: Recent results from lattice calculations*, *Nucl.Phys.* **A590** (1995) 367C–382C, [[hep-lat/9503010](#)].
- [21] J. Y. Ollitrault, *Anisotropy as a signature of transverse collective flow*, *Phys.Rev.* **D46** (1992) 229–245.
- [22] R. Snellings, *Elliptic Flow: A Brief Review*, *New J.Phys.* **13** (2011) 055008, [[arXiv:1102.3010](#)].
- [23] H. Holopainen, S. Rasanen, and K. J. Eskola, *Elliptic flow of thermal photons in heavy-ion collisions at Relativistic Heavy Ion Collider and Large Hadron Collider*, *Phys.Rev.* **C84** (2011) 064903, [[arXiv:1104.5371](#)].

- [24] **ALICE** Collaboration, K. Aamodt et al., *Elliptic flow of charged particles in Pb-Pb collisions at 2.76 TeV*, *Phys.Rev.Lett.* **105** (2010) 252302, [[arXiv:1011.3914](#)].
- [25] M. Petráň, J. Letessier, V. Petráček, and J. Rafelski, *Hadron production and quark-gluon plasma hadronization in Pb-Pb collisions at $\sqrt{s_{NN}} = 2.76$ TeV*, *Phys.Rev.* **C88** (2013), no. 3 034907, [[arXiv:1303.2098](#)].
- [26] H. Song, *QGP viscosity at RHIC and the LHC - a 2012 status report*, *Nucl.Phys.* **A904-905** (2013) 114c–121c, [[arXiv:1210.5778](#)].
- [27] A. Buzzatti and M. Gyulassy, *A running coupling explanation of the surprising transparency of the QGP at LHC*, *Nucl.Phys.* **A904-905** (2013) 779c–782c, [[arXiv:1210.6417](#)].
- [28] K. Osterwalder and E. Seiler, *Gauge Field Theories on the Lattice*, *Annals Phys.* **110** (1978) 440.
- [29] K. Becker, M. Becker, and J. H. Schwarz, *String Theory and M theory. A Modern Introduction*. Cambridge University Press, 2007.
- [30] J. Polchinski, *String Theory*. Cambridge University Press, 2008.
- [31] E. Kiritsis, *Introduction to superstring theory*, [hep-th/9709062](#).
- [32] C. G. Callan, E. J. Martinec, M. J. Perry, and D. Friedan, *Strings in Background Fields*, *Nucl.Phys.* **B262** (1985) 593.
- [33] J. D. Bekenstein, *Entropy bounds and black hole remnants*, *Phys.Rev.* **D49** (1994) 1912–1921, [[gr-qc/9307035](#)].
- [34] G. 't Hooft, *Dimensional reduction in quantum gravity*, [gr-qc/9310026](#).
- [35] L. Susskind, *The World as a hologram*, *J.Math.Phys.* **36** (1995) 6377–6396, [[hep-th/9409089](#)].
- [36] S. Hawking, *Particle Creation by Black Holes*, *Commun.Math.Phys.* **43** (1975) 199–220.
- [37] G. Policastro, D. T. Son, and A. O. Starinets, *From AdS / CFT correspondence to hydrodynamics*, *JHEP* **0209** (2002) 043, [[hep-th/0205052](#)].

- [38] G. Policastro, D. T. Son, and A. O. Starinets, *The Shear viscosity of strongly coupled $N=4$ supersymmetric Yang-Mills plasma*, *Phys.Rev.Lett.* **87** (2001) 081601, [[hep-th/0104066](#)].
- [39] G. Policastro, D. T. Son, and A. O. Starinets, *From AdS / CFT correspondence to hydrodynamics. 2. Sound waves*, *JHEP* **0212** (2002) 054, [[hep-th/0210220](#)].
- [40] P. Kovtun, D. T. Son, and A. O. Starinets, *Viscosity in strongly interacting quantum field theories from black hole physics*, *Phys.Rev.Lett.* **94** (2005) 111601, [[hep-th/0405231](#)].
- [41] S. Bhattacharyya, V. Hubeny, S. Minwalla, and M. Rangamani, *Nonlinear Fluid Dynamics from Gravity*, *JHEP* **0802** (2008) 045, [[arXiv:0712.2456](#)].
- [42] H. Nastase, *On high energy scattering inside gravitational backgrounds*, [hep-th/0410124](#).
- [43] H. Nastase, *More on the RHIC fireball and dual black holes*, [hep-th/0603176](#).
- [44] J. B. Griffiths, *Colliding Plane Waves in General Relativity*. Oxford University Press, 1991.
- [45] D. Grumiller and P. Romatschke, *On the collision of two shock waves in AdS(5)*, *JHEP* **0808** (2008) 027, [[arXiv:0803.3226](#)].
- [46] R. Penrose *Seminar at Cambridge University (unpublished)* (1974).
- [47] P. D'Eath and P. Payne, *Gravitational radiation in high speed black hole collisions. 1. Perturbation treatment of the axisymmetric speed of light collision*, *Phys.Rev.* **D46** (1992) 658–674.
- [48] P. D'Eath and P. Payne, *Gravitational radiation in high speed black hole collisions. 2. Reduction to two independent variables and calculation of the second order news function*, *Phys.Rev.* **D46** (1992) 675–693.
- [49] P. D'Eath and P. Payne, *Gravitational radiation in high speed black hole collisions. 3. Results and conclusions*, *Phys.Rev.* **D46** (1992) 694–701.
- [50] D. M. Eardley and S. B. Giddings, *Classical black hole production in high-energy collisions*, *Phys.Rev.* **D66** (2002) 044011, [[gr-qc/0201034](#)].

-
- [51] S. S. Gubser, S. S. Pufu, and A. Yarom, *Entropy production in collisions of gravitational shock waves and of heavy ions*, *Phys.Rev.* **D78** (2008) 066014, [[arXiv:0805.1551](#)].
- [52] S. Lin and E. Shuryak, *Grazing Collisions of Gravitational Shock Waves and Entropy Production in Heavy Ion Collision*, *Phys.Rev.* **D79** (2009) 124015, [[arXiv:0902.1508](#)].
- [53] S. S. Gubser, S. S. Pufu, and A. Yarom, *Off-center collisions in AdS(5) with applications to multiplicity estimates in heavy-ion collisions*, *JHEP* **0911** (2009) 050, [[arXiv:0902.4062](#)].
- [54] P. Aichelburg and R. Sexl, *On the Gravitational field of a massless particle*, *Gen.Rel.Grav.* **2** (1971) 303–312.
- [55] A. Duenas-Vidal and M. A. Vazquez-Mozo, *Colliding AdS gravitational shock waves in various dimensions and holography*, *JHEP* **1007** (2010) 021, [[arXiv:1004.2609](#)].
- [56] H. Yoshino and Y. Nambu, *Black hole formation in the grazing collision of high-energy particles*, *Phys.Rev.* **D67** (2003) 024009, [[gr-qc/0209003](#)].
- [57] L. Alvarez-Gaume, C. Gomez, A. Sabio Vera, A. Tavanfar, and M. A. Vazquez-Mozo, *Critical formation of trapped surfaces in the collision of gravitational shock waves*, *JHEP* **0902** (2009) 009, [[arXiv:0811.3969](#)].
- [58] A. Duenas-Vidal and M. A. Vazquez-Mozo *Unpublished* (2013).
- [59] I. Y. Aref’eva, A. Bagrov, and L. Joukovskaya, *Critical Trapped Surfaces Formation in the Collision of Ultrarelativistic Charges in (A)dS*, *JHEP* **1003** (2010) 002, [[arXiv:0909.1294](#)].
- [60] A. Duenas-Vidal and M. Vazquez-Mozo, *A Note on the Collision of Reissner-Nordström Gravitational Shock Waves in AdS*, *Phys.Lett.* **B713** (2012) 500–504, [[arXiv:1203.1046](#)].
- [61] H. Yoshino and R. B. Mann, *Black hole formation in the head-on collision of ultrarelativistic charges*, *Phys.Rev.* **D74** (2006) 044003, [[gr-qc/0605131](#)].
- [62] R. J. Szabo, *Quantum field theory on noncommutative spaces*, *Phys.Rept.* **378** (2003) 207–299, [[hep-th/0109162](#)].

- [63] M. R. Douglas and N. A. Nekrasov, *Noncommutative field theory*, *Rev.Mod.Phys.* **73** (2001) 977–1029, [[hep-th/0106048](#)].
- [64] J. Barbon, *Introduction to noncommutative field theory*, .
- [65] S. Minwalla, M. Van Raamsdonk, and N. Seiberg, *Noncommutative perturbative dynamics*, *JHEP* **0002** (2000) 020, [[hep-th/9912072](#)].
- [66] H. S. Snyder, *Quantized space-time*, *Phys.Rev.* **71** (1947) 38–41.
- [67] A. Connes, *Noncommutative Geometry*. Academic Press, 1994.
- [68] F. Meyer, *Noncommutative spaces and gravity*, [hep-th/0510188](#).
- [69] S. Giller, C. Gonera, P. Kosinski, and P. Maslanka, *On the Consistency of Twisted Gauge Theory*, *Phys.Lett.* **B655** (2007) 80–83, [[hep-th/0701014](#)].
- [70] L. Alvarez-Gaume, F. Meyer, and M. A. Vazquez-Mozo, *Comments on noncommutative gravity*, *Nucl.Phys.* **B753** (2006) 92–127, [[hep-th/0605113](#)].
- [71] N. Seiberg and E. Witten, *String theory and noncommutative geometry*, *JHEP* **9909** (1999) 032, [[hep-th/9908142](#)].
- [72] A. Duenas-Vidal and M. A. Vazquez-Mozo, *Twisted invariances of noncommutative gauge theories*, *Phys.Lett.* **B668** (2008) 57–62, [[arXiv:0802.4201](#)].
- [73] R. Hulse and J. Taylor, *Discovery of a pulsar in a binary system*, *Astrophys.J.* **195** (1975) L51–L53.
- [74] J. Weisberg and J. Taylor, *Gravitational radiation from an orbiting pulsar*, *Gen.Rel.Grav.* **13** (1981) 1–6.
- [75] **BICEP2** Collaboration, *Detection of B-Mode Polarization at Degree Angular Scales by BICEP2*, *Phys.Rev.Lett.* **112** (2014) 241101, [[arXiv:1403.3985](#)].
- [76] M. J. Mortonson and U. Seljak, *A joint analysis of Planck and BICEP2 B modes including dust polarization uncertainty*, *JCAP* **1410** (2014), no. 10 035, [[arXiv:1405.5857](#)].
- [77] L. D. Landau and M. E. Lifshitz, *Course of Theoretical Physics. Volume 2: The Classical Theory of Fields*. Cambridge University Press, 1947.

- [78] R. M. Wald, *General Relativity*. The University of Chicago Press, 1984.
- [79] C. W. Misner, K. S. Thorne, and J. A. Wheeler, *Gravitation*. W. H. Freeman and Company, 1973.
- [80] T. Padmanabhan, *Gravitation: Foundations and Frontiers*. Cambridge University Press, 2010.
- [81] J. B. Griffiths and J. Podolsky, *Exact Space-Times in Einstein's General Relativity*. Cambridge University Press, 2009.
- [82] H. Stephani et al., *Exact solutions of Einstein's field equations*. Cambridge University Press, 2003.
- [83] T. Dray and G. 't Hooft, *The Gravitational Shock Wave of a Massless Particle*, *Nucl.Phys.* **B253** (1985) 173–188.
- [84] C. Lousto and N. Sanchez, *The Curved Shock Wave Space-Time of Ultrarelativistic Charged Particles and their Scattering*, *Int.J.Mod.Phys.* **A5** (1990) 915.
- [85] C. Lousto and N. Sanchez, *The Ultrarelativistic Limit of the Boosted Kerr-Newman Geometry and the Scattering of Spin 1/2 Particles*, *Nucl.Phys.* **B383** (1992) 377–394.
- [86] K. Khan and R. Penrose, *Scattering of two impulsive gravitational plane waves*, *Nature* **229** (1971) 185–186.
- [87] S. S. Gubser, I. R. Klebanov, and A. A. Tseytlin, *String theory and classical absorption by three-branes*, *Nucl.Phys.* **B499** (1997) 217–240, [[hep-th/9703040](#)].
- [88] S. S. Gubser and I. R. Klebanov, *Absorption by branes and Schwinger terms in the world volume theory*, *Phys.Lett.* **B413** (1997) 41–48, [[hep-th/9708005](#)].
- [89] R. C. Myers, *Stress tensors and Casimir energies in the AdS / CFT correspondence*, *Phys.Rev.* **D60** (1999) 046002, [[hep-th/9903203](#)].
- [90] V. Balasubramanian and P. Kraus, *A Stress tensor for Anti-de Sitter gravity*, *Commun.Math.Phys.* **208** (1999) 413–428, [[hep-th/9902121](#)].
- [91] J. D. Brown and J. W. York, *Quasilocal energy and conserved charges derived from the gravitational action*, *Phys.Rev.* **D47** (1993) 1407–1419, [[gr-qc/9209012](#)].

- [92] S. de Haro, S. N. Solodukhin, and K. Skenderis, *Holographic reconstruction of space-time and renormalization in the AdS / CFT correspondence*, *Commun.Math.Phys.* **217** (2001) 595–622, [[hep-th/0002230](#)].
- [93] L. Alvarez-Gaume and M. Vazquez-Mozo, *Critical gravitational collapse: towards a holographic understanding of the Regge region*, *Nucl.Phys.* **B806** (2009) 327–385, [[arXiv:0804.1464](#)].
- [94] L. Susskind and E. Witten, *The Holographic bound in anti-de Sitter space*, [hep-th/9805114](#).
- [95] A. W. Peet and J. Polchinski, *UV / IR relations in AdS dynamics*, *Phys.Rev.* **D59** (1999) 065011, [[hep-th/9809022](#)].
- [96] A. Chamblin, R. Emparan, C. V. Johnson, and R. C. Myers, *Charged AdS black holes and catastrophic holography*, *Phys.Rev.* **D60** (1999) 064018, [[hep-th/9902170](#)].
- [97] S. Hawking and H. Reall, *Charged and rotating AdS black holes and their CFT duals*, *Phys.Rev.* **D61** (2000) 024014, [[hep-th/9908109](#)].
- [98] A. Chamblin, R. Emparan, C. V. Johnson, and R. C. Myers, *Holography, thermodynamics and fluctuations of charged AdS black holes*, *Phys.Rev.* **D60** (1999) 104026, [[hep-th/9904197](#)].
- [99] J. Gomis and T. Mehen, *Space-time noncommutative field theories and unitarity*, *Nucl.Phys.* **B591** (2000) 265–276, [[hep-th/0005129](#)].
- [100] F. Bayen, M. Flato, C. Fronsdal, A. Lichnerowicz, and D. Sternheimer, *Deformation Theory and Quantization. 1. Deformations of Symplectic Structures*, *Annals Phys.* **111** (1978) 61.
- [101] M. Van Raamsdonk and N. Seiberg, *Comments on noncommutative perturbative dynamics*, *JHEP* **0003** (2000) 035, [[hep-th/0002186](#)].
- [102] F. R. Ruiz, *Gauge fixing independence of IR divergences in noncommutative U(1), perturbative tachyonic instabilities and supersymmetry*, *Phys.Lett.* **B502** (2001) 274–278, [[hep-th/0012171](#)].
- [103] L. Alvarez-Gaume and M. Vazquez-Mozo, *General properties of noncommutative field theories*, *Nucl.Phys.* **B668** (2003) 293–321, [[hep-th/0305093](#)].

- [104] M. Hayakawa, *Perturbative analysis on infrared aspects of noncommutative QED on R^{**4}* , *Phys.Lett.* **B478** (2000) 394–400, [[hep-th/9912094](#)].
- [105] M. Chaichian, P. Presnajder, M. Sheikh-Jabbari, and A. Tureanu, *Noncommutative gauge field theories: A No go theorem*, *Phys.Lett.* **B526** (2002) 132–136, [[hep-th/0107037](#)].
- [106] V. Chari and A. N. Pressley, *Quantum Groups*. Cambridge University Press, 1995.
- [107] D. Vassilevich, *Symmetries in noncommutative field theories: Hopf versus Lie*, *Sao Paulo J.Math.Sci.* **4** (2010) 121–133, [[arXiv:0711.4091](#)].
- [108] C. Herdeiro, M. O. Sampaio, and C. Rebelo, *Radiation from a D-dimensional collision of shock waves: First order perturbation theory*, *JHEP* **1107** (2011) 121, [[arXiv:1105.2298](#)].
- [109] F. S. Coelho, C. Herdeiro, and M. O. Sampaio, *Radiation from a D-dimensional collision of shock waves: a remarkably simple fit formula*, *Phys.Rev.Lett.* **108** (2012) 181102, [[arXiv:1203.5355](#)].
- [110] F. S. Coelho, C. Herdeiro, C. Rebelo, and M. Sampaio, *Radiation from a D-dimensional collision of shock waves: Higher-order setup and perturbation theory validity*, *Phys.Rev.* **D87** (2013) 084034, [[arXiv:1206.5839](#)].
- [111] F. S. Coelho, C. Herdeiro, and M. O. P. Sampaio, *Radiation from a D-dimensional collision of shock waves: proof of first order formula and angular factorisation at all orders*, *JHEP* **1412** (2014) 119, [[arXiv:1410.0964](#)].
- [112] J. B. Griffiths and J. Podolsky, *Exact Space-Times in Einstein's General Relativity*. Cambridge University Press, 2009.
- [113] J. D. York *Found. Phys.* **16** (1986) 249.
- [114] E. Poisson, *A Relativist's Toolkit. The Mathematics of Black-Hole Mechanics*. Cambridge University Press, 2004.
- [115] M. Abramowitz and I. Stegun, *Handbook of Mathematical Functions with Formulas, Graphs, and Mathematical Tables*. National Bureau of Standards Applied Mathematics Series, 1964.

